


NASA Tech Briefs

National
Aeronautics and
Space
Administration

May/June 1986
Volume 10 Number 3

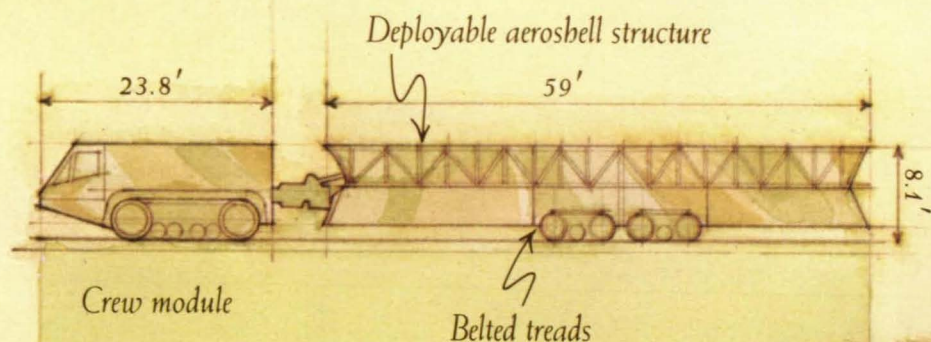


Nuclear Magnetic Resonance Imaging:

**Adapting Outer
Space Technology
to Explore the
Human Brain**

Missile launchers that go just about anywhere.

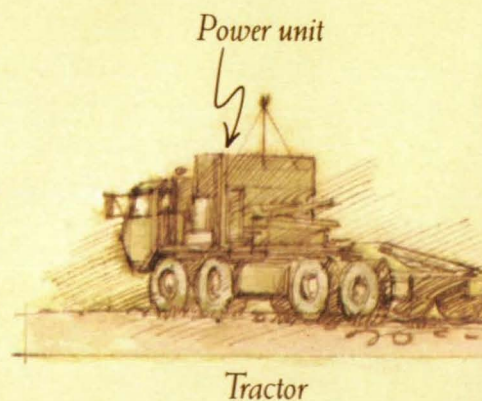
A missile system's effectiveness can depend heavily on high mobility as well as survivability. In some 30 years of meeting these two goals, Martin Marietta has addressed virtually all of the engineering and integration challenges facing planners of next-generation mobile missiles. These issues include transporting, protecting, checking out, aiming and launching from a wide range of surfaces in all kinds of climates.



Hard Mobile Launcher

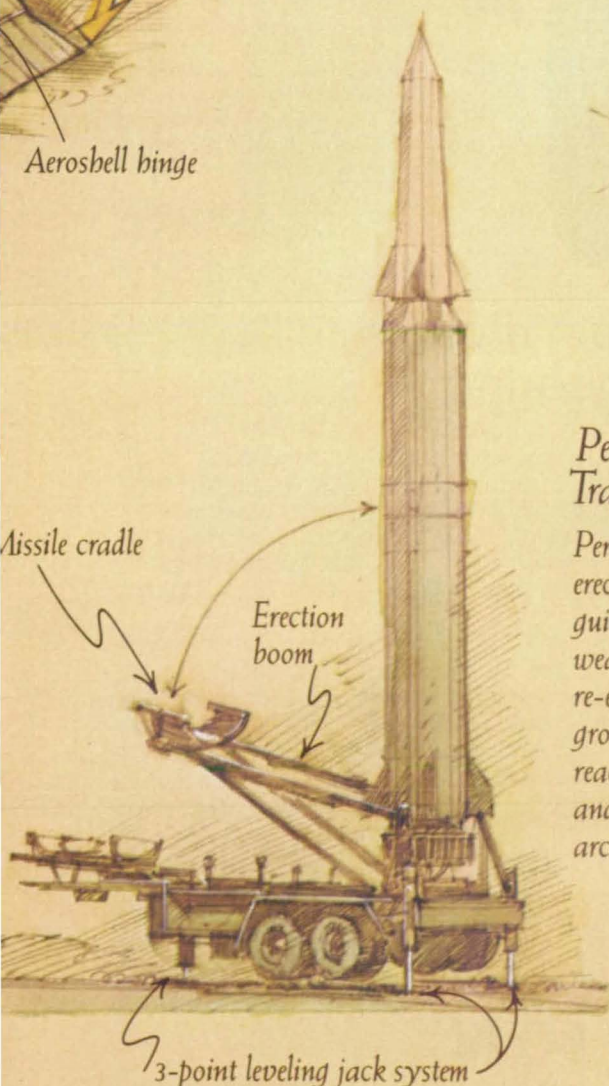
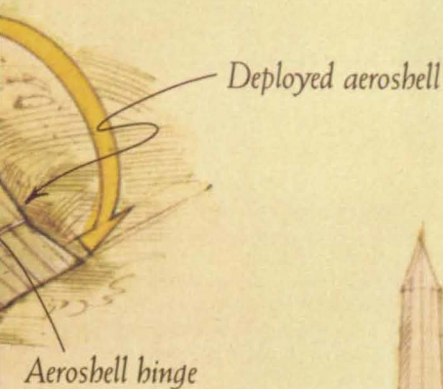
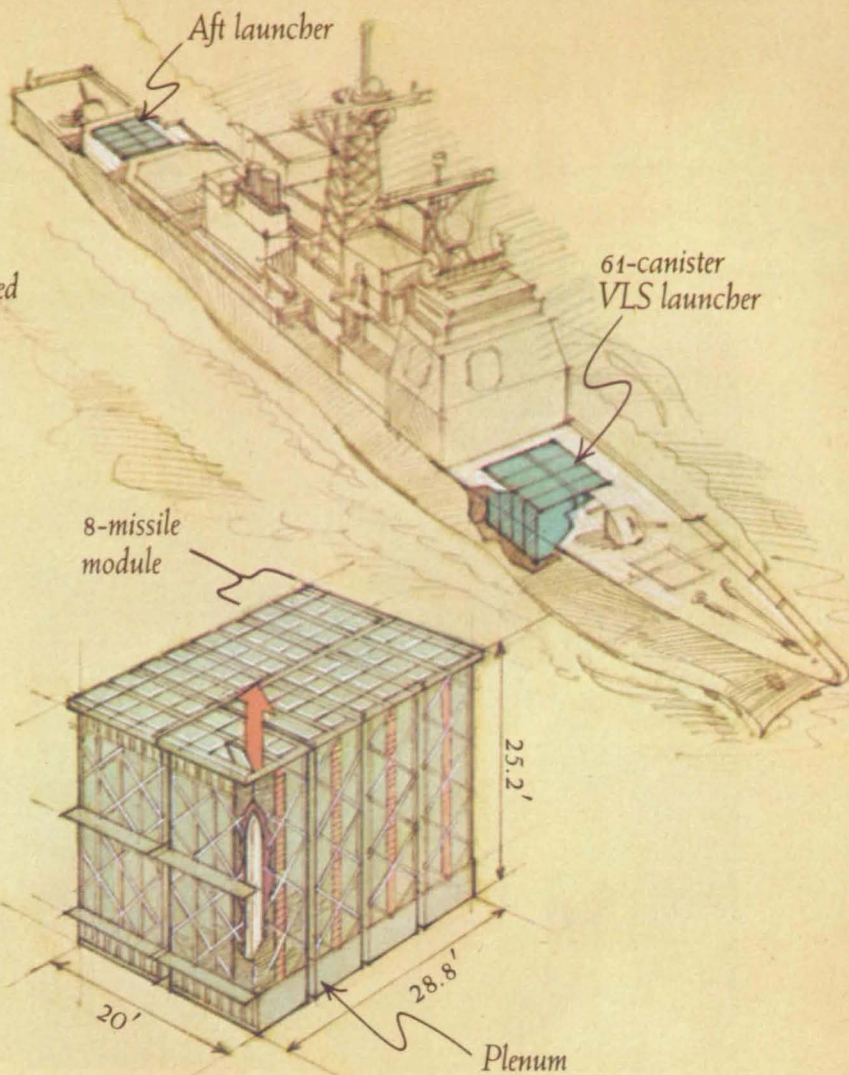
With belted treads for maximum on/off road, all-weather mobility, this launching system for the Small ICBM requires no site preparation.

Ground-conforming seals



Vertical Launching System

A mix of canister-stored missiles, stowed in protected below-deck locations, combats surface, air and underwater threats.



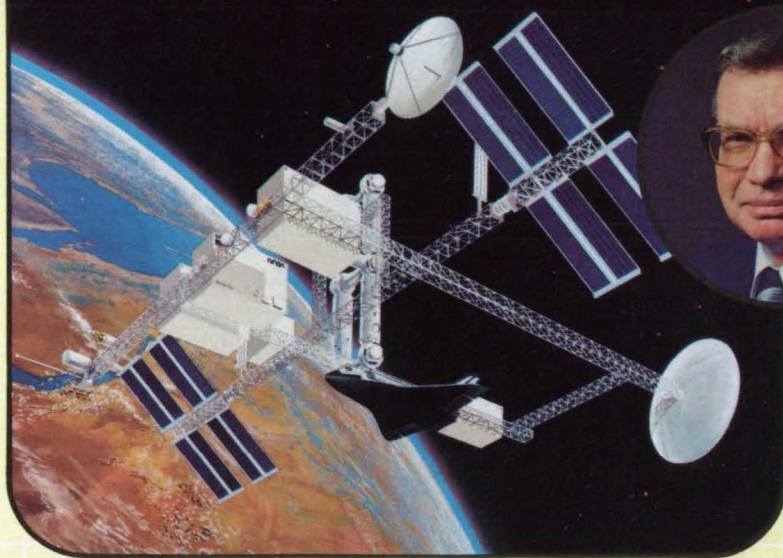
Pershing II Transporter/launcher

Pershing II, with its mobile erector/launcher, inertial guidance system and all-weather terminally guided re-entry vehicle, provides ground forces with quick-reaction firepower in terrain and climates ranging from arctic to desert.

MARTIN MARIETTA

Martin Marietta Corporation
6801 Rockledge Drive, Bethesda, Maryland 20817, USA

Making sure it works



"We provide the engineering and management assistance required for successful space operations. With 6,000 employees worldwide, we comprise a large experience base for aerospace engineering and operations, from system concept and design through integration, test, launch, and mission support."

Harry Clark
Space Operations Manager

The Space Transportation System must! Vitro Aerospace Systems Engineering

This Vitro experience accounts for much of our success in helping NASA meet the complex demands of the space transportation system and space station.

The Vitro staff has the experience, knowledge, skill, and familiarity with space systems hardware, software, management, and operations to provide effective overall program integration. Their aerospace engineering, management, and operations experience includes commercial and government space launch vehicles, payloads, and launch and mission operations systems and facilities.

In addition to expertise in aerospace engineering, management, and operations, Vitro has developed a comprehensive array of supporting technical skills. These include software development, maintenance and maintainability planning, information management, and logistic support.

Vitro meets mission requirements on time and within budget. We stand ready to meet your aerospace needs with our experience, teamwork, flexibility, and rapid response. . .to continue a tradition of engineering excellence.

Vitro *Turning Today's
Technologies
Into Tomorrow's Systems*
CORPORATION

14000 Georgia Avenue, Silver Spring, Maryland 20910
For information call our Marketing Manager, (301) 231-1300

A Unit of the Penn Central Federal Systems Company
Circle Reader Action No. 394

Special Features and Departments

10 Editorial Notebook

**National Space Technology
Laboratories: High-Tech**

12 Mecca in the Deep South

157 Framework for Action (III)

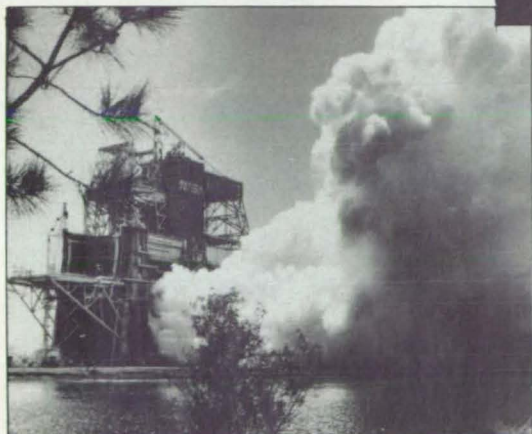
162 Letters

Advertising

163 Index

164 About This Publication

165 Mission Accomplished



NASA's National Space Technology Laboratories, near Bay St. Louis, Mississippi, is the test site for the space shuttle's main engines. In addition to NASA, 17 other federal agencies are in residence at NSTL . . . page 12.



Remote sensing technology is being applied in disciplines as diverse as geology and pathology. The medical application is currently being advanced by an applications engineering project linking radiologists from Washington

University Medical Center, St. Louis, Missouri, and NASA scientists at NSTL . . . page 165.



This computer-generated image served as a point of departure for archeologists studying Poverty Point, LA . . . page 12.

This document was prepared under the sponsorship of the National Aeronautics and Space Administration. Neither Associated Business Publications, Inc., nor anyone acting on behalf of Associated Business Publications, Inc., nor the United States Government nor any person acting on behalf of the United States Government assumes any liability resulting from the use of the information contained in this document, or warrants that such use will be free from privately owned rights. The U.S. Government does not endorse any commercial product, process, or activity identified in this publication.

NASA Tech Briefs, ISSN 0145-319X, copyright © 1986 in U.S., is published bi-monthly by Associated Business Publications, Inc., 41 E. 42nd St., New York, NY 10017-5391. The copyrighted information does not include the individual Tech Briefs which are supplied by NASA. Editorial, sales, production and circulation offices at 41 E. 42nd Street, New York, NY 10017-5391. Subscriptions for non-qualified subscribers in the U.S., Panama Canal Zone, and Puerto Rico, \$50.00 for 1 year; \$100.00 for 2 years; \$150 for 3 years. Single copies \$15.00. Remit by check, draft, postal or express orders. Other remittances at sender's risk. Address all communications for subscriptions or circulation to NASA Tech Briefs, 41 E. 42nd Street, New York, NY 10017-5391. Application to mail at second-class postage rates is pending at New York, NY 10017 and additional mailing offices.

POSTMASTER: please send address changes to NASA Tech Briefs, 41 E. 42nd Street, Suite 921, New York, NY 10017-5391.

Technical Section Thumb Index

28 NASA TV Services

22 New Product Ideas

30 Electronic Components and Circuits

44 Electronic Systems

54 Physical Sciences

62 Materials

74 Computer Programs

92 Mechanics

106 Machinery

128 Fabrication Technology

146 Mathematics and Information Sciences

152 Life Sciences

154 Subject Index

**Thumb Index
Technical Section**

The story behind IBM's new 32-bit RISC PCs.

These aren't your ordinary workstations.

For IBM RT Personal Computers—6150 and 6151—are built around a revolutionary 32-bit, virtual memory, RISC-based microprocessor. Developed and manufactured by IBM.

The significance? Far faster throughput. Because RISC (for Reduced Instruction Set Computer) architecture eliminates many of the unnecessary bells and whistles found in conventional chip design.

What's more, an IBM RT PC can directly address up to four megabytes (Mb) of real memory, over a trillion bytes of virtual memory and up to 210 Mb of DASD, or disk storage.

All of which makes IBM RT PC microprocessors particularly well suited for the total application requirements of technical professionals working in engineering, scientific, industrial and academic environments.

CADAM® and CIEDS¹ Software

One of the key programs available for the IBM RT PC—attached to the IBM 5080 Graphics System—is Professional CADAM. And it's compatible with established host-based CADAM.

There's also Computer-Integrated Electrical Design Series (CIEDS), which allows for the schematic capture of integrated circuit designs.

And there is a growing list of applications available from software companies in the following fields: mechanical and electrical CAD/CAM, petroleum production, artificial intelligence, software engineering, project management and graphics.

UNIX² System V

The primary operating system is derived from the UNIX System V—with some very important enhancements added by IBM. These enhancements make this operating system—Advanced Interactive Executive or AIX³—much easier to use, give it improved performance and reliability, and also add a virtual storage capability.

This operating system gives you multi-user and multi-tasking operations for up to eight concurrent local or remote users working on low-cost ASCII

terminals such as the IBM 3161.

There is also a full-function IBM SQL/RT relational data base management facility available.

Understands Many Languages

The IBM RT PCs are highly literate. You'll be able to write and run applications in C, Fortran 77, BASIC, PASCAL and Assembler.

And as for general-purpose applications, you'll be able to run UNIRAS⁴ (for engineering and business graphics), RS/1⁵ (for data analysis and graphing functions), IMSL⁶ (a library of Fortran subroutines), Interleaf's Workstation Publishing Software,⁷ Solomon III⁸ (for accounting), SAMNA+⁹ (for spreadsheet and word processing) and Applix IA¹⁰ (for integrated office functions).

PC Compatible

The IBM RT PCs can incorporate as an optional feature an Intel 80286 coprocessor (in effect a PC AT on-a-board) that runs concurrently with the 32-bit RISC processor. That means the RT PCs can support many existing IBM PC applications and the interchange of their related data. It also means the RT PC I/O bus can accept standard PC cards.

Contact your IBM marketing representative. Or call 1 800 IBM-2468, Ext. CZ/710, for participating Authorized Dealers, or for free literature. Software companies interested in writing programs for the IBM RT PC should call 1 203 783-7141.



The IBM RT PC 6150 Model 20
Floor-standing unit

IBM	5/86
DRM, Dept. CZ/710	
101 Paragon Drive, Montvale, NJ 07645	
<input type="checkbox"/> Please send me information on the IBM RT PCs.	
<input type="checkbox"/> Please have an IBM marketing representative call me.	
Name _____	Title _____
Company _____	
Address _____	
City _____	State _____ Zip _____
Phone _____	



**The IBM RT PC 6151 Model 10
Desk-top unit**

CADAM® is a registered trademark of CADAM INC. 1. CIEDS is a trademark of the International Business Machines Corp. 2. UNIX is a trademark of AT&T Laboratories. 3. AIX is a trademark of the International Business Machines Corp. 4. UNIRAS is a trademark of UNIRAS Incorporated. 5. RS/1 is a trademark of Bolt, Beranek and Newman, Inc. 6. IMSL is a trademark of IMSL, Incorporated. 7. Workstation Publishing Software and Interleaf are trademarks of Interleaf, Inc. 8. SOLOMON III is a trademark of TLB Incorporated. 9. SAMNA+ is a trademark of SAMNA Corporation. 10. Applix IA is a trademark of Applix, Incorporated.

Circle Reader Action No. 325

ENHANCE YOUR PRODUCT RELIABILITY!

Manufacturers nationwide rely on the high quality and timely delivery of Aurora Bearing Company products. Select from a complete family of general purpose, economy, extra strength and heavy-duty rod ends to 2" bore size. Quality 1-piece race, swaged construction, precision ground balls for maximum trouble-free performance. Aurora Bearing, THE MOTION TRANSFER SPECIALISTS, will customize units to your special materials and linkage requirements.

Aurora Bearing is an OEM supplier of rod ends and special linkages to the following industries:

- HEAVY TRUCKING & TRANSPORTATION
- PRINTING EQUIPMENT
- AUTOMATION & PACKAGING MACHINERY
- AIRCRAFT—AEROSPACE
- OFF-HIGHWAY CONSTRUCTION EQUIPMENT
- FARM MACHINERY AND EQUIPMENT
- RACING CARS OF ALL TYPES
- AND MANY MORE...

Let Aurora Bearing apply its manufacturing, application, and design expertise to your needs. Call or write today for technical assistance, price and delivery on your rod end and special linkage applications.

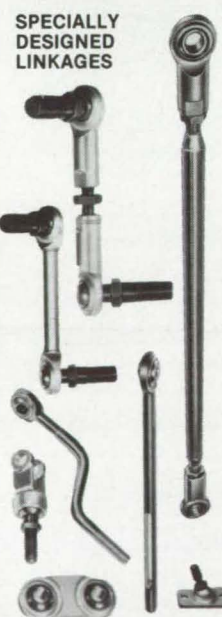


**WRITE FOR
CURRENT
CATALOG**

**TELEX: 280079 AUR BRGS
THE MOTION-TRANSFER SPECIALISTS**

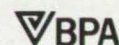


AURORA BEARING COMPANY
970 South Lake Street
Aurora, IL 60506 • Phone (312) 859-2030



NASA Tech Briefs

National Aeronautics and
Space Administration



NASA Tech Briefs:

Published by **Associated Business Publications**
Editor-in-Chief/Publisher **Bill Schnirring**
Managing Editor **R.J. Laer**
Associate Editor **Judith Mann**
Assistant Editor **Elena Nacanthier**
Technical Advisor **Dr. Robert E. Waterman**
Art Director **Melanie Gottlieb**
Assistant Art Director **Michelle Schmitz**
Production Manager **Rita Nothaft**
Traffic Manager **Joe Pramberger**
Circulation Manager **Anita Weissman**
Fulfillment Manager **Elizabeth Kuzio**
Controller **Neil B. Rose**

Technical Staff:

Briefs prepared for National Aeronautics and Space Administration by **Logical Technical Services Corp.**, NY, NY
Technical Editor **Jay Kirschenbaum**
Art Director **Ernest Gillespie**
Managing Editor **Ted Selinsky**
Administrator **Elizabeth Teixeira**
Chief Copy Editor **Pamela Touboul**
Staff Editors **James Boyd, Theron Cole, Jr., Larry Grunberger, Jordan Randjelovich, George Watson**
Graphics **Luis Martinez, Huburn Proffitt, Joe Renzler**
Editorial & Production **Lorne Bullen, Leonard Dalfino, Bill Little, Frank Ponce, Ivonne Valdes,**

NASA:

NASA Tech Briefs are provided by the National Aeronautics and Space Administration, Technology Transfer Division, Washington, DC:
Acting Administrator **Dr. William R. Graham**
Assistant Administrator for Commercial Programs **Isaac T. Gillam IV**
Acting Director Technology Utilization Division **Henry J. Clarks**
Publications Manager **Leonard A. Ault**

Associated Business Publications

**41 East 42nd Street, Suite 921
New York, NY 10017-5391
(212) 490-3999**

President **Bill Schnirring**
Executive Vice President **Frank Nothaft**
Vice President—Sales **Wayne Pierce**
Vice President **Patricia Neri**

Advertising:

New York Office: (212) 490-3999

Vice President—Sales **Wayne Pierce**
Sales Manager **Robin DuCharme**
Account Executive **Dick Soule**
Advertising Assistant **Erving Dockery, Jr.**

Chicago Office: (312) 848-8144

Account Executive **Irene Froehlich**

Los Angeles Office: (213) 477-5866

Account Executive **Robert Bruder**

The Normalization Pairing



The Normalization Pairing

A scientist at the General Motors Research Laboratories has developed a new method for accurately determining the effectiveness of safety belts in preventing traffic fatalities. The approach may be used to answer a wide variety of questions using data bases that lack conventional measures of exposure.

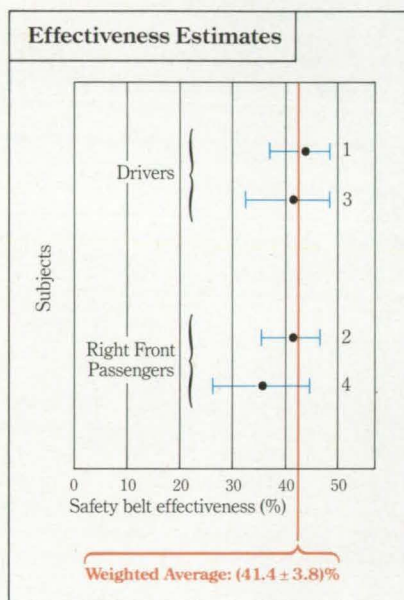


Figure 1: Weighted estimates of safety-belt effectiveness by subject, with standard error. Estimate 1 pairs subjects with right-front passengers; 2 pairs subjects with drivers; 3 and 4 pair subjects with occupants of all other seating positions.

Figure 2: Schematic representation of a sample double-pair comparison.

THERE IS A serious problem that researchers often encounter when trying to analyze large collections of information. It is the problem of measuring exposure. Though a collection of data may contain a large number of cases, and though the facts in each case may be highly detailed, there may be no way of comparing events selected for inclusion in the collection against the normal occurrence of similar events in the world at large.

One such data base is the Fatal Accident Reporting System (FARS) maintained by the U.S. Department of Transportation's National Highway Traffic Safety Administration. FARS details all fatal accidents in the U.S. since January 1, 1975—more than 300,000 crashes. However, it lacks an explicit measure of exposure.

FARS contains, for example, the number of fatalities classified by safety belt use. But fatalities among users depend on two considerations: first, the effectiveness of safety belts; and second, the crash involvement

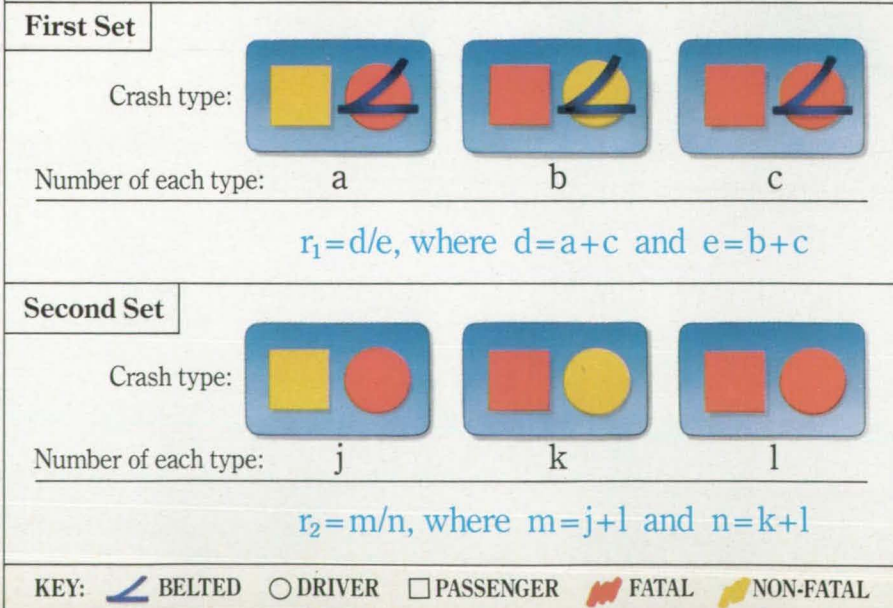
differences between users and non-users—that is, the exposure of belt users to crash involvement. If crash involvement were independent of belt use, it would be a simple matter to calculate the effectiveness of safety belts in preventing fatalities. However, belted drivers have fewer crashes, and the crashes they do have tend to be of lower average severity than those of unbelted drivers.

Now a scientist at the General Motors Research Laboratories has developed an approach to drawing inferences from FARS using only the information contained in the file. Dr. Leonard Evans has designed a method for comparing the effects of isolated characteristics by using two sets of crashes. In each set, a *subject* occupant is paired with an *other* occupant. In the first set, the subject exhibits the characteristic to be studied; in the second, the subject does not. The *other* occupant is chosen to have similar characteristics in both sets of crashes (e.g. always unbelted), and thereby acts as a measure of exposure.

To illustrate the workings of the method of double-pair comparison, Dr. Evans first applied it to a study of the effects of safety belt use on fatality risk. He could define the effectiveness of safety belts in terms of the ratio:

$$R_{\text{true}} = \frac{N_b}{N_u} = \frac{N' \int q_{D,b}(s)f_u(s)ds}{N' \int q_{D,u}(s)f_u(s)ds}$$

where N' is the number of crashes per year by unbelted drivers, s is crash severity, $f_u(s)$ is the probability that a crash involving an unbelted driver has a severity s , $q_{D,u}(s)$ is the probability that an unbelted driver will become a fatality in a crash of severity s , and $q_{D,b}(s)$ is the probability that a belted driver will become a fatality in a crash of severity s . R_{true} is a ratio of new to



old fatalities—assuming a formerly unbelted population became a belted population, with nothing else changing. But while N_u , the number of unbelted driver fatalities, can be determined from the FARS data, N_b , the number of these who would still have been fatalities had they been wearing safety belts, clearly is not coded in the data base.

Dr. Evans applied the double-pair comparison method to determine a quantity, R , that would, under plausible assumptions, accurately estimate R_{true} . Figure 2 shows the pattern of the first application. In it, one set of crashes paired belted drivers and accompanying unbelted front-seat passengers, generating a ratio, r_1 , of belted driver fatalities per unbelted passenger fatality. The second set paired unbelted drivers with unbelted front-seat passengers, leading to a ratio, r_2 , of unbelted driver fatalities per unbelted passenger fatality. This yields a value of $R = r_1/r_2$ as a measure of safety-belt effectiveness.

IN ADDITION to calculating R for driver *subjects* using front-seat passenger *others*, effectiveness was also calculated for right-front passenger *subjects* using driver *others*. Additional calculations were made pairing driver or right-front passenger *subjects* with passengers in any other seating position. Figure 1 reflects the synthesis of these estimates. Estimates 1 and 2 represent *subject* and *other* occupants disaggregated into three age categories and averaged. Estimates 3 and 4 represent pairings of *subjects* with occupants in other seating positions and averaged.

In all, Dr. Evans calculated 46 estimates of R . The weighted average of these gives a safety-belt effectiveness of $(41.4 \pm 3.8)\%$. This should be an accurate estimate whenever the

distribution of severities is the same for both sets of crashes in each double-pair comparison.

Moreover, a formal analysis showed r_1/r_2 to be an accurate estimate of R_{true} under much less stringent restrictions. Even when the distributions of crash severity differ for belted and unbelted drivers, Dr. Evans concluded that the simple ratio $R = r_1/r_2 = nd/me$ is indeed an accurate estimate of safety-belt effectiveness.

Dr. Evans' confidence in the method rests on some key assumptions. But, as he points out: "One of the beauties of the method is its ability to remove the biasing effects of confounding interactions that may undermine those assumptions. It is necessary only to disaggregate occupants into different categories of the suspect variable.

"Because of bias elimination, and the ability to create a measure of exposure, the method of double-pair comparison lends itself to a broad range of investigations. We can estimate, for example, fatality risk as a function of helmet use by motorcyclists, or safety-belt effectiveness in different accident types. More broadly, we can estimate fatality risk as a function of age, sex, or alcohol use. We may even have revealed a trend in trauma response, in general, as a function of sex and age."

General Motors



THE MAN BEHIND THE WORK



Dr. Leonard Evans is a Senior Staff Research Scientist in the Operating Systems Research Department at the General Motors Research Laboratories.

He received his undergraduate degree in physics from The Queen's University of Belfast, and holds a D. Phil. in the same discipline from Oxford University. He was a Post-Doctorate Fellow at the National Research Council of Canada in Ottawa.

Since joining GM in 1967, Dr. Evans has published research on such diverse topics as atomic physics and trauma analyses. His current area of concentration is traffic safety research.

He is a member of the Human Factors Society and is a Past President of the Society's Southeastern Michigan Chapter. In 1985, Dr. Evans received the Society's A. R. Lauer Award "for outstanding contributions to the human factors aspects of highway safety."

Editorial Notebook

Getting the Word Out

Every so often I get the feeling that this column resembles the form letters I sometimes receive at Christmas from well-intentioned friends. I like hearing from them, but I'd like it better if I got some personal communication.

So when I tell all of you that those of us associated with *Tech Briefs* like hearing from you via the feedback cards, I feel I ought to be sending more personal responses. Considering the amount of feedback we receive, this just isn't possible. Still, I think it's important for me to note that I read every single card.

Closing the loop on my analogy, thank you all for your responses, and please keep them coming. We appreciate your ideas for new approaches, and the positive and negative criticism. We're gratified that the positive-to-negative ratio is 99-to-1.

Some of the feedback cards we receive note the use of NASA-derived technology.

We like to follow up on these for possible inclusion in *Spinoff*, an annual NASA publication designed to tell the public about products and services that have come about because of, or been enhanced by, NASA's ongoing technology transfer efforts. Sometimes we find that people are a little nervous about having used the NASA technology they've read about in *Tech Briefs*. This shouldn't be. The reason we publish *Tech Briefs* is to get the technology used. If a given invention or process needs a license, it says so in the brief. If it doesn't, use it.

The benefits of being published in *Spinoff* sometimes go beyond the realm of education into the cold, crass world of cash. What brings this to mind is the EcoSphere® a technology transfer first published in *Spinoff* and republished in "Mission Accomplished" in the last issue of *Tech Briefs*. As we reported, Engineer-



ing and Research Associates of Tucson, Ariz., has sold some 4,000 EcoSpheres as a sideline, and last issue's republication brought about a rash of new inquiries.

It could happen to you and your company... if you let us know what you've done. □

Eric Schaeffer

**FOR TURBINE TESTING,
PSI BLOWS THE
COMPETITION AWAY.**

Our 780B pressure scanning system gives you speed, accuracy and reliability that are unmatched in the industry.

You get faster data acquisition rates, improved accuracy and repeatable results. Along with computer compatibility (IEEE-488) to interface with almost any system.

Help your testing productivity really take off. Call or write today for more information on the 780B from PSI...the leaders in digital pressure measurement technology.

- 20,000 measurements per second
- $\pm 0.1\%$ FS worst case inaccuracy
- ± 1.0 psid to 500 psid ranges
- Automatic on-line calibration
- Direct computer interfacing

PSI PRESSURE SYSTEMS

34 Research Drive, Hampton, VA 23666
804/865-1243

Product/Research Developments®

Third of a series

General

3M's commitment to innovation has been responsible for the more than 40,000 3M products that help you get jobs done faster, easier, and more efficiently.

Because new products are constantly being developed, we began this series to make you aware that there *may* be an easier way to do a job that you are responsible for.

To make procurement even easier, two years ago 3M set up the Federal Systems Department to meet the special needs and requirements of the U.S. Government.

We're here to prove that "3M hears you" is more than just a slogan.

Super fiber

Nextel™ 312 and 440 Ceramic Fiber Products offer performance far beyond the useful limits of other high-temperature textiles such as glass, asbestos, fused silica, and leached silica.

Nextel 312 and 440 are transparent, smooth, non-asbestos, continuous polycrystalline metal oxide fibers which retain strength and flexibility at continuous temperatures to 2200°F and 2500°F, respectively.

Available in braided sleeveings, sewing threads, woven tape, and woven fabrics, all *Nextel* products are designed to meet the toughest thermal and electrical requirements.

In addition to *Nextel* fibers, 3M has developed several other ceramic fiber compositions for different high-temperature applications. Call us at the number below to discuss finding the fiber to fit *your* specific design requirements.

Static-free videocassettes

As the signal-carrying area for videotape has grown smaller and smaller, the amount of "dropout" that a single speck can cause has increased. Today, a smoke or dust particle, human hair, or fingerprint can be disastrous.

Because static electricity attracts dust and debris, 3M ¾" Master Broadcast (*MBR*™) videocassettes and 3M ½" Broadcast videocassettes receive a special *Anti-Stat*™ System treatment that virtually eliminates static buildup and therefore minimizes resulting dropouts.

3M videocassettes also register the most desirable combination of color noise and signal-to-noise ratios among leading competitors and feature a dimensionally stabilized polyester backing to withstand environmental extremes.

(Contract number: GSOOK86AGSO214)

Recycle oil

Messy clay granules pick up their own weight in oil at best. Rags are not much better. But one compact roll of 3M Brand Oil Sorbent does the work of 700 pounds of granules — soaking from 13 to 25 times its weight in oil.

Available in rolls, sheets, pillows, and particulate, Oil Sorbent eliminates oil and hazardous liquids from both wet and dry environments. In sumps and ponds, it removes the oil, leaves the water, and can be left in the water for months without sinking or deteriorating.

A big plus is that Oil Sorbent can be wrung out, reused, and the oil reclaimed. Please follow local regulations for disposal.

(Contract number: GS-OOF-79538)

Conclusion

When you deal with 3M, you get more than just the scientific, research, manufacturing, and distribution capabilities behind 40,000 diverse products. You also get 3M's ironclad commitment to *service*.

3M has expert service technicians available anywhere in the U.S. and in more than 50 other countries. Our services include a toll-free hotline operating 24 hours a day, 365 days a year. We also provide third party service (*TPS*) support to owners of all types of office, personal computer, and data communications equipment. This fast, dependable, efficient service utilizes the latest technology — like remote diagnostics — while still giving you immediate, personal attention.

3M's *TPS* can eliminate the need for separate service contracts with several manufacturers. But, more importantly, it is *flexible*: We will listen to your requirements, and respond with service arrangements that will meet those requirements.

For more information about our products or our service arrangements, call 800-328-1684 toll-free (or 800-792-1072 in Minnesota). Descriptive literature will be mailed to you without cost or obligation. Or, if you wish, a 3M representative will call you for an appointment at your convenience to discuss your particular needs.

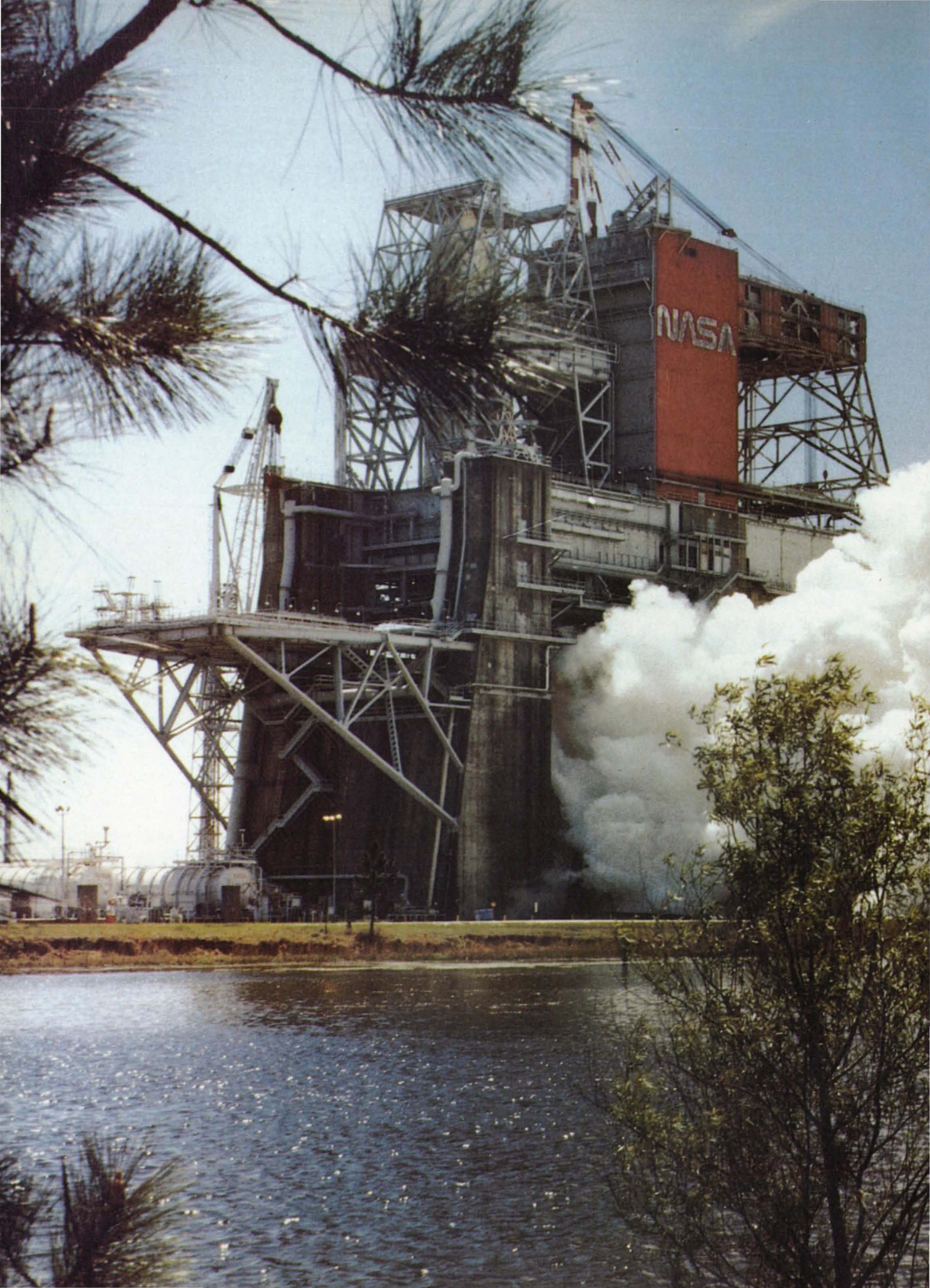
Just call **800-328-1684**

(In Minnesota 800-792-1072)

Note: If you are not already familiar with the distinctive style of office communication created by *Post-it*™ brand notes from 3M, we will be pleased to send you a sample pad while supplies for this special offer last. Just give us a call at the number above.

Nextel, *MBR*, *Anti-Stat*, *Post-it*, and 3M are registered trademarks of 3M.

3M hears you. . .

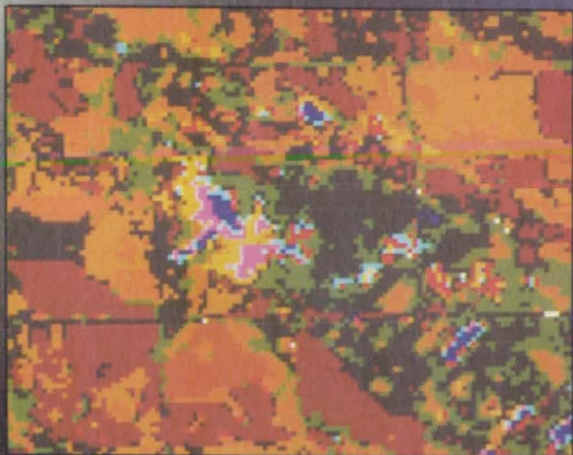


National Space Technology Laboratories:

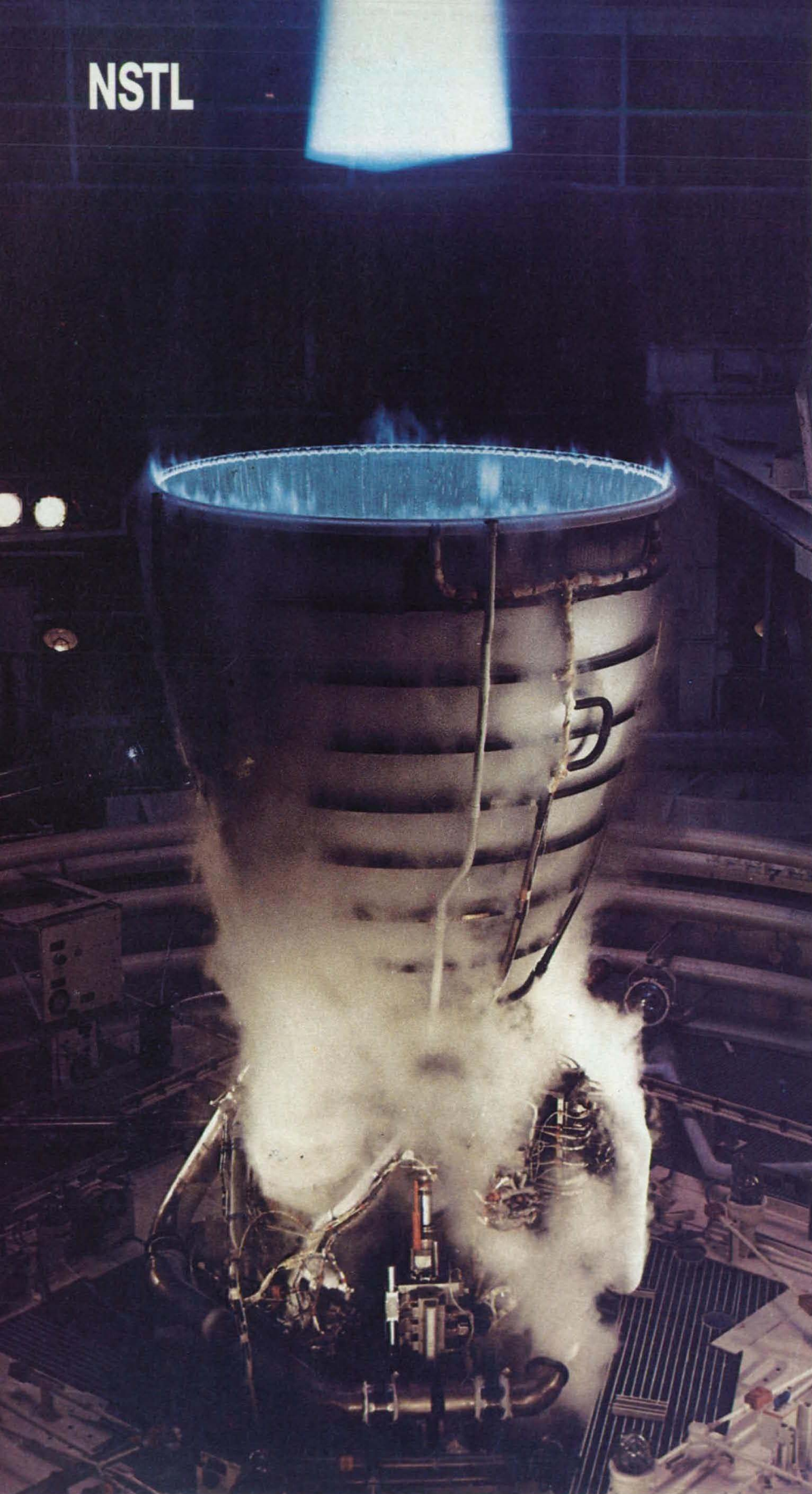
High-Tech Mecca In The Deep South

From the Civil War to the civil rights era, Mississippi has played an important role in shaping the political history of this nation. On the cultural horizon, many a bright star has risen out of Mississippi, among them the singers Elvis Presley and Leontyne Price, and the award-winning writers William Faulkner, Tennessee Williams and Eudora Welty. Still Mississippi has a reputation as a rural, agrarian, poor and—in a word—backward kind of place. Few of us would think to look there when trolling for high technology.

To find high technology anywhere, you have to know where to look. In Mississippi, the place to start is along the Gulf Coast, in southeastern Hancock County near Bay St. Louis, at NASA's National Space Technology Laboratories. ►



Against the backdrop of a shuttle main engine test firing are four images generated from remotely-sensed data at NSTL's Earth Resources Laboratory. Top to bottom they are: A thematic map of Poverty Point, Louisiana, showing a subterranean system of archeological interest. The 400-acre site may date back to 1800 B.C., making it one of the oldest sites in the Americas; A satellite view of the Mississippi Gulf Coast; A thematic map of Arrow Point, Manitoba, that delineates land cover categories for use in surveying waterfowl nesting habitats; Before- and after-eruption images of Mount St. Helens generated from digital terrain data.



A single shuttle main engine undergoes test firing at NSTL. The engines are tested singly and in the three-engine cluster that, along with two solid rocket boosters, powers the shuttle during its 8½-minute flight to low-earth orbit.

NASA's presence in Mississippi dates back to the Apollo era, when the expanding agency acquired a new site for test firing the Saturn V rockets that would boost man to the moon. In the early 1960s, NASA purchased several thousand acres of land adjacent to Mississippi's East Pearl River and negotiated a perpetual easement on an additional 125,000 acres. The extra acreage would provide an acoustical buffer zone to ensure that the tremor-like vibrations and low-frequency roars that accompanied the test firing of the Saturn V would go relatively unnoticed. Even so, one test engineer who worked at the facility during this period recalled conferring with a NASA colleague in Mobile, Alabama, after a test-firing. The colleague was able to pinpoint the time and duration of the test, saying he'd felt the vibrations even though he was 100 miles away. Closer to the Mississippi site, the test engineer added, "You were more likely to feel that the shirt was being shaken right off your back."

While its remote setting was definitely a factor, the southern Mississippi site was also an appropriate choice because it falls within the boundaries of NASA's "space crescent," a geographic area stretching east from Houston to Cape Kennedy and north to Marshall Space Flight Center in Huntsville, Alabama. But finally, the Mississippi site was selected primarily for its proximity to water. Site development involved constructing nearly eight miles of canals to link the Mississippi Test Facility with the East Pearl River. The man-made canal system allowed the huge Saturn V rocket stages to be transported via barges from the Michoud Assembly Facility, near New Orleans, to the test facility. After testing, they were turned around—via the canals, the East Pearl and the Intracoastal Waterway—for launch at Cape Kennedy.

Other site development included the building of three mammoth concrete and steel test stands adjacent to the canals, plus associated test facilities, including a 64 million gallon reservoir, a power generation plant and a large gas pressure complex. Control centers, laboratories and administration and engineering offices were also constructed, along with roads to link the facility with the state's highway system.

When the Mississippi Test Facility became operational in 1966, it had developed into a city unto itself, complete with post office, fire department and hospital. The southern Mississippi metamorphosis that began with the transition of rural, wet, snake-infested farmland into a space-age technological outpost was underway.

An Expanding Focus

Between 1966 and 1970, all the first and second stages of the Saturn V rocket used for the Apollo missions were test fired at the Mississippi Test Facility. When the Apollo era drew to a close in the early '70s, the Mississippi Test Facility entered a tran-

Performance That's Out Of This World.



For Real World Applications.

Performance—Mainframe, multi-user performance in an office-compatible package. That's what Celerity Computing's distributed Super-minicomputer Systems bring to you. They redefine the way compute-intensive tasks are accomplished in the engineering design environment.

Real world application software—ANSYS, PATRAN II, NASTRAN, MARC, MENTAT, SINDA, ADAMS, DYNA and others.

Productivity, Economy, Flexibility: Available NOW from Celerity Computing.

CELERITY COMPUTING



Corporate Headquarters: 9692 Via Excelencia, San Diego, CA 92126 (619) 271-9940.

ANSYS, PATRAN, NASTRAN, MARC AND MENTAT, and ADAMS are registered trademarks of SWANSON ANALYSIS SYSTEMS, INC., PDA ENGINEERING, NATIONAL AERONAUTICS AND SPACE ADMINISTRATION, MARC ANALYSIS RESEARCH CORPORATION and MECHANICAL DYNAMICS, INC., respectively.

Circle Reader Action No. 352

In 1992, we set sail for a New World.

In 1492, a Genoese navigator and an intrepid crew crossed uncharted waters in search of a west passage to India. In the process, they uncovered the vast resources of two continents. And they opened up a new base for exploration, progress, and the hopes of mankind.



In 1992, coincident with the 500th anniversary of Columbus's voyage, we plan to set sail for another New World. That year, or shortly thereafter, the United States and the world will begin benefiting from the first manned Space Station. The Station will be more than another giant step for mankind. It will be our stepping stone to living in new realms, and it will result in thousands of discoveries that will benefit earth.

This New World, free from gravity and atmospheric impurity, will provide that ideal environment for experimentation and production that is impossible on earth. Simultaneously we will have a permanent station for scanning the earth and the heavens — an unparalleled vantage point for predicting weather, aiding agriculture, and understanding the universe.

Of course, like Columbus, we cannot foresee all the benefits ahead. But we do know that we will have a new arena in which to conquer disease, transform the materials of earth, and generate precious energy. The resulting knowledge from countless discoveries will come down to earth for our well-being.

But, unlike Columbus, our craft will be in constant contact with the Old World. Harris Aerospace, as a member of the Rockwell, Grumman and Sperry team, is responsible for the Space Station's communications and tracking system. We are totally committed to this great endeavor, and we bring to the challenge the capabilities and experience necessary for success.

Harris has had 27 years of successful involvement with the kind of space communications and tracking required for the manned Space Station. Our space experience includes programs from Telstar to the Tracking and Data Relay Satellite as well as the manned programs of Apollo, Lunar Module, and Space Shuttle. We are also a leader in the architecture and design of large communication networks.

Now Harris is ready for the Space Station. Over the next years and centuries, the scope of scientific, commercial and technological opportunities and breadth of results are sure to exceed our wildest expectations.

For in 1992, we, too, will be very much like Columbus: carrying the sum of our knowledge into the unknown. And, like him, we, too, shall return with the bountiful gifts of a New World.

**HARRIS**

Circle Reader Action No. 410

For your information,



our name is Harris.

NSTL

sitional phase. Before the decade was out, the southern Mississippi site would metamorphose yet again, this time from a single-agency, single-mission test facility into a multi-agency, multi-mission federal laboratory. Highlighting all this was a simple name change. In 1974, the Mississippi Test Facility was renamed the National Space Technology Laboratories (NSTL) and given full NASA field center status.

At about the same time test engineers wrapped up their initial Saturn V assignment, NASA selected the facility to test the space shuttle's main engines and main propulsion system. Since the actual testing would not take place for several years, NASA began searching for ways to keep its \$350 million facility economically and technically viable in the interim. In its characteristically innovative way, NASA succeeded in finding not one, but two solutions.

The first solution was to locate NASA's newly-established Earth Resources Laboratory at NSTL. This enhanced NSTL's technical and scientific base, and obviated the need for new construction or facilities. In 1970, NASA's Earth Resources Laboratory took up residence at NSTL, and research and development of space-related technology for earth observations got underway. Remote sensing and data systems development were designated as the primary research focus of the lab, and an applications program revolving around earth science disciplines—forestry, ecology and geology among them—was instituted alongside the R&D program.

The second solution involved opening the gates of NASA's southern Mississippi "city" to other federal agencies. In exchange for paying part of the cost of maintaining and operating the facility, other federal agencies could take advantage of the site's resources and NASA's support service contracts without incurring any long-term liabilities. NASA, in turn, agreed to act as mayor and city council of NSTL by supplying technical and installation support services to resident agencies.

Federal and state agencies alike took NASA up on its offer, and by the time NSTL had geared up for its primary mission—testing the shuttle main engines and main propulsion system—the Navy, the Army, the Department of Commerce and the Department of Interior, among others, had established offices at NSTL.

Full Steam Ahead

The transitions that occurred at NSTL during the '70s defined the center's agenda for the '80s, pointing up three distinct missions for the facility—space shuttle main engine testing, research and development of remote sensing technology and applications, and acting as a host agency in managing the installation. Activities in all three areas have expanded in recent years. ▶

Building High Technology from the Ground Up

NSTL senior research scientist Dr. B.C. Wolverton will show you a slide of a grazing goat and laughingly say, "NASA—high technology." Although he's laughing, Dr. Wolverton is not kidding. For the past 12 years, he and his associates at NSTL have been applying natural biological processes in solving a variety of environmental problems. The goat represents one harvesting option for NASA's plant-based, wastewater purification program.

The development of this innovative NSTL bio-technology began with the discovery that the roots of the water hyacinth, a vascular aquatic plant common in the South, are ideally suited for removing excess nutrients and organics from over-enriched lakes. Dr. Wolverton first applied the experimental water hyacinth technology in the sewage lagoon at NSTL. Racks of floating water hyacinths were placed in the 40-acre lagoon. The result? The roots of the water hyacinths absorbed the lagoon's excess nutrients, the plants themselves thrived (to the point where they required harvesting—enter the goats), and the lagoon was purified. The success of this original application paved the way for others, among them a wastewater purification system for the city of San Diego, California.

A serious water shortage prompted the city of San Diego to investigate methods of reclaiming potable water from sewage. In 1981 the city built an experimental wastewater purification system based on the NSTL water hyacinth technology. The success of the experimental system, which treated 25,000 gallons of sewage a day, inspired the city to build a one million gallon per day facility in 1984. This new facility combines water hyacinths with a new NSTL-developed reed/rock filtration system, or artificial marsh, for wastewater purification.

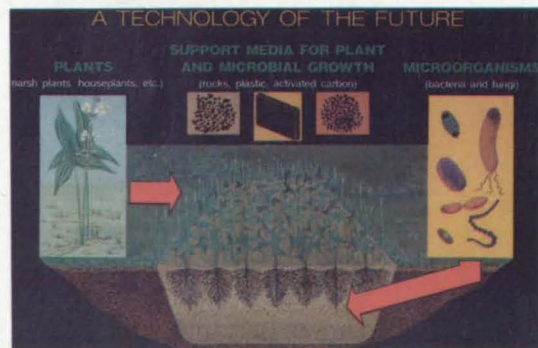
Several southern towns, the New Orleans Nature Center, and Walt Disney World's EPCOT Center also utilize the NSTL plant-based purification systems, either for wastewater treatment or experimental purposes. Individual homeowners can construct artificial marshes in lieu of septic tanks for sewage treatment. Recently, the technology has been applied in removing chemicals and heavy metals from industrial wastewaters, and for purifying the water used in seafood processing.

Another focus of the NSTL environmental research is the problem of indoor air pollution, particularly in buildings which have been sealed for energy efficiency. Again, plants are the basis of the purification system, but in this case, the leaves rather than the roots do the work. Dr. Wolverton and associates determined that, in addition to carbon dioxide, plant leaves will remove harmful gases, such as benzene and formaldehyde, from the indoor environment. By pulling air through a plant-filled greenhouse, homeowners can ensure that their sealed homes are healthful as well as energy-efficient.

The ultimate application for NASA's plant-based purification technology will be the space station. Because it will be a closed system with no direct source of air or water, methods for recycling these elements will be extremely important. But for now and for years to come, this technology promises to be quite useful and beneficial right here on earth. □



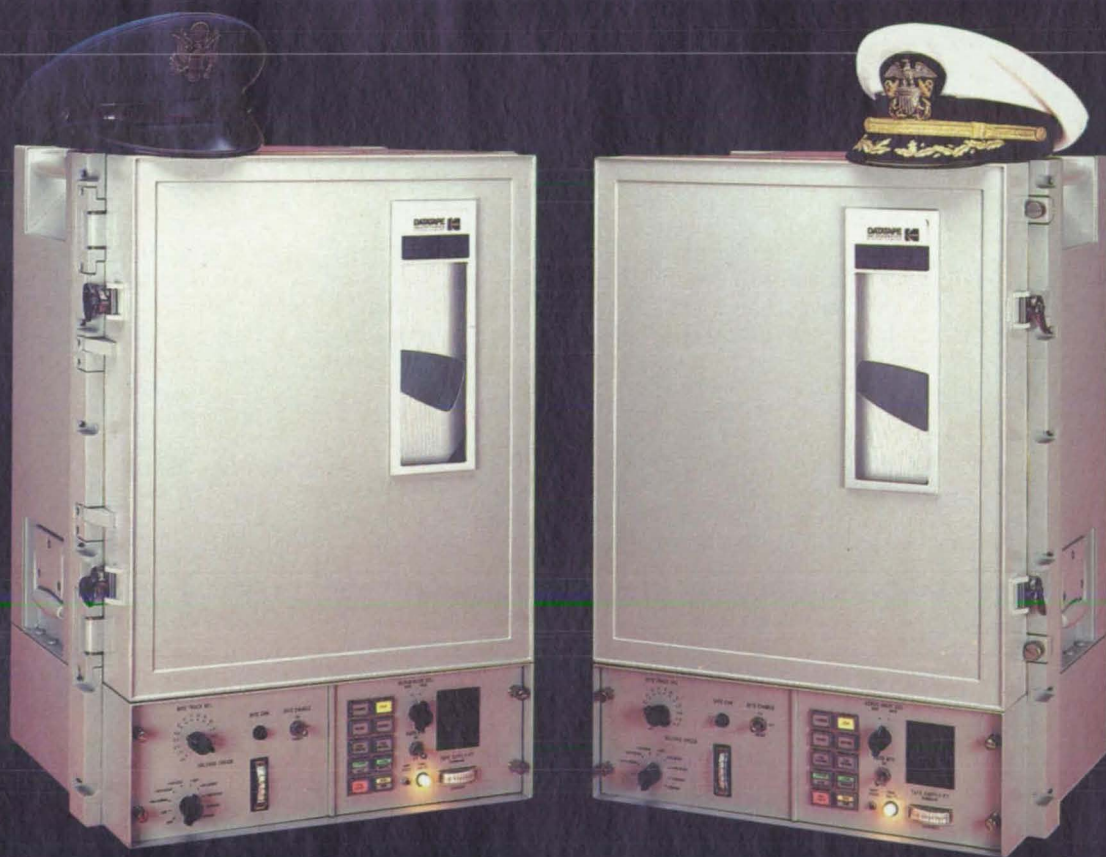
Because it can clog lakes and streams, the prolific water hyacinth was once considered a nuisance. A new bio-technology casts the aquatic plant in a beneficial role.



The NSTL-developed reed/rock filtration system is applicable in colder climates which are inhospitable to the semi-tropical water hyacinth.

TEMPEST APPROVED

The AN/USH-24(V) is here to serve you and your specific recorder requirements. Now add Tempest approved to MIL-E-5400 and MIL STD 16400.



The AN/USH-24(V). The *only* magnetic tape recorder/reproducer system available that is *multi* service approved for airborne, shipboard, and ground hostile environment adds the additional capability of meeting your requirements for Tempest approved equipments.

DATATAPE
INCORPORATED
A KODAK COMPANY



NSTL

so that today NSTL is a fully-utilized, multi-mission facility.

NSTL's primary mission is to provide operational and technical support in the testing of the shuttle main engines and main propulsion system. NASA's Marshall Space Flight Center in Huntsville, Alabama, has design and development responsibilities for the shuttle main engines. A group of Marshall engineers is in residence at NSTL to monitor the tests, which are conducted by the engine private contractor, Rockwell International, Rocketdyne Division. NSTL's responsibility is to provide facilities, properly maintained and properly configured, and any and all technical support services required to test the engines.

In the beginning, this involved modifying one of the test stands to incorporate a simulated orbiter aft section, which holds the shuttle three main engines, and an external fuel tank, which feeds propellants to the engines. The propellants, liquid oxygen and liquid hydrogen, are ferried from New Orleans via NSTL's nine barges and NASA's only tugboat, the Clermont II. The barges store the propellants as well, and they're moored in the canals adjacent to the test stands. During tests, the barges service the test stands' run tanks with fuel as needed.

NSTL's 64 million gallon reservoir is connected to the test stands by pipelines 96 inches in diameter. During test runs, the reservoir supplies 300,000 gallons of water per minute at 200 psi to the stands for cooling. The reservoir also functions as a source of power generation.

Tests on both single shuttle engines and the three-engine cluster that, in conjunction with the solid rocket boosters, powers the shuttle during flight are conducted at NSTL. The initial R&D testing began in 1975, and today the emphasis is on increasing the engine's thrust level to 109%, meaning that each engine will generate 417,300 pounds of thrust at sea-level during liftoff. To date, shuttle engines have been tested for an accumulated 172,000 seconds at NSTL, or the equivalent of 340 launches.

Beyond the initial certification and flight acceptance testing, reacceptance tests are also conducted at NSTL. After an engine reaches the end of its mission life, it is returned to NSTL for reacceptance testing before being sent back to the Cape for reuse.

Unlike the Saturn V rockets that preceded them, the shuttle engines are relatively good neighbors. Although they're nearly as loud, the fuel that powers them produces a nice, clean steam. And while the gargantuan Saturn rocket engines were Cleopatras of a sort, coming and going on barges, the smaller shuttle engines are transported over land by trucks.

"Over land" brings up the second of NSTL's three missions, conducting research and development of remote sen-

sing technology for use here on earth. NSTL's Earth Resources Laboratory applies its efforts in three areas—earth science and applied research and commercialization, with supporting sensor and data systems engineering.

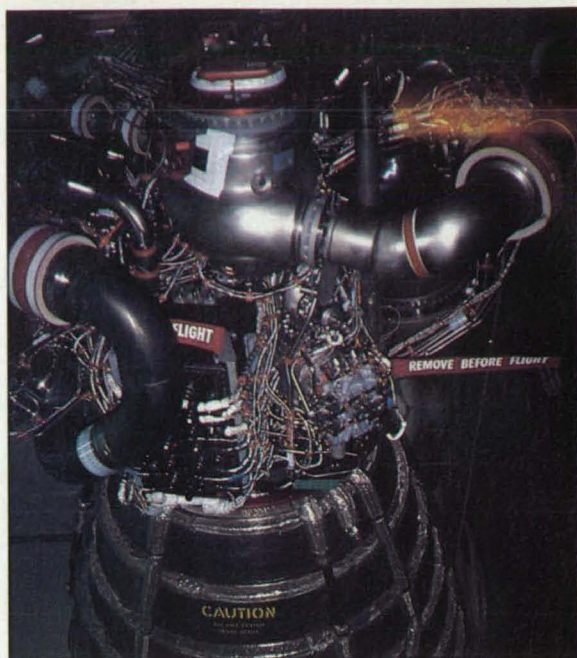
The Earth Resources Laboratory's science program focuses on the physical, biological and chemical processes occurring in tropical forests and aquatic ecosystems. The ERL is working cooperatively with the academic community to form a better understanding of these processes in the role that remote sensing will play in future global monitoring and assessment.

The lab's applied research and commercialization program is working with the private sector and medical community to develop remote sensing techniques for use in earth resources assessments and medical diagnostics.

NSTL's Earth Resources Laboratory is also supporting NASA's space station program, both in terms of finding potential commercial sponsors for earth and ocean observation missions on the space station, and in developing data systems that simulate space station payloads. In the commercialization function, the laboratory is supporting one of NASA's five Centers for the Commercial Development of Space. The Space Remote Sensing Center was established at NSTL earlier this year by Mississippi's Institute for Technology Development. The Center will be developing applied research programs and, with industry, joint research projects that exploit the commercial applications of remote sensing technology, whether in land or resource management, or medical and scientific applications.

The laboratory's data systems engineering group designs and develops ground data processing and analysis systems that handle the massive amounts of data transmitted by remote sensors. The engineering group supports the laboratory's science and applied research and commercialization programs, in addition to developing and managing the entire NSTL automated data processing capability.

Supplying data processing capabilities to the entire facility is one aspect of NSTL's third mission—to manage the installation and provide technical and support services to the site's 17 resident agencies. Another aspect of this mission is the cooperative programs that have grown out of NSTL's unique arrangements with its resident agencies. For example, the Earth Resources Laboratory's data systems engineering group is upgrading the data analysis system that the U.S. Navy uses to guide its fleet of ships. This arrangement



After powering Atlantis on its maiden flight, this shuttle main engine is back at NSTL for recertification tests.

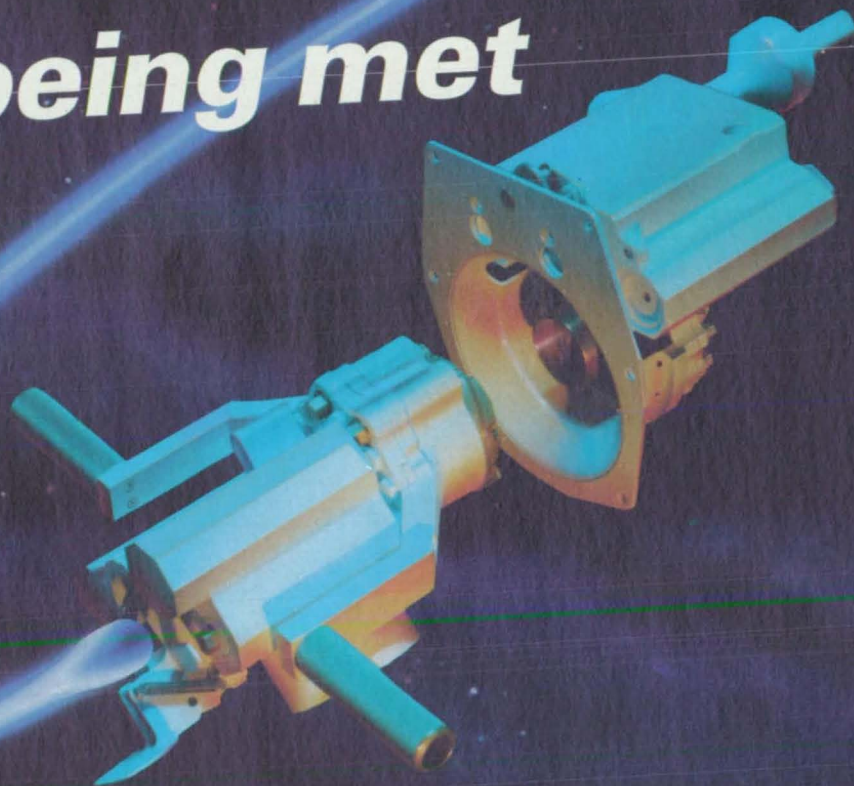
was sparked by the presence of the Navy's Oceanographic Command at NSTL.

This sort of interactive utilization of technology and resources has attracted two state agencies to NSTL. Both Louisiana and Mississippi have established technology transfer offices at NSTL, with the aim of improving the productivity and economic viability of their industries. Mississippi, widely perceived as the poorest state in the nation, has made a substantial commitment to utilizing technology for economic development. In 1985, the state appropriated \$4 million for the construction of a new building at NSTL. When completed, it will house new federal agency personnel and various state agency offices. It is anticipated that the state will profit from its investment by utilizing advanced technology to foster industrial expansion and economic growth.

In the words of Dr. James Miller, director of the Mississippi Technology Transfer Office, "Mississippi is making a concentrated effort to link its economic future to people-based industry," most of which is founded on high technology. Its linkage with NASA is part of a cohesive array of initiatives that will bring Mississippi from the agricultural phase straight into the information age. According to Dr. Miller, the initiatives are designed not to help Mississippi catch up with the rest of the country, but to help it leap ahead.

It's still too early to tell just how well Mississippi's plan will work, especially since its home base, the new NSTL building, is still under construction. But as a point of departure, the far-reaching plan to bolster economic development through high technology sounds promising. Mississippi, it seems, has a lot to look forward to, and the rest of us, well, we may just learn a thing or two from our enigmatically high-tech Southern cousin. □

The challenge of transferring fluids in space is being met



FAIRCHILD CONTROL SYSTEMS DEVELOPED THE STANDARDIZED SPACECRAFT REFUELING COUPLING

Until now, the useful life of a spacecraft has been limited by the quantity of propellant and other consumables on board at launch. At Fairchild today, that's being changed. The first steps toward indefinite spacecraft utility are being taken through the development of the Standardized Refueling Coupling. Under the auspices of the NASA Johnson Space Center, Fairchild is working to make spacecraft serviceability a reality. The Standardized Refueling

Coupling will allow payloads like TRW's Gamma Ray Observatory to be resupplied with hydrazine in orbit. Designed to be safe for manual servicing, the Standardized Refueling Coupling is easily adapted to automated operation. If your future involves serviceable spacecraft, contact Fairchild Control Systems Company to learn how the Standardized Refueling Coupling can make the future happen.



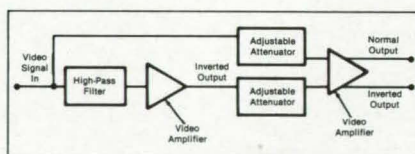
FAIRCHILD
CONTROL SYSTEMS COMPANY

Fairchild Control Systems Company
1800 Rosecrans Avenue
Manhattan Beach, California 90266
Tel: (213) 643-9222
Telex: 910-325-6216

New Product Ideas are just a few of the many innovations described in this issue of *NASA Tech Briefs* and having promising commercial applications. Each is discussed further on the referenced page in the appropriate section in this issue. If you are interested in developing a product from these or other NASA innovations, you can receive further technical information by requesting the TSP referenced at the end of the full-length article or by writing the Technology Utilization Office of the sponsoring NASA center (see page 29). NASA's patent-licensing program to encourage commercial development is described on page 29.

Analog Video Image-Enhancing Device

A real-time analog video image-enhancing device improves the appearance of technical photographs by selectively compressing their overall dynamic ranges while accentuating edges or small details of greatest interest. The system includes a video camera connected to a video monitor to which a circuit (see figure) is added for analog video enhancement. The video signal is high-pass filtered, amplified, and then added in a second video amplifier to the unfiltered signal; the sum is sent back to the monitor. Black-and-white reversal is possible in the second amplifier, allowing negatives as well as prints to be examined directly. Adjustments of the new image parameters along with the conventional variability of monitor brightness and contrast allows a wide range of image enhancement. In addition, the time constant on the high-pass filter results in a pseudo-three-dimensional effect, which sometimes shows detail more clearly. (See page 46.)



Measuring Thicknesses of Coatings on Metals

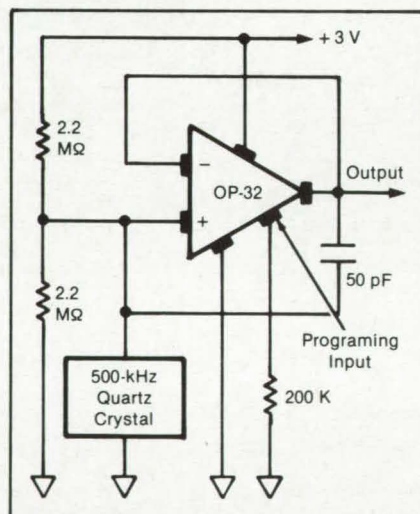
Using laser-beam reflections and eddy-current sensing, an instrument measures the thicknesses of nonconductive coatings on metal substrates; the eddy-current sensor maintains a reflected-light triangulation sensor at a fixed distance from the surface of the substrate as the substrate moves under it, while the light sensor determines the angle and therefore the perpendicular distance of the laser-beam spot on the coating surface. When the capabilities of available components are fully exploited, the instrument will be able to measure coatings from 0.001 to 6 in. (0.0025 to 15 cm) thick, with an accuracy of 1 part in 4,000. The instrument can readily be incorporated in automatic production and inspection systems; for example, it can be used to inspect thermal insulation layers, paint, protective coatings, or to control the application of coatings to preset thicknesses.

(See page 94.)

Temperature-Sensitive Oscillator

A quartz-crystal oscillator—the frequency of which depends on its temperature—serves as a small, inexpensive, low-power, temperature-sensing circuit that can be used as an ingestible thermometer for measuring internal body temperature. Because the circuit does not depend on any temperature sensitivity of the crystal itself, readily-available, inexpensive crystals can be used. The circuit also avoids the linearity and stability problems of thermistor-based temperature-sensing circuits. The oscillator operates at about 500 kHz, a frequency that is readily transmitted through the body. With the component values shown in the figure (OP-32 is a high-gain, programmable operational amplifier), the change of capacitance with temperature causes the oscillator frequency to increase linearly, at about 4 Hz per °C, over the temperature range of 30 to 40 °C.

(See page 39.)



Lightweight Ceramic Insulation

Prepared by a process of sacrificial burnout, a rigid ceramic insulation having a low density of 2 to 6 lb/ft³ (32 to 96 kg/m³) can replace flexible insulation in applications where low weight is essential. Unlike the loose fibers or blankets of flexible insulation, the new insulation does not pack together or shift. It is thermally stable, and its flexural strength of 25 to 75 lb/in.² (170 to 500 kN/m²) enables it to retain its shape under light loading. The rigid insulation can be machined to the requisite shape and bonded.

(See page 65.)

A REPAIR SHOP LIKE NO PLACE ON EARTH.

In low orbits around the Earth, satellites gather, analyze and transmit critical information—for scientists, for corporations, for countries.

Because of the high cost of getting them up there in the first place, some of these satellites are designed to be repaired where they are if something goes wrong.

A manned space station could act as the neighborhood garage—the local spare parts and repair facility for these valuable satellites. That's one reason why

McDonnell Douglas is working to put a space station in orbit by the 1990s.

Since 1960, when we did the first Manned Orbiting Research Laboratory studies, we've been a world leader in space systems. We built the original space station—Skylab. And we've been a pioneer in space systems operations, from launches to payload integration.

Now we're devoting our space experience, systems expertise, and technological ingenuity to taking America the next step into

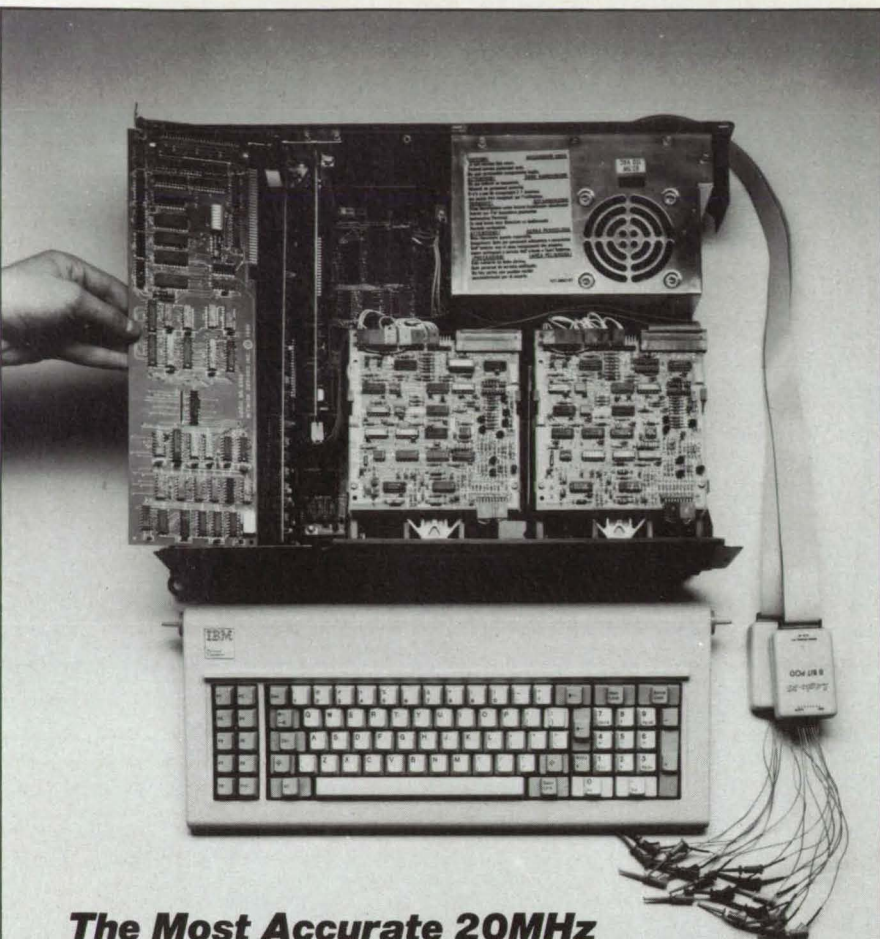
space—with a manned station.

Such a station could lower the cost of technological upkeep—for science, for industry. We think that's a very good reason to build a repair shop like no place on Earth.



MCDONNELL DOUGLAS

Circle Reader Action No. 374



The Most Accurate 20MHz Logic Analyzer Available For Only \$1,495.

Only with the Logic-20™ Only from BitWise Designs

The true criterion of a logic analyzer's accuracy is not its sample speed, but its set-up time — that period of time prior to the clock edge in which it cannot accurately sample data.

With a set-up time of only 2 ns., the Logic-20 from BitWise Designs blows away its nearest 20 MHz competitors — which are totally unreliable for a monstrous 25 ns. before the clock edge.

The Logic-20 is a single IBM PC (or compatible) expansion card, offering 16 channels of 20 MHz sampling with less than one ns. channel-to-channel skew. Optionally, for those with unusually fast sampling speed applications, the Doubler™ pod is available that allows 40 MHz sampling over eight channels.

And because the Logic-20 is an add on to your personal computer, you can have it right on your

desktop when you need it. You can interrupt development at any time to use your PC to write a memo or document your progress, and then go right back to where you left off. All in your office, all right at your desk.

Need to know more about logic analyzer accuracy or the Logic-20?



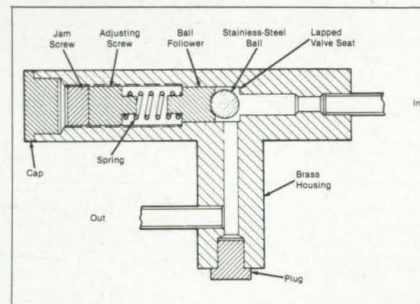
Logic That Makes Sense

1223 PEOPLES AVE.
TROY • NY • 12180
518 • 274 • 0755

IBM and IBM PC are trademarks of International Business Machines Corporation.
Logic-20 is a trademark of BitWise Designs, Inc.

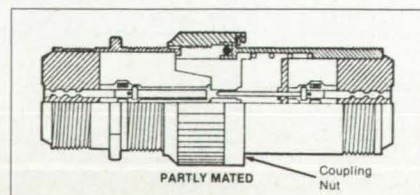
Spring-Loaded Joule-Thomson Valve

A spring-loaded Joule-Thomson (J-T) valve (see figure) permits optimal cooling-power regulation of a helium refrigerator by allowing independent adjustment of the flow rate and pressure drop through the valve. Because the spring-loaded J-T valve maintains a constant pressure drop, an upstream room-temperature throttle valve can adjust the flow rate precisely for any given upstream pressure, even while the helium is flowing. In addition, the new valve is relatively invulnerable to frozen gas contaminants, which can clog fixed-opening J-T valves. (See page 101.)

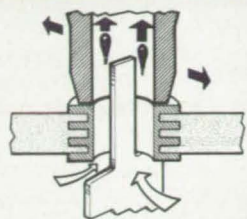


Self-Alining Electrical Connector

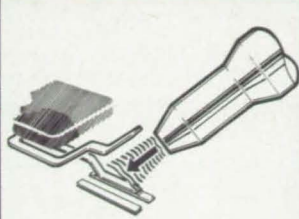
A self-aligning, multipin electrical connector prevents the breaking or bending of male pins that occurs with conventional connectors when misaligned contacts are carelessly pressed together. The new design features tapered insulators that are keyed to mate each other before the male pins touch the female sockets. The contacts mate when the coupling nut draws the aligned plug and socket together, depressing one of the aligning insulators against a spring. The compressed spring applies tension on the mated threads of the assembly, helping the connector resist loosening under vibration or shock. This connector should be particularly useful in locations that are out of sight or difficultly accessed. The design could also be useful in high voltage applications because the mating insulators eliminate air spaces that could otherwise become electrical-leakage pathways. (See page 33.)



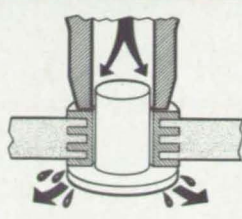
REPAIR PCB'S



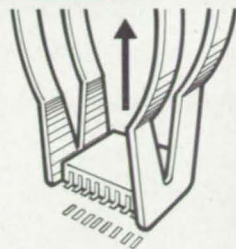
Spike Free
Vacuum Desoldering



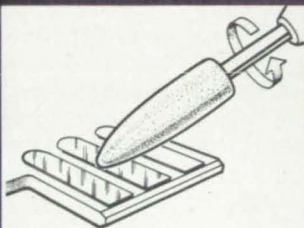
Hot Air Jet
Flat Pack Removal



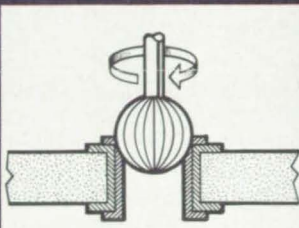
Blind Joint
Pressure Desoldering



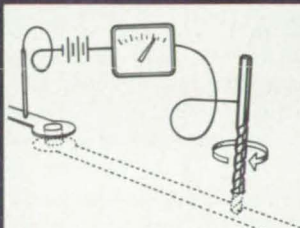
Multi-terminal
Chip Removal



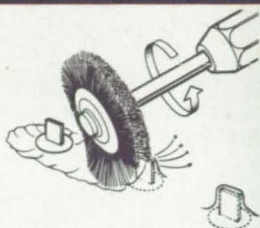
Precision Abrading
Thin Coatings



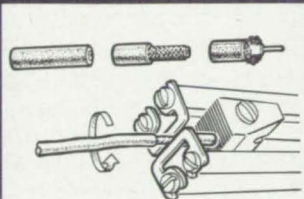
High Torque - Low RPM
Drilling and Milling



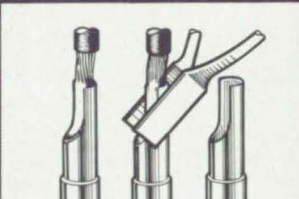
Drilling Test Probe
Spike Free



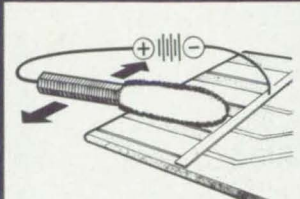
Conforming
Coating Removal



Thermal Stripping
Coax and Teflon



Resistance Soldering
Cup Terminals



Gold Plating
Edge Connectors



Lapflow Soldering
Circuit Repair

The Pace PRC - 151 Repair System Improves Reliability ... Saves Money.

The PRC - 151 repair system gives you full repair capability for any electronic assembly. It performs all the functions shown above, plus many more.

Proven through diverse industrial, military and commercial usage in factory and field. It's the low cost way to high reliability repair. Call or write today for literature and a demonstration.

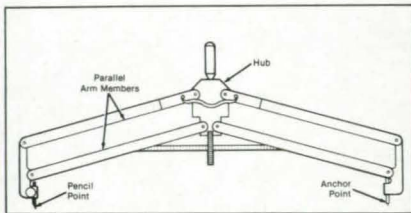
PAGE
Repair Systems
Systems for PCB Repair Anywhere™

9893 Brewers Court
Laurel, MD 20707, U.S.A.
(301) 490-9860
Telex 87446



Parallel-End-Point Drafting Compass

A drafting compass employs a parallelogram linkage between its ends and its hub to keep its pointed ends in parallel when it is closed, when it is fully open, and at all positions in between (see figure). A pair of omega-shaped springs secures the linkage arms in the position set by the user until the user readjusts the end spacing. The parallelogram-linkage principle can be used on dividers as well as on compasses. When the pointed ends are in parallel, distance measurements become more precise than with inexpensive compasses or dividers that have their pointed ends extending radially from the hub. At the same time, the new compass/dividers are more convenient than the more expensive compasses and dividers that have adjustable points that have to be set individually for each new radius to keep the pointed ends in parallel. (See page 103.)



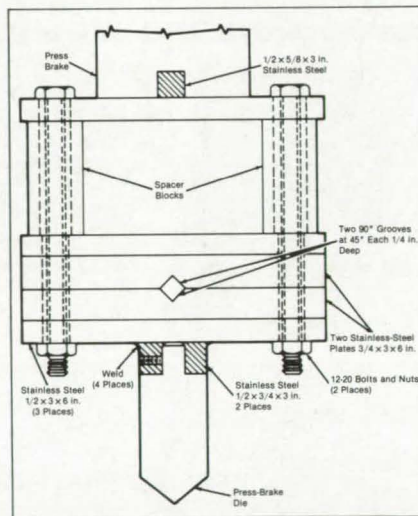
Small-Portion Water Dispenser

A dispenser provides a measured amount of water for reconstituting dehydrated foods. The dispenser holds the food or beverage package while it is being filled with either cold or room-temperature water (see figure, which shows the dispensing needle about to penetrate a plastic food package). Other uses might include the dispensing of fluids or medicine. A pressure regulator in the dispenser reduces the varying pressure of the water supply to a constant pressure. An electronic timer stops the flow after a predetermined length of time, ensuring that a controlled volume of water is dispensed. (See page 152.)



Adjustable Tooling for Bending Brake

An adjustable tooling jig for a bending-brake accommodates spacing blocks and either a standard male press-brake die or a bar die. By increasing the free space available for bending sheet-metal parts, the jig makes it easier to fabricate such items as deep metal boxes or brackets with right-angle bends. To make deep metal boxes, the jig is interposed between the press brake and one of the press-brake dies; spacer blocks are fabricated to the required dimensions as needed by cutting them from metal scraps. To fabricate smaller parts with multiple right-angle bends, the press-brake die is removed from the bottom of the jig, and a round or square bar is clamped between the upper and lower 90° grooves. The bar then serves as the male bending die, cooperating with a female die consisting of a grooved block placed on the lower press-brake surface. (See page 124.)



Material for Fast Cutting

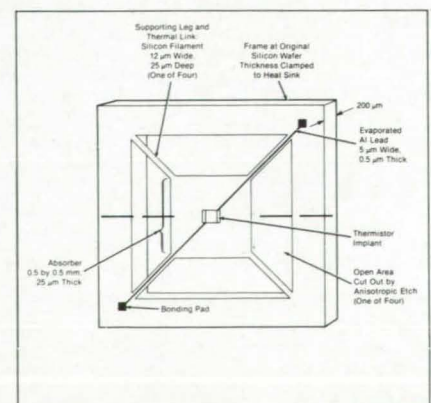
A new material based on silicon nitride and containing more than 90 percent silicon combines impact resistance close to that of coated carbides with heat and wear resistance close to those of aluminum oxide ceramics. Because tools made of this material can operate at relatively high cutting speed, they will remove more material than will a conventional tool operating at the same pressure. Consequently, a high removal rate can be accomplished with relatively low pressure, which greatly reduces vibration, workpiece slippage, and tool breakage. With its relatively long life, this material reduces the amount of cutting time lost to indexing, gauging, and adjustments. (See page 70.)

Rotating Apparatus for Isoelectric Focusing

An improved isoelectric focusing apparatus helps to prevent electro-osmosis and convection, both of which cause the remixing of separated fractions. The apparatus is slowly rotated continuously or rocked about its horizontal axis at a rotational amplitude of at least 180° so that the average gravitational vector experienced by the fluid is zero, and the convection is therefore suppressed. Use of filters to separate the column into dislike compartments along its length further suppresses convection and suppresses electro-osmosis. Experiments have shown that the dimensions of the apparatus are not critical. Typical compartment and column volumes are 2 and 40 ml, respectively. Rotation speeds can lie between 3 and 30 rpm. (See page 152.)

High-Resolution Thermal X-Ray Detector

A thermal X-ray detector, tested successfully in prototype, in theory can operate as a spectrometer with a resolution less than 5 eV full width at half height — 100 times the spectral resolution of conventional solid-state detectors — with high efficiency from 100 eV to 9 keV. It could be used to detect trace constituents in minerals by X-ray fluorescence. It also could be used for measuring the energies of energetic electrons and weak pulses of light. The figure shows a version of the detector, which consists of an X-ray absorber, a temperature sensor in the absorber, and a thermal link from the absorber to a heat sink. An X-ray photon is detected by measuring the temperature rise immediately following the absorption of the photon. (See page 37.)



"It's the quality of the ideas..."

Sometimes the impossible is within your reach.

The development and implementation of an Ada® compiler is a complex challenge. Because Ada has it all – strong typing, packaging, concurrency, exception handling, separate compilation, overloading – it seems an impossible task to develop an Ada compiler for a specific processor.

Now there's a solution to hand.

By using a systematic and formal approach during development, an approach which prevents coding a single line before you know exactly how and why the entire compiler should be coded, DDC International has found the solution to the Ada Problem – the Portable DDC Ada Compiler System.

Our solution can be yours.

The DDC Ada Compiler System can be ported to another processor in less than a year. Ask Honeywell in Boston – we started in January 1984 and Honeywell had a validated Ada compiler for their DPS6 computer in December the same year. Or ask some of the other companies that wanted a validated solution to their Ada Problems – companies like Rockwell International and CDC in the US or ICL in Britain.

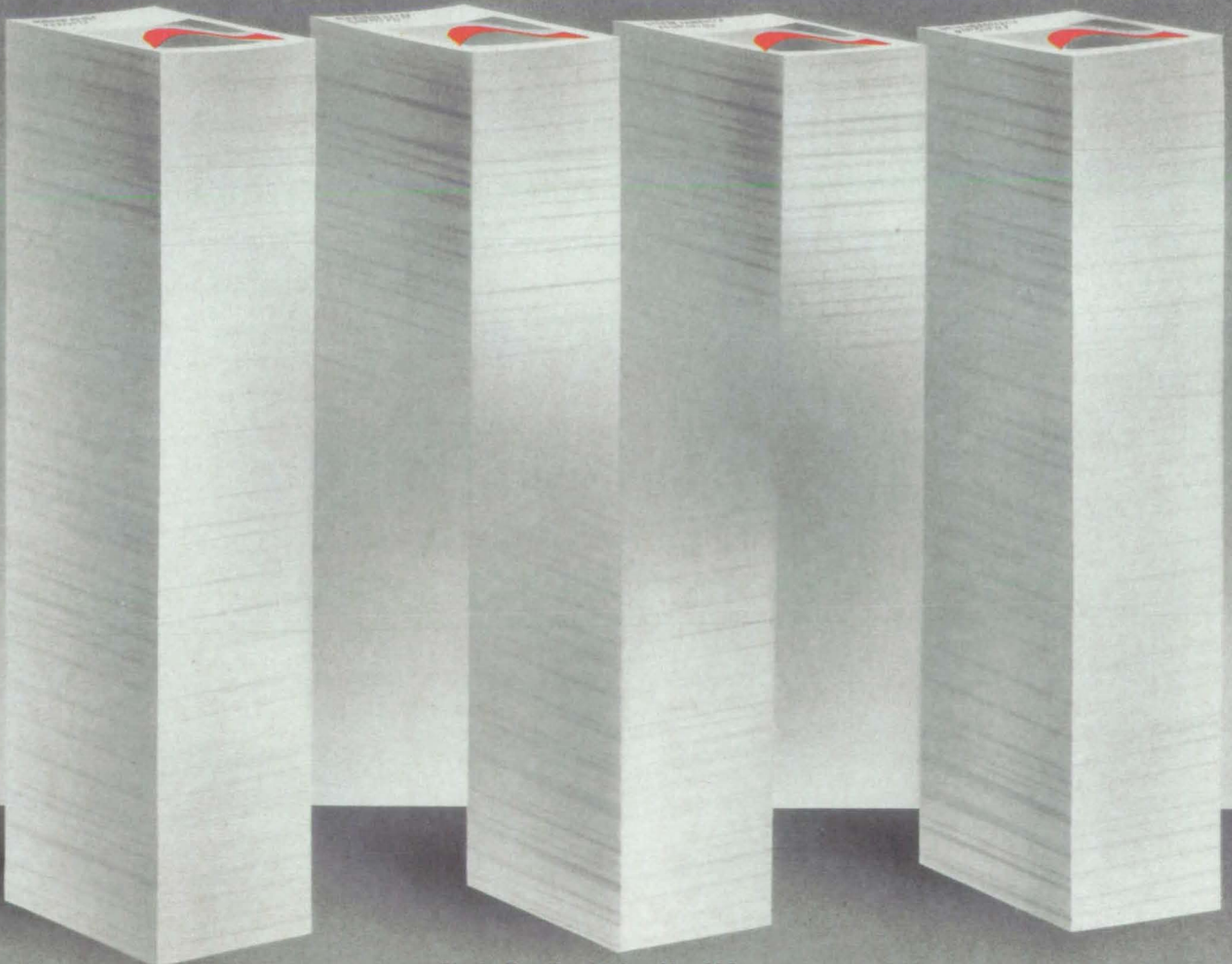
®Ada is a registered trademark of the US Dept. of Defense (AJPO).

"and the way you implement them."



The DDC Ada Compiler System. The Portable Solution.

DDC International, Lundtoftevej 1C
DK-2800 Lyngby, Denmark
Tel.: (+45) 2 87 11 44, Telex: 37704 ddc dk



HOW YOU CAN BENEFIT FROM NASA'S TECHNOLOGY UTILIZATION SERVICES



HOW YOU CAN UTILIZE NASA'S Industrial Applications Centers

A nationwide network offering a broad range of technical services, including computerized access to over 100 million documents worldwide.

You can contact NASA's network of Industrial Applications Centers (IACs) for assistance in solving a specific technical problem or meeting your information needs. The "user friendly" IACs are staffed by technology transfer experts who provide computerized information retrieval from one of the world's largest banks of technical data. Nearly 500 computerized data bases, ranging from NASA's own data base to Chemical Abstracts and INSPEC, are accessible through the nine IACs, which are located throughout the nation. The IACs also offer technical consultation services and/or linkage with other experts in the field.

You can obtain more information about these services by calling or writing the nearest IAC. User fees are charged for IAC information services.

Aerospace Research Applications Center (ARAC)

Indianapolis Center for Advanced Research
611 N. Capitol Avenue
Indianapolis, IN 46204
Dr. F. Timothy Janis, Director
(317) 262-5003

Kerr Industrial Applications Center (KIAC)

Southeastern Oklahoma State University
Station A, Box 2584
Durant, OK 74701
Tom J. McRorey, Director
(405) 924-6822

NASA Industrial Applications Center

823 William Pitt Union
University of Pittsburgh
Pittsburgh, PA 15260
Paul A. McWilliams, Executive Director
(412) 624-5211

NASA/Southern Technology Applications Center

State University System of Florida
307 Weil Hall
Gainesville, FL 32611
J. Ronald Thornton, Director
(904) 392-6760

NASA/UK Technology Applications Center

University of Kentucky
109 Kinkead Hall
Lexington, KY 40506-0057
William R. Strong, Director
(606) 257-6322

NERAC, Inc.

Mansfield Professional Park
Storrs, CT 06268
Daniel U. Wilde, President
(203) 429-3000

North Carolina Science and Technology Research Center (NC/STRC)

Post Office Box 12235
Research Triangle Park, NC 27709
J. Graves Vann, Jr., Acting Director
(919) 549-0671

Technology Application Center (TAC)

University of New Mexico
Albuquerque, NM 87131
Stanley A. Morain, Director
(505) 277-3622

NASA Industrial Applications Center (WESRAC)

University of Southern California
Research Annex
3716 South Hope Street
Room 200
Los Angeles, CA 90007
Radford G. King, Acting Director
(213) 743-6132
(800) 642-2872 (CA only)
(800) 872-7477 (toll-free US)

If you represent a public sector organization with a particular need, you can contact NASA's Application Team for technology matching and problem solving assistance. Staffed by professional engineers from a variety of disciplines, the Application Team works with public sector organizations to identify and solve critical problems with existing NASA technology.

Technology Application Team

Research Triangle Institute
P.O. Box 12194
Research Triangle Park, NC 27709
Doris Rouse, Director
(919) 541-6980

A SHORTCUT TO SOFTWARE:

COSMIC®

An economical source of computer programs developed by NASA & other gov't. agencies.

Software developed by the U.S. government may be applicable to your needs. To tap this valuable resource, contact COSMIC, NASA's Computer Software Management and Information Center. Approximately 1100 computer programs and related documentation comprise the current library. New and updated programs are announced regularly in NASA Tech Briefs' Computer Programs section, and COSMIC publishes an annual software catalog.

More information about COSMIC's services can be obtained by calling or writing:

COSMIC®
Computer Services Annex
University of Georgia
Athens, GA 30602
John A. Gibson, Director
(404) 542-3265

HOW YOU CAN ACCESS TECHNOLOGY TRANSFER SERVICES AT NASA FIELD CENTERS:

Technology Utilization Officers & Patent Counsels

Each NASA Field Center has designated a Technology Utilization Officer and a Patent Counsel to facilitate technology transfer between NASA and the private sector.

If you need further information about new technologies presented in NASA Tech Briefs, you should request the Technical Support Package (TSP) that accompanies the brief. In the event that a TSP is not available, you can contact the Technology Utilization Officer at the NASA Field Center that sponsored the research. He can arrange for expert assistance in applying the technology by putting you in touch with the people who developed it.

If you want additional information about the patent status of a particular technology or are interested in licensing a NASA invention, contact the Patent Counsel at the NASA Field Center that sponsored the research. Be sure to refer to the NASA reference number at the end of the tech brief.

Ames Research Center

Technology Utilization Officer:

Laurance A. Milov
Mail Code 204-10
Moffett Field, CA 94035
(415) 694-5761

Patent Counsel:

Darrell G. Brekke
Mail Code 200-11
Moffett Field, CA 94035
(415) 694-5104

Goddard Space Flight Center

Technology Utilization Officer:

Donald S. Friedman
Mail Code 702-1
Greenbelt, MD 20771
(301) 344-6242

Patent Counsel:

John O. Tresansky
Mail Code 204
Greenbelt, MD 20771
(301) 344-7351

Lyndon B. Johnson Space Center

Technology Utilization Officer:

William Chmylak
Mail Code AL32
Houston TX 77058
(713) 483-3809

Patent Counsel:

Marvin F. Matthews
Mail Code AL3
Houston, TX 77058
(713) 483-4871

John F. Kennedy Space Center

Acting Technology Utilization

Officer: Thomas M. Hammond
Mail Stop PT-TPO-A
Kennedy Space Center, FL 32899
(305) 867-3017

Patent Counsel:

James O. Harrell
Mail Code PT-PAT
Kennedy Space Center, FL 32899
(305) 867-2544

Langley Research Center

Technology Utilization Officer:

John Samos
Mail Stop 139A
Hampton, VA 23665
(804) 865-3281

Patent Counsel:

Howard J. Osborn
Mail Code 279
Hampton, VA 23665
(804) 865-3725

Lewis Research Center

Technology Utilization Officer:

Daniel G. Soltis
Mail Stop 7-3
21000 Brookpark Road
Cleveland, OH 44135
(216) 433-5567

Patent Counsel:

Gene E. Shook
Mail Code 60-2
21000 Brookpark Road
Cleveland, OH 44135
(216) 433-5753

Jet Propulsion Laboratory

Technology Utilization Manager:

Norman L. Chalfin
Mail Stop 201-110
4800 Oak Grove Drive
Pasadena, CA 91109
(818) 354-2240

NASA Resident Office-JPL

Technology Utilization Officer:

Gordon S. Chapman
Mail Stop 180-801
4800 Oak Grove Drive
Pasadena, CA 91109
(818) 354-4849

Patent Counsel:

Paul F. McCaul
Mail Code 180-801
4800 Oak Grove Drive
Pasadena, CA 91109
(818) 354-2734

George C. Marshall Space Flight Center

Technology Utilization Officer:

Isamil Akbay
Code AT01
Marshall Space Flight Center,
AL 35812
(205) 544-0962

Patent Counsel:

Leon D. Wofford, Jr.
Mail Code CC01
Marshall Space Flight Center,
AL 35812
(205) 544-0014

National Space Technology Laboratories

Technology Utilization Officer:

Robert M. Barlow
Code GA-10
NSTL Station, MS 39529
(601) 388-1929

NASA Headquarters

Technology Utilization Officer:

Leonard A. Ault
Code IU
Washington, DC 20546
(202) 453-1920
Assistant General Counsel for
Patent Matters: Robert F. Kempf
Code GP
Washington, DC 20546
(202) 453-2424

IF YOU HAVE A QUESTION...

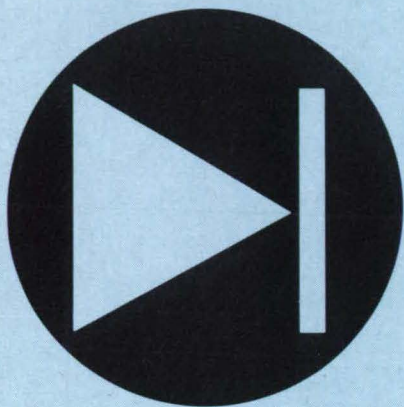
NASA Scientific & Technical Information Facility

If you have a general or specific question about NASA's Technology Utilization Network or its services and documents, you can contact the STI facility for assistance. The STI staff can answer your questions, supply documents and provide referrals to meet your needs. You can use the feedback card in this issue to contact STI directly.

NASA Scientific and Technical Information Facility

Technology Utilization Office
P.O. Box 8757
BWI Airport, MD 21240
Walter M. Heiland, Manager
(301) 859-5300, Ext.242, 243

Electronic Components & Circuits



Hardware, Techniques, and Processes

- 30 Fabrication of an X-Ray Imaging Detector
- 33 Self-Alining Electrical Connector
- 34 ROM-Based Plan-Position-Indicator Sweep Driver
- 36 Variable Synthetic Capacitance
- 37 High-Resolution Thermal X-Ray Detector
- 38 Two-Element Transducer for Ultrasound
- 39 Temperature-Sensitive Oscillator
- 39 Multikilowatt Bipolar Nickel/Hydrogen Battery
- 40 Unbalanced-to-Balanced Video Interface
- 41 Passive Element Shapes Antenna Radiation Pattern

Books & Reports

- 42 Reliability Research for Photovoltaic Modules
- 42 Guidelines for SEU-Resistant Integrated Circuits

Fabrication of an X-Ray Imaging Detector

A silicon wafer would be divided into an array of X-ray detectors.

Goddard Space Flight Center, Greenbelt, Maryland

An X-ray detector array that could yield a mosaic image of an object emitting in the 1- to 30-keV range could be fabricated from an n-doped silicon wafer. The detector is an improved version of the device described in "X-Ray Detector for 1 to 30 keV" (GSC-12682), *NASA Tech Briefs*, Vol. 7, No. 3 (Spring, 1983), page 248.

In the proposed fabrication technique, thin walls of diffused n^+ dopant would divide the wafer into pixels of rectangular cross section, each containing a central electrode of thermally migrated p-type metal. This pnn^+ arrangement would reduce the leakage current by preventing the transistor action caused by the pnp structure of the earlier version.

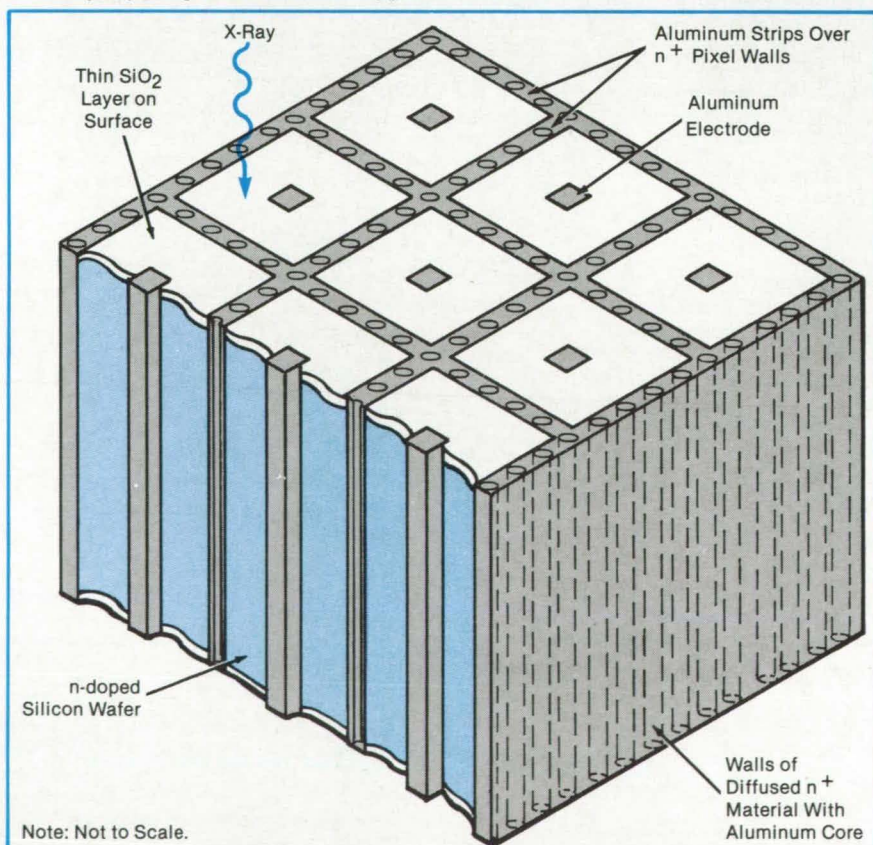
The n-type conductivity in the silicon wafer would be produced by doping it lightly with phosphorus. For 1- to 30-keV X-rays the wafer thickness would be about 50 mil (1.27 mm). Relatively thin layers (about 2,000 Å thick) of silicon dioxide would be formed on the wafer surfaces by exposing it to steam and oxygen

while its temperature is maintained at about 1,000 °C.

In the first step in the pixel formation, a photoresist mask is applied to the upper surface of the wafer to delineate the walls. The surface is etched in a buffered hydrofluoric acid solution to remove selectively the upper silicon dioxide layer in a pattern defining the pixel walls.

A laser is used to drill circular openings, about 1 mil (0.025 mm) in diameter, centered every 2 mil (0.05 mm) along the etched pattern and passing perpendicularly completely through the wafer. The wafer, placed in a furnace at 1,100 °C, would then be exposed to a phosphorus gas dopant ($POCl_3$ in a mixture of gaseous nitrogen and oxygen) for a time sufficient to assure diffusion of the dopant atoms to a distance of 1 mil (0.025 mm) from the axis of each opening, the phosphorus atoms diffusing from adjacent openings thus coming into contact to produce continuous walls of n^+ atoms.

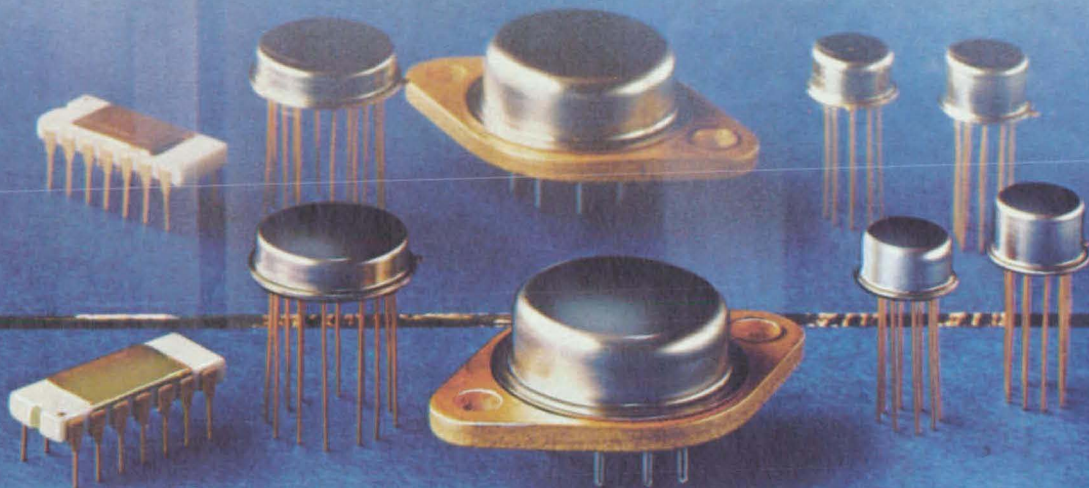
Metallic strips, preferably aluminum,



An **X-Ray Detector Array** fabricated from a single silicon wafer consists of pixels of n-doped silicon separated by n^+ walls and containing aluminum (p) electrodes.

NASA Tech Briefs, May/June 1986

CTS is the source for standard military hybrids



Need special screening, environmental testing, data logging or specific electrical testing? Contact us.

What a great alternate source for standard pin-for-pin Military Hybrid replacements! When you are faced with the "take-it-or-leave-it" attitude that some major suppliers have adopted on Military Hybrid standards—look to CTS Corporation, Microelectronics Division. CTS will provide Military Hybrids just as you want them. And, our prices are very competitive.

CTS has been a leading producer of custom Military Hybrids for over 20 years. Our hybrids are designed and screened to Mil-Std-883 requirements. We have complete quality conformance evaluation

capabilities as required in Mil-M-38510.

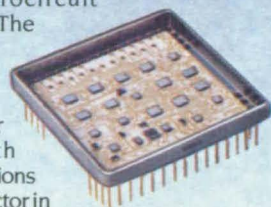
Don't settle for standard hybrids that don't meet your individual needs. Ask about the CTS0002, 6, 8, 21, 32, 33, 34 and 41 as alternates for the LH and DH series. We'll make your standards to custom requirements.

Write today for a product-for-product comparison chart, and technical data on customized "standards" that meet *your* specs. Contact: CTS Corporation, 1201 Cumberland Ave., West Lafayette, IN 47906. (317) 463-2565.



Advanced Air Force Communications System uses CTS Military Hybrid

The prime contractor for the Air Force SEEK TALK anti-jam voice communication system selected a CTS Hi-Rel unit as a primary microcircuit component. The need for high reliability in this system linking fighter aircraft with command stations was a major factor in the selection of CTS.



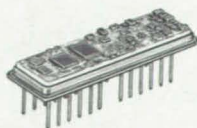
Circle Reader Action No. 351

CTS® MEANS RELIABILITY

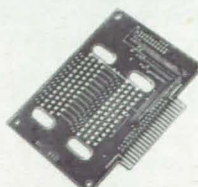
CTS CORPORATION • ELKHART, INDIANA



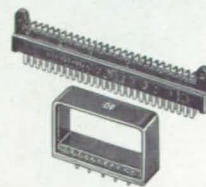
Voltage Controlled Crystal Oscillators
Standard and hybrid designs.
Phone: (815) 786-8411
CIRCLE NO. 350



Custom Hybrid Circuits
for demanding medical electronics.
Phone: (317) 463-2565
CIRCLE NO. 375

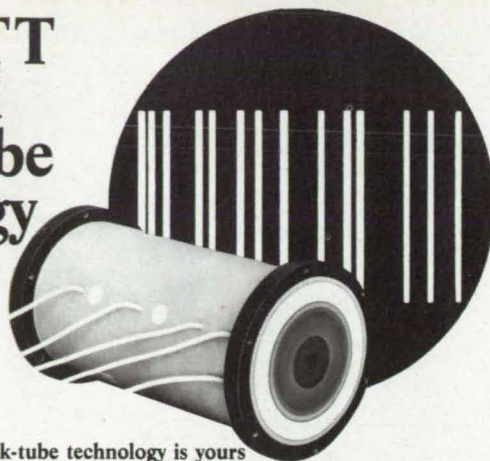


PC Boards Complex double-sided and multilayer.
Phone: (415) 659-1770
CIRCLE NO. 376



Connectors Custom PC board and military styles.
Phone: (612) 941-9100
CIRCLE NO. 377

Specify ITT Advanced Streak-Tube Technology



Advanced, customized streak-tube technology is yours

ITT/Electro-Optical Products Division can now offer you the latest streak-tube advancements developed for Lawrence Livermore and Los Alamos National Laboratories. The ITT Model F4157 series features a variety of windows, wide dynamic range, and high-sensitivity photocathodes. Extinction ratio has been greatly improved in gated operation. Minimal system modifications are needed to retrofit these devices into existing installations.

High photocathode uniformity and a wide variety of spectral responses, including high-red-sensitivity, can be offered through ITT's remote process technique. And, a wide choice of window materials can be accommodated by ITT's advanced indium seal techniques.

ITT's new streak-tubes are low-voltage-gateable and feature all-electrostatic design with improved spatial resolution, low distortion and wide dynamic range. Streak-tubes are encapsulated in high-voltage-insulated and magnetically shielded assemblies.

A standard line of photoelectronic products is also available. Ask for our catalog by contacting: ITT Electro-Optical Products Division, P.O. Box 3700, Fort Wayne, IN 46801, (219) 423-4341, TWX: 810-332-1413, Telex: 232-429.

ELECTRO-OPTICAL PRODUCTS DIVISION

ITT

Circle Reader Action No. 403

would then be evaporated over the exposed wall areas of the top surface to contact the diffused phosphorus, forming the interconnected configuration shown in the figure. A similar array of aluminum strips, contacting the diffused phosphorus at the openings, would be produced evaporatively on the lower wafer surface.

To locate the thin aluminum electrodes centered in each pixel, a photoresist mask with openings at the pixel centers is applied to the upper wafer surface. The masked wafer is etched with hydrofluoric acid to expose the silicon in the center. Then, after the photoresist mask is stripped using hot chromic acid and the wafer rinsed clean, aluminum is evaporated over the top wafer surface. A second photoresist mask is then applied to protect the aluminum film at the future electrode sites while the rest of the film is etched with phosphoric acid.

After the second mask is stripped with chromic acid and the wafer rinsed clean, the lower surface of the wafer is heated to about 1,150 °C, while the upper surface is kept slightly cooler at about 1,100 °C. The resulting thermal gradient causes the aluminum deposited in the etched opening on the cooler surface to form the central electrodes by diffusing completely through the wafer to the opposite surface. The aluminum strips connecting the n^+ -diffused regions also diffuse through the wafer to form aluminum walls between the pixels.

Since this rapid diffusion allows little time for lateral diffusion, the cross section of each electrode is small compared to the cross section of each pixel, thereby minimizing the probability of X-rays impinging directly on the central electrodes. To enhance the spatial resolution of an X-ray image, the horizontal cross section of each pixel is kept small: The separation between the central electrodes of adjacent pixels is about 1 mm.

The array of detector cells comprises a deep diode array, since both the n^+ pixel walls and the metal electrodes extend completely through the wafer. The application of bias potentials between the central electrodes and the walls creates a depletion region extending laterally from the central electrode to the walls of each pixel through the entire wafer thickness.

In this configuration, incident X-rays impinging on the wafer with a penetration depth less than its thickness; i.e., with energies up to 30 keV, precipitate photoelectron interactions with the wafer material. Regardless where the interaction occurs within a pixel, the resulting photoelectrons are attracted to the central electrode, thereby providing a signal for the detection of the incident X-rays. The central electrode of each pixel could be connected to a separate element of a

SPACE

...on board NASA Tech Briefs' next launch

"NASA Tech Briefs WORKS for advertisers."

That's according to Bill Waskey, Director of Business Development for Fairchild Industries Control Systems Division, and other executives now advertising in NASA Tech Briefs. Companies like Rockwell, Amoco, Data General, and DuPont have already received more than 7500 top-quality responses to their ads in just one issue of NASA Tech Briefs. If your company is on the leading edge of technology, shouldn't you be marketing in the #1 magazine on the leading edge of technology?

Confirm Your Space on Board.

To find out how you can be on board the next launch of NASA's official magazine, call Robin DuCharme, Dick Soule or Wayne Pierce in New York at (212) 490-3999; Irene Froehlich in Chicago at (312) 848-8144; or Bob Bruder in Los Angeles at (213) 477-5866.

NASA Tech Briefs
is published by
Associated Business Publications
41 East 42nd Street, Suite 921
New York, NY 10017

charge-coupled-device processor, enabling the processor to read sequentially each pixel and generate a composite image of it as it appears on the illuminated

surface of the detector array.

This work was done by George E. Alcorn and Andre S. Burgess of **Goddard Space Flight Center**. For further infor-

mation, Circle 82 on the TSP Request Card.

GSC-12956

Self-Alining Electrical Connector

A mating pair of insulators forces the initial alinement of a plug and socket.

*Marshall Space Flight Center,
Alabama*

A self-aligning multipin electrical connector features tapered insulators that are keyed to mate each other before the male pins come into contact with the female sockets. This arrangement prevents the breakage or bending of the male pins as on conventional connectors when misaligned contacts are carelessly pressed together.

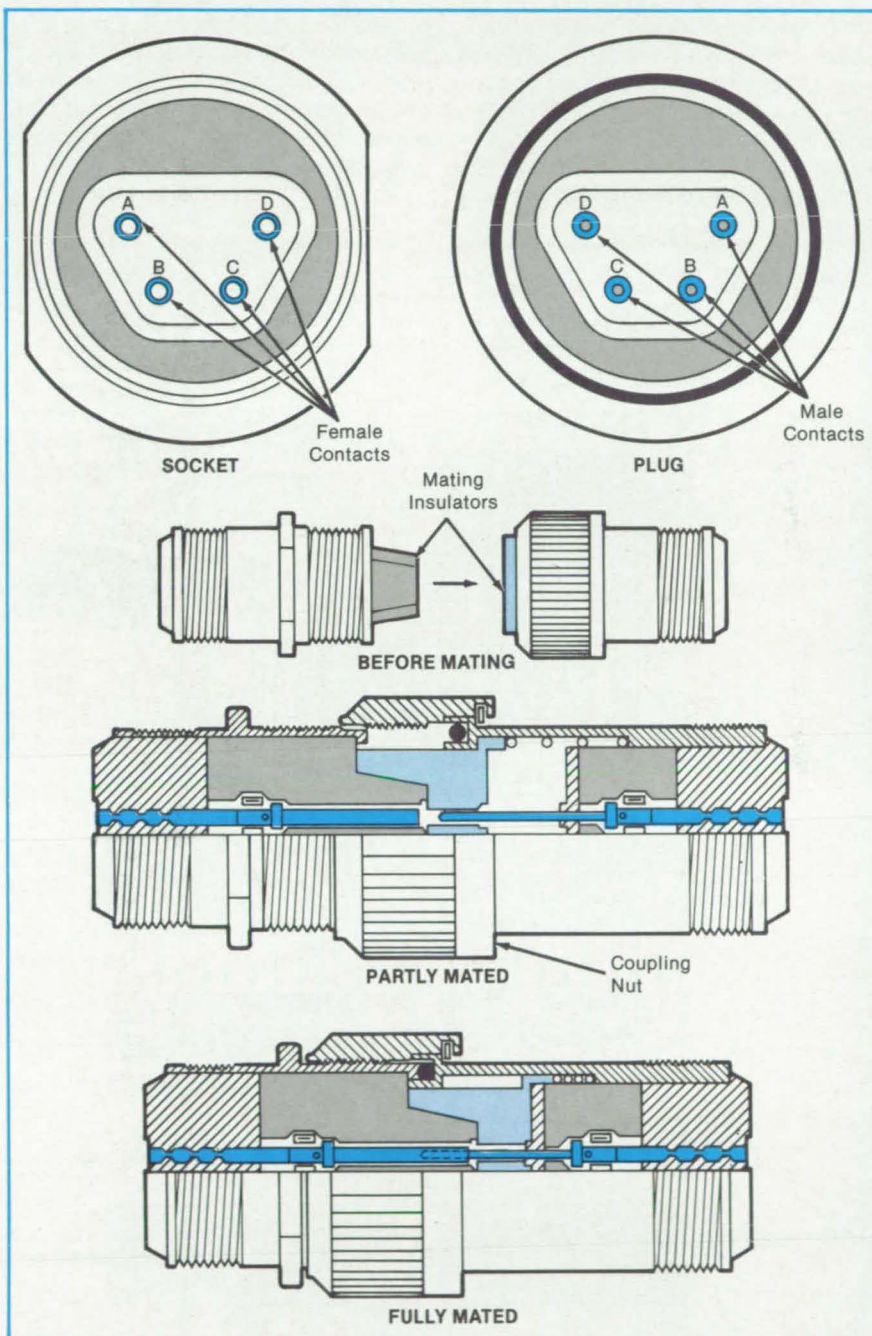
In the new design (see figure), the male pins are recessed behind one of the alining insulators so that they cannot touch the female contacts before the plug and socket are properly aligned. The contacts mate when the coupling nut draws the aligned plug and socket together, depressing one of the alining insulators against a spring. The compressed spring provides tension on the mated threads of the assembly, helping the connector to resist loosening under vibration or shock.

In contrast, conventional connectors must be aligned precisely before the contact to prevent the pin damage. By providing the alinement before the mating, the new design effectively extends the contact life. Furthermore, the accurate alinement would simplify the mating of connectors having high contact densities.

The new connector should be both faster and easier to use than are conventional circular multipin connectors, particularly if the user is wearing gloves or the connector is located out of sight, in a confined space, or in a hard-to-reach location. The new connector concept could be used in fiber-optic connectors or in hybrid electrical/fiber-optic connectors.

Connectors embodying the concept can be packaged in housings suitable for such severe environments as high altitude, outer space, under water, high or low temperatures, or high pressures. The design would also be useful in high-voltage applications because the tapered alining insulators would press against each other when the coupling nut is fully tightened, eliminating air spaces, which could otherwise become electrical-leakage paths.

This work was done by Anthony Swanic of Arbus, Inc., for **Marshall Space Flight Center**. For further information, Circle 1 on the TSP Request NASA Tech Briefs, May/June 1986



The **Plug and Socket** have tapered, trapezoidally shaped insulators, which guide alinement. Partially-cutaway side views show the connector pair at two stages in the mating process: In the first, the tapered insulators have touched and forced each other into alinement prior to contact mating; in the second, tightening the coupling nut on the plug has pushed the plug further into the socket, compressing the spring behind the plug insulator, and forcing the electrical contacts to mate.

Card.

Inquiries concerning rights for the commercial use of this invention should

be addressed to the Patent Counsel, Marshall Space Flight Center [see page 29]. Refer to MFS-26022.

ROM-Based Plan-Position-Indicator Sweep Driver

The circuit produces a PPI display on a conventional X-Y oscilloscope.

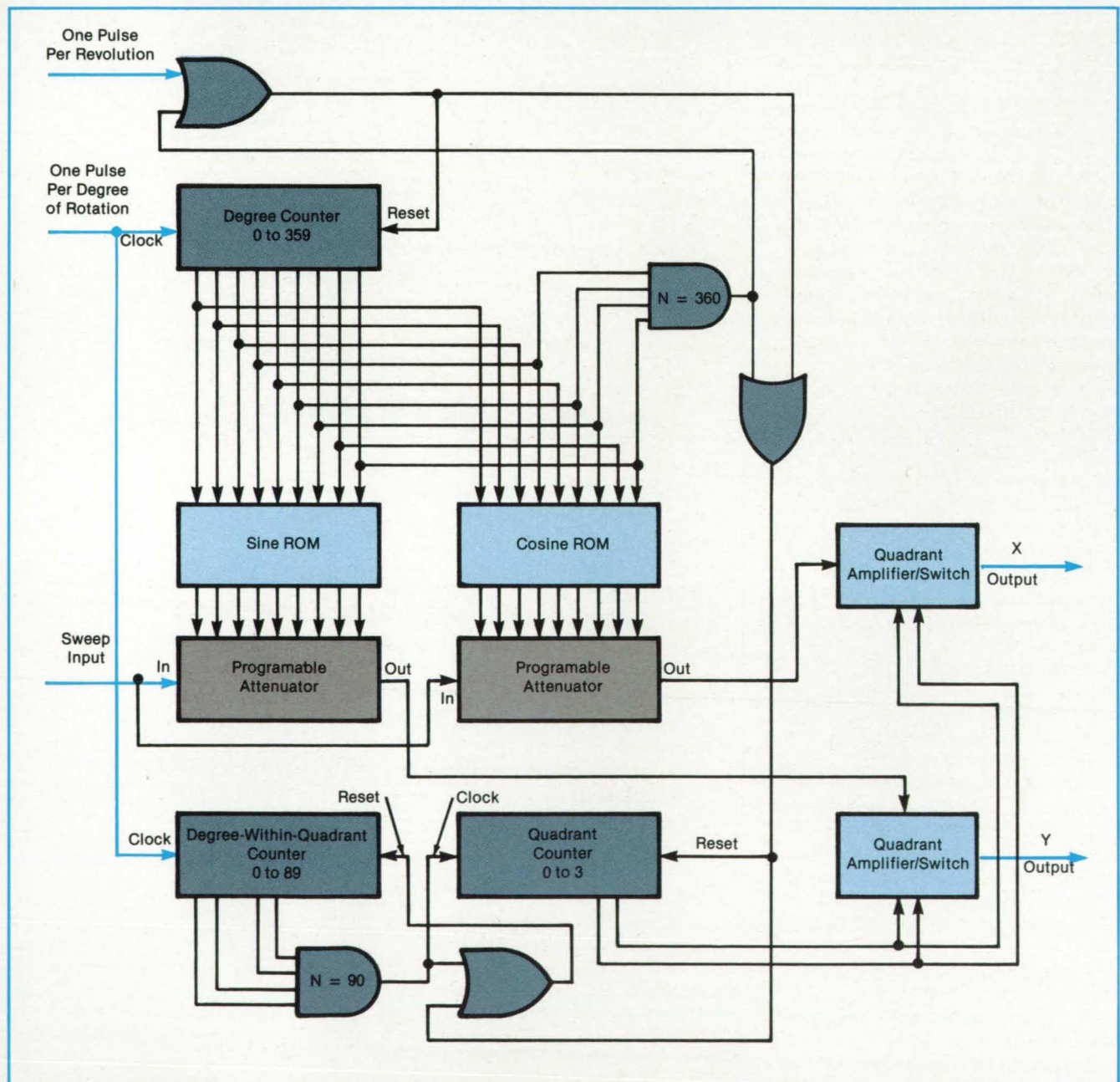
Langley Research Center, Hampton, Virginia

The read-only-memory-based (ROM-based) plan-position-indicator (PPI) sweep driver electronically generates circular radar presentations on a conventional X-Y oscilloscope. Conventional methods to accomplish this task have used mechanically-driven deflection coils

or mechanically-driven sine and cosine potentiometers, requiring mechanical preventive maintenance plus a dedicated display indicator. The new method can display the radar sweep on any conventional storage oscilloscope.

The ROM-based system uses a pro-

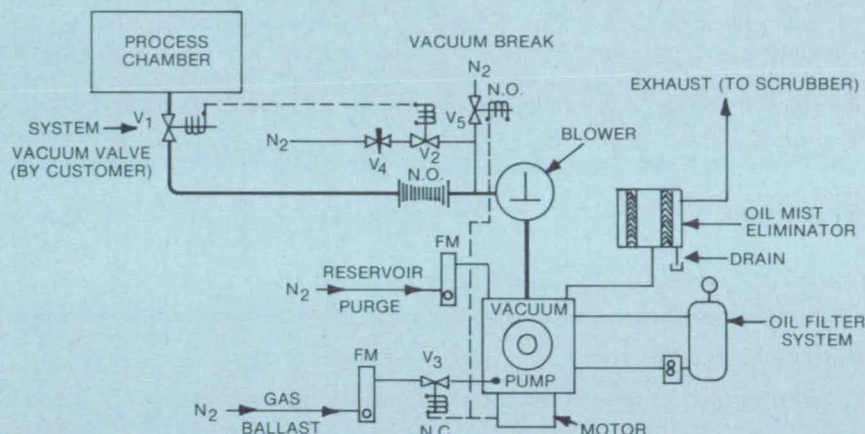
gramable memory to define the sweep function. Because the sweep function thus becomes essentially a table-lookup function, other presentation formats can be accommodated by changing or electrically selecting different memory chips. For example, the normal search-radar



This **Sweep Driver** generates a PPI display on a conventional X-Y oscilloscope. The mechanically-driven deflection coils or potentiometers of prior PPI display units are not needed.

How to stop water vapor from destroying your vacuum system when you're plasma etching.

DRY PLASMA ETCHING SYSTEM
TYPICAL VACUUM SYSTEM SCHEMATIC



- NOTES:
1. ALL NITROGEN GAS BLEEDS—1 PSIG MAXIMUM
 2. SYSTEM VALVE V₁ INTERLOCKED WITH VALVE V₂. WHEN V₁ CLOSED V₂ OPEN. WITH V₁ CLOSED & VACUUM SYSTEM IN OPERATION, USE NEEDLE VALVE V₄ TO ADJUST PRESSURE IN MANIFOLD TO 50-100 MICRONS.
 3. SOLENOID VALVE V₃ CONNECTED ACROSS MOTOR LEADS, OPENS WHEN PUMP STARTS.
 4. FM = FLOW METER
 5. SOLENOID VALVE V₅ CONNECTED ACROSS MOTOR LEADS, CLOSSES WHEN PUMP STARTS.

Due to the corrosive nature of the gases used and the particulates generated, plasma etching can impose harsh requirements on your vacuum system.

The presence of water vapor makes these conditions even more severe.

To keep your vacuum system performing to its capabilities, you must prevent water vapor from entering the system. If it does, you must remove it quickly.

The following installation and operation procedures will help you keep your system operating smoothly.

The right installation.

Install PVC exhaust piping instead of galvanized or black iron pipe, and an oil mist eliminator to reduce oil loss from the pump.

The exhaust line should be installed so it can easily be disassembled for

periodic cleaning and the vacuum manifold must be leak-free.

The right operation.

Operate the vacuum system continuously and make sure the vacuum pump is gas ballasted during processing with a nitrogen flow rate of 1 to 2 L/M.

Purge the reservoir with nitrogen (in humid ambients it may be necessary to increase the nitrogen flow). Do not pump on the process chamber with the vacuum system at blank-off pressure as oil backstreaming may result. When necessary to shut down the vacuum system for over 8 hours, fill gas ballast with nitrogen for at least 4 hours before stopping.

The right maintenance.

Drain the exhaust oil mist eliminator weekly. If oil is clean, it can be reused by

returning to the pump. If it is "milky" or cloudy, it should be decanted before returning to pump reservoir. Cleaning interval is determined by the amounts of particulates accumulated.

Monitor differential pressure across the oil filter. Replace element when filter pressure shows a significant increase above baseline pressure. Actual pressures will be determined by your own process.

Open pump reservoir at 2-month intervals to remove sediment from bottom of the reservoir. And when the particulate oil filter elements are used, replace element when filter pressure as shown on the gage is exceeded.

The right vacuum system.

Stokes is America's full-line vacuum components manufacturer so we have the right pumping package for your application. So you don't have to over-design or over-purchase.

If you have a processing design question call or write: Stokes Division, Pennwalt Corporation, 5500 Tabor Road, Philadelphia, PA 19120. 215-831-5400.

**Send for free
subscription to
Vac-Tech News.**

Keep up with the latest developments and advanced technology taking place in the vacuum industry. Just call or write and we'll see that you receive each issue.



STOKES
PENNWALT
EQUIPMENT ■ CHEMICALS
HEALTH PRODUCTS

Stokes Division, Pennwalt Corporation
5500 Tabor Road, Philadelphia, PA 19120
Phone: 215-831-5400

display is the circular PPI, but it would be very simple to reprogram the memory for an offcenter sector sweep or even a bearing/range B-scan.

The circuit (see figure) requires three inputs. The first is a once-per-scan pulse to synchronize the display to the north, the relative heading, or another reference direction. The second is a once-per-degree-of-rotation pulse to advance the sweep rotation. The third input is the normal sweep ramp. The duration of the ramp corresponds to the maximum displayed range. Changing the ramp duration, while holding its peak amplitude constant, changes the maximum displayed range.

There are two main counter sections. The first section, known as the degree counter, counts from 0 to 359 and resets. This counter is also reset by the once-per-scan input pulse to synchronize the counter to the antenna. The counter

states are routed in parallel to two ROM's.

The second counter section, known as the quadrant counter, consists of two subsections. One counts from 0 to 89 and resets. It is also reset by both the once-per-scan pulse and the degree-counter reset. The output of this counter is fed to a two-stage binary counter, the 0-to-3 counter, which keeps track of what quadrant the sweep is in.

The absolute values of the sine function normalized to an integer scale of 0 to 255 are stored in the first ROM. The second ROM contains the absolute values of the cosine function normalized to an integer scale of 0 to 255. The ROM data-output lines are connected to programmable attenuators, which are fed by the sweep ramp. The outputs of the programmable attenuators are routed through the quadrant amplifier/switch units. The

quadrant switches are formed from 4066 CMOS analog gates and are driven by decoders connected to the quadrant counter. The result is a sweep ramp multiplied by the sine and the cosine of the antenna position.

These two outputs, when fed to the X and Y inputs of an oscilloscope, produce a true PPI display. The 8-bit programmable attenuators, one for the sine and one for the cosine, consist of resistor ladder networks and analog gates. The gates connect the resistors to ground or to the input signal according to the bit pattern from the respective ROM. This circuit has been built and tested and will form the heart of a display system for a bistatic IFF processor at Langley Research Center.

This work was done by John M. Franke and Bradley D. Leighty of Langley Research Center. No further documentation is available. LAR-13328

Variable Synthetic Capacitance

Small oscillator-frequency changes are produced by digital signals.

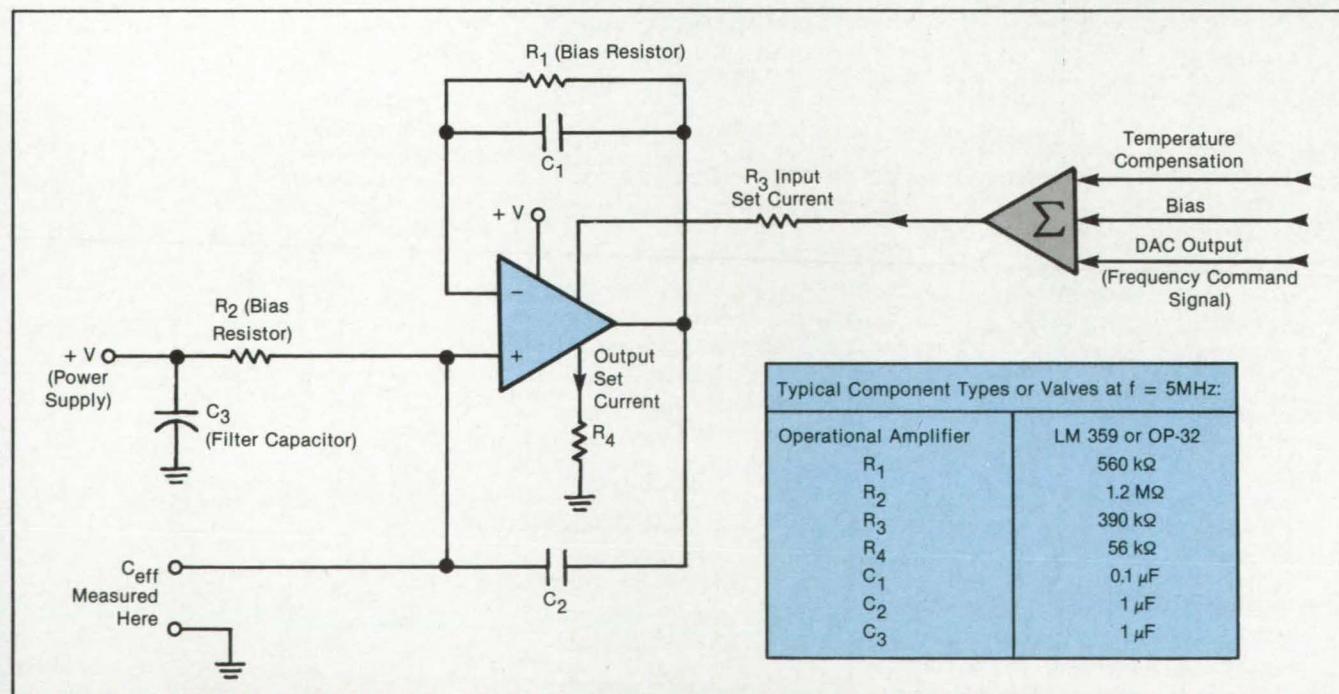
Goddard Space Flight Center, Greenbelt, Maryland

A feedback amplifier circuit synthesizes an electronically variable capacitance. Because the changes in the effective capacitance are relatively small even with large control-signal voltages, the circuit is insensitive to input noise. The circuit is especially suitable for fine frequency adjustments of piezoelectric-crystal or inductor/capacitor resonant oscillators.

The circuit (see figure) includes an operational amplifier, the gain-bandwidth product of which varies with an input set current, and the output impedance of which varies with an output set current. The inverting input is connected to the output through bias resistor R_1 and parallel bypass capacitor C_1 . This capacitor is

large enough so that for practical purposes it can be regarded as a short circuit at the intended oscillator frequency. Thus, the signal at the inverting input follows the output signal. Capacitor C_2 is connected in a feedback loop from the output to the inverting input.

In this follower configuration, the voltage gain K_v (output signal voltage divided by input signal voltage at the noninverting



The **Variable Synthetic Capacitor** is an amplifier circuit with a follower/feedback configuration. The effective input capacitance depends on the input set current. If the synthetic capacitor is connected across the resonant element of an oscillator, the oscillator frequency can be controlled via the input set current.

input) is given by $K_r = K/(1 + K)$, where K = the open-loop gain of the operational amplifier alone. At a frequency f in the intended operating range of several megahertz to one gigahertz, K can be approximated as $-jf_g/f$, where f_g = the gain-bandwidth product.

These values of K_r and K are used to calculate the circuit input admittance, Y , at the noninverting input. The result is $Y = 2\pi C_2[jf - f_g]/[1 + (f_g/f)^2]$, which is equivalent to the admittance of a large negative resistance in parallel with an effective (synthetic) capacitance of $C_{eff} = C_2[1 + (f_g/f)^2]$. (The negative resistance can be ignored because it is large in comparison to the resistance with which it is connected in parallel.)

The synthetic capacitance is normally connected across the piezoelectric crys-

tal or other resonant element of an oscillator. The ungrounded side of the element is connected to the noninverting input while the grounded side of the element is connected to the circuit ground. Although C_{eff} and the oscillator frequency, f , depend on each other, the variation in f is so small in practice that C_{eff} and f can both be considered to depend only on f_g .

The input set current is varied to adjust f via its effect on f_g . The input set current is fed through resistor R_3 from a summing circuit. The summing-circuit inputs are a temperature-compensating voltage, a bias voltage, and the output of a digital-to-analog converter (DAC).

The digital input to the DAC is the main frequency-control signal. It can be generated locally or transmitted over a long distance. A typical DAC might have

1,024 steps, with analog output increments of about 5 mV per step. Thus, the oscillator frequency is varied in 512 small steps above and below a central value.

For a 5-MHz crystal oscillator connected to this circuit and using typical component values, each step of the DAC can be made to correspond to a frequency change of 0.005 Hz or even less (≤ 1 part in 10^9). This small change in frequency is achieved with relatively large digital signal voltages so that noise is not a primary consideration. The noise at the DAC output is of the order of nanovolts and thus has no appreciable effect on the frequency.

This work was done by Leonard L. Kleinberg of Goddard Space Flight Center. For further information, Circle 81 on the TSP Request Card. GSC-12961

High-Resolution Thermal X-Ray Detector

Thermal pulses from single photons can be measured.

Goddard Space Flight Center, Greenbelt, Maryland

A thermal X-ray detector, tested successfully in prototype, in theory can operate as a spectrometer that provides 100 times the spectral resolution of conventional solid-state detectors, with high efficiency from 100 eV to 9 keV. It could be used to detect trace constituents in materials by X-ray fluorescence. It also could be used for measuring the energies of energetic electrons and weak pulses of light.

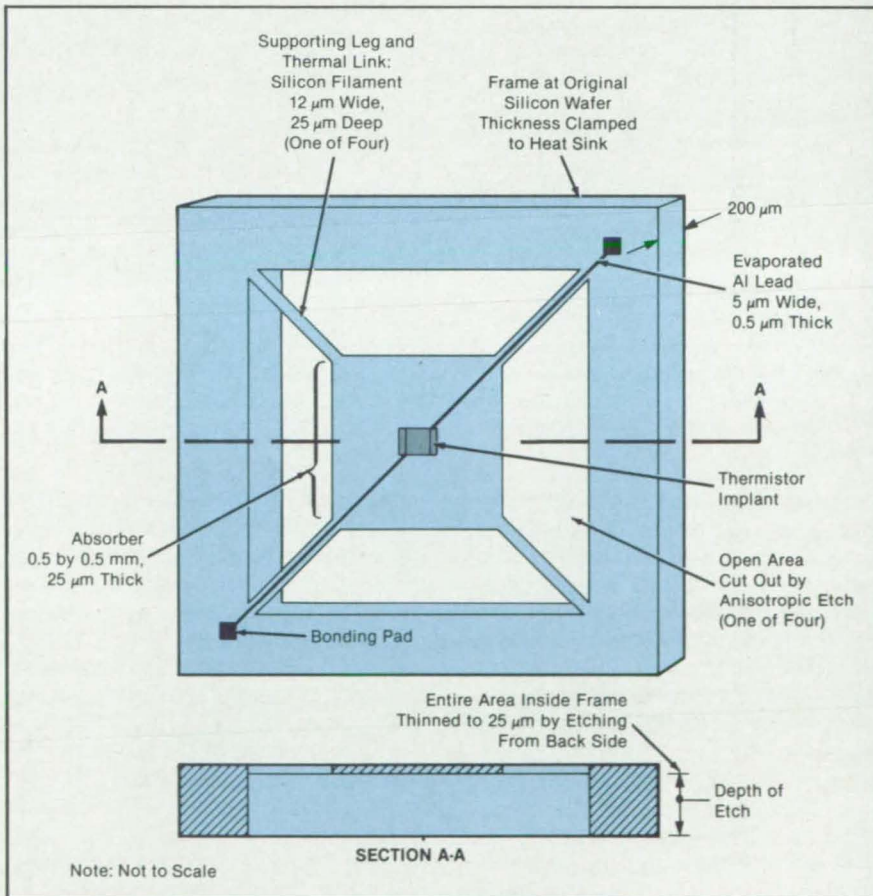
The figure shows a version of the detector, which consists of an X-ray absorber, a temperature sensor in the absorber, and a thermal link from the absorber to a heat sink. An X-ray photon is detected by measuring the temperature rise immediately following the absorption of the photon.

The temperature rise is approximately $\Delta T = U/C$, where U is the X-ray energy and C is the detector heat capacity. If the thermal conductance of the thermal link equals G , then the detector element decays back toward the heat-sink temperature exponentially with a time constant $\tau = C/G$.

In a practical detector, the time constant of the output pulse is changed by electrothermal feedback from τ to an effective time constant τ_e . Therefore in the time domain an impulse of absorbed energy U at time $t = 0$ produces a decaying exponential pulse of voltage

$$V(t) = (US(0)/\tau_e) \exp(-t/\tau_e)$$

where $S(0)$ is the detector responsivity at zero frequency (measured in V/W). The



The **Thermal X-Ray Detector** is made on a silicon wafer as an integrated circuit. The temperature sensor is implanted in the square absorber in the middle.

utility of this device as a detector depends on the ability to measure this pulse height accurately.

The fundamental limit to the sensitivity of such a device is imposed by the thermodynamic temperature fluctuations of

the sensor. The rms temperature fluctuations can be written as

$$\Delta T_{\text{rms}} = (k_B/C)^{1/2} T$$

so that $\Delta U_{\text{rms}} = (k_B C)^{1/2} T$, where k_B is Boltzman's constant. With a proper choice of materials, adequate X-ray absorption out to energies of 9 keV can be achieved while maintaining sufficiently low heat capacity to offer good spectral resolution ($\Delta U \leq 5$ eV full width at half maximum). To achieve the excellent resolution offered by this technique, the de-

vices must be cooled to less than 0.3 K.

The device shown in the figure includes a silicon photon-absorbing element, a semiconductor on the insulating side of the metal/insulator transition to sense the absorber temperatures, and etched silicon filaments at the corners as the thermal link from the absorber to the heat sink. Many alternative designs are possible.

In laboratory tests, devices of this type exhibited a resolution of 130 eV full width at half maximum at 6 keV photon energy. This is better than the 155 eV, which is the

best achieved using solid-state detectors at this energy. These results were obtained with a detector of relatively high heat capacity operating at 0.3 K and are in good agreement with theory: The implication is that devices of lower heat capacity operating at 0.1 K will come near the theoretical predictions.

This work was done by S. Harvey Moseley of Goddard Space Flight Center. For further information, Circle 31 on the TSP Request Card.
GSC-12953

Two-Element Transducer for Ultrasound

The separation of transmitting and receiving units improves the probing of deep tissue.

NASA's Jet Propulsion Laboratory, Pasadena, California

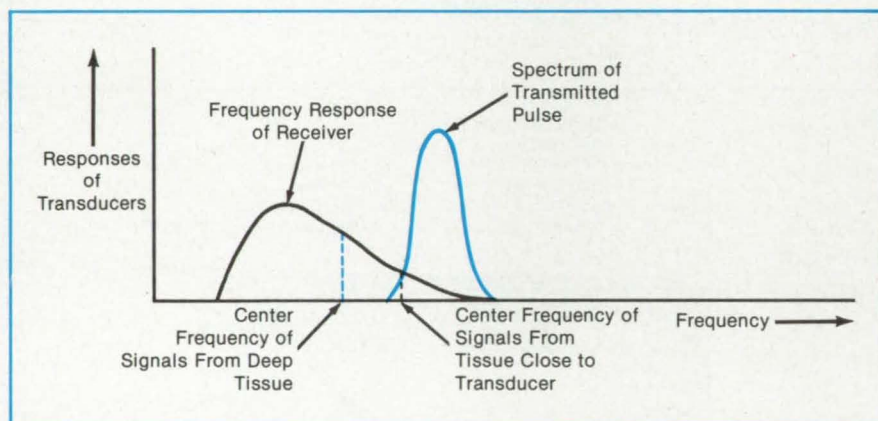


Figure 1. The **Frequency Responses of the Receiver and Transmitter Would Be Different** in a new dual-element ultrasonic transducer. The receiver would peak at lower frequencies more characteristic of the spectrum of the ultrasound pulse after passage through tissue.

A proposed ultrasonic transducer would have dual elements to increase the depth at which sonic images can be made of biological tissue. Present transducers use the same elements for transmitting and receiving ultrasonic signals. The proposed transducer would use separate transmitting and receiving elements, and the frequency response of the receiving element would be independently designed to accommodate the attenuation of higher frequencies by the tissue.

The new transducer is intended for pulse-echo ultrasonic systems, in which reflected sound pulses reveal features in tissue.

Soft tissue attenuates sound at a rate of about 1 decibel per megahertz per centimeter of round-trip path length. Thus, the higher frequencies in a pulse are attenuated more as the pulse pene-

trates tissue, and the center frequency in a received pulse may be significantly lower than in the transmitted pulse. The new center frequency may not correspond to the most sensitive receiving region of the transmitter/receiver. The received signal will thus seem weak, and details of the reflecting features will be lost.

In the proposed dual transducer, the receiver characteristics would not have to be as much of a compromise with the required transmitter characteristics. The receiver would be designed to be most sensitive to the expected range of echo-pulse center frequencies (see Figure 1). The transducers could be concentric; for example, a circular concave piezoelectric element encircled by an annular concave piezoelectric element (see Figure 2).

This work was done by Dennis H. Le

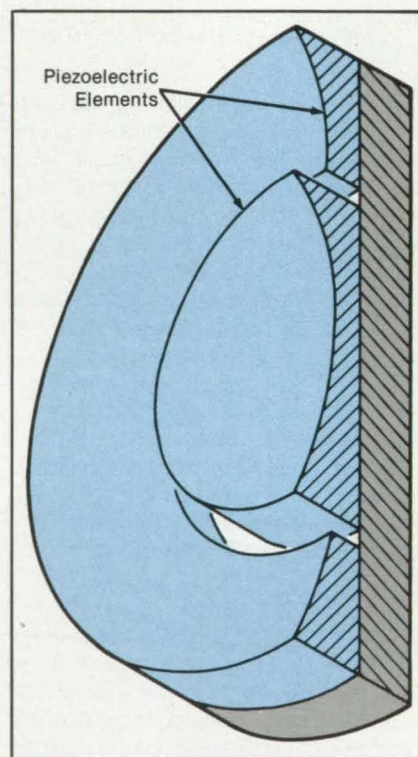


Figure 2. Two **Piezoelectric Elements**, shown here in a cutaway view, would be the transducers in an ultrasound transmitter/receiver.

Croissette and Richard C. Heyser of Caltech for NASA's Jet Propulsion Laboratory. For further information, Circle 43 on the TSP Request Card.
NPO-16591

Temperature-Sensitive Oscillator

An ingestible thermometer consists of an oscillator with temperature-dependent frequency.

Goddard Space Flight Center, Greenbelt, Maryland

A new, small, inexpensive, low-power, temperature-sensing circuit is suitable for use as an ingestible thermometer for measuring internal body temperature. The device is a quartz-crystal oscillator, the frequency of which changes in proportion to the change in temperature.

The circuit does not depend on any temperature sensitivity of the crystal itself. Thus, readily-available, inexpensive, crystals can be used. Previous crystal-oscillator temperature-sensing circuits required expensive crystals which had to be specially cut to provide large, linear temperature coefficients. The new circuit also avoids the linearity and stability problems of thermistor-based temperature-sensing circuits.

The circuit includes an operational amplifier, the gain-bandwidth product of which can be varied by varying the bias current at the programming input. Because of the temperature variation of a forward voltage drop across two internal diodes, the bias current (through resistor R_3) varies with temperature, thereby varying the gain-bandwidth product. The value of R_3 is selected to set the bias and gain-bandwidth product to the desired values at a given temperature (for example, normal body temperature).

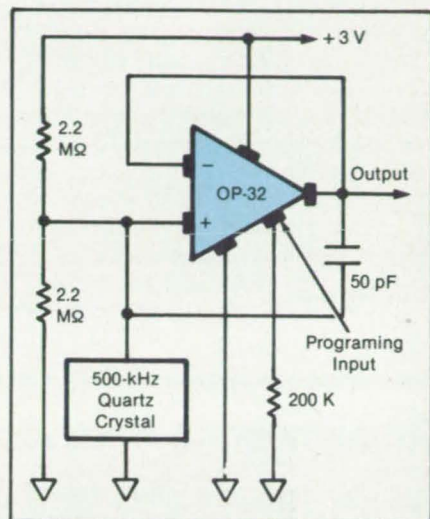
The oscillator operates in the rolloff re-

gion of the gain-versus-frequency characteristic of the amplifier. With the capacitor connected between the output and the non-inverting input, the effective capacitance across the crystal changes with the gain-bandwidth product and therefore with temperature. This, in turn, changes the crystal resonant frequency slightly.

The oscillator (see figure) operates at about 500 kHz, a frequency that is readily transmitted through the body and for which miniature crystals are available. Using the component values shown, the capacitance varies with temperature in such a way that the oscillator frequency increases linearly over the temperature range of 30° to 40°C, at about 4 Hz per °C. In general, achieving linearity depends on selecting an operational amplifier with a sufficient change in gain-bandwidth product for a given set current and a crystal with large enough motional capacitance to allow it to be pulled over a relatively large frequency range with a relatively small capacitance change.

This work was done by Leonard L. Kleinberg of Goddard Space Flight Center. For further information, Circle 105 on the TSP Request Card.

This invention is owned by NASA, and a patent application has been filed. Inquiries concerning nonexclusive or ex-



A Temperature-Sensitive Oscillator with a nearly linear temperature coefficient of frequency can be obtained by using a high-speed, high-gain, programmable operational amplifier such as the OP-32 to produce a temperature-varying reflected capacitance across a quartz crystal.

clusive license for its commercial development should be addressed to the Patent Counsel, Goddard Space Flight Center [see page 29]. Refer to GSC-12958.

Multikilowatt Bipolar Nickel/Hydrogen Battery

High energy densities appear feasible.

Lewis Research Center, Cleveland, Ohio

A nickel/hydrogen battery utilizing a bipolar construction in a common pressure vessel, which addresses the needs for multikilowatt storage for low-Earth-orbit applications, has been designed and a 10-cell prototype model tested. The modular-concept-design 35-kW battery projected energy densities of 20 to 24 Wh/lb (160 to 190 kJ/kg) and 700 to 900 Wh/ft³ (90 to 110 MJ/m³) and incorporated significant improvements over state-of-the-art storage systems.

Results of low-Earth-orbit multikilowatt-mission studies have indicated a need for electrochemical storage subsystems that NASA Tech Briefs, May/June 1986

will be quite different from those in current use. The general trend for the multikilowatt application is toward higher cell capacity and higher battery voltage. It is generally conceded that the nickel/hydrogen system would represent the best candidate for scaleup from its current size of from 30 to 50 Ah to a size more compatible with the multikilowatt missions.

An advanced configuration for the nickel/hydrogen system that fulfills the requirements of future multikilowatt low-Earth-orbit missions was designed. The result was a complete battery system

that incorporated active cooling for thermal control, an improved oxygen-recombination method, and pore-size engineering to facilitate electrolyte management. The individual cells are constructed in a bipolar manner and are contained within a common pressure vessel. The cell stack resembles that of a fuel cell where only one electrode pair is housed in each cell compartment. Thus, the electrode/battery ampere-hour capacity is a function of the electrode dimensions.

Active cooling is accomplished by a liquid coolant or other suitable means. The battery power output was designed to



(130 MJ/m³), a threefold to fourfold improvement over an IPV battery.

The bipolar design is especially attractive when looking at cost and system integration. With the bipolar design, there is only one stack and vessel; whereas about 450 state-of-the-art IPV cells are needed in series/parallel combination to match the 35-kW power requirements.

Two 10-cell, 6.5-Ah batteries based on the design were fabricated and tested. The test results of these first bipolar batteries are very encouraging. A total of 4,000 cycles at 80-percent depth-of-discharge has been obtained. A cycle-life goal of 30,000 cycles at lesser depth-of-discharge (50 percent) appears achievable with minor design changes.

The discharge-rate capability of this design exceeds 20 C. At the 10-C discharge rate, 80 percent of the battery capacity can be withdrawn in 6 min. Low-polarization voltages that result in cyclic

watt-hour efficiency of 75 to 80 percent have been demonstrated. This demonstration indicates that a high-voltage bipolar battery within a common pressure vessel makes an ideal building block for such large, advanced energy-storage systems as the space station.

This work was done by the Electrochemistry Branch of **Lewis Research Center**. Further information may be found in NASA TM-82844 [N82-24647/NSP], "Design of a 35 kilowatt Bipolar Nickel-Hydrogen Battery for Low Earth Orbit Applications."

Copies may be purchased [prepayment required] from the National Technical Information Service, Springfield, Virginia 22161, Telephone No. (703) 487-4650. Rush orders may be placed for an extra fee by calling (800) 336-4700.
LEW-14244

Unbalanced-to-Balanced Video Interface

Equal but opposite video waveforms are generated.

Lyndon B. Johnson Space Center, Houston, Texas

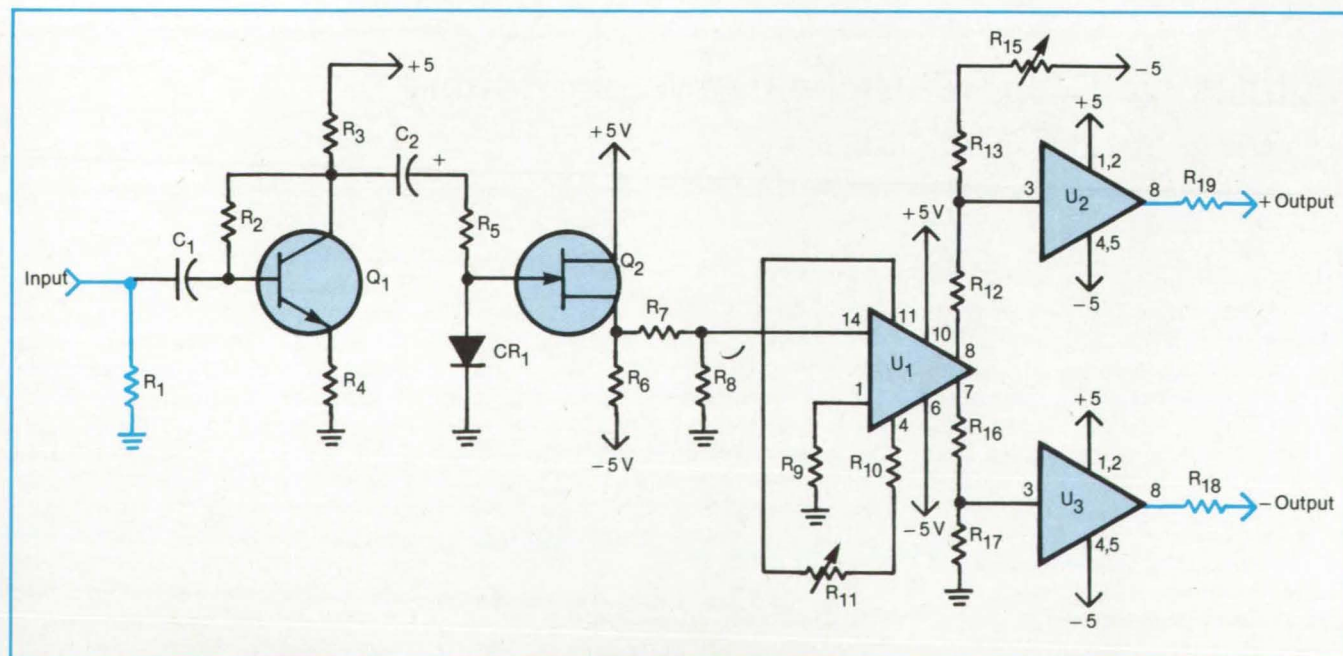
An interface circuit for video signals converts a 75-ohm unbalanced input to a 75-ohm balanced output. The circuit (see figure) is intended for use with an input television signal having polarity, amplitude, and dc bias such that the tips of the synchronizing pulses lie at zero volts while the reference white level is a specified positive dc level

(typically about 1 volt).

The unbalanced input line is terminated in a 75-ohm resistor, R_1 . Capacitor C_1 blocks the dc component of the input so that only the time-varying component is fed to Q_1 and is inverted in polarity.

The combination of capacitor C_2 , resistor R_5 , and diode CR_1 acts as a dc restorer

for the inverted waveform. Since the tips of the synchronizing pulses are at the positive extremity of the inverted waveform, the diode clamps them near zero volts, while allowing the negative-polarity remainder of the signal to be fed to buffer amplifier Q₂. The input impedance of Q₂ is high enough to prevent the loss of dc restoration during



This **Interface Circuit** converts a 75-ohm unbalanced video input to a 75-ohm balanced output.

the horizontal-line picture-transmission time between synchronizing pulses.

Integrated circuit U_1 takes the unbalanced output of Q_2 and produces a balanced output to drive integrated-circuit current amplifiers U_2 and U_3 . R_{11} is used to adjust the output-signal amplitude. R_{15} is a

fine-adjustment control to set the synchronizing-pulse tips to zero output voltage. R_{13} and R_{19} match the amplifier outputs to the two conductors of the balanced 75-ohm output transmission line. Thus, the output-line conductors carry opposite-polarity replicas of the input video

signal.

This work was done by James E. Richardson of Taft Broadcasting Corp. for **Johnson Space Center**. For further information, Circle 108 on the TSP Request Card. MSC-20950

Passive Element Shapes Antenna Radiation Pattern

A parasitic waveguide element suppresses ground-reflected multipath radiation.

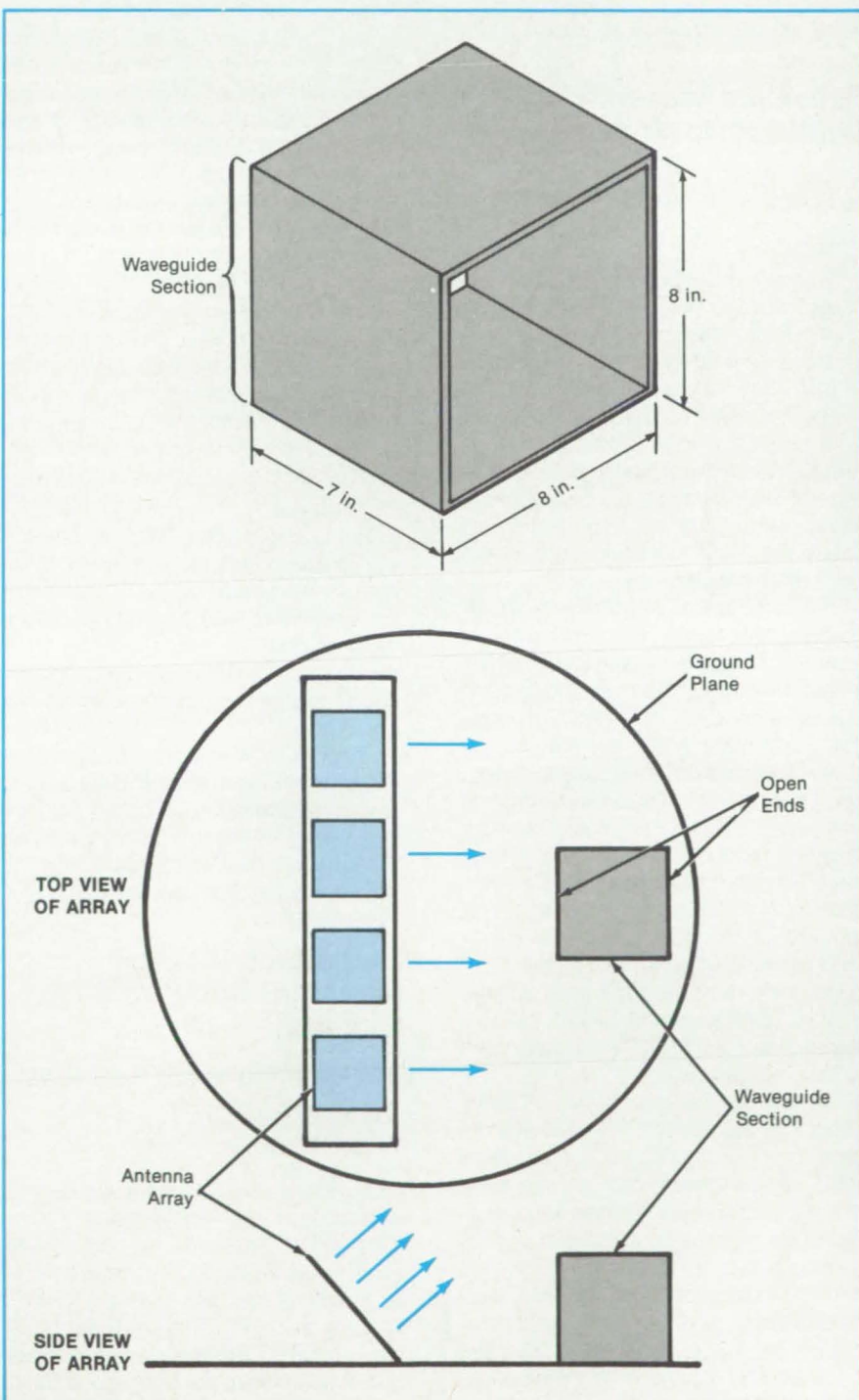
NASA's Jet Propulsion Laboratory, Pasadena, California

A small section of waveguide placed in front of a phased-array antenna operating at 850 MHz (see figure) modifies the radiation field by reducing power density parallel to and below the ground plane without significantly affecting the primary radiation at angles greater than 20° above the horizontal. The waveguide acts as a parasitic radiator that shifts the phase of a portion of the wavefront by approximately 180° , causing partial cancellation in the ground plane, thereby reducing the radiation intensity in that direction by about 10 dB. This produces a corresponding reduction in multipath radiation scattered from the ground.

This waveguide technique could also be used to decouple two nearby antennas. A piece of waveguide would be positioned to create a null in the pattern of one of the antennas in the direction of the other antenna. The technique could be used at both antennas if necessary.

The waveguide dimensions are chosen so that the phase velocity in the waveguide is twice that in free space at the operating wavelength. The waveguide works with circularly and linearly polarized radiations. In contrast with such other ground-plane radiation-suppression devices or techniques as varying the shape or length of a ground plane, inductive gratings, or absorbers, the waveguide takes up less room. Also, in contrast with other techniques, the waveguide allows the radiation to retain a more nearly circular polarization down to and below the ground plane. The new technique is also quite economical, since the short length of waveguide required is relatively inexpensive.

A Passive Waveguide Element modifies the radiation pattern of a phased-array antenna. In the case shown, the goal is to reduce the radiation along and toward the ground.



When the technique was tested in the 850-MHz system, the length and the placement of the waveguide element were determined empirically. A 7-in. (17.8-cm) long, 8-in. (20.3-cm) square waveguide proved to be optimum.

This work done by Mark E. Bonebright

and Derling Killion of Cubic Corp. for **NASA's Jet Propulsion Laboratory**. For further information, Circle 107 on the TSP Request Card.

This invention is owned by NASA, and a patent application has been filed. Inquiries concerning nonexclusive or ex-

clusive license for its commercial development should be addressed to the Patent Counsel, NASA Resident Office — JPL [see page 29]. Refer to NPO-16632.

Books and Reports

These reports, studies, and handbooks are available from NASA as Technical Support Packages (TSP's) when a Request Card number is cited; otherwise they are available from the National Technical Information Service.

Reliability Research for Photovoltaic Modules

Problems of reliability analysis are described.

A report describes the research approach used to improve the reliability of photovoltaic modules. The research is aimed at raising the useful module lifetime to 20 to 30 years.

The first research task is to identify the principal degradation mechanisms. This requires the documentation of failures in service and in laboratory accelerated-aging tests. Thus far, experience has shown that increased temperature is the most reliable aging accelerator.

The next task is to establish reliability goals specific to each degradation mechanism. This requires quantification of the economic importance, at the system level, of each failure or instance of degradation. Included in this analysis are the power loss due to encapsulant soiling, open- or short-circuit failures of individual cells, statistical and economic properties of circuit redundancy, and the effects of these and other features on the life-cycle cost per unit of energy. For example, one analysis of 13 failure mechanisms in a module with a 30-year design life chose component reliability goals such that the cost of energy would be 20 percent higher than it would be if the system were to have no failures.

To achieve the quantitative reliability goals, it is necessary to measure the dependencies of the degradation or failure rates on the parameters of operating stresses, component designs, and manufacturing processes. This is a complicated problem requiring detailed physical and chemical studies and statistical analyses of failure-test data.

Degradation prediction involves the application of the parametric dependencies to mathematical models of the time

histories of applied stresses. For example, a simplified characterization of the daily thermal cycling coupled with a knowledge of the thermal-expansion and fatigue characteristics of a module would enable a prediction of the time to fatigue failure of one of the metal interconnections or a calculation of the accelerating factor of a thermal-cycling test.

The development of cost-effective solutions to the module-lifetime problem requires compromises between degradation rates, failure rates, and lifetimes, on one hand, and the costs of initial manufacture, maintenance, and lost energy, on the other hand. Life-cycle costing integrates the disparate economic terms, allowing cost effectiveness to be quantified, thereby allowing the comparison of different design alternatives. The system design may evolve somewhat from the original concept as the designer iteratively focuses in on the cost-optimum solution. An important consideration is to minimize the sensitivity of the system life and cost to processing variations and design uncertainties.

The last step in the reliability program is extensive testing of the product. By the end of the program, data with quantitative correlations to field applications should be available. The testing must be realistic, including likely interactions with users' equipment under adverse field conditions.

This work was done by Ronald G. Ross, Jr., of Caltech for NASA's Jet Propulsion Laboratory. To obtain a copy of the report, "Reliability Research Toward 30-Year-Life Photovoltaic Modules," Circle 103 on the TSP Request Card. NPO-16595

Guidelines for SEU-Resistant Integrated Circuits

Designs are examined that immunize chips to single-event upsets.

A paper presents recent results of a continuing program for increasing the resistance of integrated circuits to single-event upset (SEU). The results are based on a study of test data for heavy-ion SEU in more than 180 different types of devices. (Some of the devices perform identical functions but are made by different processes.)

A single-event upset — an error caused by a single atomic particle interacting with an integrated circuit chip — is usually "soft"; that is, it can be corrected by subsequent electrical input. Soft errors occur in random-access memories, microprocessors, programmable read-only memories, and logic devices. They are less likely to occur in logic circuits but are more difficult to detect and correct there. SEU has been a problem primarily in integrated circuits in space vehicles. However, terrestrial cosmic rays, which contain trace quantities of protons and neutrons, pose a threat to very-large-scale integrated chips as their circuit features approach submicron dimensions.

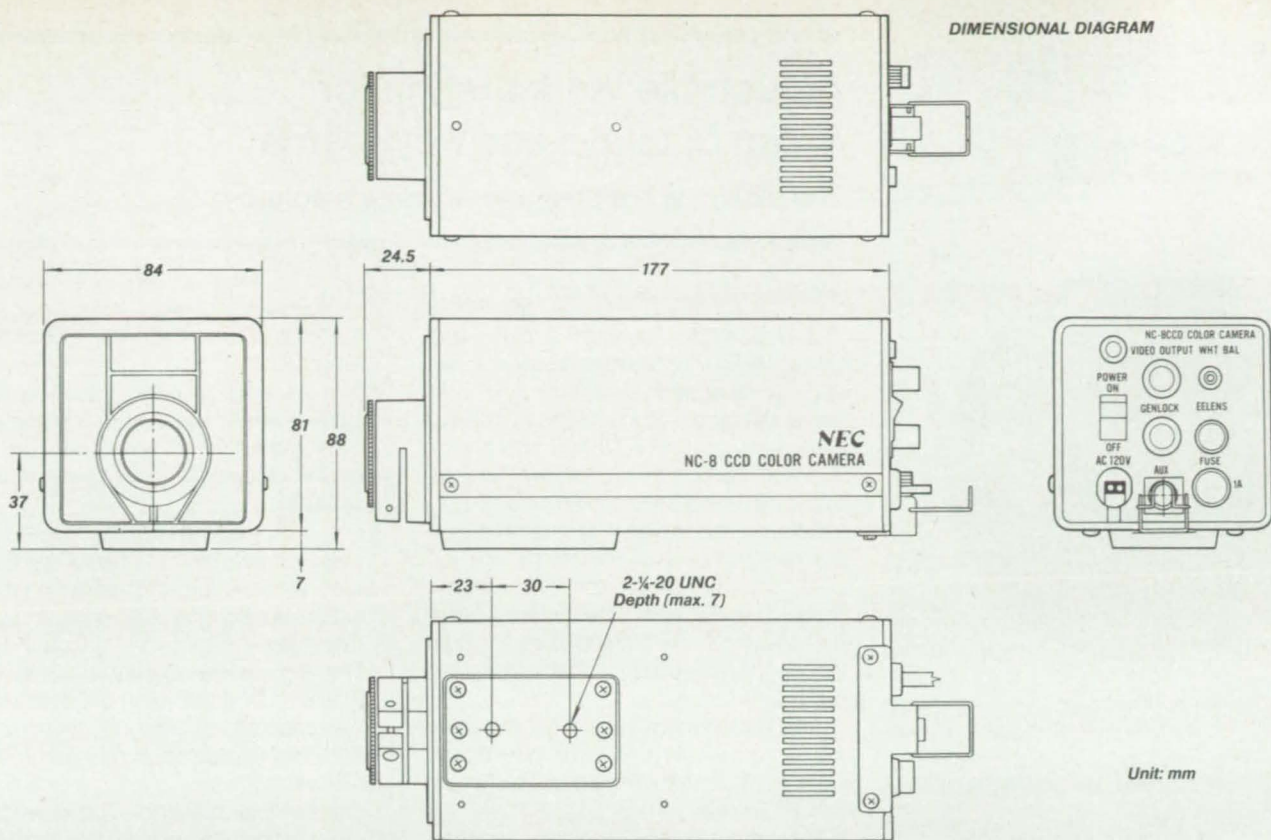
The program is examining the test data to extract generalizations about the SEU resistance of parts in terms of fabrication technology. The report notes that certain conclusions can already be drawn. For example, a broad ranking of SEU resistance, or "hardness," would place complementary metal-oxide-semiconductor/silicon-on-sapphire (CMOS/SOS) devices at the top of the list. Following in order of decreasing hardness would be CMOS on bulk silicon chips, n-channel MOS (NMOS), p-channel MOS (PMOS) and bipolar devices, and dynamic NMOS devices.

The susceptibility to upset increases with decreasing feature size, and this effect is more dominant than the differences in technology. Newer versions of a given device are more susceptible to SEU than their larger feature size predecessors. Faster parts are more susceptible than slower parts. However, individual device variability is great so that predictions cannot substitute for tests.

The program is also examining developments in mathematical models for SEU. Mathematical models can be used to a certain extent in designing devices resistant to SEU, but actually making such devices requires close collaboration between an experienced modeler and a fabrication group with expertise in various manufacturing processes, devices, and circuit design.

This work was done by Donald K. Nichols of Caltech for NASA's Jet Propulsion Laboratory. To obtain a copy of the paper, "Guidelines for Designing Parts Resistant to Single Event Upset," Circle 109 on the TSP Request Card. NPO-16596

NASA Tech Briefs, May/June 1986



OUR DESIGN FITS YOUR SPECS.

NEC invites you to take a look inside the NC-8 single chip color camera — the camera designed with your specifications in mind. With the lightweight, flexible NC-8, you get high definition and resolution, very low lag and no burn in. It resists shocks, is immune to magnetic distortion, and because its pixels are arranged in a high precision matrix, there is no geometric distortion. It includes Gen Lock as a standard feature. It is equipped for any C-mount lens including auto iris.

This durable little camera is a match for any of your toughest video camera requirements and is easily adaptable to a wide variety of settings.

NEC, the world's largest manufacturer of semiconductors, offers an entire line of solid state industrial cameras—all high quality, hard-working products from a respected source.

NEC

IMAGINE WHAT WE'LL DO FOR YOU



C&C

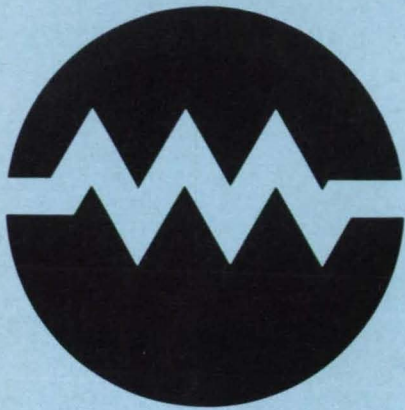
COMPUTERS AND COMMUNICATIONS

Specifications

Pickup	Interline transfer type CCD x1
Number of picture element	H427xV492
S/N ratio	47dB (illumination channel, standard recording conditions, AGC: off)
Resolution	Horizontal: 280 lines Vertical: 350 lines
Sensitivity	1,600 Lux F4.0
Minimum illumination	10 Lux F1.4 AGC: ON (20% signal output level)
White balance adjustment	Manual/Remote
Lens mount	C-Mount
Power consumption	Approx. 6.5W (less than 9VA)
Weight	Approx. 1.4kg [3.1 lbs] (excluding lens)

For more information about the NC-8, TI-22AII, TI-22PII and TI-26A industrial cameras, contact the Industrial Video Group, Broadcast Equipment Division, NEC America, Inc., 130 Martin Lane, Elk Grove Village, IL 60007. Toll free 1-800-323-6656. In Illinois phone 312/640-3792.

Electronic Systems



Hardware, Techniques, and Processes

- 44 Adjustable Work Station for Video Displays and Keyboards
- 46 Analog Video Image-Enhancing Device
- 48 Automated Signal-to-Noise Ratio Measurement
- 49 Phase-Measuring System
- 49 Wireless "Jump" Starts for Partly Disabled Equipment

Books & Reports

- 50 Radiation Hardening of Computers
- 53 Laser Inertial Navigation System

Computer Programs

- 74 Economic-Analysis Program for a Communication System

Adjustable Work Station for Video Displays and Keyboards

The station is adaptable to operator's comfort.

Marshall Space Flight Center, Alabama

A work station for video displays and keyboards is adaptable to the operational and anthropometric requirements of individual operators. Visual displays can be placed beyond the keyboard and in line with the inclination of the keyboard to minimize the operator's head movement. In addition, the station is arranged so that the operator's eyes and hands are focused onto three primary control and display areas. This quickens operating response and decreases the chance of error, since the input devices and feedback to the operator are collocated.

The figure shows the work station and the three primary and three secondary work surfaces. A brief description of each feature follows:

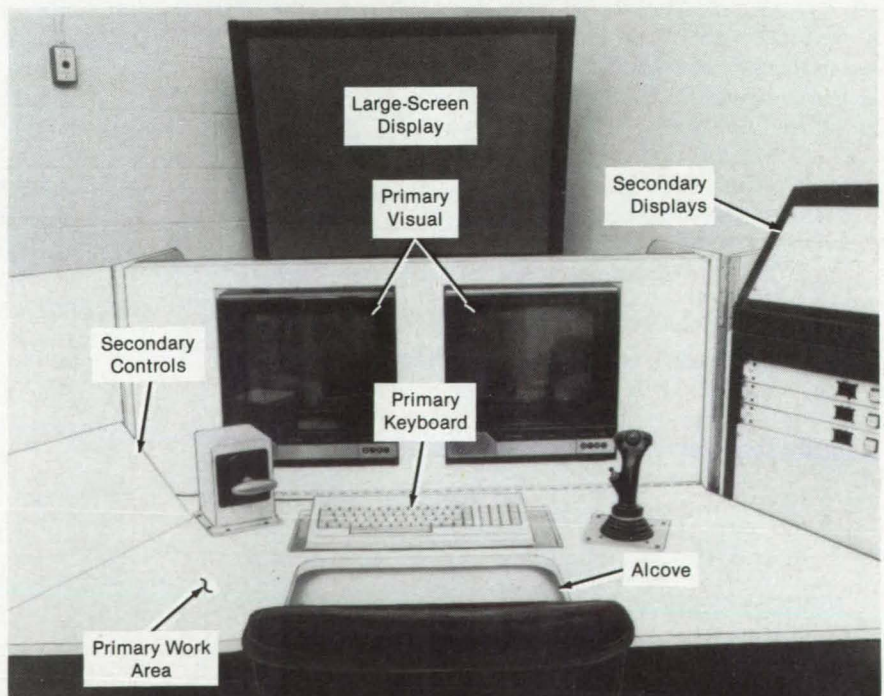
- The primary visual panel accommodates two video-display units of up to 19 in. (47.5 cm) diagonal and their associated controls.
- The primary keyboard panel is designed for a wide range of keyboard configurations. The panel is rotatable through a 30° arc.
- The primary work panel is a desk top with an alcove in front of the keyboard. The panel, which can be outfitted for hand controls, can be adjusted to tilt down, away from the operator, allowing

the full support of the arms during hand movements.

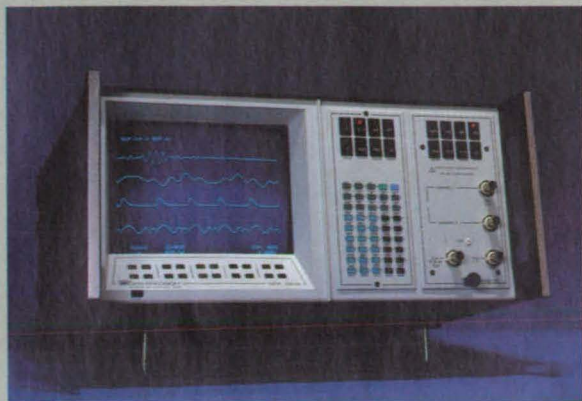
- The secondary control panels are slanted wings attached to the primary work table. These wings can be removed independently to permit reconfiguration.
- The secondary display panels are located on two vertical side wings. They form an environmental enclosure and allow the mounting of infrequently used displays.
- The large-screen display is a 3- by 4-ft (0.9- by 1.2-m) television projection display mounted in front of the workstation. This display, showing either of the two primary visual monitors or a third independent display, can be viewed by other people without disturbing the operator.

This work was done by Fred Roe of Marshall Space Flight Center and by Nicholas Shields, Jr., Mary Frances Fagg, and David Henderson of Essex Corp. For further information, Circle 36 on the TSP Request Card.

Inquiries concerning rights for the commercial use of this invention should be addressed to the Patent Counsel, Marshall Space Flight Center [see page 29]. Refer to MFS-26009.



The **Work Station** includes an adjustable work surface and equipment that can be tilted to suit the operator. The equipment is placed to minimize operator fatigue and errors.



DATA 6000 Waveform Analyzer



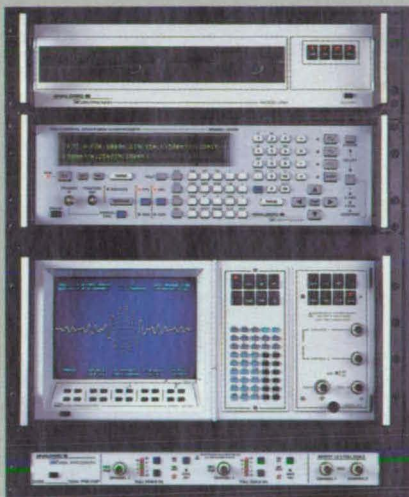
DATA 2020 Waveform Generator

Rule the Waves

Coming... or Going.

The DATA 6000 Universal Waveform Analyzer offers the ultimate in signal acquisition and on-board waveform analysis in one unit—without programming. Front panel commands are available for complex waveform operations, such as FFT and Correlation as well as scalar parameters such as Max., Min., Width, Rise, or PK-PK, using the display cursor and crosshair. For specialized measurements, the 6000 can also store analytical routines internally.

- Digitizing Plug-Ins from millihertz to 100MHz sample rates.
- An ultra-high dynamic range digitizing plug-in: 1MHz at 16 bits.
- Simultaneous multi-channel sampling with pre- and post-trigger transient capture.
- FFT (Magnitude and Phase), Convolution, Correlation, Waveform Average, Amplitude Histogram, etc.
- Direct plotter drive for HP-GL compatible plotters.
- Companion Model 681 Flexible Disk Drive for waveform and program storage.
- Full Programmability for ATE via IEEE-488 or RS-232 interface.



Combining the DATA 2020 and DATA 6000 yields an unbeatable system for signal acquisition, analysis and regeneration. Capture actual signals with the DATA 6000. They can then be modified or combined with other waveforms and down-loaded into the 2020 for regeneration. What was transient can become repetitive, available on call. Shown above, from top to bottom, are the 681 Flexible Disk, the DATA 2020, DATA 6000 and D-1000 Pre-Amplifier: products which give you the power to rule the waves both coming and going.

The DATA 2020 Polynomial Waveform Synthesizer provides an unprecedented ability to emulate real world signals, creating desired waveforms from mathematical definitions. Modify the ideal waveforms to add distortion, noise or glitches. Simulate degraded rise times, phase shifts . . . test the limits. Your systems and products must live in the real world. Emulate it with the 2020.

- Direct front panel or remote entry of mathematical equations of the form $Y=f(t)$.
- High-speed waveform generation—up to 25 megapoints per second at 12 bits (100 megapoints at 12 bits, optional).
- Large waveform output memory—up to 512K points, combined with non-volatile storage of hundreds of waveform equations.
- Standard Functions—sine, square, triangle with variable symmetry, plus white noise which can be summed with any signal.
- Arbitrary Mode including point entry, scope draw, and down-loading of the waveform memory.
- Full Programmability for ATE via IEEE-488 or RS-232 interface.

ANALOGIC ■

DATA PRECISION®

HEADQUARTERS: DATA PRECISION, Division of Analogic Corporation, Electronics Avenue, Danvers, MA 01923. Tel: 617-246-1600. Telex: 6817144.

ANALOGIC Ltd., The Center, Weybridge, Surrey, England KT138BN. Tel: 0932-56011. Telex: 928030 ANALOG G.

ANALOGIC GmbH, Daimlerstr. 2, 6200 Wiesbaden-Nordenstadt, W. Germany. Tel: 06122-4071. Telex: 4182587 ANA D.

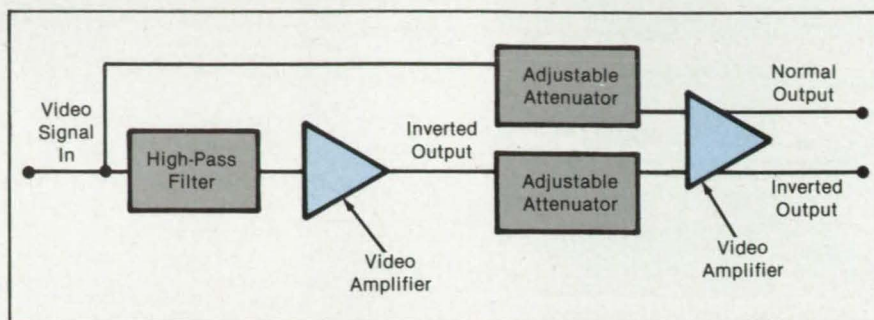
Please see us at ELECTRO booth #577 and ATE EAST booth #843.

For additional information Circle RAC No. 432
For a demonstration Circle RAC No. 433

Analog Video Image-Enhancing Device

This inexpensive system also yields a pseudo-three-dimensional effect.

Langley Research Center,
Hampton, Virginia



This **Analog Video Device** is added to a video monitor for image enhancement. The circuit is inexpensive, easy to use, and can be adapted to many closed-circuit video systems.

High Power Nd:YAG Laser Systems

- 30 kW TEM₀₀ @ 2 kHz
 - <100 nS Pulswidth @ 2 kHz
 - 10% Stability @ 30 kHz
 - Ultra Simple & Reliable
 - Low Maintenance



APPLICATIONS

- Marking
- Cutting
- Soldering & Welding
- Thick & thin film trimming
- Annealing
- Mask repairing
- Pumping Dye, F-center, and Raman lasers

Lee Laser staff personnel have designed and built over 2,000 CW:YAG lasers for OEM applications. They also have had extensive experience designing and integrating lasers into scientific, industrial and medical turnkey systems.

LEE LASER, INC.

3718 VINELAND ROAD, ORLANDO, FLORIDA 32811
305-422-2476

An analog video image-enhancing device improves the appearance of technical photographs by selectively compressing their overall dynamic ranges while accentuating edges or small details of greatest interest. Analog video circuitry is used to provide an inexpensive real-time image processing technique.


The system includes a video camera with a lens, connected to a video monitor. A circuit (see figure) is added to the monitor for analog video enhancement. The video signal is obtained from the monitor at a point beyond where the synchronization signals are detected, thus eliminating the need to regenerate a composite video signal.

The signal is high-pass filtered with an adjustable resistor/capacitor filter. The high-pass signal is then amplified with an adjustable-gain video amplifier. The unfiltered signal is also adjustable from a gain of near zero to about two. The two signals are added in a second video amplifier, and the sum is sent back to the monitor. Black-and-white reversal is possible in the second amplifier, allowing negatives as well as prints to be examined directly, as indicated in the figure.

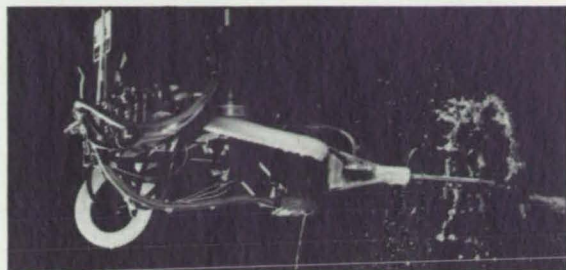
Adjustments of the new image parameters along with the conventional variability of monitor brightness and contrast enable the control of a wide range of image enhancement. In addition, the time constant on the high-pass filter results in a pseudo-three-dimensional effect, which, in some cases, shows detail more clearly.

This work was done by Leonard M. Weinstein of **Langley Research Center**. No further documentation is available.

This invention is owned by NASA, and a patent application has been filed. Inquiries concerning nonexclusive or exclusive license for its commercial development should be addressed to the Patent Counsel, Langley Research Center, [see page 29]. Refer to LAR-13336.



THE WAVE OF THE FUTURE IN NON-DESTRUCTIVE TESTING IS AVAILABLE TODAY.



As the industry leader in the use of composite parts, we understand the need for non-destructive testing that's fast, reliable and cost-efficient. To meet this need, we rely on AUSS IV, our Automated Ultrasonic Scanning System.

AUSS IV is a computer-controlled test and data handling system that automatically checks composite parts for delaminations, voids, ply slippage, foreign objects or other anomalies. AUSS IV is the result of intensive design development that began in 1973. It's thoroughly production proven, and it's the most advanced ultrasonic scanning system available today.

The system offers fully automatic inspection and plotting. Its high speed graphics terminal provides real-time display of ultrasonic data in true shades of gray. AUSS IV requires no programming knowledge for set-up or operation.

To find out more about AUSS IV and how it can help increase productivity while reducing costs, call Jim Dunn at (314) 233-8185, or Paul Fleetwood at (314) 234-9000. Or write:
AUSS, Dept. 080
McDonnell Aircraft Company
P. O. Box 516
St. Louis, MO 63166

**MCDONNELL
DOUGLAS**

Automated Signal-to-Noise Ratio Measurement

Computer-controlled spectrum analysis gives rapid results for communication systems.

Lyndon B. Johnson Space Center, Houston, Texas

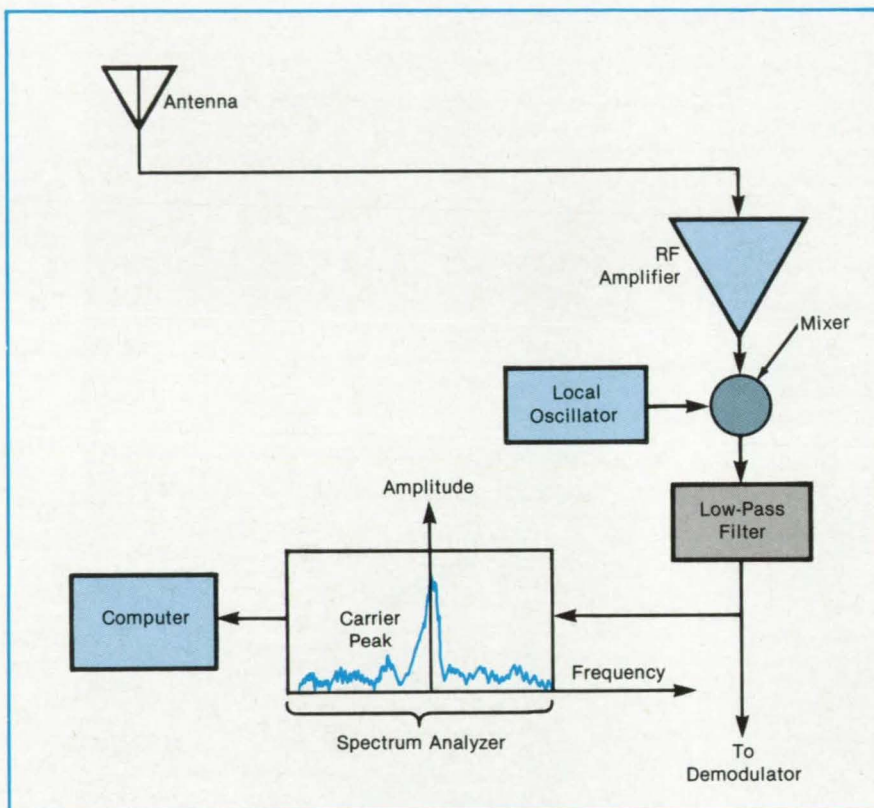
Based on spectrum analysis, an automated procedure for measuring the signal-to-noise ratio (S/N) in a radio-frequency (RF) signal has several advantages over the customary manual method:

- Measurements can be made quickly, without physical disruption of the communication link.
- The dynamic range is greater than with the power-meter method, making it possible to examine weak signals.
- The signal and noise can be differentiated without the adjustment of a variable attenuator, which cannot always be used when a signal is received from a remote transmitter.
- No external bandpass filter is required to find the S/N spectral density ratio.
- The old signal-on/signal-off technique requires the assumption that the system is linear, which is rarely the case. The new method requires no such assumption and provides more-accurate measurements because there is always a signal in the channel.

The new method was developed to obtain accurate and rapid measurements of the S/N ratio in digitally modulated signals transmitted from remote stations. The ratio is used to plot the received bit-error rate. This plot can be compared to a "best possible" curve to see how well a communication system is performing. The measurement of S/N is also needed to assess the radiated power, signal quality, and signal-tracking threshold.

As illustrated schematically in the figure, a spectrum analyzer is used to make several (e.g., 10) noise-amplitude measurements uniformly distributed in a pass band selected by the user and centered on the receiver intermediate frequency. The numerical average of these measurements is deemed to be the noise.

The spectrum analyzer finds the signal peak through its ability to find the strongest signal in a specified bandwidth. The search algorithm is performed four times, with a gradually-narrowing search bandwidth, the final search bandwidth, being a



A **Computer-Controlled Spectrum Analyzer** locates the carrier signal in the intermediate-frequency band and measures both the carrier amplitude and the amplitude of noise in several channels near the carrier frequency. The computer then computes the ratio of the signal to the average noise. Because the measurements and calculations are rapid, this system can be used in fading communication channels.

few hundred Hertz. The amplitude of this peak is measured and deemed to be the amplitude of the desired signal.

The corresponding S/N is then calculated by division of the measured signal by the measured noise. The algorithm used in the measurements and calculations is programmed into a micro-computer. The control of the spectrum analyzer is given to the computer, which can repeat the process for many data points, depending upon the type of communications-performance testing taking place.

This method of determining S/N cannot be applied to a modulated carrier signal; modulation suppresses the carrier

and produces sidebands that look like noise to the spectrum analyzer. Nevertheless, the high speed of the automated S/N-measurement process permits it to be carried out during brief periods when modulation is off. Hence, this method does not interfere appreciably with normal transmissions and does not incur a large delay that would cause a lack of correspondence between the bit-error rate and the S/N.

This work was done by Joseph E. Pineda of Lockheed Engineering and Management Services Co., Inc., for Johnson Space Center. For further information, Circle 59 on the TSP Request Card.
MSC-21021

Phase-Measuring System

The phase difference between a signal and its harmonic is displayed directly.

Langley Research Center, Hampton, Virginia

A system developed and in use at Langley Research Center measures the phase between two signals of the same frequency or between two signals, one of which is the harmonic multiple of the other. This simple and inexpensive device combines digital and analog components to give accurate phase measurements.

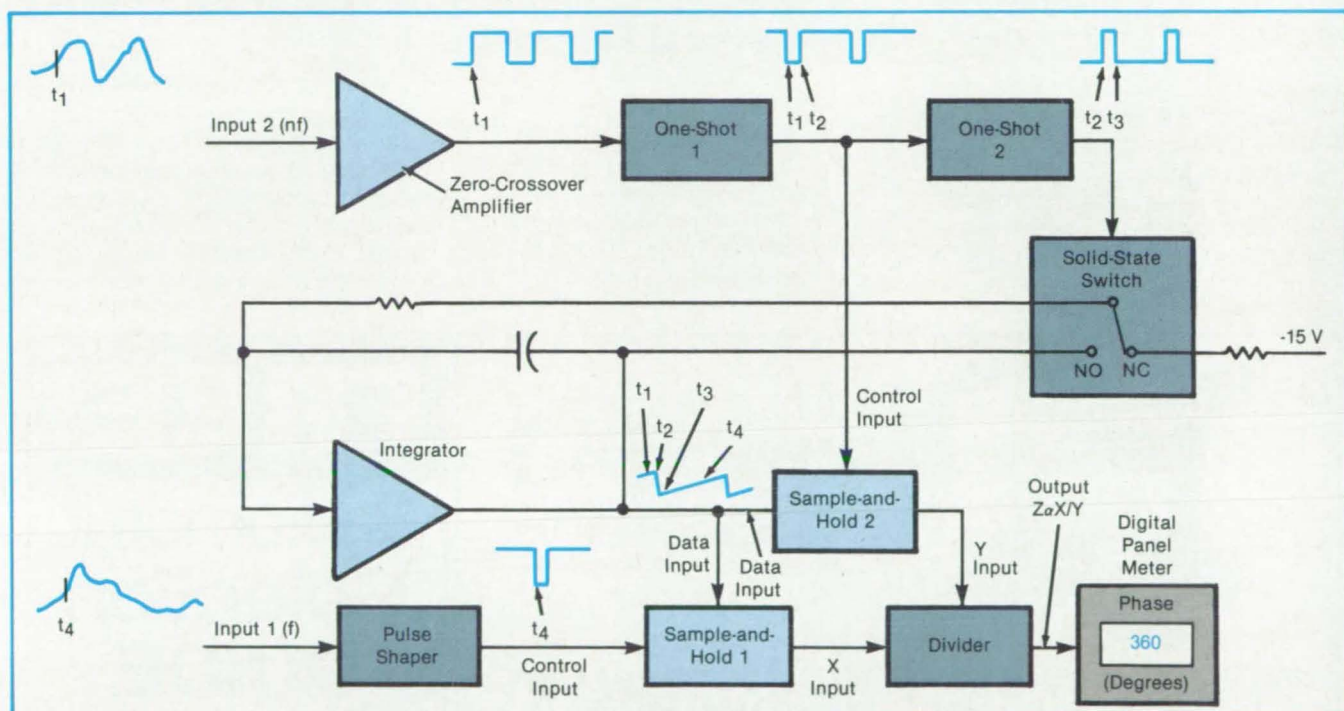
As shown in the figure, one signal at frequency f is fed to a pulse shaper, which produces a negative pulse at time t_4 . This pulse is applied to the control input of sample-and-hold module 1. The second signal, at frequency nf , is fed to a

zero-crossover amplifier, which produces a square wave at time t_1 . This signal drives the first one-shot, which produces a narrow negative pulse at t_1 . This signal then drives a second one-shot, which produces a narrow positive pulse at time t_2 . This pulse is used to turn on a solid-state switch and reset an integrator circuit to zero.

The output of the integrator is fed to the data inputs of the two sample-and-hold modules. Sample-and-hold module 2 receives its control pulse from one-shot 1 at t_1 and produces a dc output equal to

the maximum output of the integrator. This signal is fed to the Y input of the divider module. The output of sample-and-hold module 1 is a dc voltage equal to the integrator output level at time t_4 ; this voltage is fed to the X input of the divider. The output of the divider is a dc voltage proportional to X/Y and to the phase angle between the two input signals. The dc voltage is fed to a digital panel meter which, with proper scaling, displays the phase angle directly.

This work was done by William T. Davis of Langley Research Center. No further documentation is available.
LAR-13439



The Digital Panel Meter displays the difference in phase between harmonically related inputs 1 and 2.

Wireless "Jump" Starts for Partly Disabled Equipment

Equipment might be activated when normal remote starting does not work.

Lyndon B. Johnson Space Center, Houston, Texas

A scheme for activating a satellite crippled by discharged storage batteries would allow the Space Shuttle crew to turn on the satellite even though it does not respond to the normal initiation signals from Earth. The scheme would make extravehicular activity by the crew unnecessary for

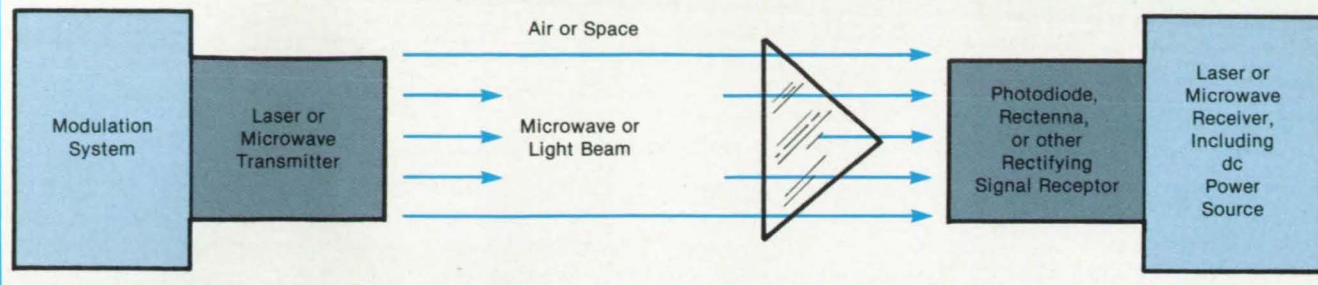
starting the satellite. Potential terrestrial applications for the scheme could include the starting of robots on such remotely-controlled hazardous tasks as the handling of explosives or retrieval or deposition of objects in hostile environments.

Ordinarily, the satellite is activated

by a telecommunication link from an Earth station or perhaps another satellite. If this primary activation method fails to get the equipment started, the proposed backup method would be implemented. The Space Shuttle or other mobile control/service station would project a powerful microwave beam or

MOBILE CONTROL/SERVICE STATION

REMOTELY CONTROLLED EQUIPMENT



A Beam From a Nearby Station first carries raw energy and then the subsystem-activating signals to equipment crippled by the discharged storage batteries. With this scheme, operators can start up the equipment without approaching it under hazardous conditions.

intense light beam toward the disabled equipment (see figure). Rectifying antennas, Shockley diodes, photosensors, or other devices on the equipment would receive the beam energy and convert it to direct current. This electrical power would provide the boost the equipment needs to activate its batteries or solar cells or both. The command signals then would be superimposed on the beam so that the control and communication systems on the equipment could be activated.

At this point, control would revert to the Earth station or other normal remote-control point. Normal deployment of the equipment would resume. To prevent unauthorized startup of the equipment, the Space Shuttle or mo-

bile control/service station would first transmit the normal remote-control security code to the equipment.

This work was done by Kent D. Castle of Johnson Space Center. No further documentation is available. MSC-21010

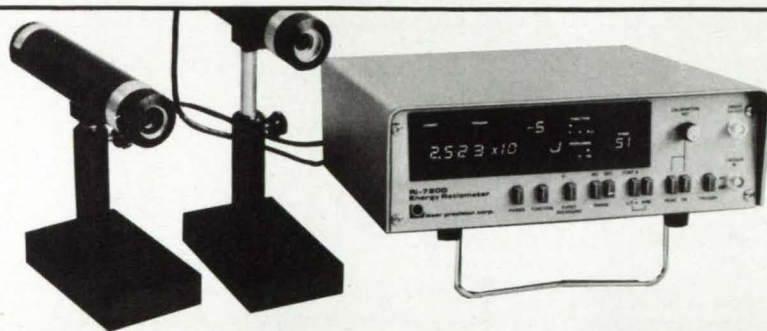
Books and Reports

These reports, studies, and handbooks are available from NASA as Technical Support Packages (TSP's) when a Request Card number is cited; otherwise they are available from the National Technical Information Service.

Radiation Hardening of Computers

Single-event upsets are reduced by use of oversize transistors.

Computers can be made less susceptible to ionizing radiation by replacing bipolar integrated circuits with properly designed, complementary metal-oxide-semiconductor (CMOS) circuits, according to a report. CMOS circuit chips can be made highly resistant to single-event upset (SEU), especially when certain



PULSED ENERGY MEASUREMENT

*"unsurpassed for speed, sensitivity, & accuracy
... UV to Far IR, picojoule to joules"*

Rjp-7000 SERIES microprocessor based ENERGY METERS, available in single or dual channel readout. Features scientific notation readout, autoranging, BCD output, EMI rejection, and wide dynamic range. Direct readout of individual pulse energies with repetition rates up to 40pps and pulse length from picoseconds to one millisecond. The measurement range is from 10^{-8} to 10 joules (pyroelectric), down to 10^{-13} with the silicon probe. A broad selection of probes are available to meet your requirements.

PROBE SPECIFICATIONS (with either readout)

MODEL	TYPE	AREA	RESOLUTION*	MAX. SIGNAL	SPECTRAL RESPONSE
Rjp-734	Cavity	5.0cm ²	1x10 ⁻⁵	1x10 ⁶ W/cm ²	$\pm 1/2\%$ (0.4-3 μ m); $+1/2\%$, -4% (0.25-16 μ m)
Rjp-735	Cavity	1.0cm ²	1x10 ⁻⁷	1x10 ⁶ W/cm ²	$\pm 1/2\%$ (0.4-3 μ m); $+1/2\%$, -4% (0.25-16 μ m)
Rjp-736	Flat	20.0cm ²	1x10 ⁻⁴	1x10 ⁶ W/cm ²	$\pm 3\%$ (0.4-1 μ m); $+3\%$, -9% (0.35-11 μ m)
Rjp-765	Silicon	1.0cm ²	5x10 ⁻¹³	5W/cm ²	0.3-1.1 μ m (not flat)

*Single event, 10X and 100X averaging available

from the leader
in optical radiation
measurements.....



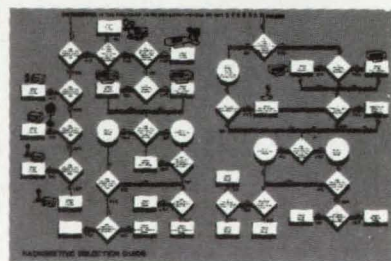
For more information, contact:

laser precision

1231 Hart Street, Utica, NY 13502 (315) 797-4449

FREE!

Radiometric Selection Guide



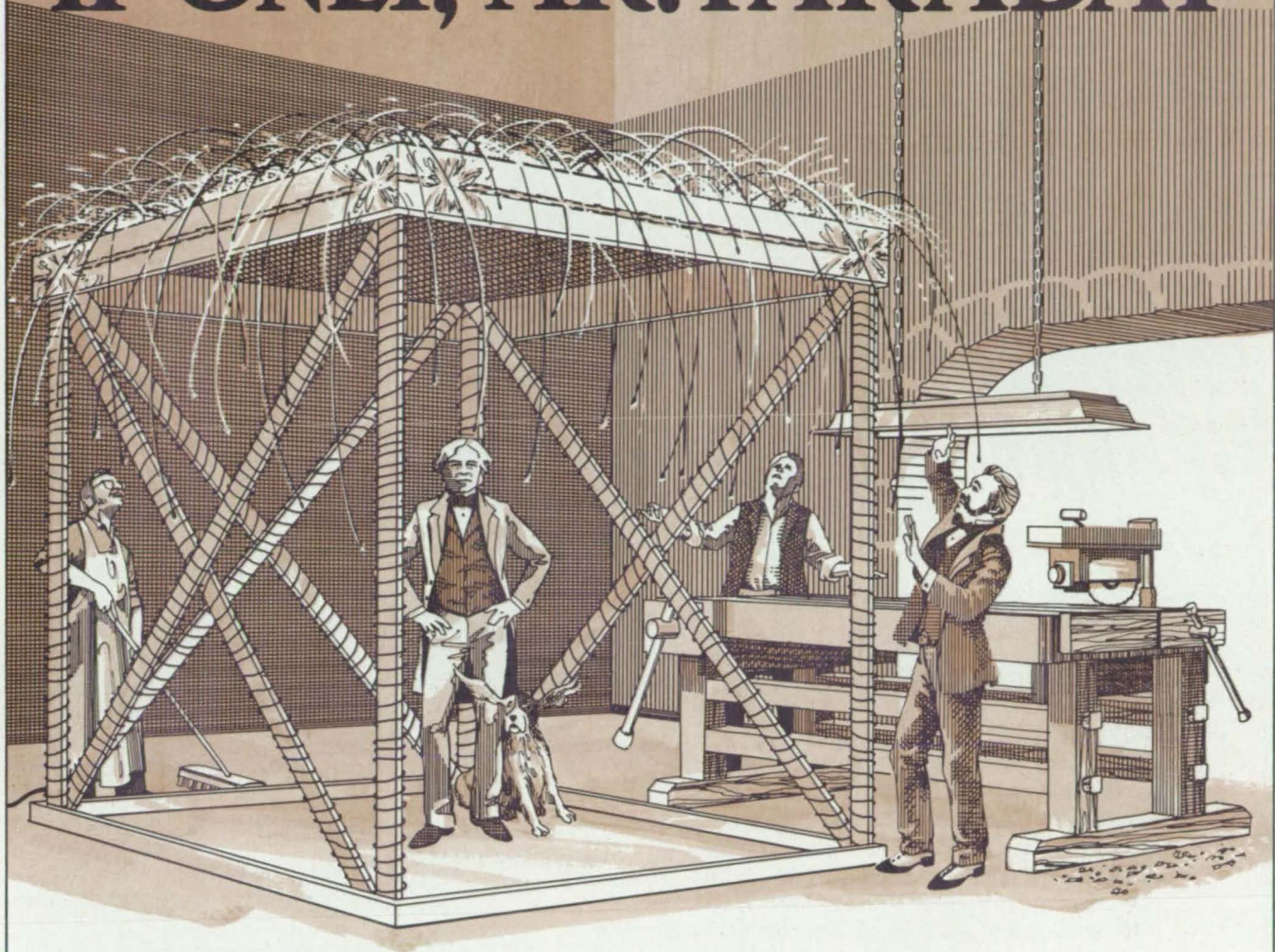
The easy way to select the right power meter, energy meter, radiometer, or detector to fit your requirements.

(UV to far IR, picowatt to kilowatt, picojoule to joules)



CIRCLE NO. 302

IF ONLY, MR. FARADAY



...had gone through on-screen prototyping of his electromagnet with the AOS/MAGNETIC™ Analysis Program. He could have learned its optimum electrical efficiency without making costly physical prototypes.

Imagine how the AOS/MAGNETIC Analysis Program would have helped Mr. Faraday design his electromagnet faster and with a great deal more efficiency.

It may be too late for Mr. Faraday, but not for you to vastly improve your designs by

using the AOS/MAGNETIC Analysis Program. You only need to call us and we'll show you how we can help you look great while we save you money.

CALL US AT

1-800-MAG-6442
IN WISCONSIN 414-357-2706



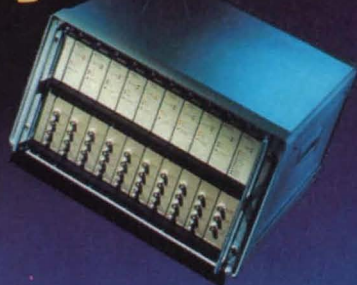
A. O. SMITH
DATA SYSTEMS, INC.

A SUBSIDIARY OF A. O. SMITH CORPORATION
8901 N. Kildeer Ct., • Milwaukee, WI 53209

While you're chatting, ask our representative to deliver a poster of Faraday at work, suitable for hanging in your office.

In 1836, James Faraday stood inside a 12' x 12' x 12' box he constructed to prove that electricity follows pathways. His experiments led to the practical use of electricity.

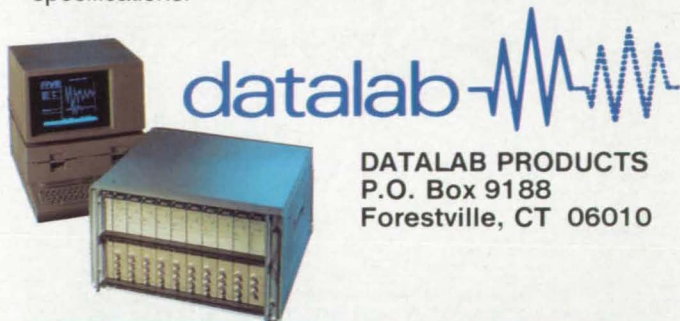
Track Tomorrow Today



Use multichannel transient waveform recording to put you on a course you'll find hard to believe. MULTITRAP is an easy-to-use system with the flexibility to do hundreds of different tasks. It is totally software controlled. Elimination of front panel controls (no dials, knobs or buttons) assures accuracy and reliability. Individual modules let you choose the sampling rate, number of channels, record lengths, timebases and transfer rates needed for your application.

Easy to setup and record; MULTITRAP also provides immediate access to results and complete software for analysis and integration of acquired data. A/D performance certification is also available.

Find out more about MULTITRAP, the expandable signal capture system from Datalab Products, Inc. Call George Wedge at 203-582-3898. Or write for our capabilities and specifications.



DATALAB PRODUCTS
P.O. Box 9188
Forestville, CT 06010

Lease or rental available for short term needs.

Inquire now for rates and availability 203-582-3898

feedback resistors are incorporated. The redesigned chips also consume less power than do the original chips.

CMOS replacements for nine types of bipolar logic circuits were constructed. Two techniques were used to increase the resistance to radiation. One is the use of oversize transistors. Feedback resistors are also inserted in the regeneration path of most latches to increase the time of responses to particle hits to well beyond the durations of the disturbances.

The use of larger-than-minimum transistors helps in two ways: The increased current drive causes a struck node to be restored more quickly, and the higher gate capacitance permits a corresponding decrease in the size of the feedback resistor required to achieve a given regeneration time. The increase in size beyond the minimum required for sufficient speed, reduces the dependence on resistors to the point where they are not critical to adequate immunity to SEU. Moreover, because the CMOS chips are small relative to area constraints imposed by processing yield, it is feasible to use oversize transistors without making the replacement chips unduly large.

When resistors are used to enhance the resistance to SEU, they are incorporated into the chips by one additional processing mask step; it is thus possible to fabricate in parts with and without the extra resistors in one wafer lot. The resistors are positioned in circuits so that the read-access times of memories and the propagation delays of latches are not significantly degraded. The resistors degrade the computer speed somewhat. For example, the write time for memories and the setup time for latches are increased by about 12 ns and 2 ns, respectively, for a 2901 4-bit microprocessor slice when 80-k Ω resistors are added.

Tests were conducted to determine the linear-energy-transfer (LET) thresholds for the CMOS replacement parts by subjecting them to 165-MeV krypton ions at a minimum fluence of 2×10^7 particles/cm² in a cyclotron. All data were taken with a power supply operating at 4.5 V, making the devices more susceptible to SEU than at their normal 5.0 V operation. The LET thresholds of all the tested CMOS circuits, both with and without resistors, were above the desired LET value of 37 MeV/mg/cm².

This work was done by Donald K. Nichols, Lawrence S. Smith, and John A. Zoutendyk of NASA's Jet Propulsion Laboratory and Alfred E. Giddings, Frank W. Hewlett, and R. Keith Treece of Sandia National Laboratories. To obtain a copy of the report, "SEU Immune ICs for Project Galileo," Circle 26 on the TSP Request Card. NPO-16767

Laser Inertial Navigation System

Acceptable accuracy is obtained with short alignment time.

A report describes successful helicopter tests of laser inertial navigational equipment. The tests were conducted over a 3-year period, both in a laboratory and in flight. The inertial system was used as a position/velocity/attitude indicator and later also served as part of an automatic flight-control system.

The inertial-system sensing head includes integrating laser gyroscopes and linear accelerometers. Each laser gyroscope senses the rotation about a single axis in terms of the phase shift between two laser beams launched along opposite paths about the axis. Each linear accelerometer operates similarly, except that the paths and the sensed motion are along the axis.

There are two variations on the sensing-head design: The triad version has three mutually-perpendicular sensing axes, while the tetrad version includes an additional skewed sensing axis along the diagonal of the cube represented by the first three axes. The fourth gyroscope-and-accelerometer set provides redundant sensory data for fault detection and for studies of redundancy management.

The sensing head is of the "strap-down" type; that is, it is simply mounted in the aircraft and not gimballed. Associated with the sensing head are a control-and-display unit, a system to record flight data, and a dual navigational computer.

The computer program includes provisions for detecting malfunctions in the sensors. As an example, one indication of sensor failure would be that the scalar difference (called the "parity residual") between the skewed-sensor output and the vector sum of the orthogonal-sensor outputs exceeds the background noise by a prescribed amount. When a fault is detected in any of the four axes, the sensor data for that axis can be excluded from the navigation calculation, allowing the system to continue operating with the three remaining sensors.

In the flight tests of the triad and tetrad systems, acceptable navigational accuracy was obtained after computer-controlled alignment procedures lasting 5 minutes or less before each flight. (Alignment is performed with the sensing head in place.) Failure detection using the four-axis parity residual was successful at failure levels far below the noise threshold of flight-sensing requirements.

NASA Tech Briefs, May/June 1986

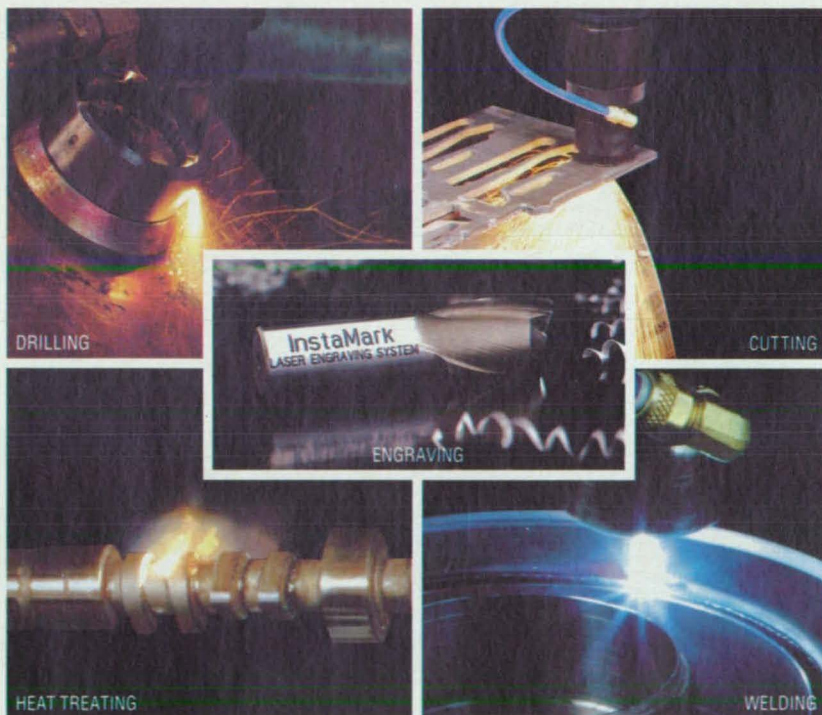
In the digital navigation-and-control system, the laser inertial equipment provides attitude, position, and velocity information that is combined with information from a microwave landing system and with control signals from the pilot. The processed combination of inputs is fed to the aircraft servocontrol system. Such a navigation-and-control system performed well in automatic-flight tests in which a helicopter landed from straight and level flight by first entering a two-turn descending helix, then emerging from the helix in line with a runway, and then decelerating to a hover 4.7 m above the

landing point.

This work was done by Ronald J. Hruby and G. Xenakis of **Ames Research Center**, Ralph A. Carestia of the University of Southern Colorado, William S. Bjorkman and S. F. Schmit of Analytical Mechanics Associates, Inc., and L. D. Corliss of the U.S. Army Aeromechanics Laboratory. For further information Circle 45 on the TSP Request Card.

Inquiries concerning rights for the commercial use of this invention should be addressed to the Patent Counsel, Ames Research Center [see page 29]. Refer to ARC-11473.

WE HAVE THE LASER SYSTEMS TO MATCH YOUR APPLICATIONS



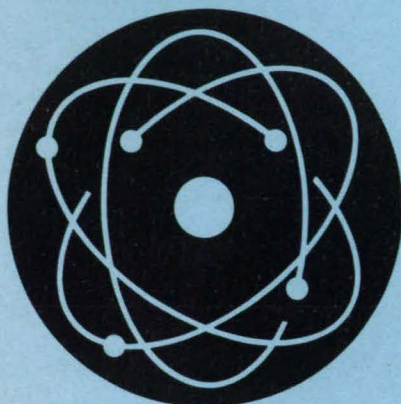
Control Laser makes the widest range of industrial laser systems and machining centers available anywhere in the world. Thus, we are uniquely able to offer the type of laser — CW and Q-switched CW Nd:YAG, pulsed Nd:YAG or CO₂ — required to meet a customer's cutting, welding, drilling, heat treating and engraving requirements. If you have a material processing problem, call CLC and discuss it with our knowledgeable sales engineers — perhaps laser machining is the answer!

Control Laser

11222 ASTRONAUT BLVD. • ORLANDO, FLORIDA 32821 • 305/851-2540 • TELEX 564407 • WATS 800/327-6036

Circle Reader Action No. 315

Physical Sciences



Hardware, Techniques, and Processes

- 54 Echelle/Grism Spectrograph
- 56 Vacuum-Ultraviolet Intensity-Calibration Standard
- 57 Measuring Seebeck Coefficients with Large Thermal Gradients
- 58 Sunlight Simulator for Photovoltaic Testing

Books & Reports

- 59 Electron-Diffraction Analysis of Growth of GaAs

Computer Programs

- 78 Predicting the Cosmic-Ray Environment Near Earth

Echelle/Grism Spectrograph

More even spectral dispersion over the detector area makes all wavelengths more distinguishable.

Goddard Space Flight Center, Greenbelt, Maryland

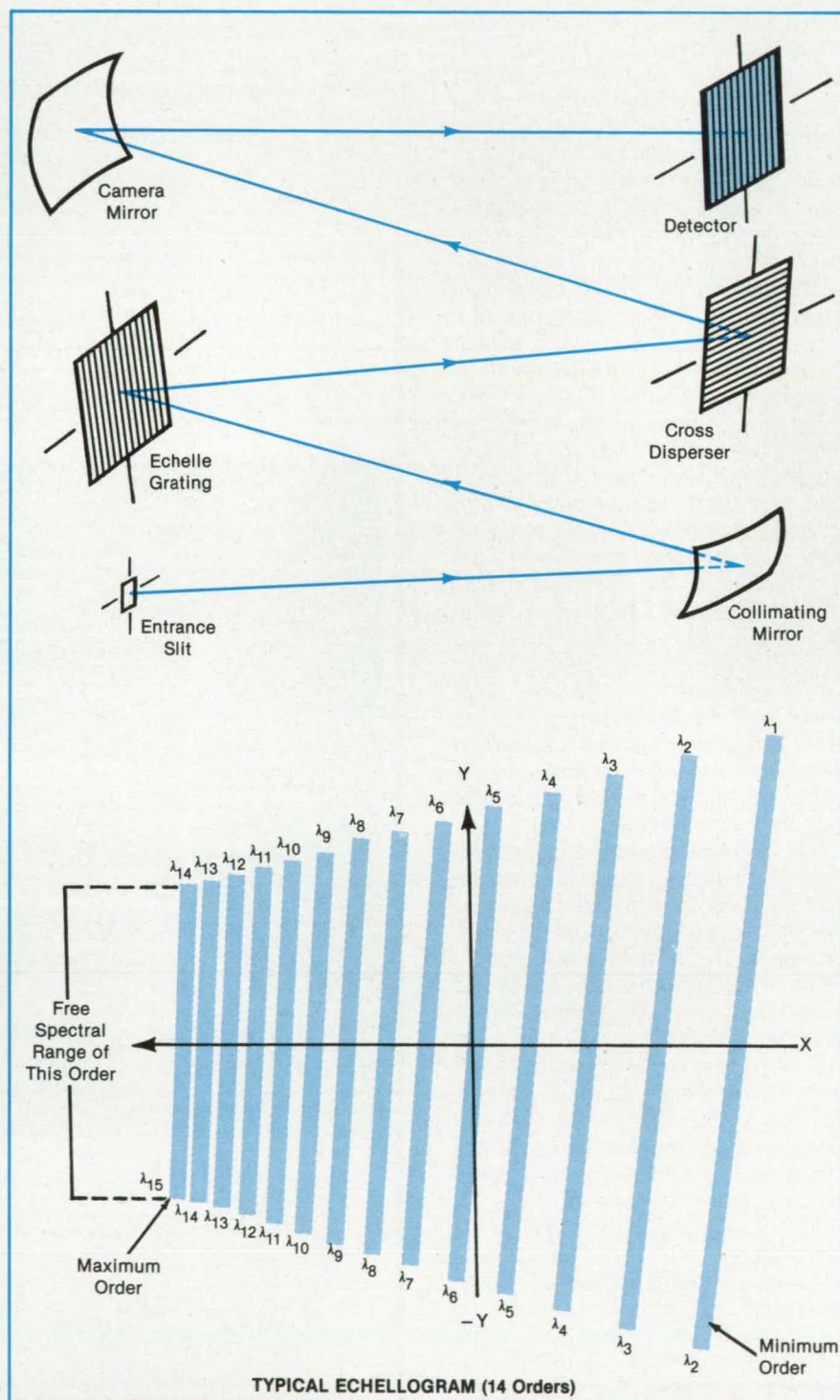
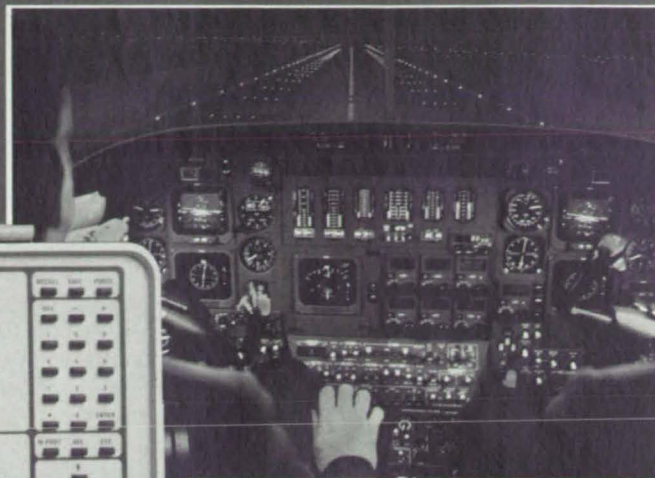


Figure 1. A **Conventional Echelle Spectrograph** (above) includes two diffraction gratings operating in two perpendicular planes. The instrument produces a two-dimensional spectrogram (below) showing several lines that correspond to different diffraction orders.

**The Precision Approach to Microwave Landing
Simulation...When
Accurate Calibration
is Critical**

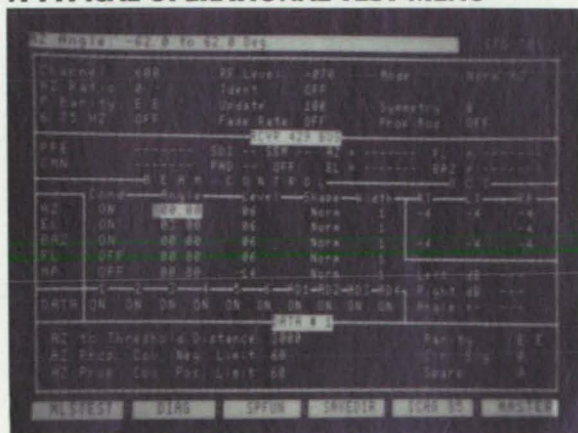


THE MLS-800

MICROWAVE LANDING SYSTEM TEST SET

*High-precision test equipment for the industry's most
precise landing system*

A TYPICAL OPERATIONAL TEST MENU



The parameters displayed on the MLS test menu are in accordance with the RTCA/DO-177 specifications, FAA STD 22b of October, 1983, ICAO SARPS of April, 1981 and the proposed ICAO SARPS of 1985.



The MLS-800: A microprocessor controlled simulator, designed to test airborne MLS angle receivers on the bench or verify system operation on the ramp.

Impressive Standard Features Include:

- Complete mainpath simulation
- Multipath simulation capability
- Control of all beam parameters
- Simulates all basic data words plus auxiliary data words with parity selection
- Full range of MLS channels
- ARINC 429 receiver data with PFE (Path Following Error) and CMN (Control Motion Noise) calculations

Remember IFR. The name you respect in test equipment. Write or call your IFR Distributor today and arrange for a demonstration. *The best is cost effective.*

IFR SYSTEMS, INC. 10200 West York Street / Wichita, Kansas 67215 U.S.A. / 316 / 522-4981 / TWX 910-741-6952

Circle Reader Action No. 317

A proposed echelle spectrograph would include a grating/prism combination, called a "grism," to make the spectral dispersion over the detector more even than it usually is in such instruments. The instrument performance would thus be improved, with little additional manufacturing effort. Furthermore, since the grism would be placed within collimated light and its faces would be optically flat, it would introduce no aberrations into the optical system.

In a conventional echelle spectrograph (top of Figure 1), collimated light is first diffracted by an echelle grating to a high order in one plane, then diffracted by a second grating (called a "cross disperser") in a perpendicular plane. The resulting dispersion spreads the spectrum out on the detector plane in two dimensions as several diffraction-order lines side by side, with the wavelength varying with its position along each line.

The diffraction angle in each diffraction plane, and therefore the placement of each order line on the detector plane, varies nonlinearly as $\sin^{-1}(C_1 \lambda + C_2)$, where C_1 and C_2 are constants, m = the diffraction order, and λ = wavelength. If large spectral coverage or resolving power or both are required, then as shown at the bottom of Figure 1, the order lines become crowded near one end of the spectrogram. Crowded order lines tend to make the wavelength lines within the order lines indistinguishable,

thereby rendering the instrument useless in the affected portion of the spectrum.

In the improved spectrograph, the cross disperser is replaced by the grating/prism combination of Figure 2. The light from the echelle grating is refracted into the prism, diffracted by the grating, then refracted back out of the prism. The sum of the direction changes introduced by refraction at the prism surface varies with the wavelength and order in such a way that the sum compensates for part of the order-line crowding of the grating.

The final position of each spectral component at the detector is now an even-more-complicated nonlinear function of the angle of incidence, prism vertex angle, prism index of refraction, wavelength, and order. However, the prism parameters can be chosen to reduce the order-line crowding, even to almost completely eliminate the nonlinear effect of the cross disperser. Thus, the orders would be spread out almost evenly, allowing more of the detector area to record useful information. The instrument can therefore be designed for greater spectral coverage, resolving power, or both.

This work was done by Andrew A. Dantzler of Goddard Space Flight Center. For further information, Circle 83 on the TSP Request Card.
GSC-12977

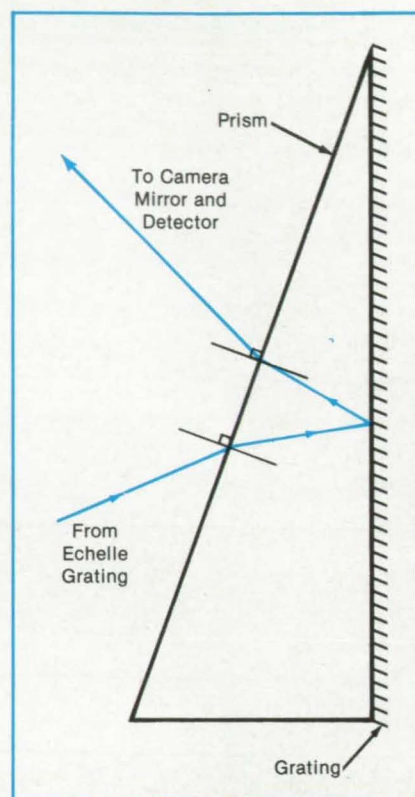


Figure 2. The Grating/Prism Combination "Grism" is used in place of the cross disperser of Figure 1. The refractive property of the prism can be exploited to compensate for some or most of the nonlinearity introduced by the grating.

Vacuum-Ultraviolet Intensity-Calibration Standard

A portable light source enables the calibration of spectrometers.

NASA's Jet Propulsion Laboratory, Pasadena, California

Spectrometers equipped with photo-detectors can be calibrated on a relative basis in the full vacuum-ultraviolet (VUV) wavelength range of 40 to 200 nm, by use of a simple, compact laboratory source of radiation and a theoretical model that relates the emission intensity as a function of wavelength to the molecular constants of the gaseous emitters in the source. Previously, there were blackbody standards in the visible and near ultraviolet, but there were no intensity-calibration standards in the VUV.

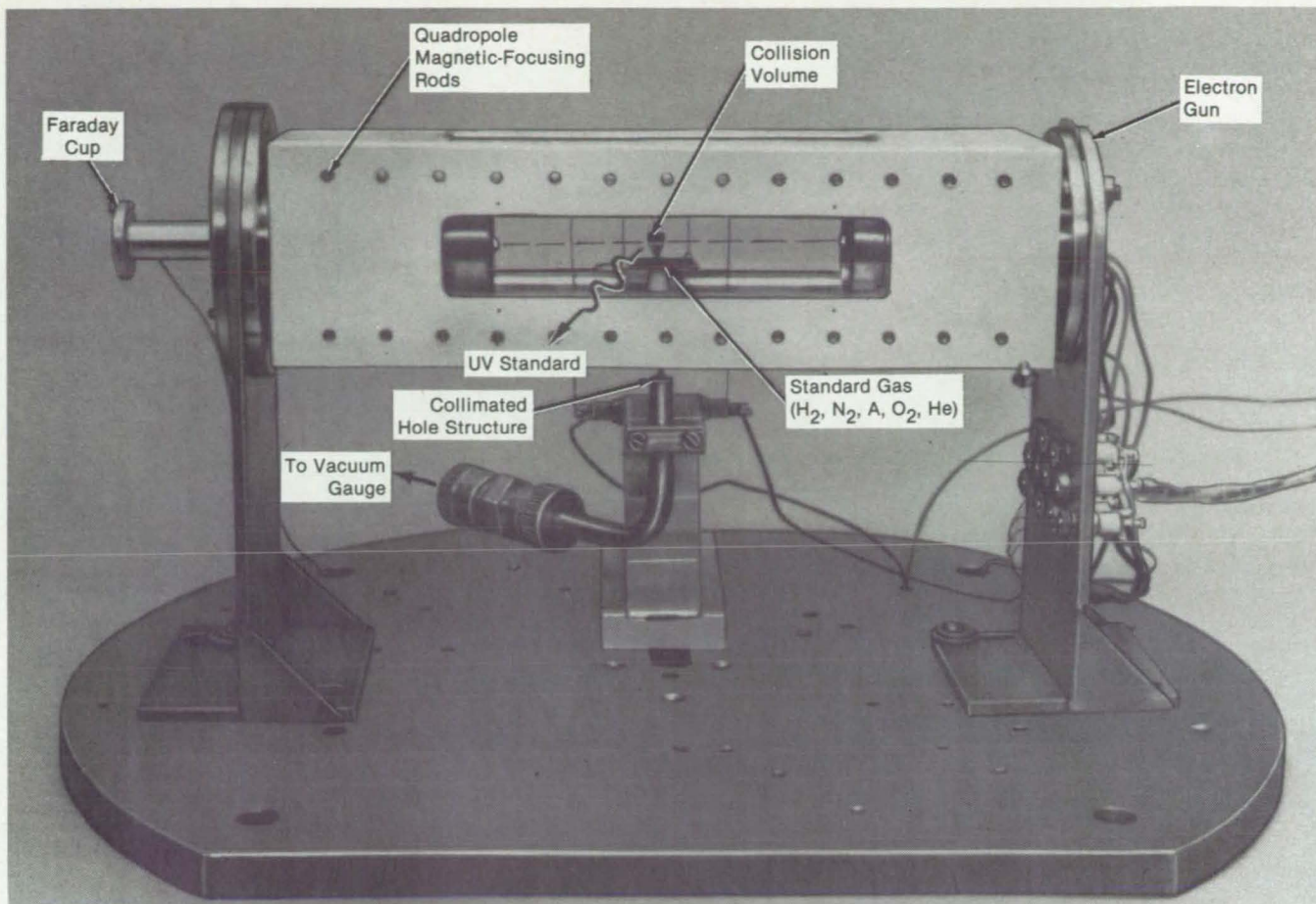
The source in which various gases are excited by electron impact is shown in the figure. In an electron-impact emission chamber, a magnetically collimated beam of electrons of variable energy (1 eV to 1 keV) is crossed with a beam of gas formed by a capillary array. The adjustable background gas pressure varies

from 1×10^{-7} to 2×10^{-5} torr (1.3×10^{-5} to 2.6×10^{-3} N/m²). Inelastic collisions between electrons and molecules cause the emission of photons, which are observed perpendicularly to the electron beam.

This source was used to measure laboratory standard electron-impact VUV spectra for important band systems of H₂ and N₂, which include two Rydberg series of H₂, L α , and L β dissociatively excited from H₂ and the N₂ ($a^1\Pi_g \rightarrow X^1\Sigma_g^+$) band system. The H₂ standard spectrum extends from 80 to 170 nm, and the N₂ standard spectrum extends from 110 to 260 nm. These spectral measurements agreed within 10 percent of those calculated from a theoretical model, which included vibrational and rotational structures of the electron-excited systems at the resolution of the laboratory spectrometer. Such

a close agreement shows that this source can serve as a relative intensity-calibration standard for VUV instruments in the region of 80 to 170 nm, provided that account is taken of optical-depth effects for foreground abundances greater than 3×10^{12} cm⁻² with H₂ as the calibration gas.

In a typical laboratory procedure, for example, in calibrating a spectrometer in the range of 80 to 170 nm, the H₂ pressure in the capillary array is 0.1 torr (13 N/m²), and a 100-eV, 200- μ A electron beam is produced by a Pierce electron gun, magnetically focused by quadrupole rods. The electron beam is collected and monitored by a Faraday cup to ensure that all electrons leaving the electron-gun aperture are collected. To be calibrated, the source spectrum is then recorded by the spectrometer. The desired relative



Vacuum Ultraviolet Light (40 to 200 nm) is produced in an electron-impact emission chamber by leading a beam of gas across an electron beam. The photons are observed at right angles to the electron-beam axis.

sensitivity of the spectrometer is the measured spectrum divided by the synthetic (theoretical) spectrum of the same resolution. The flight Galileo Ultraviolet spectrometer and the Spartan Halley Ultraviolet spectrometer were calibrated at the University of Colorado by this portable UV light source.

Current work on argon will allow calibration to be extended to the lower wavelength limit of 40 nm. The absolute calibration can be determined by normalization at a single wavelength by other means: (a) blackbody standard near 200 nm, (b) comparison to a calibrated photodiode, and (c) same electron beam

source described above in static gas mode using a standard cross section; e.g., He (58.4 nm).

This work was done by Joseph M. Ajello and Brian O. Franklin of Caltech for NASA's Jet Propulsion Laboratory. For further information, Circle 32 on the TSP Request Card.
NPO-16621

Measuring Seebeck Coefficients With Large Thermal Gradients

An apparatus takes measurements and analyzes data automatically.

NASA's Jet Propulsion Laboratory, Pasadena, California

The search for thermoelectric materials for the conversion of heat to power will be aided by a highly automated apparatus that measures Seebeck coefficients rapidly and accurately. Conveniently shaped samples are used, and the results are calculated by a microcomputer and printed out.

The Seebeck coefficient is obtained from short, rod-shaped samples by the NASA Tech Briefs, May/June 1986

"integral" method of measuring the Seebeck voltage, $V(T)$, in which one end of a sample is held at a fixed temperature, T_c , while the other end is varied automatically through the temperature range of interest (up to a maximum temperature, T , of 1,300K). The Seebeck coefficient, $S(T)$, is obtained from $S(T) = dV(T)/dT$.

As shown in the figure, the sample is

pressed (by external springs) between a resistance-heated molybdenum cylindrical furnace and a copper water-cooled plate. Thermal insulation between the hot and cold plates is provided by either bulk fiber or, preferably, multiple molybdenum radiation shields. The entire apparatus is inside a bell jar evacuated to about 10^{-7} torr (10^{-5} N/m²).

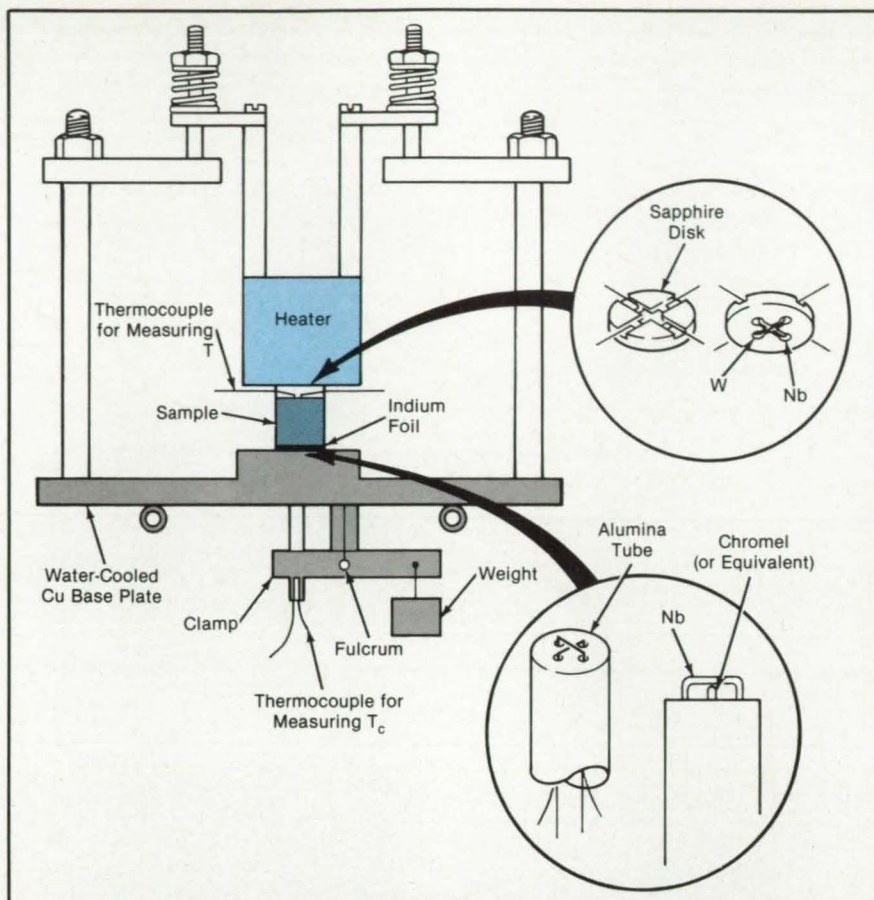
For the cold junction, a single strand of

Nb thermocouple wire is threaded through two diametrically opposite holes of a four-bore Al_2O_3 tube, and a single strand of w Chromel (or equivalent) wire is threaded through the other two holes; the two wires cross at the tube end and form the thermocouple junction. The wires are pressed against the bottom of the sample by means of a lever and a weight. An In washer is used to lower the thermal resistance between the sample and the cold plate.

A similar thermocouple configuration is used for the hot junction, except that the Al_2O_3 tube is replaced by a sapphire button. The external spring pressure on the hot plate presses this junction on the end of the sample. The voltages produced by the two thermocouples provide both T_c and T and the Seebeck voltage, $V(T)$. In this way the ideal is approached of measuring the temperature (T) and the Seebeck voltage at the same points on the specimen.

The temperature of the hot-plate furnace is automatically increased slowly above room temperature by increasing the input from a variable transformer driven by a geared-down electric motor. A W/Nb thermocouple is used to monitor the furnace temperature and provide input to a set-point temperature controller. At a predetermined temperature, the output of the controller causes the motor to reverse and the temperature to decrease slowly back to room temperature. Throughout each cycle, the Seebeck data are fed to a microcomputer; the final results are printed in tabular form and plotted.

This work was done by Charles Wood,



In this **Apparatus for Measuring Seebeck Coefficients**, a cylindrical sample is pressed between a heater and a water-cooled baseplate. Thermocouples at opposite ends of the sample provide both the temperatures and the Seebeck voltages.

Artur Chmielewski, and L. Daniel Zoltan
of Caltech for **NASA's Jet Propulsion
Laboratory**. For further information, Cir-

cle 7 on the TSP Request Card.
NPO-16667

Sunlight Simulator for Photovoltaic Testing

A flashlamp array and a filter provide spectral irradiance resembling that of sunlight.

NASA's Jet Propulsion Laboratory, Pasadena, California

Light with normalized spectral irradiance resembling that of air mass 1.5 sunlight striking the surface of the Earth is produced by use of an ultraviolet filter to modify the output of a set of flashlamps used as a large-area pulsed solar simulator (LAPSS). This filtered LAPSS light allows more realistic measurements of the output of photovoltaic devices when using a silicon reference cell having a different spectral response characteristic.

Spectral mismatches between light sources can cause errors in the measurement of the output of photovoltaic devices. These errors are large when the

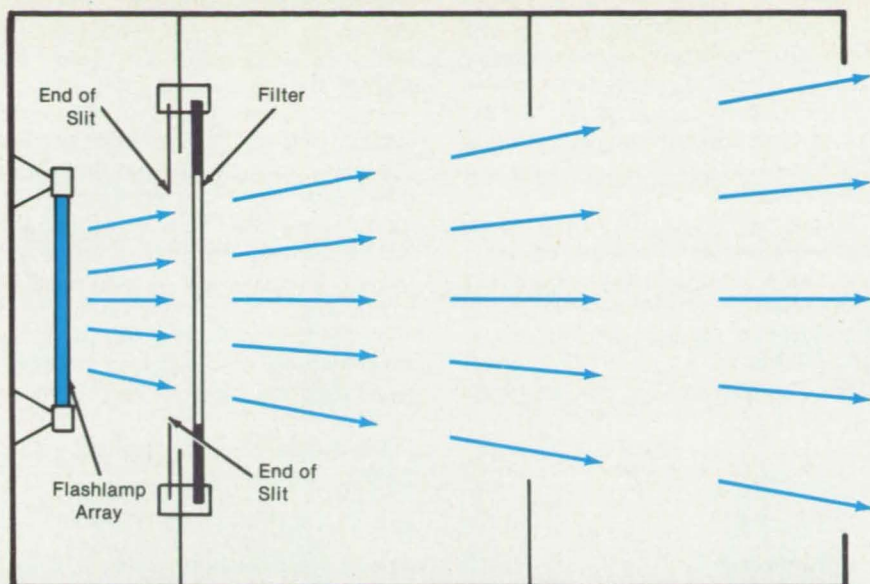
reference cells used to measure light-source intensities have spectral responses different from those of the photovoltaic devices being tested. The spectrum of the filtered light is more realistic for evaluating such devices, especially the new narrow-band, thin-film devices.

Measurement errors can be reduced to 1 percent by use of a 1-mm-thick Schott GG-395 (or equivalent) filter with a slit sized to insure uniformity of illumination at the target plane and restore the desired intensity. As shown in the figure, the filter reduces the ultraviolet portion of the unfiltered flashlamp irradiance curve,

thus producing a curve that averages well with the standard air mass 1.5 global curve.

For five wavelength bands, covering the intervals between 300 nm and 1,100 nm, the minimum ratio of normalized irradiance of the filtered light to that of standard air mass 1.5 global light is 0.884, and the maximum ratio is 1.099. This is substantially better than the ratio range of 0.75 to 1.25 allowed for a Class A solar simulator.

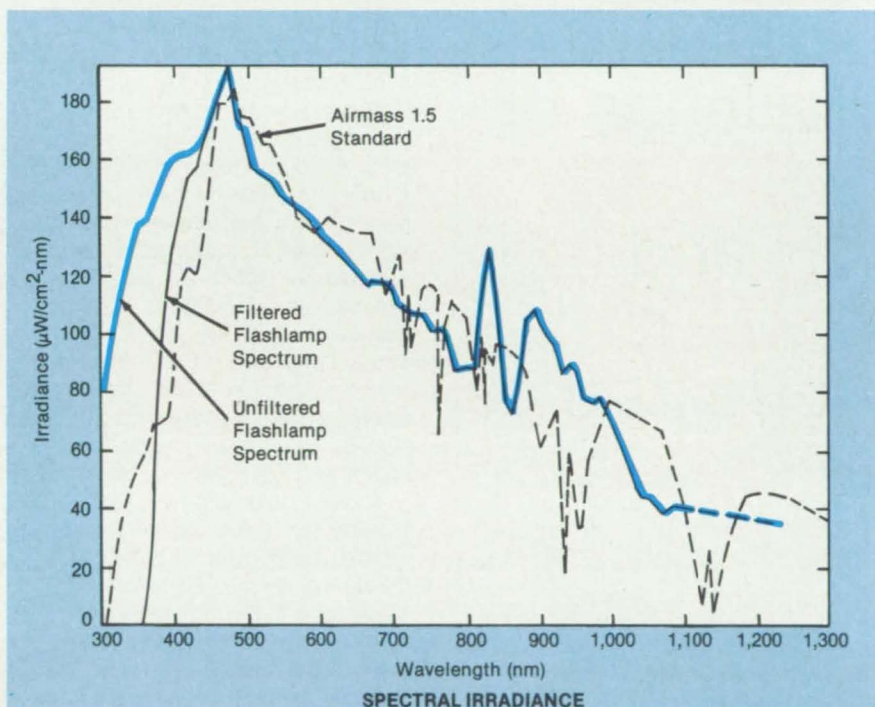
The performance of the filtered LAPSS is also better than that of a Class A simulator in several other regards. The nonuni-



LARGE-AREA PULSED SOLAR SIMULATOR WITH FILTER

formity of total irradiance is within 1 percent, vs. 2 percent for a Class A simulator. The total irradiance within a 30° field of view is greater than 99 percent, vs. 95 percent for the Class A unit. Finally, the temporal instability of irradiance is within 1 percent, vs. 2 percent for the Class A unit. There has been no detectable change in the spectral transmission of the filter after 10,000 flashes during 10 months.

This work was done by Robert L. Mueller of Caltech for NASA's Jet Propulsion Laboratory. For further information, Circle 17 on the TSP Request Card. NPO-16696



A **Filter** reduces the ultraviolet portion of the unfiltered flashlamp spectral curve, yielding an irradiance that averages well with that of standard airmass 1.5 global sunlight.

Books and Reports

These reports, studies, and handbooks are available from NASA as Technical Support Packages (TSP's) when a Request Card number is cited; otherwise they are available from the National Technical Information Service.

Electron-Diffraction Analysis of Growth of GaAs

This technique elucidates the mechanisms of GaAs crystal growth.

A report describes experiments that used reflection high-energy-electron diffraction (RHEED) to investigate the behavior of GaAs surfaces during and

after growth by molecular-beam epitaxy (MBE). The experimental results show that dynamic RHEED measurements are useful both as probes of surface and growth kinetics and as methods for determining and reproducing surface and growth conditions.

The experiments were performed in a Riber 1000-2 MBE system. The (001) semi-insulating GaAs substrates were maintained at 600 °C. For all RHEED measurements, the electron beam was incident along the [110] axis of the surface. An off-Bragg angle of incidence caused interference between beams that dif-

fracted from adjacent layers, resulting in high sensitivity to step behavior. Gallium fluxes were determined by measurement of the periods of oscillations in the RHEED pattern during growth; arsenic fluxes were determined by previous calibrations of an ion gauge near the sample position.

In one experiment, the RHEED specular-beam intensity was measured during and after short depositions ranging from a small fraction of a monolayer to several monolayers of Ga while the As pressure was held at 2.2×10^{-7} torr (2.9×10^{-5} N/m²). This gave an As incorporation rate

of 2.9 monolayers per second. After each deposition, the specular beam intensity was measured until it recovered its pregrowth value.

The recovery behavior depends strongly on the amount of Ga deposition. The initial intensity recovery is fastest after the growth of an integral number of monolayers and slowest after half-integral growths. This effect is largest for 0.5 to 1.0 monolayers and still remains significant after 13 monolayers. However, the time to recover completely to the predeposition intensity is longer for integral depositions than for fractional depositions.

The recovery curves generally follow the form

$$I = A_0 - A_1 e^{-t/\tau_1} - A_2 e^{-t/\tau_2}$$

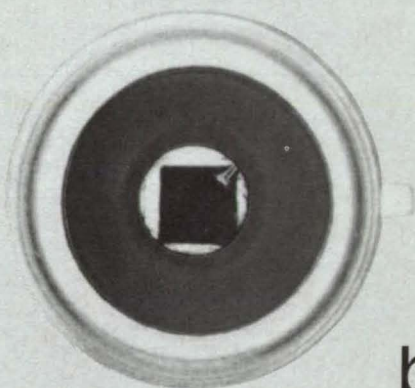
where I is the RHEED intensity, A_0 is the pregrowth intensity, A_1 and A_2 are constants, and τ_1 and τ_2 represent time constants for fast and slow recovery processes, respectively. The least-squares fit of this equation to the data is excellent, except after integral or integral minus 0.12 monolayer depositions.

Another experiment was designed to show the dependence of the RHEED intensity oscillations on the As pressure. At high As flux, the intensity oscillations have a small amplitude, which is rapidly damped out. When the As pressure is reduced, the damping is continuously reduced, while the amplitude of the oscillations first increases and then decreases again at low As pressure. Below an As pressure of 8×10^{-8} torr (1×10^{-5} N/m²), there are no oscillations, and growth is stabilized by Ga.

These results can be understood by considering the fast recovery process as a rapid smoothing of the growth front and the slow process as the recovery of long-range order in the form of the rearrangement of terraces, the reduction of one-dimensional disorder, or both. The fast process produces the largest change at low As pressure, suggesting the migration of Ga atoms. The slow process is fastest at high As pressure, suggesting the reduction of disorder. The slow recovery after the deposition of 1.0 monolayers indicates that such surfaces are very different from the equilibrium no-growth surface.

This work was done by Blair F. Lewis, Frank J. Grunthaner, Anupam Madhukar, T. C. Lee, and Rouel Fernandez of Caltech for NASA's Jet Propulsion Laboratory. To obtain a copy of the report, "RHEED Intensity Behavior During Homoepitaxial MBE Growth of GaAs and Implications for Growth Kinetics and Mechanics," Circle 3 on the TSP Request Card. NPO-16755

EG&G's New HFD Silicon Detector Meets the Challenge of **SPEED** and **GAIN** but Beats the Alternative on **COST.**



- Speed: 16 ns rise time
- Gain: 5×10^4 V/W
- Voltage: -15V, ± 5 V
- Temperature and voltage stable
- Ideal for laser rangefinders, short link communications, and analytical instruments.



Available from stock



EG&G ELECTRO-OPTICS

For further information, contact EG&G Electro-Optics
35 Congress Street, Salem, MA 01970. (617) 745-3200.
No. California (408) 735-1450. So. California (818) 344-3696.
Central States (312) 253-0335. Mid-Atlantic States (609) 452-7772.
Southeastern States (904) 383-0758.

THE KLINGER ARGUMENT AGAINST COMPROMISE:

**ONLY OUR MOTOR-DRIVEN LINEAR POSITIONERS
OFFER 4 MICROINCH RESOLUTION
OVER THE WIDEST TRAVEL RANGE.**



Whether your work involves laser machining, automated fiber optic alignment, semiconductor research or any high precision application, Klinger's wide selection of motor-driven linear stages will deliver unmatched precision.

All our linear stages can be used in combination to create XY or XYZ positioning systems. Incremental encoders for position verification are available. Other options include homing, clean room and vacuum preparation.

Don't compromise. The best is always a bargain. Klinger standards of engineering and manufacturing, as exemplified by our linear positioning stages, have made us the world leader in micropositioning systems. Get our free 212-page micropositioning handbook for complete specifications on these and thousands of other components.

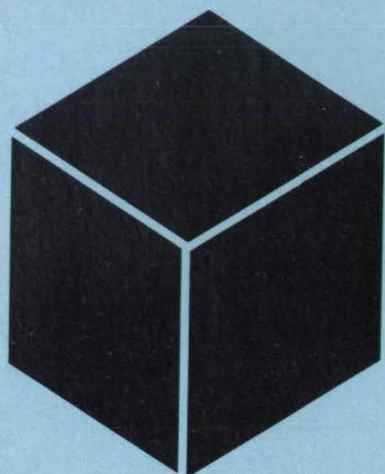
Write or phone Klinger Scientific Corporation, 110-20 Jamaica Avenue, Richmond Hill, NY 11418. (718) 846-3700.

KLINGER

SCIENTIFIC



Worldwide Network to Meet Your Needs • France: Micro Controle, Evry, (tel.) 6-077-82-83 • West Germany: Spindler & Hoyer, Göttingen, (tel.) 49/551/620/16
Canada: Optikon Corp. Ltd., Waterloo, Ontario, (tel.) 519/885/2551 • England: Unimatic Engineers Ltd., London, (tel.) 44/1/455.00.12
Netherlands: Elmekanik N.V., Hilversum, (tel.) 31/35/43.070 • Sweden: Martinsson & Co. Hagersten, (tel.) 03/744/03/00
Switzerland: G.M.P.S.A., Lausanne, (tel.) 41/21/33/33/28 • Italy: Leitz Italiana, Milano, (tel.) 39/2/27/55/46 • Japan: Hakuto Co. Ltd., Tokyo, (tel.) 03/341/2611.



Hardware, Techniques, and Processes

- 62 Etching Silicon Films with Xenon Difluoride
- 64 Preventing Delamination of Silverized FEP Films
- 65 Lightweight Ceramic Insulation
- 65 Tougher Addition Polyimides Containing Siloxane
- 66 Fast Glazing of Alumina/Silica Tiles
- 67 A Method for Characterizing PMR-15 Resin
- 70 Reinforcing the Separators for Lithium/Carbon Cells
- 70 Material for Fast Cutting

Books & Reports

- 71 Effects of Radiation on Coatings
- 71 Tests of Solar-Array Encapsulants
- 72 Separation in Binary Alloys
- 73 Crack Growth in Single-Crystal Silicon

Etching Silicon Films With Xenon Difluoride

Microscopic circuit structures are prepared for probing.

NASA's Jet Propulsion Laboratory, Pasadena, California

Xenon difluoride removes relatively large amounts of silicon from integrated-circuit or solar-cell structures while leaving SiO_2 , Si_3N_4 , Al_2O_3 , and other compounds intact. The etching technique using XeF_2 was developed to aid studies of the physical and chemical properties of interfaces between silicon and compounds of silicon or other elements in such structures. Using the XeF_2 technique, a silicon wafer with an oxide layer can be reduced in thickness from the standard $300\text{ }\mu\text{m}$ to as little as 10 nm without adversely affecting the oxide.

XeF_2 is a white solid with a vapor pressure of 4.5 torr ($6 \times 10^2\text{ N/m}^2$) at room temperature. It is allowed to sublime in a vacuum chamber containing the specimen to be etched (see Figure 1). The etching efficiency of XeF_2 in Si is only about 1 percent per molecular impact. The etching rate is increased, however, by balancing the partial pressure and flow rate of XeF_2 in such a way that the average number of collisions of an XeF_2 molecule with the sample is of the order of hundreds.

The XeF_2 flows from the solid source

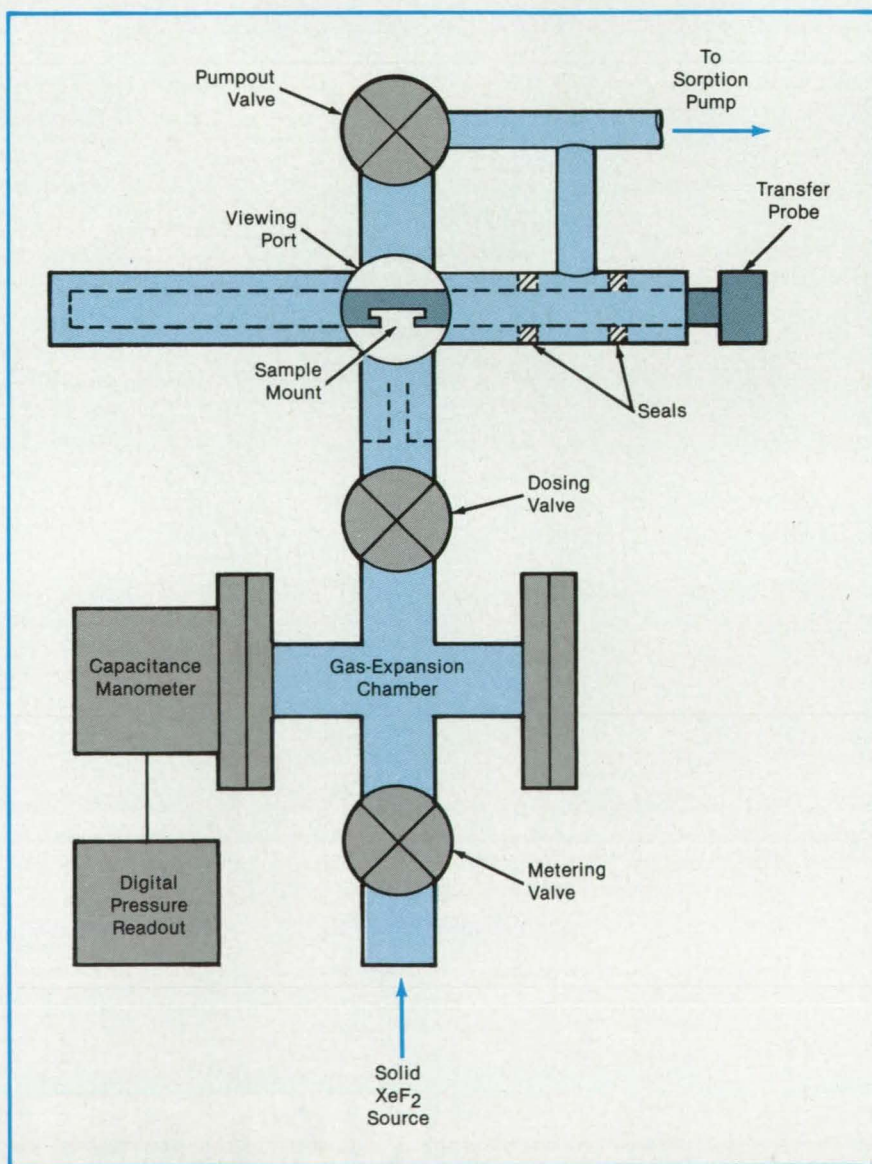
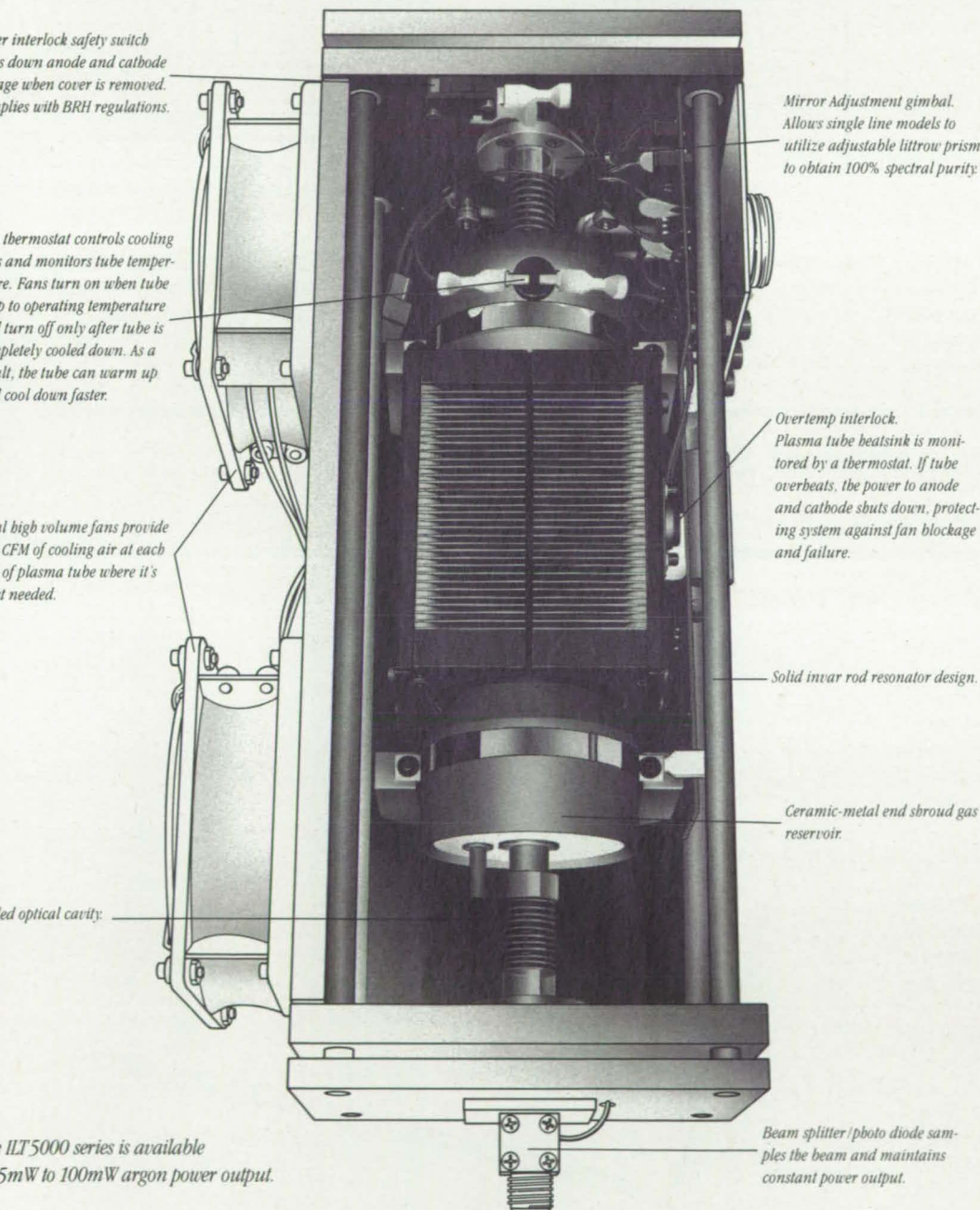


Figure 1. In the **Etching Apparatus**, solid XeF_2 is sublimated in a vacuum, then allowed to flow over the sample at a controlled rate and pressure.

For companies in search of excellence: We invite you to compare the ILT 5000 series argon laser to any other. If that's possible.



ILT 5000 series is available
5mW to 100mW argon power output.



POWER SUPPLY

We have united simplicity and technological ingenuity in a solid-state, reliable and compact switching power supply. The ILT 5000 Series power supply features a voltage doubled front end, boosts the 115 VAC line input to 340 VDC and switches to a fully isolated step-down transformer at 35 KHZ. This exclusive design prevents electrical shock and enables maximum laser energy output even at low-line voltage inputs. It is also available in 100 or 220 VAC.



REMOTE CONTROL

With the model RPC-50 remote control, the operator can control laser output power and monitor system functions. Power is displayed on a percentage available basis on a led bar graph, which also shows laser tube current.

If you would like to know more about the ILT 5000 series, contact:

Ion Laser Technology
Performance Plus Support. It Makes The Difference.

Circle Reader Action No. 362

Ion Laser Technology
263 Jimmy Doolittle Rd.
Salt Lake City, Utah 84116
801 537 1587 Telex: 3789481

through a metering valve into an expansion chamber, the pressure in which is monitored. At the appropriate pressure, a dosing valve is opened to allow the XeF_2 to impinge on the sample at the calibrated rate.

The sample mount is part of a sealed transfer probe. The sample is cooled to under 0°C to insure the uniformity of etching. A viewing port in the chamber makes it possible to observe the process directly or to use a laser-based thickness-measuring system.

Figure 2 shows an application of the technique. In this case, the objective is to study the interface between a 50-Å layer of SiO_2 and a 1,500-Å layer of Al deposited on a phosphorus-doped wafer of [100] Si. First, the front (aluminum) surface is bonded with indium solder to a gold-plated sample platen. The oxide is stripped from the exposed back surface by etching with a solution of $\text{HF}:\text{C}_2\text{H}_5\text{OH}$. The sample is then transported under N_2 to the XeF_2 -etching chamber.

The entire silicon layer is removed in 6 to 10 hours. After the XeF_2 etch, the sample is transferred in air to a wet-etching station coupled to an X-ray photoelectron spectrometer. The spectrum is recorded while the SiO_2 is slowly etched away. In one such series of experiments, the spec-

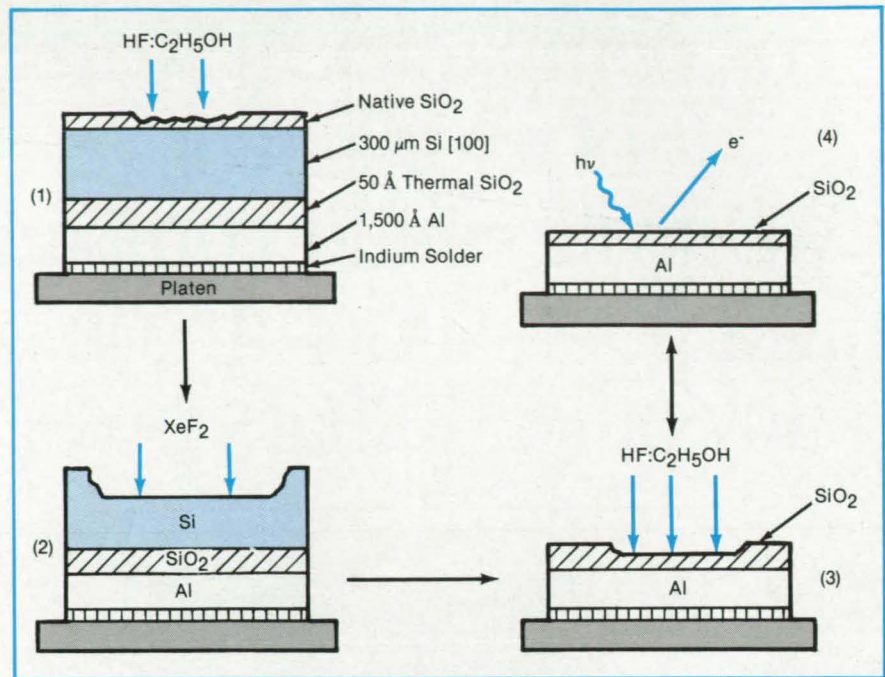


Figure 2. A Wafer Is Etched from the back to expose SiO_2 and Al layers for spectroscopic analysis of the SiO_2/Al interface.

troscopic studies showed that the interface between the Al and the SiO_2 is atomically abrupt if unannealed and includes a 0.6-nm-thick layer of Al_2O_3 if annealed.

This work was done by Michael H.

Hecht of Caltech for NASA's Jet Propulsion Laboratory. For further information, Circle 11 on the TSP Request Card. NPO-16527 and NPO-16528

Preventing Delamination of Silverized FEP Films

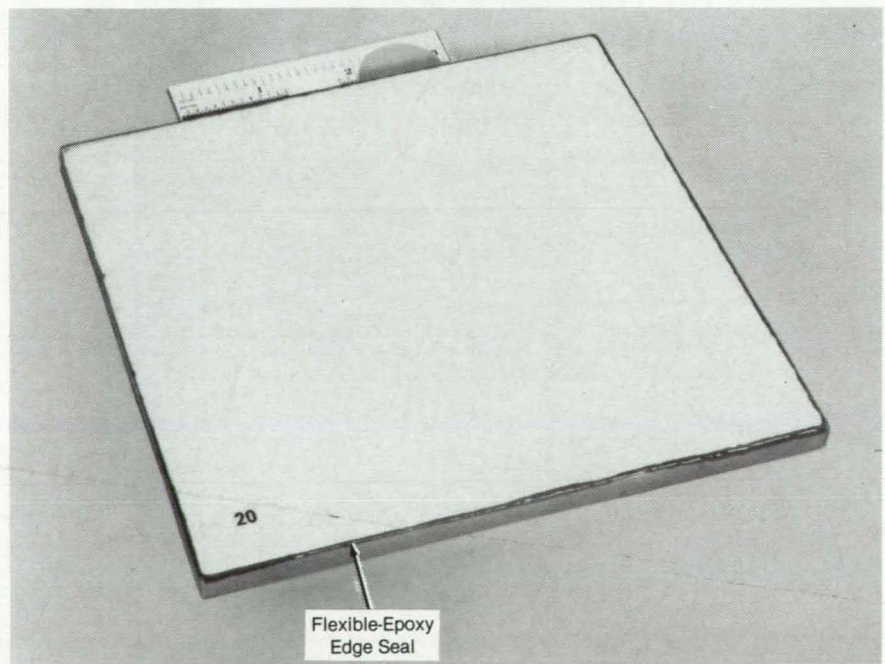
Edge treatment inhibits attack by moisture.

Lyndon B. Johnson Space Center, Houston, Texas

A novel procedure overcomes delamination of a silver-coated fluorinated ethylene/propylene (FEP) film on an aluminum substrate. FEP presents special difficulties with regard to metalization because it is formulated to actually prevent adhesion.

The delamination of untreated assemblies is apparently due to attack by moisture that migrates through the silicone adhesive between the silver and the FEP. The conclusion that failure was not a result of residual stress — perhaps from processing or simply from differential thermal expansion of the laminated layers — was reached after an extensive test program.

The new technique prevents delamination by sealing the edges where delamination starts. To ensure adhesion, the surface to be sealed is carefully prepared. The edges are abraded lightly with sandpaper to provide a roughened surface for mechanical bonding to the edge-sealing material. A bead of flexible epoxy about one-sixteenth inch (1.6 mm)



Samples of Aluminum/FEP/Silver Laminate survive humidity tests and other environmental tests when the edges of the layers are covered by an epoxy bead.

wide is applied with a syringe so that the edges of the metalization, FEP layer, and film-to-substrate adhesive are covered (see figure).

The method is easy to implement, even in the field as a repair procedure. It withstands a variety of environmental

tests, including heat and vacuum testing for 24 hours, moisture testing at 95 percent relative humidity for 5 days, and 3 weeks total water immersion at room temperature. Untreated laminates, in contrast, deteriorated seriously during such tests.

This work was done by Larissa Domnikov, Judy May, and Roberto Gallego of Hughes Aircraft Co. for Johnson Space Center. For further information, Circle 38 on the TSP Request Card.
MSC-20460

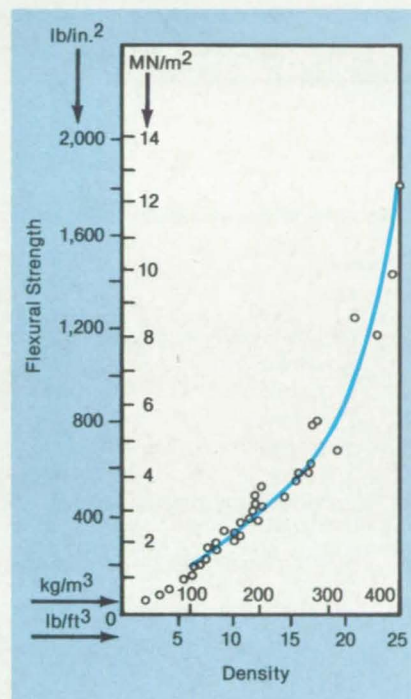
Lightweight Ceramic Insulation

A fiber burnout process yields low densities.

Lyndon B. Johnson Space Center, Houston, Texas

A rigid ceramic insulation has a density of 2 to 6 lb/ft³ (32 to 96 kg/m³) — low enough that it can replace flexible insulation in applications where low weight is essential. In contrast with the loose fibers or blankets of flexible insulation, the new insulation does not pack together or shift. It is thermally stable, and, with a flexural strength of 25 to 75 lb/in.² (170 to 500 kN/m²), it retains its shape under light loading (see figure). Originally developed for use on the Space Shuttle and other spacecraft, the rigid insulation can be machined to the requisite shape and bonded in place.

The low density is attained by a process of sacrificial burnout. Graphite or carbon fibers are mixed into a slurry of silica, alumina, and boron-compound fibers in amounts ranging from 25 to 75 percent of total fiber content by weight. The mixture is formed into blocks and dried. The blocks are placed in a kiln and heated to 1,600° F (870° C) for several hours. During this time, the graphite or carbon fibers slowly oxidize away, leaving voids and thereby reducing the block density. Final-



ly, the blocks are heated to 2,350° F (1,290° C) for 90 minutes to bond the remaining ceramic fibers together.

Before the graphite or carbon fibers are added to the casting slurry, they are chopped and dispersed in deionized water. Graphite and carbon were chosen as the materials for the burnout after experiments with cotton and nylon fibers. The graphite and carbon fibers proved to be more compatible with the rigid-insulation manufacturing process.

This work was done by William H. Wheeler and John F. Creedon of Lockheed Missiles & Space Co. Inc. for Johnson Space Center. For further information, Circle 56 on the TSP Request Card.

Inquiries concerning rights for the commercial use of this invention should be addressed to the Patent Counsel, Johnson Space Center [see page 29]. Refer to MSC-20831.

The **Flexural Strength** of lightweight rigid insulation (solid dots) follows the curve for higher density ceramic tiles of the same composition (small circles).

Tougher Addition Polyimides Containing Siloxane

Laminates show increased impact resistances and other desirable mechanical properties.

Langley Research Center, Hampton, Virginia

Aromatic addition polyimides have been developed as both matrix and adhesive resins for applications on future aircraft and spacecraft. Addition polyimides offer distinct advantages over linear polyimides, being processable in the form of short-chained oligomers end-capped with latent cross-linking groups. One particularly attractive, commercially available NASA Tech Briefs, May/June 1986

able addition polyimide results from the addition polymerization of a maleimide-terminated prepolymer prepared by the reaction of a bismaleimide with an aromatic diamino compound. However, addition polyimides of this kind tend to be highly cross-linked, insoluble, and extremely brittle on curing.

A process has been developed to ob-

tain a bismaleamic acid from the reaction of a diaminosiloxane and maleic anhydride in a 1:2 molar ratio. The bismaleamic acid may be extended by the reaction of the diaminosiloxane with maleic anhydride in a 1:1 molar ratio, followed by the reaction with half this molar ratio of an aromatic dianhydride. The bismaleamic acid may also be extended by the reac-

tion of the diaminosiloxane with maleic anhydride in a 1:2 molar ratio, followed by the reaction with half this molar ratio of an aromatic diamine (Michael-addition reaction).

The oligomer thus forms melts in the temperature range of 80° to 120° C and cures between 140° and 170° C. It can be blended with commercially available bismaleimides, with which it is compatible. All forms of the oligomer can be imidized at 130° C due to the flexibility introduced by the siloxane group and increased basicity of the aliphatic amine group, which enhances the ease of cyclization. (Oligomers of aromatic diamines require cyclization at such higher temperatures as 180° to 200° C, resulting in some isomeri-

zation to the fumaric group. Acetic acid left associated with the resin after chemical cyclization may degrade the polymer at the higher temperature where curing is effected, resulting in reduced strengths.)

Composites prepared from the oligomers can be thermoformed at elevated temperatures after an initial molding in the temperature range of 175° to 200° C due to the lowered melting temperatures. A range of service temperatures results from blending the oligomers with various bismaleimides in different proportions.

The resins can be used to coat graphite woven cloth. After drying, the resins can be thermally imidized to give material with drape and tack, and which can be cut easily and formed into shaped layups.

These layups may then be molded under heat and pressure to give the desired laminate. Such laminates have excellent properties in terms of glass-transition temperatures, flexural strengths and moduli, and short-beam shear strengths. Also, impact resistances are improved over those of the unmodified bismaleimide, showing a significant increase in toughness.

This work was done by Terry L. St. Clair of Langley Research Center and Shubha Maudgal of the National Research Council. For further information, Circle 20 on the TSP Request Card. LAR-13304

Fast Glazing of Alumina/Silica Tiles

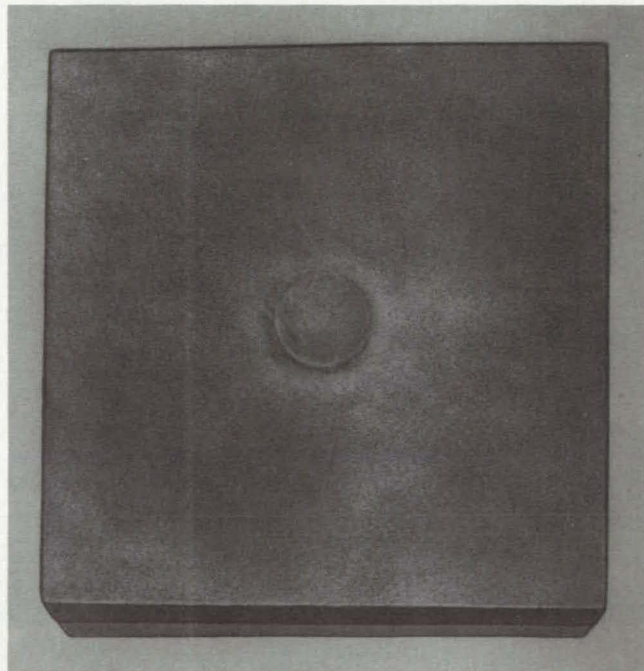
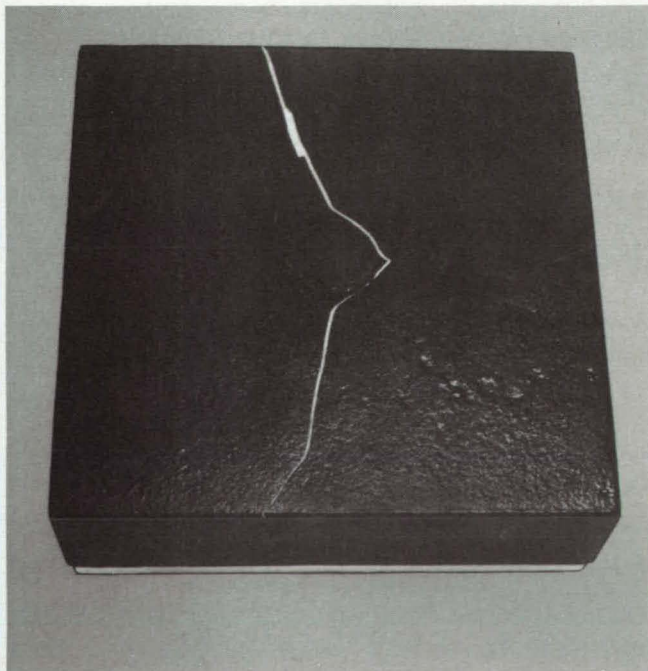
This technique prevents cracking of substrates or coatings.

Lyndon B. Johnson Space Center, Houston, Texas

A new technique for applying a ceramic coating to fibrous silica/alumina insulation tiles prevents cracks and substantially reduces firing time. This technique can be used to repair tiles with damaged coatings and possibly could be used in heat-treating objects made of materials having different thermal-expansion coefficients.

The ceramic coating is applied to tiles made of alumina and silica fibers. In the previous glazing technique, the coated tiles were heated for 95 minutes in a roller-hearth kiln at 2,250 °F (1,232 °C). On various tiles of 22-percent alumina and 78-percent silica, the coatings did not crack. However, on HTP-12 tiles [45-percent alumina, 55-percent silica, density

12 lb/ft³ (192 kg/m³)], both the coatings and the substrates cracked (see left side of figure). This cracking is attributed to the difference between the coefficients of thermal expansion of the coatings and the substrates: The coating has a coefficient of $6.07 \times 10^{-7} (^\circ\text{F})^{-1}$ [$10.9 \times 10^{-7} (^\circ\text{C})^{-1}$], while the substrate has a coefficient of about $23 \times 10^{-7} (^\circ\text{F})^{-1}$ [41×10^{-7}



Surface Cracking (left) was evident after a ceramic-coated 45-percent alumina/55-percent silica tile, fired at 2,250 °F (1,232 °C) for 95 minutes, was removed from a glazing kiln. No surface cracking (right) occurred in an identical tile fired at 2,372 °F (1,300 °C) for 1.5 minutes, cooled to room temperature, and then fired at 2,660 °F (1,460 °C) for 1.5 minutes.

(°C)⁻¹].

To reduce the thermal stresses in the tile being coated, a high-temperature, short-time firing schedule was implemented. Such a schedule allows the coating to mature while the substrate remains at a relatively low temperature, thereby reducing the stress differential between the coating and substrate.

To test this approach, a 45/55 alumina/silica tile of 6 by 6 by 2 in. (15 by 15 by 5 cm) was heated for 1.5 minutes at 2,372°F (1,300°C), cooled to 75°F (24°C), then exposed to 2,660°F (1,460°C) for another 1.5 minutes. As shown on right side of the figure, no

coating or substrate fractures were observed. The conditions were not optimized for this tile and coating, and other temperature/time combinations might be satisfactory.

In addition to eliminating cracks, the new approach has the advantage of increasing production rates, because the firing time is substantially reduced. This technique might allow the elimination of the machining offsets currently applied to all tiles to allow for tile shrinkage during heating. Thus, the tiles might be machined to final (net) dimensions, with a potential saving of material and machining time. This technique also could be used to repair

tiles with damaged coatings, because sections of the tiles could be glazed without affecting the substrate dimensions.

It should be noted that this concept is applicable only to thin coatings because of the need to heat the coating rapidly. Moreover, because the coating layer is subjected to severe thermal stress during flash heating and rapid cooling, this technique might not be suitable for coatings that cannot tolerate thermal stresses.

This work was done by John F. Creedon, Edward R. Gzowski, and William H. Wheeler of Lockheed Missiles & Space Co., Inc., for Johnson Space Center. No further documentation is available.
MSC-20976

A Method for Characterizing PMR-15 Resin

The change in composition with aging makes analysis essential.

Lewis Research Center, Cleveland, Ohio

A quantitative analysis technique based on reverse-phase, high-performance liquid chromatography (HPLC) and paired-ion chromatography (PIC) was developed for PMR-15 resins. PMR-15 resin has gained acceptance as a matrix resin in carbon-fiber composites requiring thermo-oxidative stability at temperatures up to 600°F (320°C). Verification of proper resin formulation and analysis of changes in resin composition during storage are important to the manufacturers of PMR-15 polymer matrix composite parts.

The freshly-prepared resin solution consists of three monomers: BTDE, MDA, and NE, which are dissolved in methanol. A prepreg is formed by coating carbon fiber fabric with the monomer solution and then evaporating the methanol. Composite parts are manufactured by assembling plies of prepreg and curing at high temperature.

The processability and performance of the PMR-15 resin depend on its composition. However, the composition of the resin solution and prepreg changes as the solution is aged. The change is a result of the premature reaction of the monomers with each other, as well as of the reaction of the monomers with methanol in the solvent and water from the atmosphere. The components of the aged solution exhibit a wide range of molecular properties, such as molecular weight, polarity, solubility, and dissociation constant. It is difficult to find a single separation technique

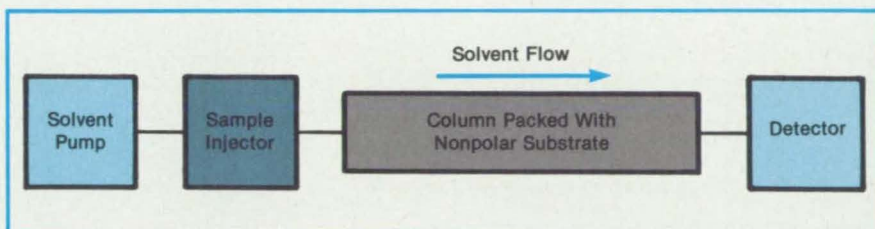


Figure 1. In a **Reverse-Phase HPLC Experiment**, a polar solvent containing the material to be analyzed is passed through a column packed with a nonpolar substrate.

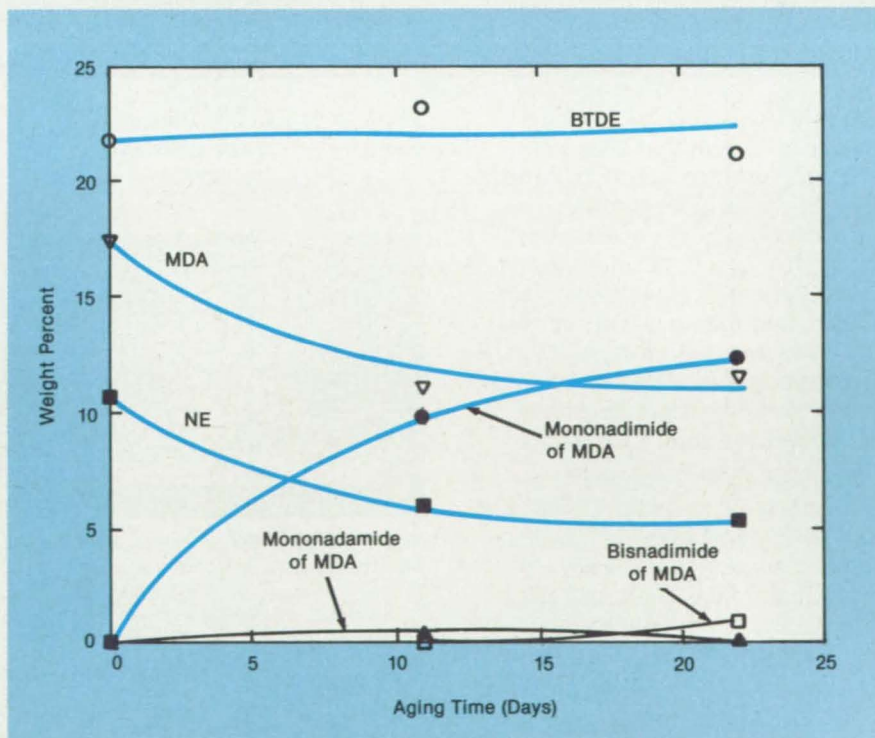
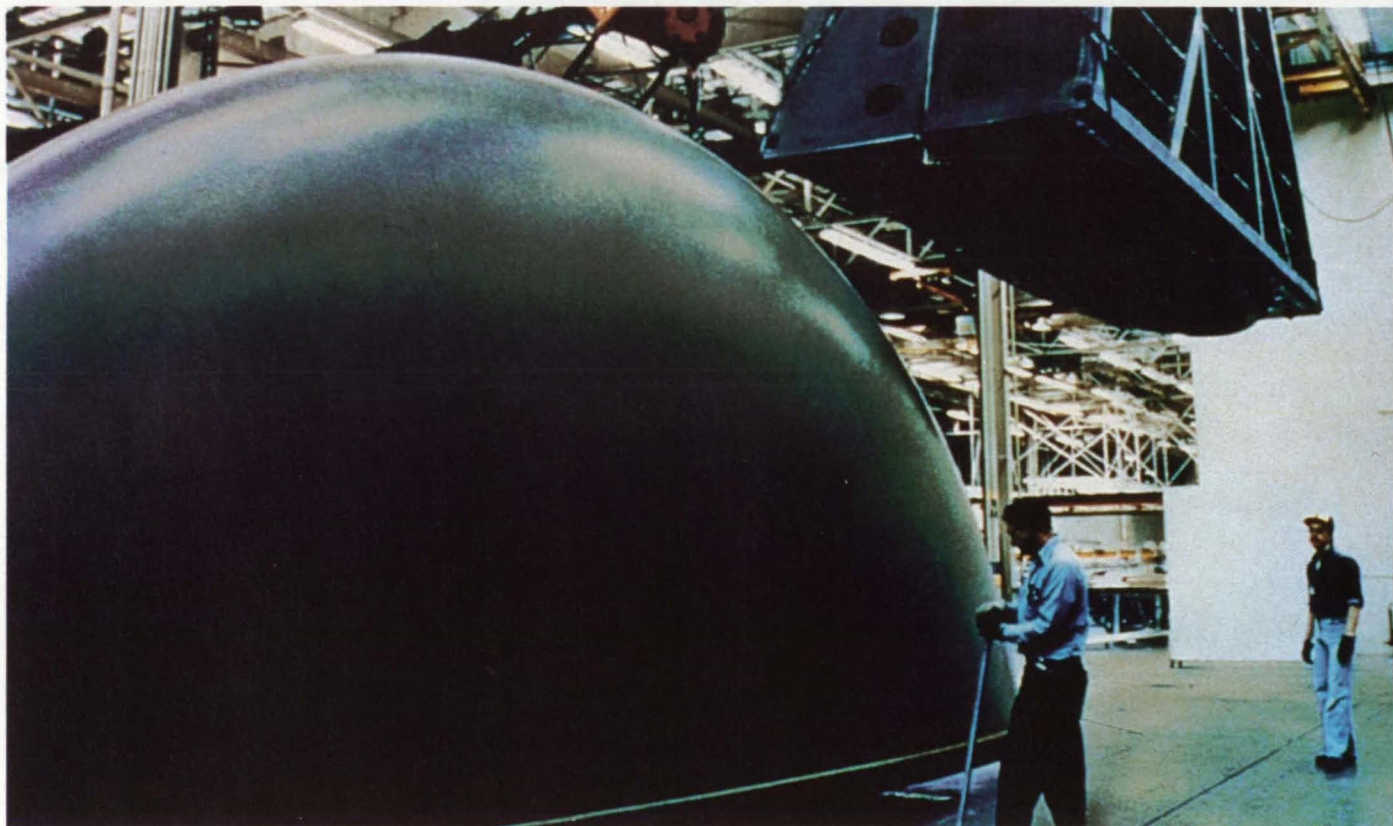


Figure 2. The **Composition of a PMR-15 Resin** of 50 weight percent changes as the resin ages at room temperature.

Introducing a revolutionary new composite materials tooling system

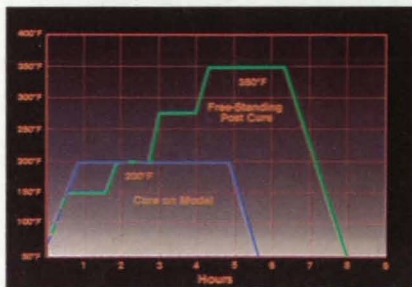


ToolRite® is a complete tooling materials system that uses low cure temperature prepregs formulated exclusively for tooling. Compared with conventional wet lay-up, it is faster, cleaner, and easier to handle. Tool life is 500% longer. And, being a prepreg system, it assures uniform resin distribution, virtually free of voids and pockets, so thermal cycling has less effect. Heat distributes evenly. Warping is 70% less.

Compared to metal tooling, the ToolRite System provides exceptional dimensional accuracy and thermal stability. Tools and parts heat up and cool down together, at the same rate. Damage and distortion

are practically eliminated. Parts come off the tool faster, too.

And because of lower mass,



The ToolRite System cures completely on a master model at 200° to 210°F. It can be removed from the master and post-cured, free-standing, at 350° to 375°F—with service temperatures of more than 400°F.

the ToolRite System saves energy—whether you cure by vacuum bag or autoclave.

ToolRite is no ivory tower idea fresh from the drawing board. It is already in use in more than 2,000 tools throughout the aerospace industry worldwide. Here is how two of these users are benefiting from the unique properties of the Fiberite ToolRite System.

Shell lay-up time on the AWACS radome tool was cut an estimated 40% due to fewer plies of thicker, more easily applied material.

One of the world's largest high temperature fiberglass/epoxy tools, the AWACS radome lay-up mandrel is 12½ ft. high, 5½ ft. wide and 30 ft. long at the base. In the past,

ToolRite[®] from Fiberite

with wet lay-up, Boeing fabricated the mandrel in two sections and cured each half separately. Thus, there were three cure cycles—Left, Right, and Spliced. With the ToolRite System, as specified by Boeing, the halves can be laid up *and spliced*, then cured in a single cycle. This saves four cycles when building the pair of mandrels required.

Large size and close dimensional tolerance make such a tool expensive to fabricate. But, with the ToolRite System, Boeing has been using the tool for three years and still does not see the end of its useful life. Also, compared with previous tooling, labor for tooling rework to retain vacuum integrity has been cut more than 90%.

As a result of the change from wet lay-up to the ToolRite System, physical properties of the tool have improved greatly. Flexural strength at 350°F is nearly twice that of the previous systems.

"To date, we have over 500 cycles on some of our prepreg tools with no indication of leakage or thermal shock cracks."

*R.T. Williams, Manager
Composites and Bonded Structures
Teledyne/Ryan Aeronautical*

Ray Williams knows prepreg tooling. He has more than 700 ToolRite tools in inventory at Teledyne/Ryan.

"If you're building graphite, aramid or glass parts, you must match the thermal characteristics of the tool with the part," Williams says. "With interlocking curvatures, projections and tight radii, the tool and the part must expand and contract at the same rate, or you lose dimension."

Uniform resin distribution is important, according to Williams,

because resin-rich areas act as a heat sink subject to thermal shock, resulting in premature tool failure. "Using graphite prepreg, we project the life of our tools somewhere near 750 cycles. In addition, the tools are light, and easy to handle and store."

Designing with the ToolRite System has significant advantages over traditional design, according to Williams. "Designing one structure of composite tooling, we've



Is it possible to make an asymmetric part with composite tooling? Using the ToolRite System, Teledyne/Ryan Aeronautical designed this split graphite tool used to fabricate an engine intake duct for the AH-64 attack helicopter. Harbor Patterns, Inc., Los Alamitos, CA, built the tool.

been able to totally design out 11 different components. By eliminating part count and secondary operations, you can really begin to save money," he says.

You can get details on the ToolRite Prepreg System for composite tooling—and arrange a technical briefing for your management and an in-shop



Add Beech Aircraft to the growing list of ToolRite System users, which already includes Boeing, MBB, CASA (AirBus), BAe, Dassault and Teledyne Ryan. The upper and lower wing skin tools for the Beech Starship I (above) were fabricated using this revolutionary new prepreg tooling system for composite parts.

demonstration—just by picking up your phone. Call Clint Juhl or Kris Ralph at (714) 639-2050, and describe your project. Or use the coupon below.

☐ Please send me a copy of your brochure showing step-by-step tool fabrication procedures using ToolRite Prepreg System. I am considering ToolRite materials for the following areas:

- | | |
|--|---|
| <input type="checkbox"/> Commercial Aircraft | <input type="checkbox"/> Missiles/Rockets |
| <input type="checkbox"/> Military Aircraft | <input type="checkbox"/> Recreational |
| <input type="checkbox"/> Helicopters | <input type="checkbox"/> Thermoforming |
| <input type="checkbox"/> Satellites/Space Vehicles | <input type="checkbox"/> Other _____ |

Name _____

Title _____

Firm _____

Address _____

City, State, Zip _____

Telephone _____ / _____

Application _____

***Mail to: June C. Nusz
Fiberite, 111 Riverfront
Winona, MN 55987***

FIBERITE[®]
AN ICI COMPANY

suitable for all components. Some of the components are not readily isolated in pure form. This makes quantitative analysis difficult since standard samples are not available.

A schematic diagram of the experiment is shown in Figure 1. In reverse-phase HPLC, a polar solvent flows through a column packed with a nonpolar substrate. A molecule passing through the column will spend some time dissolved in the flowing solvent and the remaining time adsorbed on the substrate. When a sample containing several components is injected into the column, its pure components elute

from the column in order of decreasing polarity.

Components which are ionized in solution do not adsorb onto the nonpolar substrate and are not separated by reverse-phase HPLC. Ionized components can be separated by paired-ion chromatography (PIC). The addition of a PIC reagent to the solvent during a reverse-phase HPLC experiment results in the separation of the ionized components without affecting the separation of the nonionized components. This approach was used to obtain complete separation of all components in aged PMR-15 resin.

Response factors were determined for quantitative analysis. The composition of a PMR-15 resin solution was measured as a function of room-temperature aging time (Figure 2). The composition of resin dissolved from a commercial prepreg was also measured. This technique appears to be especially suitable for commercial use by the manufacturers of high-performance composite components.

This work was done by Gary D. Roberts and Richard W. Lauver of Lewis Research Center. For further information, Circle 47 on the TSP Request Card.
LEW-14253

Reinforcing the Separators for Lithium/Carbon Cells

A backing can prevent the tearing of the very thin separators during cell assembly.

NASA's Jet Propulsion Laboratory, Pasadena, California

The fabrication of lithium/carbon batteries can be simplified by the attachment of perforated nickel-foil, graphite-cloth, or graphite-paper backings to the glass-fiber separators. These separators are so frail that they are easily torn during the assembly of cells, thereby short circuiting the cells.

The glass-fiber separators can be strengthened with a backing, which must be conductive so that it will not increase the electrical resistance of the cell. The backing must be placed on the cathode side — anything other than lithium on the anode side would short circuit the cell.

The backing on the cathode side must be either carbon or nickel, since the cathode is conductive carbon held by a nickel grid.

Both the nickel and the carbon backings appear to be viable. Because perforated nickel foil is already manufactured by electroforming, there should be no obstacle to the creation of a very thin, very porous nickel foil to serve as backing. Thicknesses of 20 μm with porosities above 50 percent are practicable.

Alternatively, conductive paper and cloth made of carbon fiber is available and could have the advantage of presenting more surface area for solvent reduc-

tion than the perforated nickel foil. The backing can be attached to the separator by polyisobutylene, a material resistant to sulfur, sulfur compounds, and oxidants (including ozone) up to at least 100°C. The polyisobutylene is expected to dissolve completely in the thionyl chloride electrolyte solvent after the cell has been assembled; the adhesive is no longer needed after the cell is assembled.

This work was done by Eugene R. du Fresne of Caltech for NASA's Jet Propulsion Laboratory. For further information, Circle 19 on the TSP Request card.
NPO-16619

Material for Fast Cutting

Silicon nitride-based tool boosts productivity and reduces costs.

Marshall Space Flight Center, Alabama

A new material for cutting tools increases the productivity of machining processes. The material, called Iscanite (or equivalent), is based on silicon nitride and contains more than 90 percent silicon. It combines impact resistance close to that of coated carbides with heat and wear resistance close to those of aluminum oxide ceramics.

Tools made of Iscanite (or equivalent) can operate at higher cutting speeds. For equal pressure on the workpiece, an

Iscanite (or equivalent) tool will therefore remove more material than will a conventional tool. The new material makes it unnecessary to use high pressure to increase the removal rate and therefore greatly reduces workpiece slippage, vibration, and tool breakage. Iscanite (or equivalent) tools last longer and therefore reduce the amount of cutting time lost to indexing, gauging, and adjustments.

The material is made by a hot-press-

ing technique that yields a product having full density. The material can be used for cutting on old or new machine tools and makes it possible to exploit fully the power and speed of a machine.

This work was done by Andrew Perez of Rockwell International Corp. for Marshall Space Flight Center. No further documentation is available.
MFS-29130

Books and Reports

These reports, studies, and handbooks are available from NASA as Technical Support Packages (TSP's) when a Request Card number is cited; otherwise they are available from the National Technical Information Service.

Effects of Radiation on Coatings

Tests help to insure reliability in a hostile environment.

Tests of radiation damage to materials used in the outer coverings of spacecraft are described in a 25-page report. The materials were exposed to ionizing radiation then examined for the degradation of desirable mechanical, electrical, and optical properties. Some of the experimental results and test methods may be applicable to aircraft, scientific instrumentation, and other equipment subject to ionizing radiation, electrostatic discharge, or both.

Electrically conductive tapes for preventing static-charge buildup were examined for decreases in peel and ultimate tensile strengths. The tests were performed on tapes with aluminum and copper coatings. The electrical grounding capability of the copper tape is superior to that of aluminum tape, but the aluminum tape retained more of its original mechanical strength after irradiation with electrons.

Two types of thermal blankets were exposed to a flux of energetic protons to match the environment expected in the vicinity of Jupiter. Both types of blanket included about 15 layers of 1/4-mil (0.006-mm) polyethylene terephthalate. One type had a front-surface layer of 1-mil (0.025-mm) polytetrafluoroethylene filled with glass fibers and carbon, while the other had a surface layer of 1.5-mil (0.038-mm) polyester over 0.5-mil (0.013-mm) polyimide. The first type showed more erosion of the front layer than did the second type (16.3 percent versus 1.8 percent by weight).

Paints and other coatings for temperature control are listed with some of their mechanical, electrical, and thermo-optical properties. The list includes both unfilled and carbon- or graphite-filled organic coatings (silicone, polyurethane, epoxy, fluorocarbon, and polyester) and inorganic coatings (silicate, titanate, ferric titanate, and zinc orthotitanate). The effects of radiation differ among the various coatings and include graying, increase in reflectance, weight loss, surface erosion, and loss of surface conductivity.

The report also describes standardized procedures and equipment for measuring

the bulk and surface electrical resistivities of coatings. While the basic techniques of resistivity measurement are simple and well known, these test specifications are useful in coping with the peculiarities of coatings; in particular, by reducing environmental variations in the samples and insuring complete contact between electrodes and samples.

This work was done by Frank L. Bouquet, Victor F. Hribar, and Edward C. Metzler of Caltech for NASA's Jet Propulsion Laboratory. For further information, Circle 111 on the TSP Request Card NPO-16533

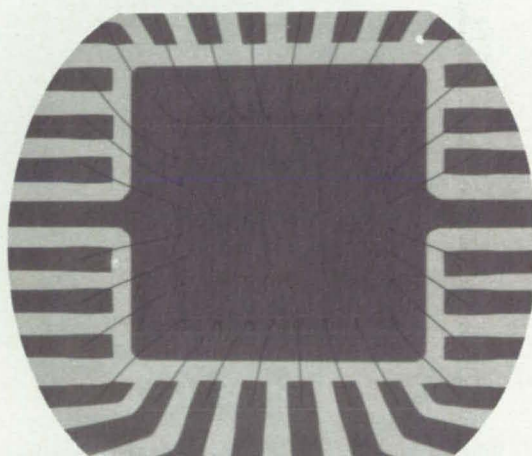
Tests of Solar-Array Encapsulants

Materials were tested for degradation by heat and light.

A report presents early results of a continuing series of photothermal aging tests of some candidate encapsulating materials for solar photovoltaic modules. The objectives of the testing program are to contribute to the development of durable, low-cost encapsulants and to predict the lifetimes of encapsulated photovol-

MICROFOCUS X-RAY TUBE

Air Cooled, Permanently Sealed



A 10 micron spot size is capable of magnifying images with little distortion, but if maneuverability and reliability are limited by typical oil cooling lines and demountable tube vacuum systems, practicality is lost. Downtime runs high.

Kevex' solution to the industry-wide problem was to develop a hermetically sealed x-ray tube more adaptable to the Quality Controller's environment and specifications.

The new KM10005S x-ray tube is air cooled and rated to 125 kV. The unique design and construction promises low maintenance, high performance, and a low cost.

Applications for x-rays are diverse, requiring application-specific solutions. If your company is involved with the inspection of ceramics, microelectronic components, turbine blades or other components requiring magnified images, contact Kevex for an answer to your needs.



Kevex Corporation X-Ray Tube Division
320 El Pueblo Rd.
Scotts Valley, CA 95066 (408) 438-5940

taic modules placed outdoors. Toward these ends, the tests are designed to reveal physical and chemical degradation mechanisms that affect the encapsulants.

The potting materials tested include ethylene vinyl acetate copolymer, polyvinyl butyral, room-temperature-vulcanizing silicone rubber, ethylene methyl acrylate copolymer, poly-n-butyl acrylate, and two aliphatic polyurethanes. Also tested were some acrylics and fluorocarbons that are likely to be used as outer-cover film materials.

Samples of these materials were aged at 55°, 70°, 85°, 105°, and 135° C. Control samples were aged in the dark while

photothermal samples were exposed to ultraviolet radiation from a mercury lamp. Some specimens were mounted between glass covers to limit the access of oxygen, while others were exposed to the air.

Changes in several material properties were observed in the aged samples. These included the following:

- Optical transmittance was measured in the wavelength range of 300 to 1,200 nm. This helps quantify chemical changes involving the formation of oxidized species, indicated the component of diminution of photovoltaic performance due to the loss of transmittance,

and gave a measure of the ultraviolet-screening ability of outer-cover films.

- Weight loss was measured to determine the loss due to evaporation of plasticizers, leaching of additives, and formation of volatile degradation products. Weight-loss measurements correlate with the formation of voids, which may cause delamination and corrosion.
- The uniaxial stress/strain response was measured to develop engineering modulus data and information on the stress-relaxation or creep behavior of the materials.
- For partially cross-linked polymers, solvent swelling and sol/gel ratios yield information on the network cross-link density and shape, which are critical structural parameters that control physical and chemical properties. Aging causes changes in these parameters; consequently, changes in swelling and sol/gel ratios are important measures of the outdoor stability of polymers.

This work was done by Ranty H. Liang, Keri L. Oda, Shirley Y. Chung, Mark V. Smith, and Amitava Gupta of Caltech for NASA's Jet Propulsion Laboratory. Further information may be found in NASA CR-172989 [N83-33339/NSP], "Handbook of Photothermal Test Data on Encapsulant Materials" [\$16]. A copy may be purchased [prepayment required] from the National Technical Information Service, Springfield, Virginia 22161. NPO-16387

How will today's events affect your project tomorrow... next week...next month?

Now available
on IBM mainframe



With VIS10N you'll know today!

Shortages, design changes, labor problems, interest fluctuations, delays... these are problems you face every day. How will they impact your project? Your schedule? Your budget?

Waiting for answers can be expensive... even disastrous. You need information to make decisions today so your project will be running smoothly tomorrow, next week, next month.

You need VIS10N...a powerful, comprehensive, easy-to-use project management system.

With VIS10N, your schedule can be updated as soon as events happen. You

can see how changes will affect your project every day. VIS10N's powerful "What-If" capability will help you analyze problems...more important, find solutions.

Put an end to surprises...send for more information on VIS10N today. Better yet, give us a call and find why so many of the Fortune 1000 companies depend on VIS10N.

SYSTONETICS

801 E. Chapman Ave., Fullerton, CA 92631
(714) 680-0910 • Telex 692-327

*VIS10N is available on DEC VAX and PR1ME minicomputers.
VIS10Nmicro now available on IBM® PC.*

DOMESTIC OFFICES: Fullerton, CA (714) 680-0910 • San Jose, CA (408) 275-0890 • Seattle, WA (206) 455-3374 • Denver, CO (303) 740-6681 • Houston, TX (713) 461-3905 • Atlanta, GA (404) 955-7740 • Oakton, VA (703) 359-2982

INTERNATIONAL AGENTS: EURO/LOG HOUSE, 25 High Street, Rickmansworth, Herts WD3 1DF, United Kingdom, Phone 923-777007, Telex: 917099 • Software Solutions Pty, Ltd., 5 Alexander Street, Crows Nest, New South Wales, Australia 2065, Phone: 2-439-3055, Telex: AA72618 • Optiim Scandinavia A.S., Lumberveien 13, P.O. Box 210, N-4620 Vagsbygd, Norway, Phone: 47-42-14200, Telex: 21603.

IBM is a trademark of International Business Machines Corporation

Separation in Binary Alloys

Studies of monotectic alloys and alloy analogs are reviewed.

A report surveys research on liquid/liquid and solid/liquid separation in binary monotectic alloys. The report emphasizes separation processes in low gravity, such as in outer space or in free fall in drop towers.

Monotectic alloys are characterized by temperature/composition regions in which the liquid phases are immiscible. In normal Earth gravity, the droplets of the minority phase do not remain dispersed uniformly in the majority phase. Instead, because their density is usually different from that of the majority phase, the droplets rise to the top or fall to the bottom of the melt. Only in nearly zero gravity can the dispersed droplets be frozen in place during solidification — hence the interest in low-gravity research on these promising alloys.

The report first reviews early experiments, including drop-tube work on bismuth and gallium, rocket flights with

NASA Tech Briefs, May/June 1986

aluminum/indium, and orbital missions with oil/water mixtures on Skylab and zinc/lead on Apollo-Soyuz. The results of these experiments prompted researchers to look more seriously at phase-separation mechanisms, especially droplet migration in thermal gradients. If interfacial tension decreases with increasing temperature, as it does in most materials, the droplets of the minority phase will drift in the direction of the thermal gradient. The report describes thermal-migration experiments with transparent solutions.

The report takes up the critical-point wetting phenomenon and its role in phase separation and solidification. Advances in methods of controlling separation in experiments are highlighted.

A major difficulty in studying metal mon-otectic systems is that most of the information must be gleaned from the final solidified products. As a result, much effort over the past several years has been devoted to developing transparent analogous systems for studying phase separation. The report surveys this work. It considers holographic techniques for investigating spinodal decomposition in transparent systems. It also considers directional-solidification experiments with succinonitrile in water, a mixture that is not only transparent but also solidifies at convenient temperatures (around 20°C).

This work was done by Donald O. Frazier, Barbara R. Facemire, William F. Kaukler, William K. Witherow, and Ursula Fanning of **Marshall Space Flight Center**. Further information may be found in NASA TM-82579 [N84-24773/NSP], "Separation Processes During Binary Mono-tectic Alloy Production" [\$8.50]. A paper copy may be purchased [prepayment required] from the National Technical Information Service, Springfield, Virginia 22161. The report is also available on microfiche at no charge. To obtain a microfiche copy, Circle 92 on the TSP Request Card. MFS-27074

Crack Growth in Single-Crystal Silicon

Experimental results suggest an absence of sub-critical crack growth.

A report describes experiments on crack growth in single-crystal silicon at room temperature in air. These results could aid in the design and fabrication of silicon photovoltaic and microelectronic devices.

Crack growth in the {111} cleavage plane of wafers, 50 by 100 by 0.76 mm in dimension, cut from Czochralski single-crystal silicon was studied by the double-torsion load-relaxation method and by acoustic-emission measurements. Scanning electron microscopy and X-ray topography were also employed.

The findings include the following:

- The critical stress-intensity factor for cleavage-crack propagation in the {111} cleavage plane of single-crystal silicon was $1 \text{ MN/m}^{3/2}$ by the double-torsion load-relaxation method. At the critical stress-intensity factor, cracks propagated by jumping.
- No load relaxation was observed during the load-holding period of the double-torsion test; hence, there was no measurable, slow-moving crack growth. This suggests the absence of subcritical crack growth.
- During loading, no acoustic-emission event was detected before the critical-stress-intensity factor was reached or during the load-relaxation-holding period. This observation also suggests the absence of subcritical crack growth.
- Acoustic-emission peak amplitudes with a signal-to-noise ratio greater than 60 dB were found at the critical stress-intensity factor for cleavage-crack pro-

pagation in the {111} plane of single-crystal silicon.

- Examinations of fracture surfaces revealed that during crack growth, the typical crack front jumped several times in a "mirror" region (where the crack surface was relatively smooth), before it propagated rapidly in a "hackle" region (where the surface was rough).
- Hackle marks on the fracture surface were associated with arrays of dislocation etch pits. Hackle marks appear to result from plastic deformation at the tips of rapidly moving cracks.
- Dislocation etch pits were not observed on the crack-front markings or in the flat areas of the "mirror" surfaces. In the mirror region, crack growth may result from interatomic bond breakage at the crack tip.
- Acoustic emission appears to be generated spontaneously from crack-front jumping (interatomic bonds broken) and hackle-mark formation (dislocation generation) during the crack growth.

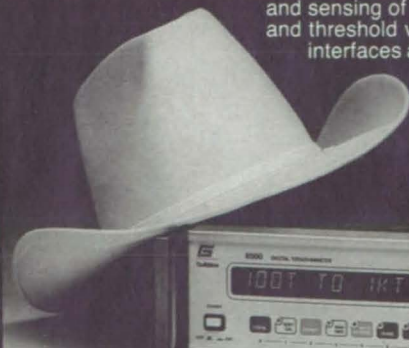
This work was done by Chern P. Chen and Martin H. Leipold of Caltech for **NASA's Jet Propulsion Laboratory**. To obtain a copy of the report, "Crack Growth in Single-Crystal Silicon," Circle 106 on the TSP Request Card. NPO-16757

OHM OHM on the range From 100 kilohms to 10,000 teraohms

The model 6500 Digital Teraohmmeter is the latest in a long and impressive line of precision resistance measurement devices from Guildline Instruments.

This new teraohmmeter is fully automatic and functions under microprocessor control and unique Sofcal™ calibration firmware. It can measure extremely high resistances, up to 10^{16} ohms, or very small currents down to 1 picoamp. Measurement time for the instrument is 5ms to 1000 seconds and sensing of instrument resistance range, integration time and threshold voltage is automatic. IEEE 488 and RS 232C interfaces are built-in as standard.

For more information contact
Guildline Instruments.



Model
6500 Digital Teraohmmeter



Guildline

Guildline Instruments Inc., 4403 Vineland Road • Suite B10
Orlando, Fla. 32811-7335 • (305) 423-8215 Telex: 856443

Guildline Instruments Ltd., P.O. Box 99 • 21 Gilroy St.
Smiths Falls, Ontario K7A 4S9 • Canada • (613) 283-3000 Telex: 053-3028

Computer Programs



Hardware, Techniques, and Processes

- 74 Economic-Analysis Program for a Communication System
- 78 Predicting the Cosmic Ray Environment Near Earth
- 78 Predicting Aircraft Spray Patterns on Crops
- 78 Estimating Average Wind Velocity Along a Trajectory
- 80 Research Program for Vibration Control in Structures
- 80 Flutter and Vibration Animation Program
- 80 Combining Structural and Substructural Mathematic Models
- 80 Analyzing Shuttle Orbiter Trajectories
- 82 Predicting Failures of Composite, Spherical Pressure Vessels
- 82 HYTESS-Hypothetical Turbofan-Engine Simplified Simulation
- 82 Aircraft Rollout Iterative Energy Simulation
- 83 Estimating Transient Pressure Surges in Cryogenic Systems
- 83 Computing Cooling Flows in Turbines
- 83 Four-Cylinder Stirling-Engine Computer Program
- 86 Graphics Programs for the DEC VAX Computer
- 86 Computing Benefits and Costs for Propulsion Systems
- 86 Analyzing Multidimensional Image Data
- 88 High Level Data-Abstraction System
- 88 Constant-Elasticity-of-Substitution Simulation
- 90 An Expert-System Engine with Operative Probabilities

COSMIC: Transferring NASA Software

COSMIC, NASA's Computer Software Management and Information Center, is the one central office established to distribute software that is developed with NASA funding. COSMIC's role as part of NASA's Technology Utilization Network is to ensure that NASA's advanced software technology is made available to industry, other government agencies, and academic institutions.

Because NASA's software development efforts are dynamic and ongoing, new programs and updates to programs are added to COSMIC's inventory on a regular basis. *Tech Briefs* will continue to report information on new programs. In addition, the 1986 edition of the *COSMIC Software Catalog* is available with descriptions and ordering information for available software. Several new programs for control systems/robotics, expert systems, thermal analysis, turbomachinery design, structural analysis, and computer graphics are offered.

For additional information on any programs described in this issue of *Tech Briefs*, circle the appropriate number on the TSP card at the back of the publication. If you don't find a program in this issue that meets your needs, you can call COSMIC directly at (404) 542-3265 and request a review of programs in your area of interest. There is no charge for this information review.

COSMIC®

Computer Services Annex, University of Georgia, Athens, GA 30602; Phone (404) 542-3265
John A. Gibson, Director

Computer Programs

These programs may be obtained at a very reasonable cost from COSMIC, a facility sponsored by NASA to provide tested and reliable software to the public. For information on program price, size and availability, circle the reference number on the TSP and COSMIC Request Card in this issue.



Economic-Analysis Program for a Communication System

Prices and profits of alternative designs can be compared.

The objective of the Land Mobile Satellite Service Finance Report (LMSS) program is to provide a means for comparing alternative designs of LMSS systems. This program is actually a Multiplan worksheet program. The labels used in the worksheet were chosen for a satellite-based cellular communication

service, but the analysis is not restricted to such cases.

A comprehensive financial model is used to calculate a figure of merit, which can be used to compare effects of equipment and operating costs, pricing strategy, and customer demand for different systems. The program also calculates the price that a company would have to charge customers to meet all its expenses and make a specified profit. A price estimate can be obtained for almost any service that is heavily dependent on capital investment and which has operating costs that depend on the amount of service sold.

The economic analysis has two main components: supplier finances and customer finances. Supplier finances include amortization, interest, insurance, taxes, and operating and maintenance expenses. Customer finances include usage rate, subscription fees, equipment costs, and estimated traffic. Prices can be defined as real or nominal to account for the effects of escalation and inflation, and the profits can be regulated or unrestricted.

LMSS is written for interactive execution with Multiplan (version 1.2) and has been implemented on an IBM PC series computer operating under DOS (version 2.11). The LMSS worksheet program has a space requirement of approximately 38K of 8-bit bytes. This worksheet program was developed in 1984.

This program was written by R. G. Chamberlain of NASA's Jet Propulsion Laboratory. For further information, Circle 88 on the TSP Request Card.
NPO-16606

NOW THERE'S ONLY ONE THING KEEPING YOU FROM PROGRAMMING IN ADA:

YOU.

If you're programming on an Apollo DOMAIN, SUN-2 or SUN-3 system—or considering investing in one—the language of the future is here.

Right now, validated, full-function Ada compilers are available from Alsys, the leader in Ada language systems. Compilers as advanced as Ada itself.

They're written in Ada and self-compiled, which means they meet a standard that goes beyond validation, one imposed by the language itself.

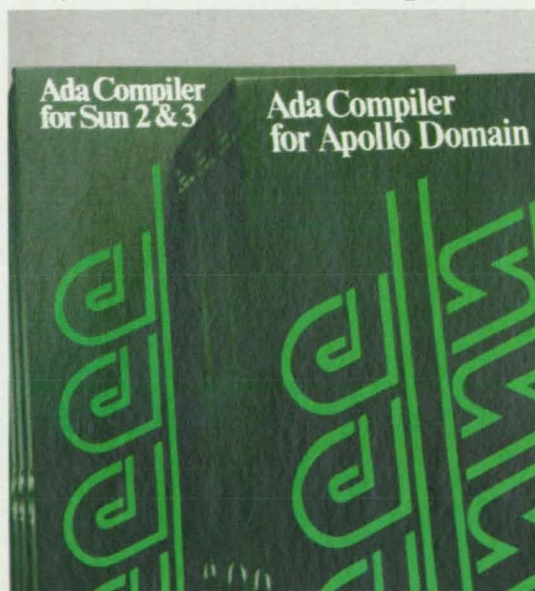
They're efficient, producing fast, compact running code. Code that even

surpasses that of many commercial compilers, including some of the best C and Pascal compilers available (according to the Ackerman Benchmarks).

They're supported with documentation that's clear and complete. And by a technical support staff of Ada experts, eager to help you get the most out of your Alsys Ada compiler.

They're available now. Call or write Alsys today for the rest of the story. Because the more you

know about our compilers, the sooner you'll be using one.



Circle Reader Action No. 341

alsys
Opening the doors to Ada

Alsys, Inc., Dept. 1432 Main Street, Waltham, MA 02154

Telephone: (617) 890-0030 Telex: 948-536

Also offices in France and the United Kingdom.

☐ Please send me more information about your Ada compiler for my _____ (please specify system).

☐ Please send me more information about Ada.

Ada is a registered trademark of the U.S. Government (AJPO).

Name _____

Title _____

Company _____

Address _____

City _____ State _____ Zip _____

Telephone (____) _____

NTB



DATA GENERAL ASKS RUSSIAN ROULETTE WITH

FOR ADVANCED COMPUTER SYSTEMS, TALK TO US. IT'S WHY SO
MANY GOVERNMENT DEPARTMENTS HAVE CHOSEN DATA GENERAL.

Government business is too critical to be taken for granted. Too much depends on it.

No wonder nineteen of the top twenty U.S. defense contractors have bought a Data General system. As have all the Armed Services and most major departments of the federal

government.

And to date, nearly thirty U.S. Senate offices and committees have chosen Data General.

TODAY'S BEST VALUE

Why such unanimity? Because Data General offers a complete range of computer solutions for government

programs, with one of the best price/performance ratios in the industry.

From our powerful superminis to the DATA GENERAL/One™ portable. From unsurpassed software to our CEO® office automation system. Plus complete systems for Ada® and Multi Level Secure Operating Systems, and a



ARE YOU PLAYING YESTERDAY'S TECHNOLOGY?

strong commitment to TEMPEST.

All Data General systems have full upward compatibility. And because they adhere to international standards, our systems protect your existing equipment investment. We give you the most cost-effective compatibility with IBM outside of IBM—and the easiest to set up and use.

SOLID SUPPORT FOR THE FUTURE


We back our systems with com-

plete service and support. As well as an investment in research and development well above the industry norm.

So instead of chancing yesterday's technology, take a closer look at the

computer company that keeps you a generation ahead. Write: Data General, Federal Systems Division, C-228, 4400 Computer Drive, Westboro, MA 01580. Or call 1-800-DATAGEN.



 **Data General**
a Generation ahead.

© 1985 Data General Corp., Westboro, MA. Ada is a registered trademark of the Department of Defense (OUSDRE-AIPO). DATA GENERAL/One is a trademark and CEO is a registered trademark of Data General Corp.

Circle Reader Action No. 353



Predicting the Cosmic-Ray Environment Near Earth

The rates of logic-circuit bit errors are estimated.

This package of computer programs was developed to predict the cosmic-ray environment for a spacecraft in orbit near Earth. A single cosmic-ray particle can deposit enough electrical charge on a sensitive area of an individual circuit to change the bit state. These single-event upsets may not cause permanent damage but can upset functioning devices. This package has been used to predict the upset rate for a space mission. The package can also calculate the time-average cosmic-ray environment for multiple circular orbits, fragments of trajectories, and isolated points.

A simple transport analysis is used to approximate the environment at the center of a spherical shield of arbitrary thickness. The effects of mass shielding and magnetic shielding are included in the computation. The principle output of the package is a Heinrich curve describing the flux of cosmic-ray particles with a given linear energy transfer (LET).

The package contains five programs: (1) GEOMAG calculates the modulating factor due to geomagnetic shielding for a given trajectory segment; (2) SPECTRUM calculates interplanetary cosmic-ray spectra and uses the GEOMAG factor to produce a time-average spectrum at the spacecraft exterior; (3) INTEGRATE converts differential spectra to integral spectra; (4) TRANSPORT computes the integral flux at the center of a spherical, shielded region; and (5) UPSET FLUX calculates the flux that causes an upset for each threshold LET. The programs are normally run in succession, but each can be used in a stand-alone fashion if the necessary input is available from outside sources.

This package is written in HPL for interactive execution and has been implemented on an HP 9825B desktop computer. This package was developed in 1985.

This program was written by L. D. Edmonds of NASA's Jet Propulsion Laboratory. For further information, Circle 78 on the TSP Request Card.
NPO-16617



Predicting Aircraft Spray Patterns on Crops

A computer program examines how aircraft designs affect the deposition of agricultural materials.

The Agricultural Dispersion Prediction (AGDISP) system was developed to predict the deposition of agricultural material released from rotary- and fixed-wing aircraft. AGDISP computes the ensemble average mean motion resulting from turbulent fluid fluctuations.

The development of the AGDISP system was motivated by the need to determine how aircraft-unique wake and propulsion-system characteristics affect the ground deposition of aerially released material. Simple aircraft-design changes, such as winglets, could potentially produce a more-desirable deposition pattern. AGDISP can be used to examine ways of making the dispersal process more efficient by insuring uniformity, reducing waste, and saving money.

AGDISP assumes that the particles are influenced by three forces: (1) aerodynamic drag, (2) forces as a consequence of evaporation, and (3) gravity. A Lagrangian approach was used to develop the equations of motion of discrete particles released from an aircraft. A predictor/corrector solution scheme is used to solve the resulting set of ordinary differential equations. The behavior of the particles is intimately connected to the local background mean-velocity and turbulence fields through which the particles are transported.

Flow-field options available in AGDISP include fixed-wing fully-rolled-up tip vortices; fixed-wing Betz rollup, propeller, helicopter in forward advance; mean-background crosswind, plant canopy, superequilibrium turbulence, terrain; and externally-computed mean-velocity and turbulence fields. The particle equations are integrated repeatedly until either the specified maximum simulation time is reached or all of the particles deposit on the surface.

The AGDISP system consists of three computer programs: The AGDISP program establishes the desired background fields and computes the particle trajectories. The AGPLOT program plots the resulting trajectories and deposition pattern. The AGLINE program constructs an

equivalent Gaussian-profile distribution from the multiparticle solution. Each of the programs is designed to run interactively, with the AGPLOT program supporting a Tektronix terminal with PLOT 10 software.

The programs in the AGDISP system are written in FORTRAN IV for interactive execution and have been implemented on a CDC CYBER 170-series computer operating under NOS 1.4 with a central-memory requirement of approximately 60K total of 60-bit words. The AGDISP system was developed in 1984.

This program was written by Milton E. Teske and Alan J. Bilanin of Continuum Dynamics, Inc., for Langley Research Center. For further information, Circle 63 on the TSP Request Card.
LAR-13432

Estimating Average Wind Velocity Along a Trajectory

The variation of wind velocity with altitude is taken into account.

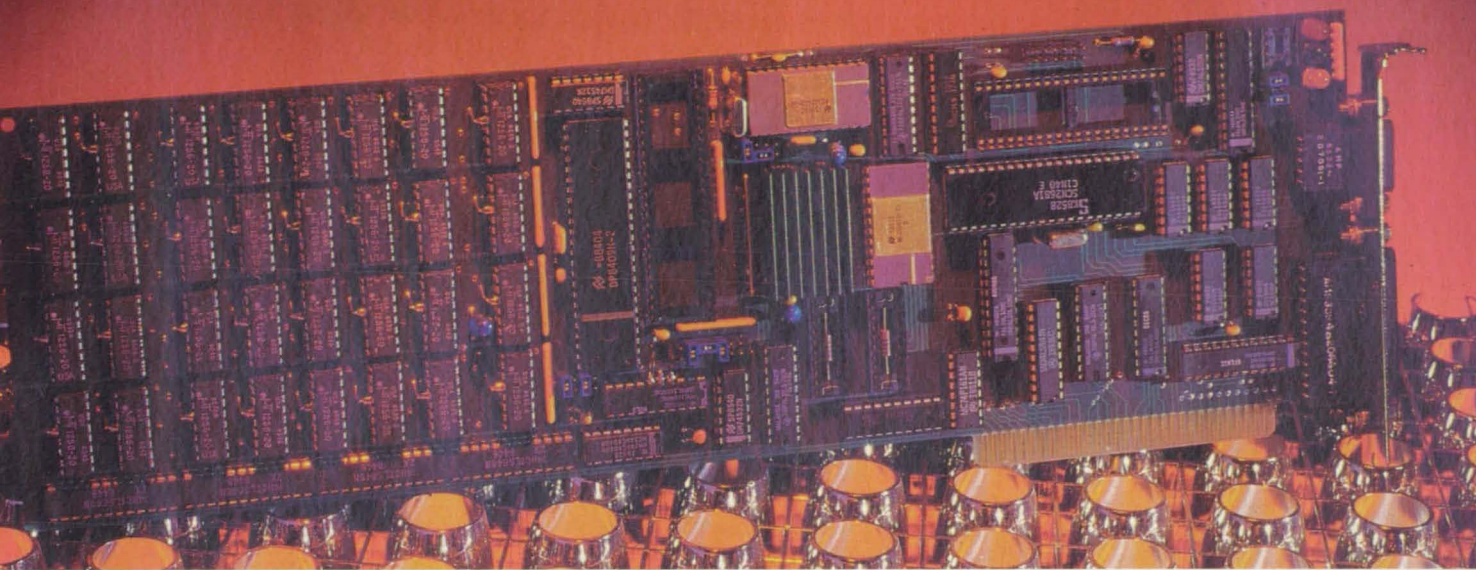
The Average Wind Velocity (VWAVE) program calculates the average wind velocity over time for a particular vehicle trajectory. The calculation is based on wind profile, which is the wind magnitude at various altitudes. The average of a wind profile over altitude does not correlate well with the actual apparent effect of wind. Wind profiles with low average velocities may be more severe than some wind profiles with high average velocities.

The amount of time a vehicle experiences each different wind level of a profile is taken into account by VWAVE. The VWAVE program produces a reliable description of the relative magnitude of wind profiles as experienced by a certain trajectory. VWAVE was developed for use in analyzing the Space Shuttle orbiter glide return to the ground, but is useful for wind effects on takeoff and landing trajectories of other aircraft, as well as performance evaluations and dispersion theory.

There are two methods of calculation: In the first, the user must enter a wind profile and the vertical velocity versus altitude. This can be done interactively with the provided elementary editor. The second method requires wind-profile-versus-time data from a trajectory simulation in the standard TRWPLT format. The VWAVE program is menu driven and has options to list or edit the input files. The final result is a calculated value of wind velocity, which, if held constant, would approximate the same effects as those of the given wind profile on that particular trajectory.

CONVERT

NOW YOUR PC CAN RUN 35 TIMES FASTER



Turn Your PC Into A Powerful 32-BIT Super-Mini

DSI-32 Ever wish your PC could have more power and speed than a VAX? The **DSI-32** Co-Processor Board is a totally self-contained 32-bit computer on a single PC board. It runs at super-mini speeds (10MHz and no wait states) using its own large 32-bit memory space and floating point processor. It's fully compatible with your standard PC MS/DOS system, no re-training or file conversions is needed. Total installation is accomplished in just a few minutes.

It enables you to port scientific or commercial applications without the grueling task of recoding or restructuring your software to accommodate Intel's architecture. **DSI-32** gives you freedom of choice, either MS/DOS or Unix, without having to commit your entire system to one or the other.

Plug it in and let **DSI-32** expand your horizons.

- Uses just one slot.
- Comes with National Semiconductor's 32032 processor running at 10MHz—a full 32-bit data path.
- 1MB to 8MB available on board. (Greater memory options available soon.)
- Choice of two Operating Systems: — MS/DOS Standard or Unix V Option.
- Operates in any IBM/PC, AT or look-alike.
- Has its own Floating Point Processor.
- Supports a variety of native high level, optimizing languages: C, Pascal, Fortran, and soon ADA. Supplied with Assembler, Linker, Loader and Debugger.
- Turns your PC into a powerful concurrent processor Mini. The host 8088 or 80286 handles all I.O. functions while the 32032 runs uninterrupted.
- Transport a large variety of Mini and Mainframe programs in minutes to run on your micro.
- Now you can run large time consuming applications on a PC at warp speeds.
- Get the power and performance of computers costing tens of thousands more for less than many micros. The Definicon DSI-32.
- Try our board now at no risk. 30 Day Money Back Evaluation Period

Sieve Benchmark

N°	IBM XT	IBM AT	VAX 750	VAX 780	DSI-32
20,000	35.30	8.13	6.11	3.04	4.52
40,000	351.50	99.71	13.13	6.38	9.07

Float Benchmark

40,000	11.46	17.71	.83	.50	.80
--------	-------	-------	-----	-----	-----

Unix Benchmarks

	DSI-32	VAX 780	VAX 750
O.S. Overhead	3.88	4.4	7.0
C Compiler Test	.55	1.0	1.7
Sieve of Eratosthenes	1.93	1.7	2.4

ECOTECH[®]
COMPUTER SYSTEMS

3711 35th Street, N.W.
Washington, D.C. 20016.

800 826-2189

202 244-3858

VWAVE is written in FORTRAN V for interactive execution and has been implemented on a UNIVAC 1100-series computer with a central-memory requirement of approximately 21K of 36-bit words. The program was developed in 1981.

This program was written by Paul Bertsch of McDonnell Douglas Corp. for Johnson Space Center. For further information, Circle 64 on the TSP Request Card.

MSC-20792

Research Program for Vibration Control in Structures

Compensating algorithms are developed from optimal-control theory.

The purpose of this research computer program is to apply control theory to large space structures (LSS's) and to design a practical compensator for suppressing vibration. LSS's often have rigid hubs or flexible struts or ribs and may have meshed surfaces. These elements produce rigid-body modes and flexible vibration modes with closely-packed structural frequencies. This program models the LSS as a distributed system. Control theory is applied to produce a compensator described by functional gains and transfer functions. This program has been used for the comparison of the robustness of low- and high-order compensators that control the surface vibrations of a realistic wrap-rib antenna.

Distributed-system theory and finite-dimensional control theory are combined by use of approximations. The ideal, or optimal, compensator for a distributed system is infinite-dimensional. This program approximates the infinite-dimensional compensator by the use of finite-dimensional linear/quadratic Gaussian optimal-control equations. Balanced realizations are used to reduce the order. The LSS itself is mathematically described as a Galerkin/component-mode finite-element model.

The program is written in FORTRAN for batch execution and has been implemented on an IBM 30xx series computer. The program was developed in 1984.

This program was written by D. L. Mingori and J. S. Gibson of H. R. Textron, Inc., for NASA's Jet Propulsion Laboratory. For further information, Circle 42 on the TSP Request Card.

NPO-16615

Flutter and Vibration Animation Program

Vibration analyses of machines and structures are converted to animated displays.

The Flutter and Vibration Animation (FLUVIAN) program produces an animated picture of a structure as it vibrates at constant amplitude. FLUVIAN permits visual observation of the fluttering motion of components as they oscillate in a combination of modes. The animated display provides an insight into local deflection patterns induced in the structure, which might be overlooked if the modal deflection patterns were separately examined and then combined mentally.

FLUVIAN uses the segment and refresh features of the Tektronix 4114 computer-graphics terminal. Each time-step picture of an oscillating structure is defined as a segment. The segments are turned on and off sequentially to produce an animated display of the motion.

The input data to FLUVIAN may consist of up to 2,000 lines per plot, with lines denoted by coordinates of the end points. The sample data provided with FLUVIAN are from the analysis of the Space Shuttle orbiter fin flutter. FLUVIAN is also applicable to motion studies of buildings, bridges, oil rigs, moving parts of automobiles, and other complex structures.

The FLUVIAN program is written in FORTRAN 77 for interactive execution and has been implemented on a CDC CYBER 170-series computer operating under NOS with a central-memory requirement of approximately 56,300 (octal) of 60-bit words. This program requires the PLOT-10 Terminal Control System and a Tektronix 4114 graphics terminal. FLUVIAN was developed in 1984.

This program was written by Richard L. Tischner of Rockwell International Corp. for Johnson Space Center. For further information, Circle 60 on the TSP Request Card.

MSC-20895

Combining Structural and Substructural Mathematical Models

Automation reduces input length and potential data-entry errors.

The Matrix Automated Reduction and Coupling (MARC) program is used for combining NASTRAN® substructural

models with a primary structural model. MARC also constructs the job-control language (JCL) stream for a NASTRAN batch job that utilizes a previously-written user library of dynamic models. This automation minimizes lengthy input and reduces potential data-entry errors. The MARC procedure has been used in assembling the Space Shuttle orbiter dynamic models since 1983 and has reduced NASTRAN modeling input time by as much as 50 percent.

MARC uses the NASTRAN Substructure Operating File (SOF) to assemble mathematical models, then reduces the stiffness and mass matrices of the substructure assemblies. The reduced matrices are then coupled to the primary structural model. Optionally, MARC adjusts the primary structure mass matrix via NASTRAN Direct Matrix Input.

Before using MARC to assemble a model, the user must create a data base containing the following information: (a) grid coordinates and data for generating the NASTRAN BDYS1 map, (b) up to 50 substructure-identification codes and the corresponding SOF names, and (c) stiffness and mass matrices for the primary structure and substructures. MARC generates map files, tape backups of substructure matrices, and the JCL stream for a batch NASTRAN job to assemble the final dynamic model.

The MARC program is written in FORTRAN IV for interactive execution and has been implemented on an IBM 370-series computer operating under OS/VS2 with a central-memory requirement of approximately 55K of 8-bit bytes. MARC was developed in 1982.

This program was written by Victor K. Choa of Rockwell International Corp. for Johnson Space Center. For further information, Circle 28 on the TSP Request Card.

MSC-20897

Analyzing Shuttle Orbiter Trajectories

Measurements are combined to produce best estimates of flight paths.

The LRBET4 program is a best-estimate-of-trajectory (BET) calculation for post-flight trajectory analysis of the Shuttle orbiter. LRBET4 produces estimated measurements for comparing the predicted and actual trajectory of an Earth-orbiting spacecraft. A Kalman filter and a smoothing filter are applied to the input data to estimate the state vector, reduce noise, and produce the BET.

LRBET4 processes up to three simul-

When the Air Force demanded Total Performance, Zenith delivered.

Total performance. It's the only option for the U.S. Air Force. To measure up is to outperform the merely superior.

After extensive evaluation, the Air Force selected one official stand-alone microcomputer. The Zenith Z-120 desktop.



Zenith Z-150 PC

Now, from the same tradition as the Zenith Z-120, come the "total performance" business computers: the Zenith Z-100 PC's. They're IBM PC-compatible, but are designed with enhanced features that go beyond IBM PC compatibility. Including greater internal expandability. Storage that can expand up to 11 megabytes. A detached keyboard with an improved key layout. And the ability to run virtually all IBM PC software. We also offer Z-150 PC's that are "Tempest Accredited." (Zenith-modified listed

on Preferred Products List under Inteq, Inc.)

For your free Zenith PC Information Kit and the name of your nearest Zenith Data Systems dealer, please call **1-800-842-9000, Ext. 1**



taneous range measurements from tactical air navigation sites, C-band radar, and S-band radar. In addition, LRBET4 accepts Doppler measurements obtained from tracking data-relay satellites. Inertial-measurement-unit data are used in the equations of motion to improve accuracy during large burns.

The program incorporates a Kalman filter to process all navigational data prior to a given time. This output is then used by a backward-smoothing filter to estimate the state vector based on data before and after the given time. The normal LRBET4 output is the state vector from the smoothing filter. Abbreviated runs can be performed using only the forward Kalman filter. The state vector is propagated at time intervals of less than 60 seconds, with its output to a magnetic tape or a printer.

LRBET4 is written in FORTRAN IV for batch execution and has been implemented on a CDC CYBER 170-series computer with a central-memory requirement of approximately 117K (octal) of 60-bit words. The program was written in 1983.

This program was written by William M. Lear of TRW, Inc., for Johnson Space Center. For further information, Circle 61 on the TSP Request Card.
MSC-20786

Predicting Failures of Composite, Spherical Pressure Vessels

Long-term viscoelastic effects are computed to predict bursts.

Spherical pressure vessels are commonly made of filamentary composites for applications in which they must be light in weight. This program was developed for predicting the failure of such a vessel over a long time span. Short-term failure pressures (bursting points) can be predicted, but the long-term structural integrity of laminated vessels is being studied only now.

This program examines the time-dependent response of a vessel by considering the linearly viscoelastic character of the matrix, which binds high-strength fibers wrapped around an inner metallic liner. Under conditions of sustained high pressurization, the burst pressures and critical strains on composite pressure vessels are shown to vary with time. A laminated Kevlar (or equivalent aromatic polyamid) resin model is evaluated, and the filament volume ratio is found to be a significant factor in long-term performance.

The spherical vessel is modeled as a pseudoisotropic composite shell. By use of the maximum-strain theory of failure, both the burst pressure and the critical-strain equations are formulated, solved in the Laplace domain, and inverted to the time domain by the method of collocation. The required inputs include the elastic modulus, Poisson's ratio, shell diameters, loads, initial strains, and volumes. An auxiliary program is included for the calculation of initial burst pressures and strains.

These programs are written in FORTRAN 77 for batch execution and have been implemented on a UNIVAC 1100-series computer with a central-memory requirement of approximately 7K of 36-bit words. The programs were developed in 1983.

These programs were written by Jan D. Dozier of Marshall Space Flight Center. For further information, Circle 62 in the TSP Request Card.
MFS-27050



Machinery

HYTESS-Hypothetical Turbofan-Engine Simplified Simulation

Simulated characteristics mimic those of advanced turbofan engines.

A computer program has been developed to offer those interested in engine dynamics and controls research an efficient, realistic, and easily-used engine simulation. This simulation was developed from linearized operating-point models but still retains essential nonlinear engine effects. The simulation is representative of a hypothetical, low-bypass-ratio, twin-spool, axial-flow turbofan engine.

Typically, turbine-engine simulations incorporate detailed nonlinear descriptions of both steady-state and dynamic engine operation through the engine flight envelope. These detailed nonlinear simulations are very accurate and realistic and, when implemented in a digital computer, require relatively large amounts of computer storage and computer-processing time. This makes these detailed simulations difficult and costly to use. HYTESS was developed as an alternative. It is structurally simpler than a full nonlinear engine simulation and therefore has reduced storage and processing requirements.

HYTESS retains the essential nonlinear effects inherent in the engine operation.

This is accomplished by modeling the engine using a linear state-space formulation and incorporating the nonlinear characteristics by representing the matrix elements within the linear state-space structure as nonlinear functions of various engine variables. The compromise implied in this process is that, although the fidelity of HYTESS is maintained for the variables considered, it is very difficult to identify individual component behavior as in a detailed simulation. Also HYTESS is restricted to operating in regions about the normal operating line of the engine.

The engine characteristics simulated by HYTESS, although hypothetical, are qualitatively similar to those of realistic advanced turbofan engines. Typical applications for this simulation would include open-loop engine dynamics studies as well as closed-loop controls analysis using a user-generated control law.

This program is written in FORTRAN IV for use on an IBM 3033 AP computer running under the TSS/370 operating system.

This program was written by W. C. Merrill of Lewis Research Center, C. Beattie and R. F. LaPrad of Pratt & Whitney Aircraft Co., and S. M. Rock and M. M. Akhter of Systems Control Technology, Inc. For further information, Circle 22 on the TSP Request Card.
LEW-14020

Aircraft Rollout Iterative Energy Simulation

A computer program evaluates the performance of aircraft brakes.

The Aircraft Rollout Iterative Energy Simulation (ARIES) program analyzes aircraft-brake performance during rollout. The program simulates a three-degree-of-freedom rollout after nose-gear touchdown. The amount of brake energy dissipated during the aircraft landing determines the life expectancy of brake pads. ARIES incorporates brake pressure, actual flight data, crosswinds, and runway characteristics to calculate the following: (a) brake energy during rollout for up to four independent brake systems; (b) time profiles of rollout distance, velocity, deceleration, and lateral runway position; and (c) all aerodynamic moments on the aircraft.

ARIES can be adapted for modeling most landing aircraft during unpowered rollout. Optimum braking procedures can be developed with ARIES to minimize brake deterioration within the specified lengths of runway. ARIES has been used to evaluate several Space Shuttle orbiter brake-pad failures.

After the input of initial runway and

landing conditions, ARIES utilizes three simulation models to evaluate the rollout at given time intervals. The brake-force simulation requires tire and brake information along with actual flight data. The equations of motion allow force and moment balances to be calculated. The aerodynamic effects are computed, including lift, drag, axial and normal forces, and roll, pitch, and yaw moments. The various aerosurface effects are obtained from interpolation of the Rockwell Aero Sciences Group Design Data Book tables. The output is in both printed and plotted forms. ARIES iterates the calculations until the computed forward velocity is below 3 knots (1.5 m/s).

ARIES is written in FORTRAN 77 for batch execution (interactive usage is possible, but high external-core memory requirements may limit its practice) and has been implemented on a CDC CYBER 170-series computer with a central-memory requirement of 64K of 60-bit words, with up to an additional 460K of 60-bit words for storing the aerodynamic-coefficient table interpolation subroutines. ARIES was developed in 1984.

This program was written by Lane Kinoshita of Rockwell International Corp. for Johnson Space Center. For further information, Circle 65 on the TSP Request Card.
MSC-20816

Estimating Transient Pressure Surges in Cryogenic Systems

Potentially-damaging pressure waves can be anticipated and, therefore, avoided.

A mathematical model has been developed for the prediction of pressure behavior in single- and two-phase cryogenic systems. A transient-liquid-flow analysis has been modified to incorporate the behavior of vapor bubbles and is used to predict maximum pressure in cryogenic transfer systems consisting of complex pipe and valve arrangements under both steady-state and transient conditions. This simulation has compared favorably with data obtained during the transfer of liquid oxygen from ground storage tanks to the Space Shuttle orbiter external tanks.

Within a cryogenic liquid-transfer system, vapor cavities can easily be formed if a localized reduction in pressure occurs. Any valve opening or closing may cause the cavities to form or collapse due to a pressure variation. The collapse of an entrapped vapor cavity causes a water hammer-type effect and the creation of

high-pressure waves, which may damage the piping system and associated instrumentation. To predict the magnitude of undesirable pressure surges, this model uses the method of characteristics and basic fluid-mechanics equations, taking into account vapor cavities. The program output includes maximum pressure at junctions, the pressure head and velocity at the upstream and downstream ends, and the length of any vapor cavities in the piping system.

This program is written in FORTRAN 77 for batch execution and has been implemented on a DEC VAX-series computer with a central-memory requirement of approximately 105K of 8-bit bytes. The program was developed in 1983.

This program was written by Phillip Pfister, F. S. Gunnerson, and E. R. Hosler of the University of Central Florida for Kennedy Space Center. For further information, Circle 87 on the TSP Request Card.

KSC-11312

Computing Cooling Flows in Turbines

The required flow and the consequent decrease in efficiency are predicted.

An algorithm has been developed for calculating both the quantity of compressor bleed flow required to cool a turbine and the resulting decrease in efficiency due to cooling air injected into the gas stream. Because of the trend toward higher turbine-inlet temperatures, it is important to predict accurately the required cooling flow. This program is intended for use with axial-flow, air-breathing, jet-propulsion engines with a variety of airfoil-cooling configurations. The algorithm results have compared extremely well with figures given by major engine manufacturers for given bulk-metal temperatures and cooling configurations.

The program calculates the required cooling flow and corresponding decrease in stage efficiency for each row of airfoils throughout the turbine. These values are combined with the thermodynamic efficiency of the uncooled turbine to predict the total bleed airflow required and the altered turbine efficiency. There are 10 airfoil-cooling configurations, and the algorithm allows a different option for each row of cooled airfoils. Materials technology is incorporated and requires the date of the first year of service for the turbine stator vane and rotor blade. The user must specify pressures, temperatures, and gas flows into the turbine.

This program is written in FORTRAN IV for batch execution and has been imple-

mented on an IBM 3080-series computer with a central-memory requirement of approximately 61K of 8-bit bytes. The program was developed in 1980.

This program was written by James Gauntner of Lewis Research Center. For further information, Circle 23 on the TSP Request Card.
LEW-13999

Four-Cylinder Stirling-Engine Computer Program

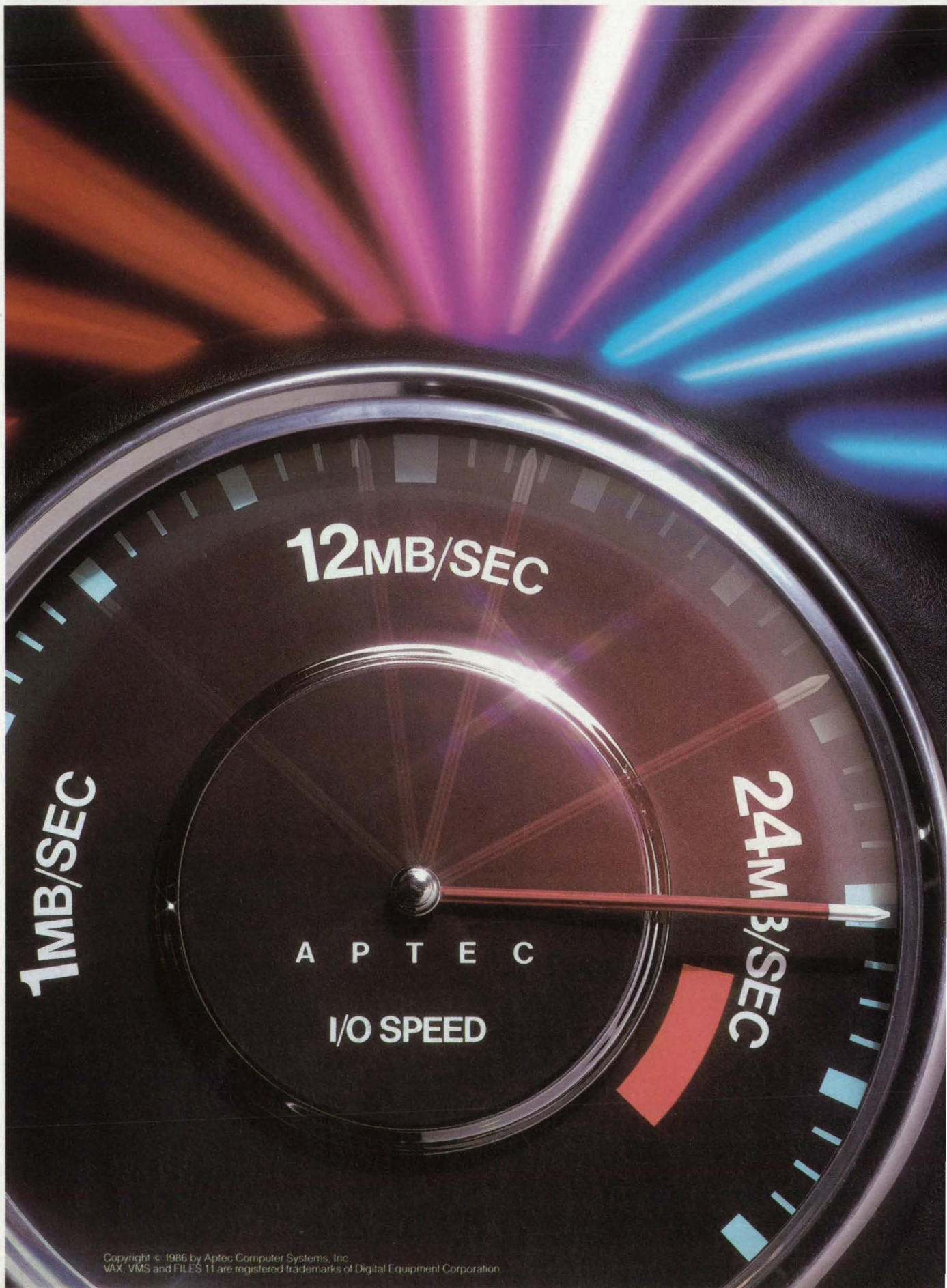
Both steady-state and transient simulations include realistic effects.

A computer program has been developed for simulating the steady-state and transient performance of a four-cylinder Stirling engine. Usual Stirling-engine models include only two pistons and the working space between them. For analysis, the working space is usually segmented into control volumes corresponding to engine components: expansion space, heater, regenerator, cooler, and compression space. More than one control volume may be used to describe each component. Also, various heat-transfer paths are included in the model. While many Stirling engines have more than one working space, the models used to predict performance generally do so for a single working space, and the resultant output power is multiplied by the number of working spaces. Although this approach is acceptable for performance calculations, it has shortcomings when the constant-pressure assumption cannot be used, such as when the amount of hydrogen within a working space varies during a cycle.

The new Stirling-engine computer model overcomes these difficulties. In the model, four cylinders are interconnected by four working spaces. Each working space contains seven volumes: one for the expansion space, heater, cooler, and compression space and three for the regenerator. A thermal time constant for the regenerator mass is associated with each regenerator gas volume.

The thermodynamic model includes both continuity and energy equations and simplified, first-order momentum terms (flow resistance). Drive dynamics and vehicle load effects are included. The computer program includes a model of a hydrogen-supply system to accelerate the engine.

The simulation can generate, at the user's option, steady-state or transient data. Steady-state power and torque predictions compare well with experimental data over a wide range of engine speeds and pressures. The model contains 70 state



Copyright © 1986 by Aptec Computer Systems, Inc.
VAX, VMS and FILES 11 are registered trademarks of Digital Equipment Corporation.

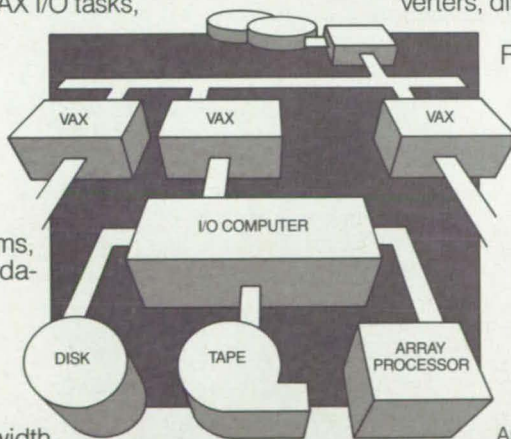
APTEC RUNS VAX TO THE MAX

Now VAX/VMS™ systems can handle high performance real time data at 24 Mbyte/sec I/O.

The VAX can be host to powerful, high-speed peripherals—and get up to 24 MB/sec throughput. Result: exceptionally fast and productive systems that easily meet real time data acquisition and processing needs.

Only the Aptec I/O Computer makes this possible. By offloading VAX I/O tasks, it extends system capabilities and performance, while assuring optimal use of peripherals. Modular and expandable, Aptec provides a cost-effective path to multiple array processor—even multiple VAX systems, with virtually no I/O degradation on even the biggest systems.

Key to offloading the VAX is Aptec's 32-bit bus structure. With a 24 MB/sec aggregate bandwidth, it handles I/O by direct communication between peripherals and Aptec mass memory.



Aptec also interfaces to high speed peripherals such as the Ibis 1400 disk system with up to 10 MB/sec data transfer rates.

Aptec frees the VAX for other tasks and frees you from frustrating host holdups.

Our extensive software supports powerful languages such as FORTRAN, STAPLE and Microcode; and familiar tools, including software drivers for array processors, A/D converters, disk and tape storage devices; all within a FILES 11™ environment.

Find out how Aptec runs VAX to the max—into new dimensions of real time processing. Call collect: (503) 620-9840. OEM arrangements are available. Aptec is a participant in Digital Equipment Corporation's Cooperative Marketing Program.

Aptec Computer Systems
P.O. Box 6750

Portland, OR
97228-6750
Telex 467167



**TEAM UP
APTEC
AND VAX/VMS
FOR HIGH
PERFORMANCE
REALTIME
SOLUTIONS**

variables. Also included in the model are piston-rod-seal leakage effects.

The simulation is modular to allow for easy modification of the model. An input routine is provided in which the user specifies the transient to be run and supplies the necessary engine geometry data. The type of output is also selected by the user. Very detailed printouts at prescribed intervals can be selected; alternatively, less detailed printouts can be selected. The integration step size and the printout interval do not have to be the same.

This computer code contains energy-equation effects and has many more volumes per working space than the previously published Stirling engine code, "Four-Cylinder Stirling Engine Control Simulation" (LEW-14106), page 148, *NASA Tech Briefs*, Vol. 9, No. 4. However, both codes give similar results and can be used together. The former code can generate results very quickly, since it has only 14 state variables with no energy equation. The current code can then be used to study various aspects of the Stirling engine in much more detail.

The program is written in FORTRAN IV for use on an IBM 370 computer.

This program was written by Carl J. Daniele and Carl F. Lorenzo of Lewis Research Center. For further information, Circle 55 on the TSP Request Card. LEW-14155



Mathematics & Information Sciences

Graphics Programs for the DEC VAX Computer

A variety of plots is available in video or printed form.

This LONGLIB library of computer programs is a set of subroutines designed for vector plotting on cathode-ray tubes and dot-matrix printers. LONGLIB subroutines are invoked by program calls similar to standard CALCOMP routines. In addition to the basic plotting routines, LONGLIB contains an extensive set of routines to allow viewport clipping, extended character sets, graphic input, gray-level plots, polar plots, and three-dimensional plotting with or without the removal of hidden lines.

LONGLIB includes "master subroutines," which are self-contained series of commonly used individual subroutines. When invoked, the master routine initializes the plotting package; plots contours, histograms, multiple curves, scatter plots, log plots, three-dimensional

plots, etc.; then closes the plot package; all with a single call.

LONGLIB was designed to produce plots on VT100's with Selnar boards, VT125's, VT240's, terminals compatible with the Tektronix 4010, and color RAMTEK 9400 devices. Printer output is available by using the raster-scan conversion routines for Printronix printers and high- or low-resolution Trilog printers. Software could easily be modified for other graphics output devices. The LONGLIB package includes the graphics library, an online help library, scan-converter programs, and command files for installing, creating, and testing the library.

LONGLIB is written in FORTRAN 77 and C (C language required for RAMTEK interface only) for batch execution and has been implemented on a DEC VAX series computer operating under VMS. These programs were developed in 1985.

This program was written by D. G. Long of Caltech for NASA's Jet Propulsion Laboratory. For further information, Circle 84 on the TSP Request Card. NPO-16666

Computing Benefits and Costs for Propulsion Systems

A weight-criteria rating approach is followed.

A flexible computer model has been developed for evaluating the benefits and costs of placing large space systems into operational orbits. With the advent of an operational space transportation system (STS), NASA will have the capability of transporting large-volume/low-density payloads to low Earth orbit (LEO). Some of these will be structures that allow the placement of very large antennas (200-m diameter), or collections of communications systems, in orbits ranging from LEO to geosynchronous Earth orbit (GEO). Currently, one approach is to deploy these large space systems (LSS) in LEO and transfer them to their operational orbits by a primary propulsion system. The vehicle thrust must be limited to assure that loading during the final acceleration will not collapse the lightweight structure. It was necessary to determine the most beneficial and cost-effective thrust level for orbit transfer of these payloads.

When subjecting a primary propulsion system to mission catalog requirements, this analytical model calculates a mission capture rating, benefit value, RDT&E costs, production costs, and launch costs, in addition to life-cycle cost at various thrust levels. The benefit section of the model follows a weighted-criteria rat-

ing approach. Ten benefit criteria, such as mission capture, engine reliability, primary propulsion system (PPS) length, and technical risk, are available for the benefit-value calculation. Each benefit criterion is assigned a weighting for flexibility. Mission capture rating is a function of thrust level, the probability of mission occurrence, and the number of STS launches.

RDT&E and PPS costs are based on vehicle subsystem masses. Government and commercial STS launch costs are taken into account. The combination of these two algorithms resulted in a benefit-and-cost model, which iterates on thrust level such that the most cost-effective and beneficial thrust level is selected for a given mission catalog.

The model at present contains the performance envelopes of three primary propulsion systems for orbit transfer based on three low-thrust engines. The model allows for any mission model to be input into the program. The model also allows the user to easily vary the program to examine the effects of various ratings and the weighting of benefit parameters for the baseline engines.

This program is written in FORTRAN IV for use on an IBM 370 computer.

This program was written by K. M. Hamlyn, R. I. Robertson, and L. J. Rose of Martin Marietta Denver Aerospace for Lewis Research Center. For further information, Circle 66 on the TSP Request Card. LEW-14129

Analyzing Multidimensional Image Data

Six computer programs perform histogram cluster analysis.

The Histogram Cluster Analysis Procedure (HICAP) was developed to perform an unsupervised classification of multidimensional image data. The clustering approach used in HICAP is based on an algorithm described by Narendra and Goldberg, which uses a multidimensional histogram to perform an unsupervised classification of four-dimensional Landsat multispectral-scanner data. HICAP generalizes this procedure to process up to 32-bit data with an arbitrary number of dimensions. HICAP also incorporates efficiency improvements so that classification requires less computation than does the original algorithm. The computational savings afforded by HICAP increase with the number of dimensions in the data.

HICAP consists of a set of six computer programs that are executed in sequence. The first program, BHISTO,



Red hair or red herring?

Digital imaging reveals the reality hidden outside our powers of perception: The body beneath the skin, the worlds beyond the stars, the strata below the surface...or the face behind the make-up.

Now there is an affordable new image processor for scientists, physicians, radiologists, geologists, designers and others who must see more than the eye can see. VisionLab from Comtal/3M.

VisionLab transforms an IBM AT or XT* or compatible into a digital imaging computer with the power of yesterday's mainframe or minicomputer-based systems. From CAT scans to LANDSAT images, VisionLab's many interactive functions enhance, process and analyze in real-time or near real-time, to expand the powers of perception.

And VisionLab does it all at a price that makes it a very tough act to follow.

VisionLab is the latest in an all-encompassing line of digital imaging equipment from Comtal/3M. For visionary design, product strength and technical support, call Comtal/3M, leaders in digital imaging technology since the dawn of the industry.

VisionLab

Comtal/3M

Pasadena, California (800) 832-2255

Expanding the Powers of Perception

*IBM AT and IBM XT are registered trademarks of International Business Machines Corporation.

CAMAC

(IEEE-583)



Your Standard Tools for Data Acquisition and Control

For 15 years, KSC has been supplying users in laboratories, plants, and R & D facilities with practical CAMAC (IEEE-583) hardware and software tools for automation. The reason is simple. CAMAC, the international standard for Computer Automated Measurement And Control, provides modular real-time data acquisition and control solutions that can be implemented a step at a time.

CAMAC features . . .

Full Standardization. Specified by the IEEE, ANSI, and IEC.

Open-end Architecture. Start as small as you like and expand when and how you want.

Multicomputer Support. Interfaces for a wide range of computers, such as DEC, CDC, MODCOMP, Gould/SYSTEMS, and Hewlett-Packard.

High Data Rates. Data transfer rates to 348,000 bytes per second with DMA interfaces.

Unsurpassed Selection of Process I/O Modules. From A/D and D/A converters and signal multiplexers to event counters and transient recorders.

Powerful Distributed Systems. Peak block rates up to three million data bytes per second over a fiber optic serial highway to as many as 62 remote stations.

Supporting Software. Easy to use CAMAC handlers, software drivers, and Process Control/Data Base System software packages.

Field-proven System Design. Used in such facilities as Boeing, Nalco Chemical, Kimberley-Clark, Digital, NASA, Bell Labs, Martin Marietta, DuPont, and General Electric.

Join the growing list of users who are specifying our CAMAC tools for their system development. Call us today.

Kinetic Systems Corporation

11 Maryknoll Dr., Lockport, IL 60441
(815) 838-0005
TWX: 910 635 2831

takes an image data file and builds a multidimensional histogram consisting of the cell indices and the frequency of occurrence of the nonzero cells. Program BKTRREE facilitates searching for cell neighbors in the histogram by reordering the raw histogram according to the K-d search trees.

Program CNSEARCH uses the re-ordered histogram and K-d search tree to locate cell neighbors in the histogram, producing a list of the cell neighbors and their respective separation distances. Program SMOOTH smooths the histogram by selectively averaging cells, replacing the frequency of occurrence of each cell by the average frequency of its neighbors as defined in the neighbor index list.

Program CLUSTER locates clusters in the histogram by locating local maximums in the frequency distribution estimate and using frequency gradients to determine the population of each cluster. Finally, the CLASSIFY program uses the clustered histogram to classify the original data by table lookup via hashing. Various utility programs are included to derive a spatial or spectral subset of an image, to print an image in integer format, and to print various files used by HICAP.

The HICAP programs are written in FORTRAN 77 for batch or interactive execution and have been implemented on a DEC VAX-series computer with the largest program having a memory requirement of approximately 740K of 8-bit bytes. HICAP was developed in 1983.

This program was written by Stephen W. Wharton of Goddard Space Flight Center. For further information, Circle 71 on the TSP Request Card.

This invention is owned by NASA, and a patent application has been filed. Inquiries concerning nonexclusive or exclusive license for its commercial development should be addressed to the Patent Counsel, Goddard Space Flight Center [see page 29]. Refer to GSC-12935.

High-Level Data-Abstraction System

Communication with the data-base processor is flexible and efficient.

The High Level Data Abstraction (HILDA) system is a three-layer system supporting the data-abstraction features of the Intel data-base processor (DBP). The purpose of HILDA is the establishment of a flexible method of efficiently communicating with the DBP. The power of HILDA lies in its extensibility with re-

gard to syntax and semantic changes. HILDA's high-level query language can be readily modified. HILDA offers powerful potential to computer sites where the DBP is attached to a DEC VAX-series computer.

Each layer within HILDA plays a specific role during communication with the DBP. The first layer is the Service Port Protocol (SPP), which provides an error-correcting asynchronous protocol to serve as the foundation for the other two layers.

The second layer of HILDA is the DBP Semantics Specification Package (DBPSSP), which enables the analyst easily to construct request blocks to be sent to the DBP. DBPSSP is a collection of assembly tools and serves as a cross-assembler. The DBP "machine code" is assembled on the host and then directed to the DBP for execution.

The third layer of HILDA is the DBP Query Language (DBPQL), which is a high-level query processor that enables the analyst to communicate with the DBP using English-like commands. DBPQL is designed to be used both by casual data-management users and by users with in-depth knowledge of DBP commands. DBPQL includes trace and performance commands to aid the analyst in implementing new commands and in analyzing the execution characteristics of the DBP. A parser generator package (PARGEN) is included to enable the analyst to create and manipulate easily the query statement syntax and semantics.

The HILDA system is written in Pascal and FORTRAN 77 for interactive execution. HILDA is designed for implementation on a DEC VAX-series computer with the VMS Level-3 operating system, an Intel DBP, and an RS-232 connection. The HILDA system was developed in 1983.

This program was written by Paul A. Fishwick of Kentron International, Inc., for Langley Research Center. For further information, Circle 70 on the TSP Request Card.
LAR-13244

Constant-Elasticity-of-Substitution Simulation

A computer program simulates production costs and uncertainties.

A program simulates the constant-elasticity-of-substitution (CES) production function. The CES function is used by economic analysts to examine production costs as well as uncertainties in production. The user provides such input parameters as the price of labor, price of capital, and dispersion levels. CES mini-

For 25 years, DCS has been shaping the future of telemetry.



4784 Bit Synchronizer

- IEEE-488 interface
- Soft decision AGC
- 10 MBPS Operation
- 1 DB of theoretical
- Card changeable for later upgrades
- Remote terminal or computer entry

We look to tomorrow with new products like this:

The DCS model 4784 PCM Bit Synchronizer is an upgraded version of an already proven design. This state-of-the-art telemetry data processing component is capable of handling serial PCM bit streams which have been degraded by noise, base line instabilities, or jitter. The 4784 utilizes a synchronous clock to reconstruct and normalize data to NRZ-L. Both filter/sample and integrate/reset detection techniques are available, providing optimum performance under varying operating conditions.

5001 PCM Decommutator

- Multiple program format storage
- Programmable bit synchronizer
- Integral PCM simulator
- Diagnostic self-test
- Remote terminal or computer entry

We continue to pioneer better ways to serve our customers.

The DCS model 5001 PCM Decommutator utilizes the most recent developments in microprocessor technology, and brings these capabilities to the field of high bit rate PCM. A dedicated microprocessor within the Decommutator interfaces with a front panel keyboard and a 16-digit alpha/numeric display. The panel displays program parameters, or data, under control of the keyboard. Up to 30 formats may be saved in nonvolatile storage.

At DCS, we always support our customers with fast, on-call maintenance in your shop or ours.

6010 High Speed Frame Synchronizer

- 30 MBPS bit rate
- ECL technology
- Adaptive pattern recognition
- Auto polarity recognition

Future advances in telemetry are being designed today.

The DCS model 6010 High Speed PCM Frame Synchronizer represents one of the most technologically advanced instruments of its kind in the industry today. It is capable of handling data rates of up to 30 MBPS utilizing an adaptive frame sync strategy consisting of search, check, and lock; based on four sequential, correct and incorrect patterns. Auto polarity inverts the incoming data when a complement of the frame synchronization pattern is detected. The 6010 and soon to be released, 4785 Bit Synchronizer are the forerunners of a whole new family of products now in advanced stages of design.

1455 Research Blvd.,
Rockville, Maryland 20850
Tel. (301) 279-8798 Twx. (710) 828-9785
8291 Westminster Ave., Suite 150,
Westminster, California 92683 Tel. (714) 894-4471 Twx. (910) 596-1802

DATA-CONTROL SYSTEMS
where the customer still comes first!



A CompuDyne Company

mizes the expected cost to produce a capital-uncertainty pair. By varying the capital-value input, one obtains a series of capital-uncertainty pairs. The capital-uncertainty pairs can then be used to generate several cost curves. The CES program is menu driven and features a specific print menu for examining selected output curves.

Certain cost-curve data are stored in two formats: a floppy diskette file and a plot file. Some of the output-curve data are as follows: (a) capital versus uncertainty, (b) expected quantity of labor versus uncertainty, (c) expected total cost versus uncertainty, and (d) expected average cost versus quantity.

The CES program is written in BASIC for interactive execution and has been implemented on an IBM PC-series computer with a central-memory requirement of 64K of 8-bit bytes. The CES program was developed in 1984.

This program was written by Gregory Reiter of Caltech for NASA's Jet Propulsion Laboratory. For further information, Circle 67 on the TSP Request Card. NPO-16524

An Expert-System Engine With Operative Probabilities

The program enables proof-of-concept tests of expert systems under development.

AESOP is a rule-based inference engine for an expert system, which makes decisions about a particular situation given user-supplied hypotheses, rules, and answers to questions drawn from the rules. If a knowledge base containing the hypotheses and rules governing an environment is available to AESOP, almost any situation within that environment can be resolved by answering the questions asked by AESOP. The questions can be answered with YES, NO, MAYBE, DON'T KNOW, DON'T CARE, or with a probability factor ranging from 0 to 10.

AESOP was developed as a tool for expert-system development. Although it is probably not suitable for the final implementation of most expert-systems applications, AESOP can serve as a fast means of developing a proof-of-concept test system. It also can be valuable in allowing the majority of the knowledge engineering to be done before commitment to a final implementation mechanism.

The sample AESOP rule file contains data for determining whether tasks in space should be automated or performed by humans. The initial prompt asks what task is under consideration, and AESOP

asks questions about feasibility and performance until one of the original hypotheses (automate or perform by humans) is confirmed.

The rule file contains the initial prompt, the rules, and mutually exclusive rules used in the decisionmaking, the hypotheses, and the probability factors for each rule in a hypothesis. AESOP builds a top-down logic-tree structure. If a reply is DON'T KNOW, the rule base is checked for existing questions that may solve the dilemma. This allows several levels of rules to exist within a particular level containing more-specific decision criteria.

When any hypothesis reaches 90-percent certainty, AESOP prints a final confirming message. The user can ask WHY or HOW for a detailed list of the evidence confirming the hypothesis. The status of all initial hypotheses posed to AESOP is stored in a file for later reference.

AESOP is written in Franz LISP for interactive execution and has been implemented on a DEC VAX-series computer. The program was developed in 1984.

This program was written by Nancy E. Orlando and Michael T. Palmer of Langley Research Center and Richard S. Wallace of Carnegie-Mellon University. For further information, Circle 68 on the TSP Request Card. LAR-13382

How to get started in expert systems ...for only \$950.

Personal Consultant™ and Personal Consultant Plus software from Texas Instruments—now you have two ways to get started in expert system development and delivery on PCs. Both run on TI Professional Computers, including the Business-Pro™ computer, as well as the IBM® PC/XT™, Personal Computer AT™ and compatibles.

Personal Consultant is the low-cost, high functionality tool for the rapid prototyping and development of expert system applications. It can get you started for only \$950.*

Personal Consultant Plus is a larger, more powerful family member with extra features to handle more complex problems, priced at \$2950.*

And, if you order Personal Consultant and decide to move up to Personal Consultant Plus, you can apply

the \$950 towards the new purchase—and keep both products!

To order, or for more information, call toll-free:

1-800-527-3500

*Suggested list price.

Personal Consultant and Business-Pro are trademarks of Texas Instruments Incorporated. IBM is a registered trademark and PC/XT and Personal Computer AT are trademarks of International Business Machines Corporation.


**TEXAS
INSTRUMENTS**

Creating useful products
and services for you.

©1986 TI 261765-03

Since the dawn of the Space Age, Ford Aerospace & Communications Corporation has forged beyond the limits of our knowledge of the universe...developing the ground and space communications concepts and techniques that are today's standards.

EXPAND YOUR HORIZONS AS WE EXPAND THE LIMITS OF THE KNOWN.

We were the pioneers in the development of satellites — today, we are the world's largest producer of both communications and meteorological satellites. We've also been privileged to serve our nation's manned space programs from the first Gemini mission through the Space Shuttles.

Today, Ford Aerospace continues to further expand technology and knowledge into the 21st century, as we perform advanced research and development of communications and control systems required by the most sophisticated projects of the Space Age.

At our Space Information Systems Operation in College Park,

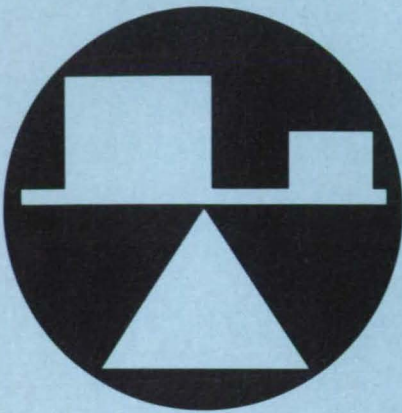
Maryland, we support the engineering and operations efforts at NASA's Goddard Space Flight Center. We're involved in the engineering, operation and maintenance of NASA's Operational Communications Network (NASCOM), with the Operational Control Center for the Hubbell Space Telescope and advanced design and technology studies for the development of the Space Station Information System.

If you'd like to become involved with these exciting Space Age projects, are ready to expand your career horizons, and have a Bachelor's or advanced degree in Engineering, Computer Science, or other hard sciences or equivalent experience, consider a career with Ford Aerospace. We offer an ideal location midway between Baltimore, Maryland and Washington, D.C., plus an excellent salary and benefits package. For consideration, send your resume with salary history in confidence to: James L. Furilla, Recruiting & Placement, 4920 Niagara Road, Suite #6, College Park, MD 20740.



**Ford Aerospace & Communications Corporation
Space Information Systems Operation**

U.S. Citizenship Required/Equal Opportunity Employer



Hardware, Techniques, and Processes

- 92 Variable-Friction Secondary Face Seals
- 94 Measuring Thicknesses of Coatings on Metals
- 96 Equations for Annular-Heat-Transfer Coefficients
- 97 Continuous, Multielement, Hot-Film Transition Gage
- 98 Two-Axis, Self-Nulling Skin-Friction Balance
- 99 Acoustic-Liner Admittance in a Duct
- 100 Sensing Horizontal Heading in Aircraft Maneuvers
- 101 Spring-Loaded Joule-Thomson Valve
- 101 Measuring Acoustic-Radiation Stresses in Materials
- 102 Feedback-Controlled Regulation of Gas Pressure
- 103 Parallel-End-Point Drafting Compass

Books & Reports

- 104 Evaluation of Mathematical Turbulence Models
- 104 Correcting for Supports in Structural Dynamic Testing

Computer Programs

- 78 Predicting Aircraft Spray Patterns on Crops
- 78 Estimating Average Wind Velocity Along a Trajectory
- 80 Research Program for Vibration Control in Structures
- 80 Combining Structural and Substructural Mathematical Models
- 80 Flutter and Vibration Animation Program
- 80 Analyzing Shuttle Orbiter Trajectories
- 82 Predicting Failures of Composite, Spherical Pressure Vessels

Variable-Friction Secondary Face Seals

Feedback-controlled friction or damping suppresses vibrations.

Lewis Research Center, Cleveland, Ohio

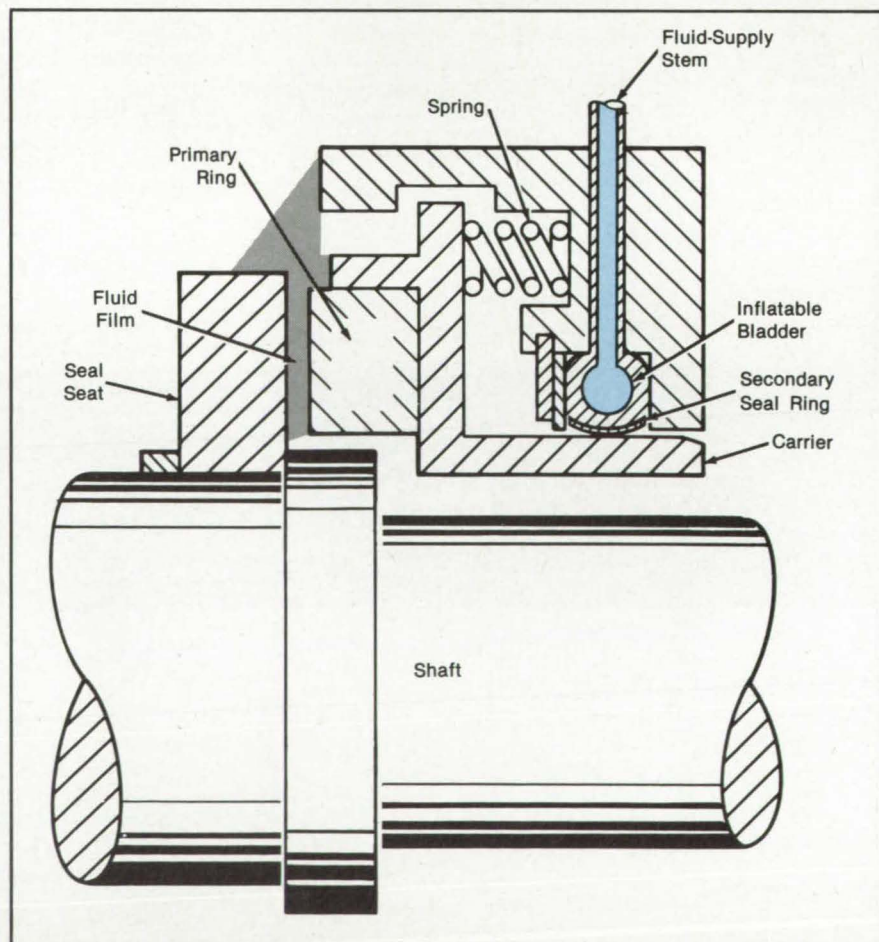
A variable-friction secondary seal has been conceived to control the vibration and stability of the primary seal ring over a wide range of conditions. By varying the friction force or damping applied to the primary seal ring, the vibration can be controlled to provide stable operation.

Self-acting face seals are a special type of face seal that operate with a very-thin liquid or gaseous film between the primary seal faces. In addition to the primary sealing face, face seals have a secondary seal, typically in the form of piston rings or elastomeric O-rings. The purpose of the secondary seal is to seal the secondary leak path in the face-seal assembly. Face seals are subject to instability due to the vibration of the primary seal ring. This results in excessive seal-face wear or failure.

Previous devices for producing the damping of primary-seal-ring vibration

were of a static nature; i.e., the friction force was optimized for one seal-operating condition only. The disadvantage was that instabilities were encountered when seal conditions deviated from the design condition or when the seal was perturbed by transients.

As a means of alleviating this situation and allowing control over a wide range of conditions, the variable-friction secondary seal was conceived. The components of the "variable-friction secondary seal" (see figure) are the bladder and secondary seal ring, which has an axial split line. Operationally, variable friction and consequently variable damping are achieved by introducing air or hydraulic pressure through the stem into the bladder, which causes the bladder to expand into the secondary-seal ring. This changes the radial force and, consequently, the friction damping applied to



The Friction Damping Applied to the Carrier is varied by changing the pressure of air or fluid in the bladder.

•M•A•G•I•N•A•T•I•O•N•



catalyst of technology

Imagination and innovation can transform worlds. At Boeing, technologies just beyond the horizon are born, technologies that help find practical solutions to complex problems. Your access to the latest in simulation, testing, consultation, and analysis is Boeing Technology Services. Contact us, we're The Boeing Company's broker for the technology you need.

**BOEING
TECHNOLOGY
SERVICES**

Circle Reader Action No. 367

the carrier.

In the event that the seal film becomes unstable or the primary ring begins to vibrate, the bladder pressure is changed to mitigate the instability or vibration. The bladder pressure can be changed manually or by means of a feedback control system, which senses primary-ring vibration amplitude. The control system then changes the bladder pressure to minimize or limit the primary-ring vibration

amplitudes within stable boundaries. The secondary-seal material may be selected to provide many different friction coefficients, and coatings may be applied to the secondary-seal ring to optimize the friction coefficient and sliding interface.

Advantages of the "variable-friction secondary seal" are that face-seal stability can be controlled as a function of primary-ring vibration amplitudes, and also the friction can be remotely changed

to achieve acceptable vibration amplitudes for a large range of seal-operating conditions without compromising the secondary-seal performance. The concept is also useful in seal testing in which the dynamic stability of face seals is under evaluation.

This work was done by Eliseo DiRusso of Lewis Research Center. No further documentation is available.
LEW-14170

Measuring Thicknesses of Coatings on Metals

A digital light sensor and eddy-current sensor measure thickness without contact.

Marshall Space Flight Center, Alabama

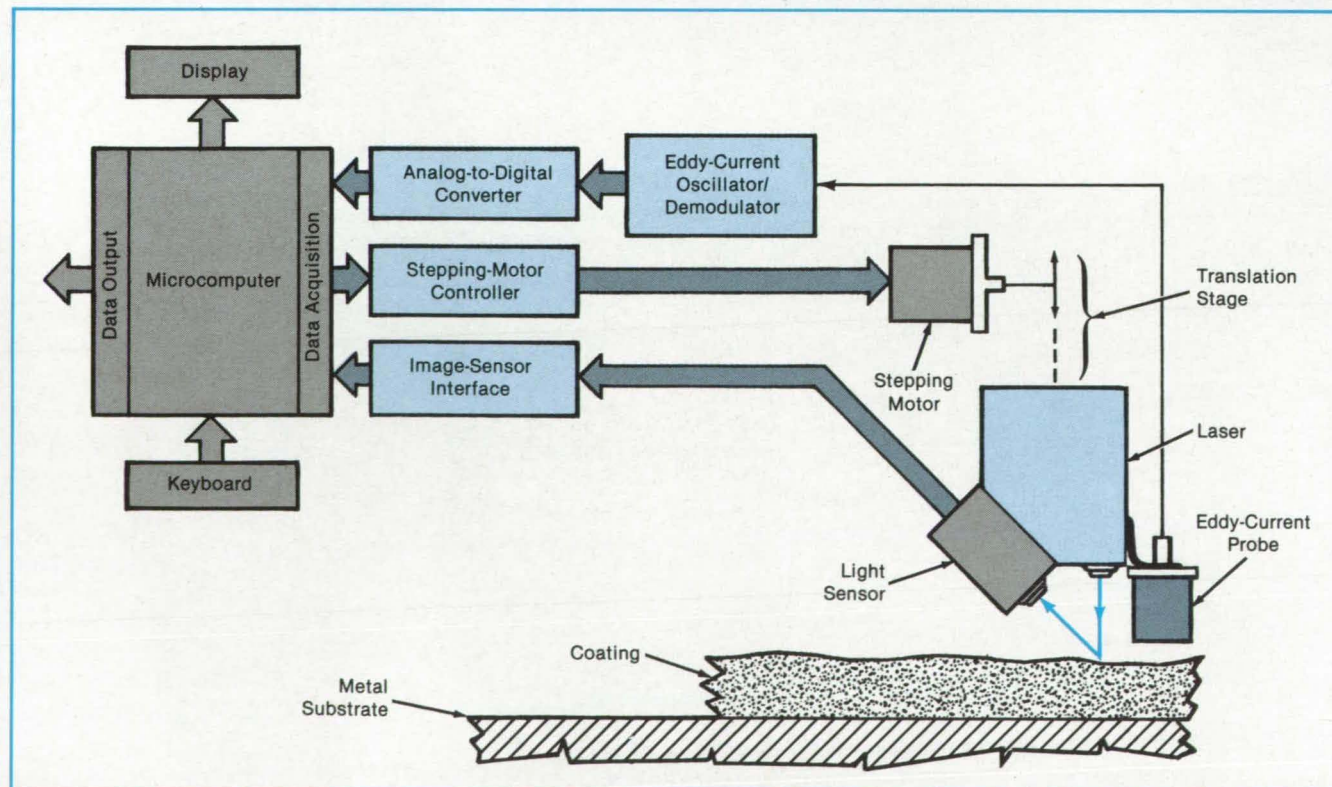
Using laser-beam reflections and eddy-current sensing, an instrument measures the thicknesses of nonconductive coatings on metal substrates. When the capabilities of available components are fully exploited, the instrument will be able to measure coatings from 0.001 to 6 in. (0.0025 to 15 cm) thick with an accuracy of 1 part in 4,000. The instrument can readily be incorporated in automatic production and inspection systems. For example, it can be used to inspect thermal-insulation layers, paint, and protective coatings. It can also be used to control

the application of coatings to preset thicknesses.

The eddy-current-sensing portion of the instrument maintains a reflected-light triangulation sensor at a fixed distance from the surface of the substrate as the substrate moves under it. The light sensor determines the angle and therefore the perpendicular distance of the laser-beam spot on the coating surface. With the laser kept at a fixed distance above the substrate by the eddy-current sensor, the angle to the laser spot is thus a function of the coating thickness. A micro-

computer computes this thickness from the light-sensor angle measurement.

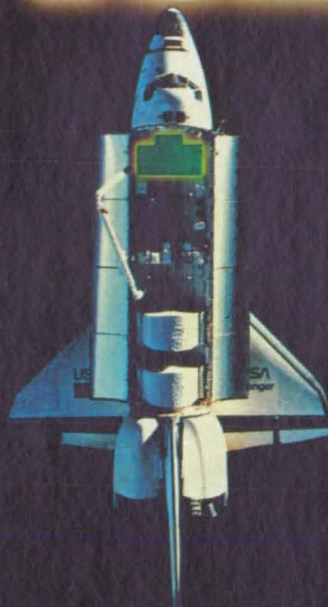
The eddy-current sensor and the light sensor are mounted together on a precise translation stage that moves toward or away from the coated substrate (see figure). The output of the eddy-current sensor is converted to a digital signal and is compared with the required sensor-to-substrate separation stored in the computer memory. The computer calculates the direction and magnitude of the separation error and sends a signal to the stepping motor that drives the translation



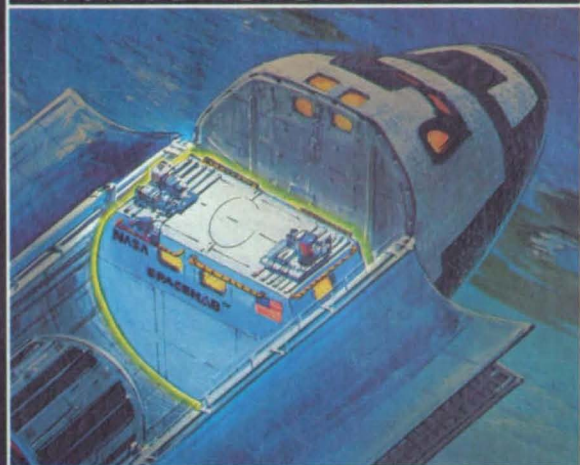
The **Surface of a Coating** reflects a laser beam to an optical sensor. The position of the reflected spot on the sensor is used by the microcomputer to calculate the coating thickness. The eddy-current sensor maintains a constant distance between the optical sensor and the metal substrate.

INTRODUCING A NEW
SPACE SHUTTLE CAPABILITY

SPACEHAB



AVAILABILITY: 1988



A PRESSURIZED MID-DECK AUGMENTATION MODULE

SPACEHAB PROVIDES:

- Additional living, working, and storage space for the flight crew (28 cubic meters/ 1,000 cu. ft.).
- A major increase in orbiter capability to support middeck class payloads at low cost.
- Simplified and fast payload integration, quick response and rapid turn-around.
- Regular and frequent flight opportunities.
- Services including NASA/Customer relations, payload development requirements, manifesting, processing, integration, and flight operations support.

FOR ADDITIONAL INFORMATION:

To obtain further information on SPACEHAB module capabilities and SPACEHAB services and costs, please write on your company or organization letterhead to:

Customer Relations Office
SPACEHAB, Inc.
Suite 510, 1107 N.E. 45th Street
Seattle, Washington 98105
(206)-545-7126

stage. This adjusts the position of the sensors accordingly.

The light source is a helium/neon laser with a 1-mW output. The light sensor is an array of light-sensitive memory cells. When struck by photons, each cell discharges at a rate proportional to the product of light intensity and length of exposure. Before each measurement, the array is first refreshed with digital ones. Light is then focused on it to discharge

the cells selectively. An image focused on the array is thus converted into a pattern of ones and zeros. The array is then read in the manner of an ordinary memory chip, and the angle information is extracted.

In addition to its other functions, the microcomputer can be used to control the movement of the sensors over the specimen surface. From a series of thickness measurements, it can also

determine the waviness of the coating surface from the valleys and peaks of the thickness values and the distance between them.

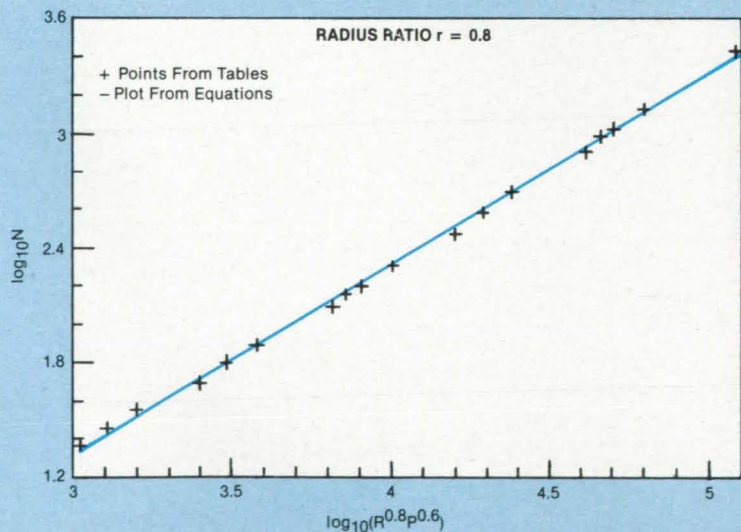
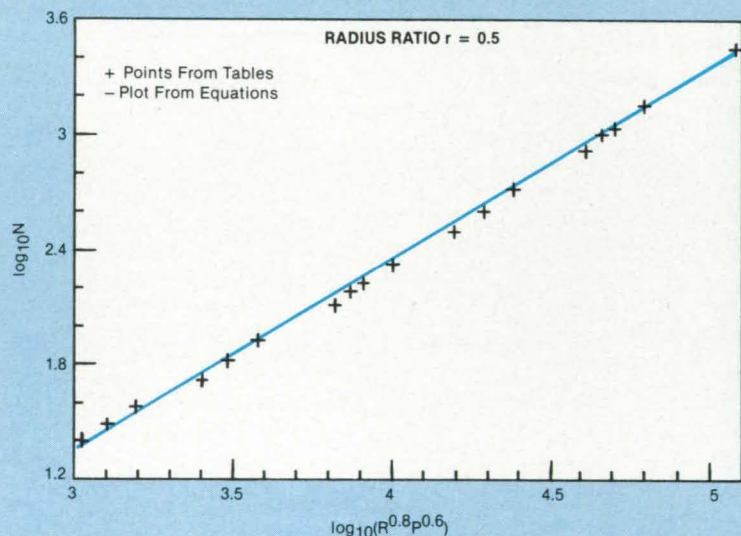
This work was done by Glenn M. Cotty, Jr., of Martin Marietta Corp. for Marshall Space Flight Center. For further information, Circle 89 on the TSP Request Card.

MFS-28126

Equations for Annular-Heat-Transfer Coefficients

Tables of coefficients have been converted to algebraic expressions.

Marshall Space Flight Center, Alabama



A set of equations has been developed for heat-transfer coefficients for the annulus between the inner and outer tubes of a concentric-tube heat exchanger. Previously, the coefficients were available only in tabular form. In equation form, the coefficients can be incorporated into mathematical models more readily than as tabular data. The equations simplify the design and analysis of heat exchangers.

The equations were obtained by a regression analysis of the tabular data of W. M. Kays and E. Y. Leung, published in the *International Journal of Heat Mass Transfer* in 1963. The Nusselt number on the inner surface of an annulus with a constant rate of heat transfer and an insulated outer surface can be calculated as a function of the Prandtl number, the Reynolds number, and the annulus radius ratio, as follows:

$$\log_{10} N = A \log_{10}(R^{0.8} P^{0.6}) + B$$

$$A = -0.123r^2 + 0.172r + 0.937$$

$$B = 0.958r^2 - 1.336r - 1.217$$

where r = the ratio of the outside diameter of the inner tube to the inside diameter of the outer tube, R = the Reynolds number, and P = the Prandtl number.

These equations are correlated with the tabular data for $10^4 \leq R \leq 10^6$, $0.5 \leq P \leq 3$, and $0.1 \leq r \leq 0.8$. The coefficient of determination of the correlation is 0.987. The curves plotted from the equations agree well with the data points in the Kays and Leung tables (see figure).

This work was done by Barry Yao of Rockwell International Corp. for Marshall Space Flight Center. No further documentation is available.

MFS-29074

A Plot of the Equation for the Nusselt Number agrees closely with points from tabulated data. The equation for the Nusselt number and those for coefficients A and B were obtained by a regression analysis of the data. Other plots (not shown) also show close agreement for radius ratios of 0.1 and 0.2.

Continuous, Multielement, Hot-Film Transition Gage

Measurements can be taken along a single line in the streamwise direction.

Langley Research Center, Hampton, Virginia

The accurate measurement of the location where a laminar boundary layer undergoes the transition to a turbulent one serves many purposes in basic aerodynamic research and developmental testing. For example, a complete understanding of performance, stability, and control of a laminar-flow airplane requires knowledge of transition locations on the wing surfaces, empennage surfaces, fuselage, and nacelles. Visual, acoustic, and electronic methods are capable of providing this transition information.

One very useful device for large-scale wind tunnel and flight applications is the thin, surface-mounted, hot-film gage. Hot films indicate transition by responding to the differences in heat transfer between laminar and turbulent flows. These gages are approximately as small as postage stamps and are applied to the test surfaces by conventional strain-gage installation techniques.

However, the wiring attached to the downstream end of each gage is large enough to cause a transition wedge (emanating downstream at about a 7° half angle); thus, these individual gages must be staggered to avoid the formation of false turbulence at the downstream gages (see Figure 1). This need for staggering is the source of the most significant disadvantages of individual hot-film gages.

The continuous, multielement, hot-film transition gage overcomes the disadvantages of the individual, hot-film gages by integrating the required number and distribution of hot-film sensing elements into a long, continuous, thin sheet. The length of the sheet covers the area of interest for transition measurements, beginning at the leading edge and continuing downstream of the transition region (Figure 2). For example, on an airplane wing of 10 ft (3 m) chord length, the gage might be as much as 7 or 8 ft (2.1 or 2.4 m) long.

The leading edge of a gage mounted on the upper surface of a wing would wrap around, beneath, and downstream of the wing leading edge. A method for installing the gage eliminates the formation of transition wedges at the lateral edges of the gage. The spanwise-facing step along the sides of the gage may be faired with thin adhesive tape, or, if necessary, filling materials can be used to fair these edges smooth. The gage adheres to the

NASA Tech Briefs, May/June 1986

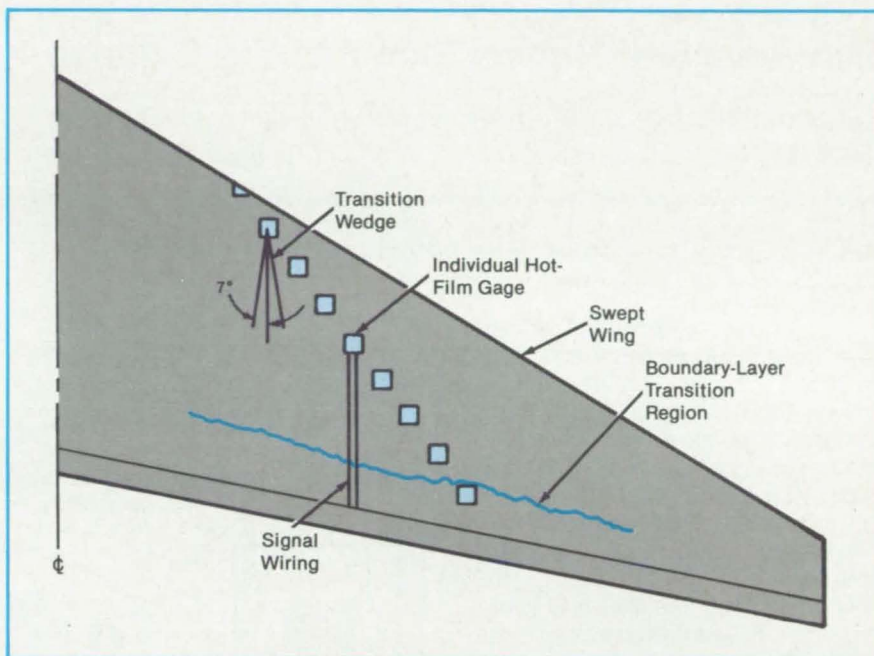


Figure 1. **Individual Gages Must Be Staggered** to prevent the formation of turbulence at the gages downstream. This arrangement precludes accurate measurements of laminar/turbulent transition regions along a streamline.

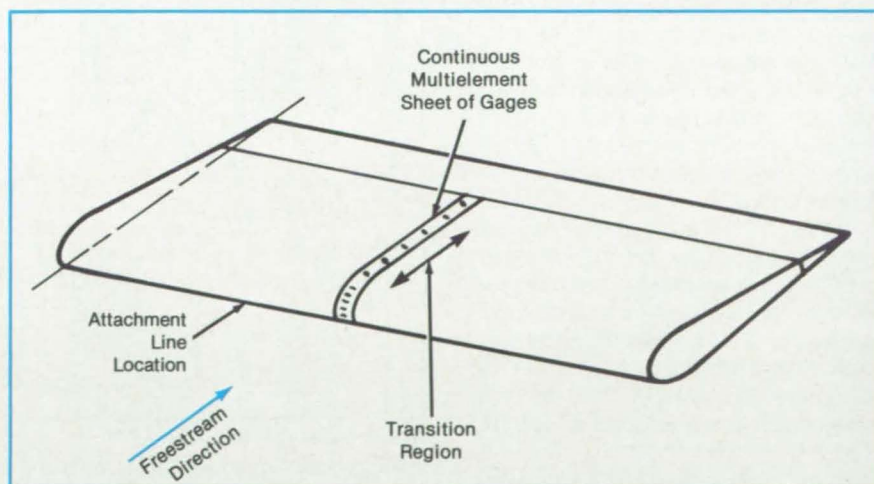


Figure 2. A **Continuous Sheet Containing Many Gage Elements** can be placed in line with the airstream without perturbing the flow and the flow measurements.

surface with a very thin [0.001-in. (0.0254-mm)] double-backed adhesive tape.

In this fashion, no disturbance from the film leading edge will cause turbulent wedges to affect the hot-film sensors in the transition region. The gage incorporates as many hot-film sensing elements as needed, distributed as needed along the

length of the sheet. Because of the close spacing of the elements near the upstream end of the sheet, the stagnation-or attachment-line location can be documented. Further downstream, the elements are more widely spaced for transition-location measurement. The width of the sheet provides space for the signal leads to be carried laterally away from each

hot-film element and longitudinally to the downstream end of the sheet where external wiring arrangements are made.

The multielement gage uses an improved circuit that serves as an electronic switch. The switch is a power MOSFET (metal oxide/semiconductor field-effect transistor). It can switch far

greater currents (10 A) than the hot-film elements require. The MOSFET switch does not oxidize as do conventional contacts, is not affected by vibration or acceleration, and is not position-sensitive. Its very high switching speed allows sensor elements to be switched into the servo loop at very high rates without damage to

the sensors.

This work was done by B. J. Holmes, J. P. McPherson, F. K. Harris, J. K. Diamond, and N. R. Johnson of **Langley Research Center** and J. J. Chapman of **Kentron International, Inc.** For further information, Circle 37 on the TSP Request Card. LAR-13319

Two-Axis, Self-Nulling Skin-Friction Balance

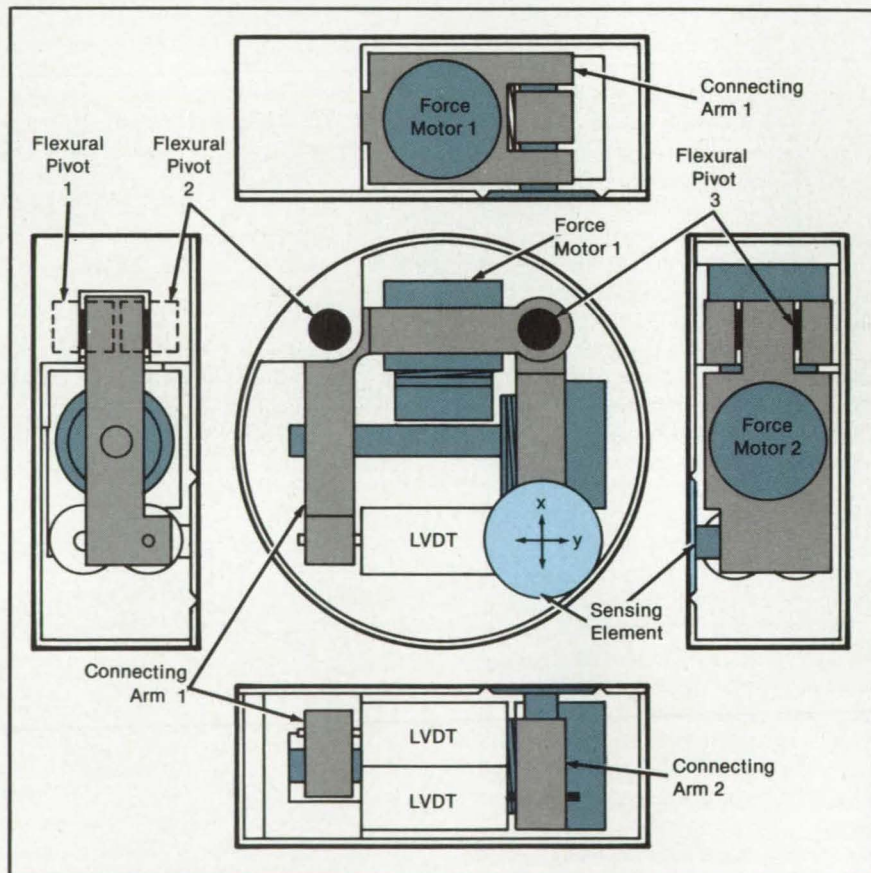
The two-dimensional aerodynamic skin-friction force is measured directly.

Langley Research Center, Hampton, Virginia

A two-axis, self-nulling skin-friction balance, designed to measure accurately the x and y components of the skin-friction force in the plane of airflow, is illustrated in the figure. The disk-shaped prototype design has overall dimensions of 1.25 inches (3.18 centimeters) diameter and 0.5 inch (1.27 centimeters) height. It is composed of two connecting arms, three flexural pivots, one sensing element, two force motors, two linear variable-differential transformers (LVDT's), and a case. A unique mechanism consisting of two flexural pivoted arms connected in tandem but at a right angle with each other is designed to impart the plane motion needed to sense the two-axis flow over the sensing element of the balance. The sensing element, 0.370 inch (0.940 centimeter) in diameter, that is attached to the end of the second arm is to be servoed by two restoring-force motors orthogonally mounted in the plane of airflow.

Two LVDT's will be used to provide the x-and y-axis displacement measurement for nulling the instrument. Care has been taken in the design of motor and LVDT housings to allow relative movements in these components only along their intended axes of operation. The balance is designed with a full-scale force range of 1 g (0.0098 N) in both x and y axes. The electronic circuit that provides the feedback signal for self-nulling operation and the continuous output signals is to be externally packaged.

A one-arm configuration with one restoring-force motor and a single LVDT can be used for the design of a miniature single-axis skin-friction balance. Also, the two-axis configuration can be converted into a three-dimensional or three-axis device by attaching a third pivoted arm in series but normal to the plane formed by



The **Skin-Friction Measuring Disk** connected to the sensing element measures the x and y components of skin friction in the plane of airflow.

the other two arms. The two- or three-axis configurations can also be designed to measure the velocity vectors of waterflow.

The present design measures directly the skin-friction force over a single sensing element. The two-axis mechanism allows the free plane motion of the sensing element with no friction, and the balance is self-nulled to provide direct plane skin-friction force measurements continuously.

This work was done by Ping Tchong and Frank H. Supplee, Jr., of **Langley Research Center**. No further documentation is available.

This invention is owned by NASA, and a patent application has been filed. Inquiries concerning nonexclusive or exclusive license for its commercial development should be addressed to the Patent Counsel, Langley Research Center [see page 29]. Refer to LAR-13294.

Acoustic-Liner Admittance in a Duct

The method calculates the admittance from easily obtainable values.

*Langley Research Center,
Hampton, Virginia*

The acoustic admittance of practical acoustic liners may be a function of the aeroacoustic environment in which they are located. The properties of these liners in such an environment are evaluated in the laboratory with a grazing-flow impedance tube. In such a tube, the acoustic material is aligned so that the sound and mean flow graze over the surface of the material in a controlled manner to simulate the environment typical of that found in a real jet engine.

Since acoustic admittance is defined as the ratio of normal particle velocity to pressure at the wall surface, the admittance could be determined experimentally by direct measurements of normal particle velocity and pressure.

In practice, measurements of particle velocity in the presence of grazing flow are currently not reliable. Instead, an indirect approach must be taken, which depends only on the measurement of acoustic pressure at selected locations in the test configuration. These measurements are then used as input to an analytical program that determines the admittance based on these measured data.

Previous methods for determining acoustic admittance in grazing flow, from measured values of the axial propagation constant and cross modes, are based on the solution to an ordinary differential equation and are restricted to mean flows with transverse gradients in one direction only. However, grazing-flow duct facilities commonly employ ducts with relatively small rectangular cross sections in which the grazing flow possesses gradients in both transverse directions of the impedance tubes. Such is the case in the flow-impedance test laboratory at Langley Research Center; therefore, the present effort was motivated by the need to account for the more realistic flow environment in laboratory flow-impedance tubes such as those in the Langley facility.


The new method for calculating acoustic-liner admittance in a rectangular duct with grazing flow is based on a finite-element discretization of the acoustic field and a reposing of the unknown admittance value as a linear eigenvalue problem on the admittance value. This eigenvalue problem is solved by Gaussian elimination. Unlike existing methods that are based on the integration of an ordinary differential equation and are thus limited to mean flows with one-

dimensional boundary layers, the present method is extendable to mean flows with two-dimensional boundary layers as well.

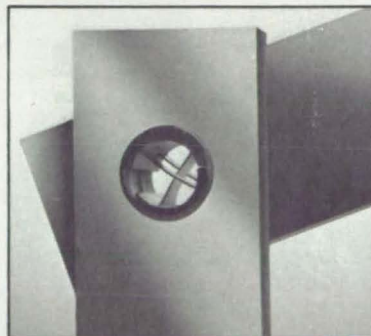
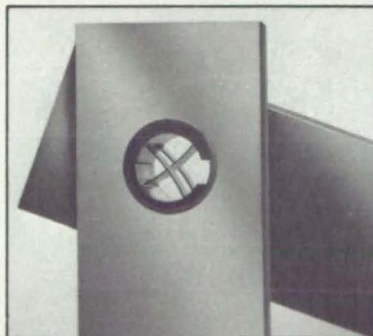
Admittance values determined from the method compared excellently with the exact solutions obtained for a constant mean flow profile. In the presence of shear, the results of the method compared well with the results of a Runge-Kutta integration technique.

This work was done by Willie R.

Watson of Langley Research Center. Further information may be found in NASA TP-2310 [N84-27543/NSP], "A New Method for Determining Acoustic-Liner Admittance in a Rectangular Duct With Grazing Flow From Experimental Data" [7]. A copy may be purchased [prepayment required] from the National Technical Information Service, Springfield, Virginia 22161. LAR-13399



BENDIX FREE FLEX® PIVOTS FRICTION-LESS ANGULAR TRAVEL BEARINGS



This patented pivot fills needs that lubricated bearings can't meet. With no required lubrication, operation in a vacuum or super clean area is possible. No rubbing surfaces permit the pivot to operate in unclean atmosphere and eliminate disadvantages of fretting and stiction. Its radial design provides low hysteresis, center shift and thermal drift. Operating through springs with low cyclic stress, indefinite life can be obtained making the pivot ideal for those hard to get at critical areas of your design.

Some typical applications are: oscillating mirrors, lever linkages, instrument nulling, weighing machines, bearing preloading, gimble rings, gyros, scanners, fuel controls, pressure and vibration transducers, etc.

With either cantilever or double ended support configuration, the Free Flex® Pivot has answered many difficult engineering requirements where reliable long-life angular travel is necessary.

When asked, "What do you like the most about Free Flex® Pivots?", engineers answer, "THEY WORK!"

Distributors located throughout United States and Europe maintain a stock of pivots from 1/8" diameter to 1" diameter. For more information contact:

Manager Flex Pivot, Marketing
Allied Corporation
Bendix Fluid Power Division
211 Seward Avenue, P.O. Box 457
Utica, NY 13503



ALLIED Bendix
Aerospace

Sensing Horizontal Heading in Aircraft Maneuvers

A modified gyroscopic system indicates the geographic heading even in nearly vertical flight.

Dryden Flight Research Center, Edwards, California

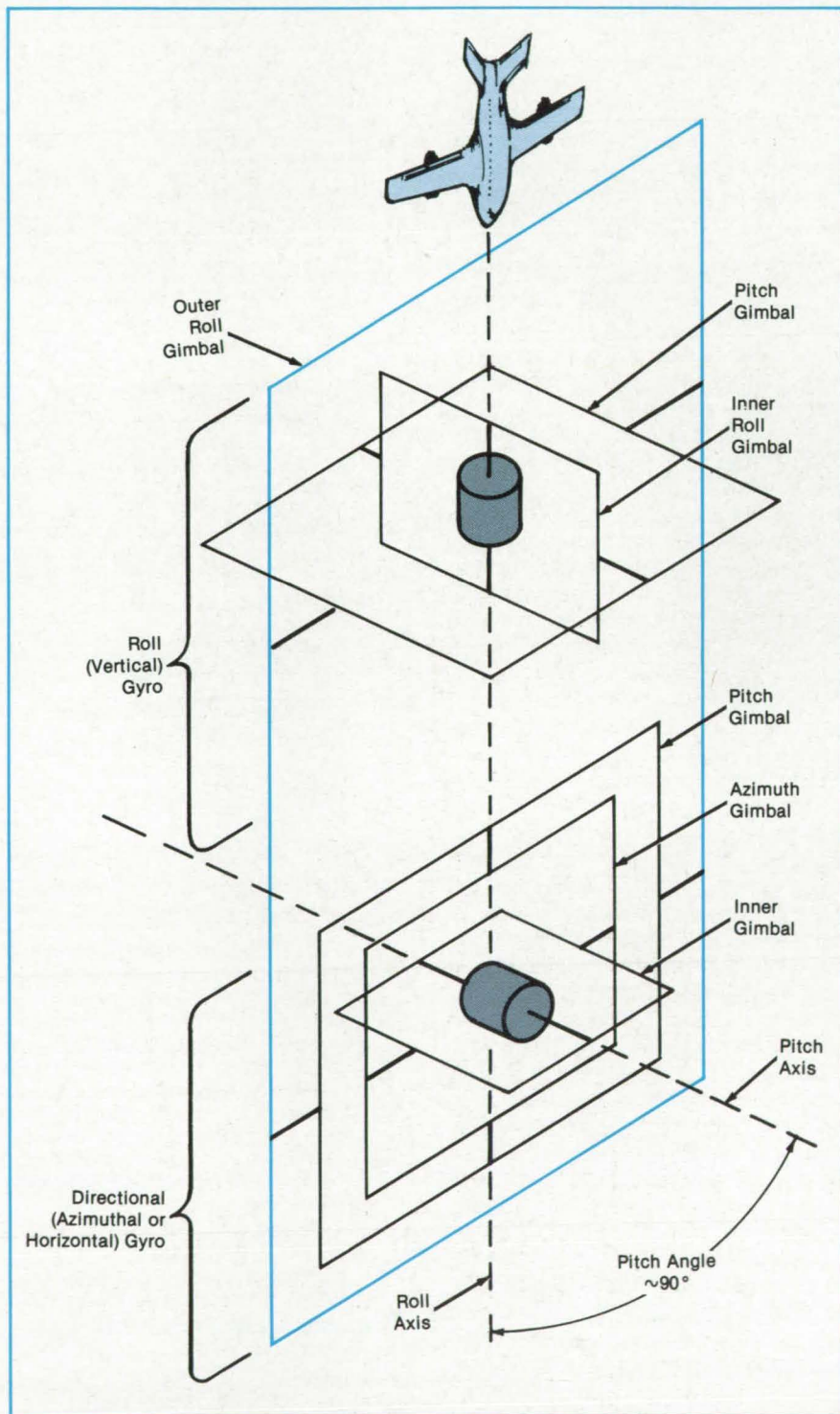
Modifications to an existing two-gyroscope attitude-sensing system supply azimuth (geographic heading) information, rather than the usual roll information when the aircraft climbs or dives within 15° of vertical. Previously, no azimuth heading was available during nearly vertical flight due to the nature of the gimbal-lock-avoidance subsystem. Now, the azimuth signal in the modified system indicates what the aircraft heading would be if it were to resume level flight from a climb or dive.

The relationship among the gimbals, gyroscopes, and aircraft axes during a nearly vertical dive is shown in the figure. In the unmodified system, the outer roll gimbal is held fixed in space when the pitch axis comes within $\pm 15^\circ$ of vertical. This causes the azimuthal gimbal to become fixed with respect to the outer roll gimbal, even when the small horizontal component of the aircraft heading changes: Thus, the horizontal (directional) gyro ceases to supply a correct azimuth-heading signal.

In the modified system, the outer roll gimbal is held fixed with respect to the aircraft frame when the pitch angle is within $\pm 15^\circ$ of vertical. A roll about the longitudinal axis then causes a movement of the pitch gimbal about the azimuthal gimbal, which gives rise to an azimuthal indication as in level flight. If the roll were to suddenly stop and the aircraft pitched back to level, the resulting aircraft azimuthal heading would be indicated correctly.

The outer roll gimbal, the pitch gimbal, and the inner gimbal of the vertical (pitch) gyro remain mutually orthogonal during nearly vertical maneuvers. Therefore, when the aircraft pitches from vertical toward horizontal flight, the outer roll gimbal is free to follow the aircraft platform without disturbing the spatial orientation of the pitch and inner roll gimbals of the vertical gyro. Similarly, departure from vertical flight induces no movement of the inner gimbals of the horizontal (directional) gyro. Thus, the probability of gyro tumble due to gimbal lock during such maneuvers is reduced.

Antitumble performance is improved over that of the original system except when the aircraft enters nearly vertical



The Gyroscopes and Gimbals of the system assume this configuration when an aircraft has pitched into a vertical dive. The outer roll gimbal is fixed with respect to the aircraft frame in this orientation.

flight while at or near a 90° roll angle. In that case, antitumble capability matches that of the original system.

This work was done by Kenneth T. Cowdin of **Dryden Flight Research**

Center. For further information, Circle 41 on the TSP Request Card.

This invention has been patented by NASA (U.S. Patent No. 4,387,513). Inquiries concerning nonexclusive or exclu-

sive license for its commercial development should be addressed to the Patent Counsel, Ames Research Center [see page 29]. Refer to FRC-11043.

Measuring Acoustic-Radiation Stresses in Materials

This system measures the nonlinearity parameters of materials.

Langley Research Center, Hampton, Virginia

The acoustic-radiation-stress measurement system was developed to provide a means to characterize quantitatively those properties of fluids and solids related to material nonlinearity. Each material has a unique set of nonlinearity parameters that characterizes the material and that is related to its thermodynamic state. The thermodynamic state is generalized here to include the degree of residual or applied stress, the atomic or molecular composition of the material, defect structures, and the state of material order or disorder. The nonlinearity parameter thus serves as an important and distinct measure of the material state and is both complementary and supplementary to acoustic-velocity and acoustic-attenuation measurements.

The nonlinearity parameter accounts for acoustic-waveform distortion leading to the generation of harmonics of the fundamental driving acoustic frequency and

to acoustic-radiation-induced static strains in the material. These strains are a manifestation of the acoustic-radiation stress in the material.

The measuring system uses the static strain generated by an acoustic wave propagating in the material. Since the static strain is effectively a "dc" component of the waveform distortion, problems associated with phase-cancellation artifacts disappear. Further, the sign of the nonlinearity parameter is obtained by simple inspection of the measured signal polarity. These features make this system very amenable to use in the field.

The theory of acoustic-radiation stress and the resulting radiation-induced static strain, only recently understood, serves as the basis for this system. The nondestructive-evaluation laboratory at Langley Research Center is using the system to characterize material nonlinearity in solids and liquids and has uncovered ma-

terial properties not previously known. The system is expected to become a standard for acoustic-radiation-stress measurements for solids and liquids and for the characterization of material properties related to strength and residual or applied stresses. It is also expected to become a standard for transducer calibration.

This work was done by John H. Cantrell, Jr., and William T. Yost of **Langley Research Center**. For further information, Circle 100 on the TSP Request Card.

This invention is owned by NASA, and a patent application has been filed. Inquiries concerning nonexclusive or exclusive license for its commercial development should be addressed to the Patent Counsel, Langley Research Center [see page 29]. Refer to LAR-13440.

Spring-Loaded Joule-Thomson Valve

The improved design reduces clogging and maintains a constant pressure drop as the flow rate varies.

NASA's Jet Propulsion Laboratory, Pasadena, California

A spring-loaded Joule-Thomson (J-T) valve permits optimal cooling-power regulation of a J-T refrigerator by allowing independent adjustment of the flow rate and pressure drop through the valve. Because the spring-loaded J-T valve maintains a constant pressure drop, an upstream room-temperature throttle valve can adjust the flow rate precisely for any given upstream pressure. In addition, the new valve is relatively invulnerable to frozen gas contaminants, which can clog fixed-orifice J-T valves.

NASA Tech Briefs, May/June 1986

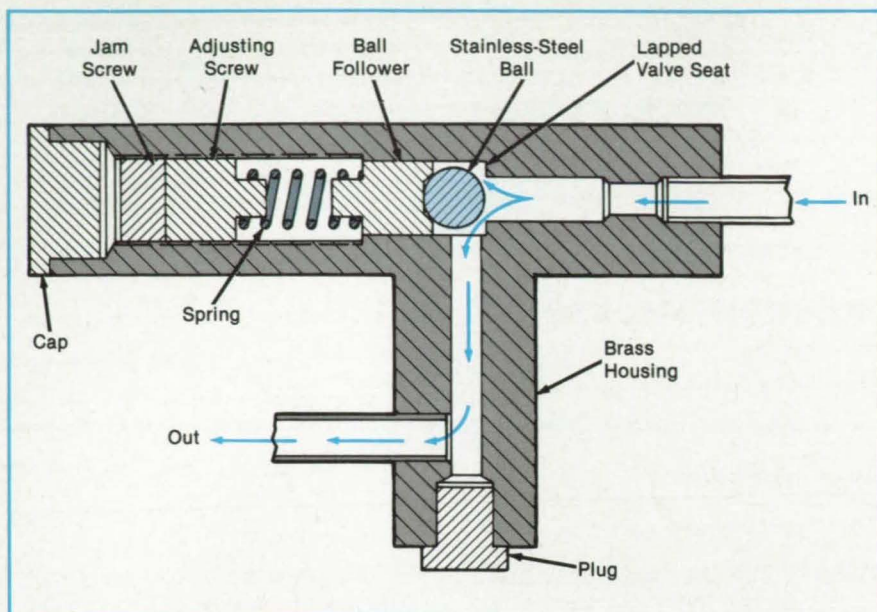
Conventional J-T expansion valves have fixed orifice openings; the pressure drop through these openings depends on the helium flow rate. Moreover, any trace amount of frozen gas contaminants could block such openings, drastically changing the cooling power of the refrigerator.

The new valve operates very much like a variably-loaded check valve. The orifice is regulated by a steel ball pushed by adjustable spring tension against a soft brass seat (see figure). The steel ball is raised off the seat whenever the force of

the upstream pressure exceeds the spring force. Thereafter, a nearly-constant pressure drop is maintained as long as the gas flows by the spring-loaded ball. An increase in the flow rate merely lifts the ball further, the pressure drop being almost unaffected. Contaminants that freeze out on the ball or seat lift the ball slightly further, but do not clog the valve permanently, as in a fixed-orifice J-T valve.

The metal-to-metal seat is more attractive for cryogenic applications than plastic





In this **Spring-Loaded Joule-Thomson Valve** the pressure drop is regulated by the spring pushing the stainless-steel ball against a soft brass seat. The pressure drop remains nearly constant, regardless of the helium flow rate and of any gas contaminants frozen on the valve seat.

seating materials, which tend to deform more than metals at low temperatures. Also the ball-and-socket approach is better than valve-poppet/O-ring designs, because a ball-and-socket design is self-centering. The new design also allows for external adjustment of the flow rate by means of a room-temperature throttle valve upstream of the J-T valve. Because the spring stiffness varies with temperature, the pressure drop at liquid-helium temperatures (typically 4.5 K) is about 4 percent higher than at room temperature.

The valve was tested on a cryogenic refrigerator used for maser receivers. At the throttle valve, the pressure dropped from 282 psia ($1.94 \times 10^6 \text{ N/m}^2$) to 262 psia ($1.81 \times 10^6 \text{ N/m}^2$); and at the spring-loaded J-T valve, from 262 psia ($1.81 \times 10^6 \text{ N/m}^2$) to 20 psia ($1.38 \times 10^5 \text{ N/m}^2$) while the temperature at the J-T valve was maintained at 4.5 K.

This work was done by Jack A. Jones and Michael J. Britcliffe of Caltech for NASA's Jet Propulsion Laboratory. For further information, Circle 8 on the TSP Request Card.
NPO-16546

Feedback-Controlled Regulation of Gas Pressure

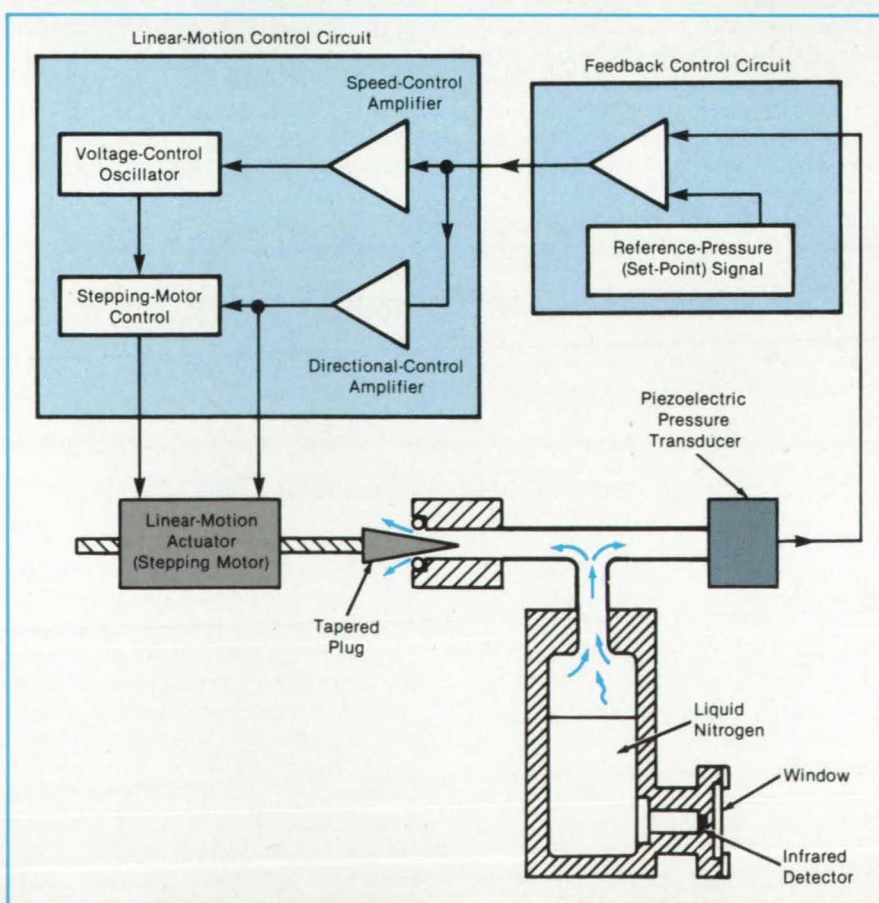
Internal pressure is maintained over a wide range of external pressures and exhaust rates.

Goddard Space Flight Center,
Greenbelt, Maryland

A feedback-controlled variable orifice regulates gaseous-nitrogen pressure in a liquid-nitrogen Dewar flask with precision of $\pm 0.001 \text{ psi}$ (7 N/m^2) over an ambient-pressure range of 26 to 756 torr (3.5 to 100 kN/m^2) and over a wide range of anticipated flow rates. Designed specifically to maintain airborne infrared detectors at a constant temperature in evaporating liquid nitrogen, this system can be modified to regulate the pressure in other enclosed systems.

Previous liquid-nitrogen pressure regulators have been of the passive mechanical type. Typically, these have a regulating accuracy no greater than $\pm 1 \text{ psi}$ (7 kN/m^2) at a given flow rate. Moreover, with these pressure regulators, the regulated pressure varies as the exhaust rate changes with the am-

The **Gaseous Pressure in a Liquid-Nitrogen Dewar** is regulated by a movable tapered plug, positioned automatically in response to signals generated by a piezoelectric pressure transducer.



bient pressure. The internal pressure also varies as system motion affects the evaporation rate of the liquid nitrogen.

The feedback-controlled, variable-orifice system is shown schematically in the figure. The exhaust opening of the liquid-nitrogen Dewar is connected to a variable-orifice mechanism that provides a variable-area port for the exhausting gaseous nitrogen. Also connected to the exhaust opening is a piezoelectric pressure transducer. The transducer sends the electronic control circuit a signal proportional to the gaseous-nitrogen pressure.

The control circuit compares the pressure-transducer signal to the set-point signal and puts out an error signal proportional to the difference between them. The error signal is sent to the linear-motion control circuit, which causes a stepping motor to move a cone-shaped plug within the exhaust orifice. The position of this plug determines the effective exhaust opening, thereby causing the Dewar pressure to be returned to the setpoint.

The use of a low-friction valve mechanism reduces the requirement for precise machining during the manufacture of the

valve parts: There is no need for the highly polished surfaces that would be necessary if the valve were designed differently. The electronic control circuit controls the valve with the same precision over its entire range of operation. The valve-operating range can be changed easily, with minimal mechanical alterations, to allow for any reasonable anticipated flow rate.

*This work was done by James C. Smith and Peter Leone of **Goddard Space Flight Center**. For further information, Circle 6 on the TSP Request Card.*

GSC-12990

Parallel-End-Point Drafting Compass

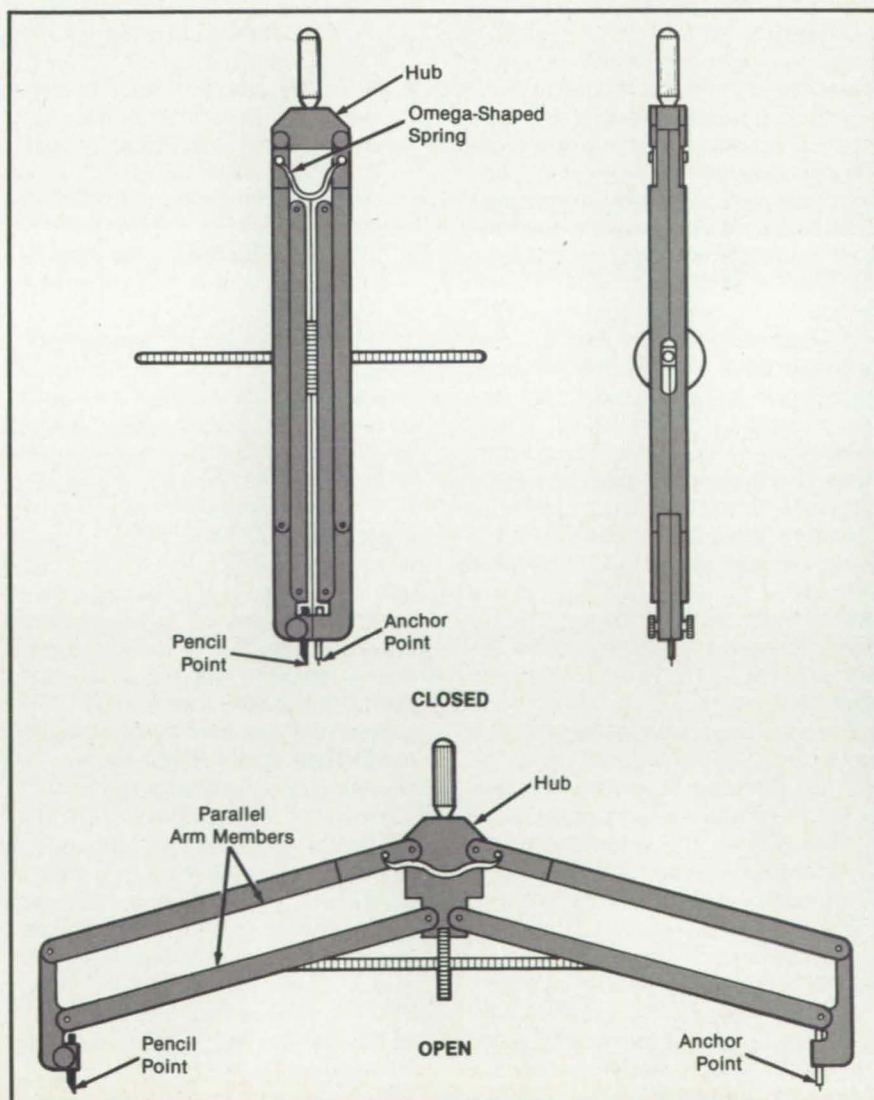
A parallelogram linkage ensures greater accuracy in drafting and scribing.

*Marshall Space Flight Center,
Alabama*

A linkage on a drafting compass keeps the pointed compass ends always in parallel, regardless how widely one opens up the compass legs. When the pointed ends are in parallel, distance measurements become more precise than with inexpensive compasses or dividers that have their pointed ends extending radially from the hub. Errors on these inexpensive instruments occur because the points sink into the paper at an angle, and the more one opens up the compass legs, the larger the angle and the greater the error. More expensive compasses and dividers have adjustable points, but these have to be set individually for each new radius to keep the pointed ends in parallel. The new compass employs a parallelogram linkage between its ends and its hub. The ends are in parallel when the compass is closed, when it is fully open, and at all positions in between. A pair of omega-shaped springs secures the linkage arms in the position set by the user until the user readjusts the end spacing. The parallelogram-linkage principle can be used on dividers as well as on compasses.

*This work was done by J. A. Cronander of Rockwell International Corp. for **Marshall Space Flight Center**. No further documentation is available.*
MFS-29070

The Two Members of an Arm of the compass remain parallel for all angles the pair makes with the hub axis. They maintain the opposing end members in parallelism.



Books and Reports

These reports, studies, and handbooks are available from NASA as Technical Support Packages (TSP's) when a Request Card number is cited; otherwise they are available from the National Technical Information Service.

Evaluation of Mathematical Turbulence Models

Simplified models for internal flow are described, and their predictions are compared with experimental results.

A report presents an account of various models used in the computation of turbulent flows. The applications of these models to internal flows are evaluated by the analysis of the predictions of various turbulence models in some important flow configurations.

Internal flows are complicated and are involved in many practical applications: These include flows in pipes, ducts, conduits, diffusers, and heat exchangers. Turbulence makes the flow equations even more complicated, necessitating the use of simplified mathematical models to obtain approximate solutions.

The report describes models of incompressible flows in which the velocities, stresses, and other dependent variables are separated into steady (that is, time-averaged) and fluctuating components. Some of the models also involve spatial averaging over such small regions as boundary layers. Attention is focused on the $k-\epsilon$ model (where k = the time-averaged local density of the kinetic energy of the turbulence and ϵ = the dissipation rate of the energy of the turbulence). The $k-\epsilon$ model relates the eddy viscosity to k and ϵ .

The main conclusions of the report are as follows:

- The $k-\epsilon$ model is the most widely used model for engineering calculations of internal flows. The performance of the standard $k-\epsilon$ model becomes poorer as one goes from attached flow to recirculating, swirling, and combusting flows, in that order.
- The standard $k-\epsilon$ model performs poorly in the prediction of apparently simple flow over a backwardly facing step. There is no significant improvement in the value of reattachment

length predicted with modified near-wall models. The algebraic stress model (a sort of extended $k-\epsilon$ model) should be used, with a modified $k-\epsilon$ equation.

- The $k-\epsilon$ model performance is rather poor for flows with streamline curvature. The algebraic stress model performs better for these flows.
- Reynolds stress models (involving approximations of diffusion, viscous dissipation, and other quantities) have not been thoroughly tested for recirculating flows and swirling flows. The computational effort required for a Reynolds stress model is much greater than that required for the $k-\epsilon$ model.
- For flows with regions of secondary flow (flows in noncircular ducts), the algebraic stress model performs fairly well for fully developed flow, but not for a developing flow. A Reynolds stress model should be used for the developing flow.
- Many computations should be viewed with caution because the dependence of the solutions on the coarseness of the computational grid has not been tested.
- The initial conditions play a crucial role in the performance of a model and the predicted solutions.
- The TEACH (Teaching Elliptic Axisymmetric Characteristics Heuristically) code, or its variant, is the most widely-used computer code in the prediction of turbulent internal flows cited in the literature.

Two important factors in the numerical solution of the model equations are discussed; namely, false diffusion and inlet boundary conditions. The existence of countergradient transport and its implications in turbulence modeling are mentioned. There are brief descriptions of other approaches to turbulent-flow computations including the vortex method (using point or line vortices), large-eddy simulation (direct solution of the Navier-Stokes equations with filtering to remove small eddies), and direct simulation (solution of the full Navier-Stokes equations).

This work was done by M. Nallasamy of Marshall Space Flight Center. Further information may be found in NASA Technical Paper 2474 [N85-25757/NSP], "A Critical Evaluation of Various Turbulence Models as Applied to Internal Fluid Flows" [\$11.95]. A paper copy may be purchased [prepayment required] from the National Technical Information Service, Springfield, Virginia 22161. The report is also available on microfiche at no charge. To obtain a microfiche copy, Circle 90 on the TSP Request Card. MFS-27118

Correcting for Supports in Structural Dynamic Testing

Testing under a variety of support conditions is combined with computer analysis to update mathematical models to match test data.

A report suggests that the dynamic characteristics of large space structures can be predicted, without full-scale testing, by a method that combines experiment and analysis. The method, multiple-boundary-condition testing, was developed for such large space structures as dish antennas, towers, and solar-cell arrays.

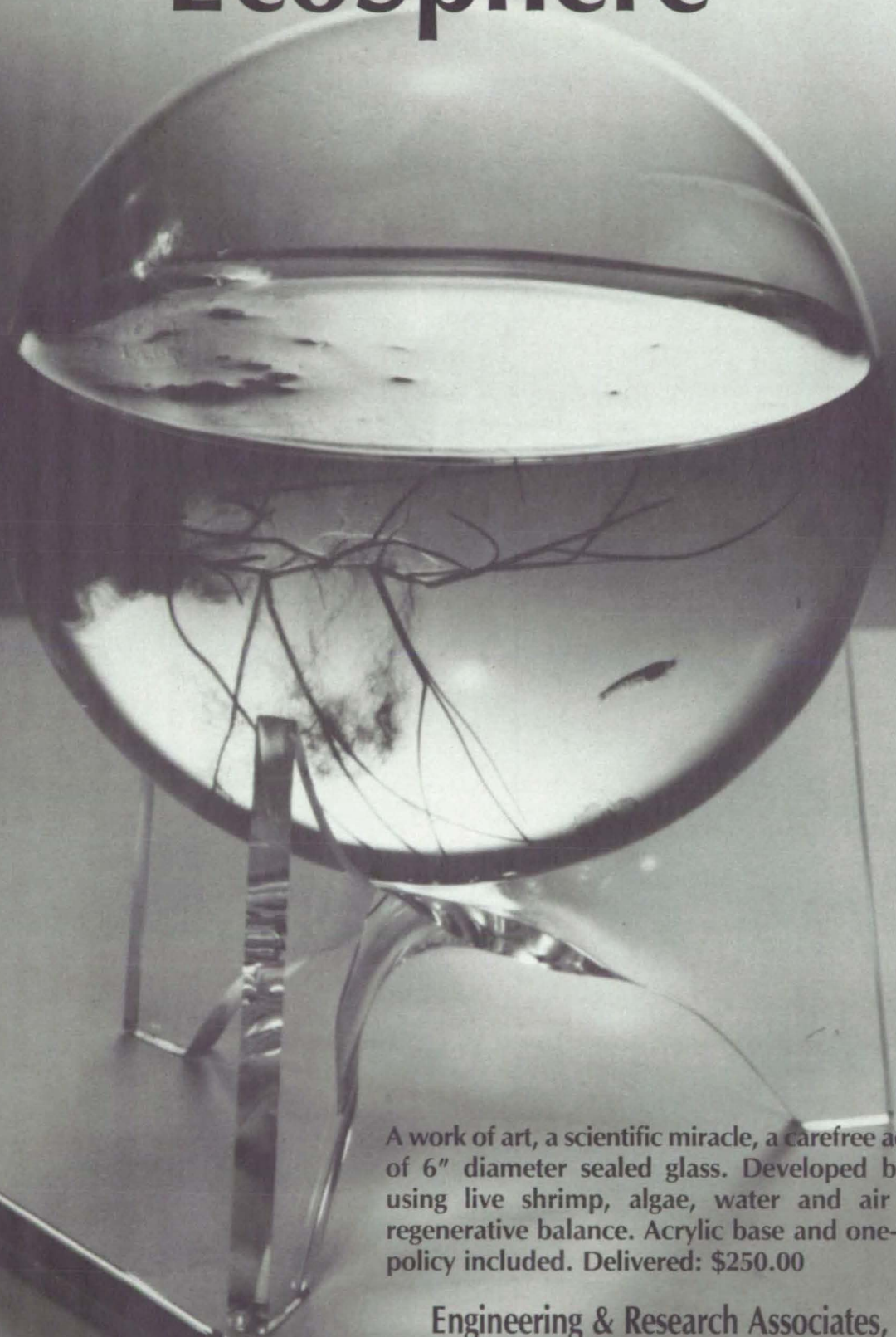
The method compensates for the effects of the supports that are needed to hold flexible and fragile space structures when they are tested in Earth's gravity. Multiple-boundary-condition testing consists of testing a structure under a variety of support conditions and support locations. The resulting data are processed according to an algorithm that separates the meaningful information about the structure from the spurious effects of the supports.

The initial input data for the mathematical model of the structure are represented by mass and stiffness matrices. The equations that give the theoretical data relating to the vibrational modes are linearized, then fitted to the test data by a least-squares method. The revised estimates are then used to calculate the data relating to the vibrational modes. This process is repeated until the correlation between the mathematical and the test results is acceptable.

The report reviews the history of the development of the method, presents the principles of the approach, discusses the results of a theoretical analysis of the accuracy of the method in comparison with conventional testing, and describes a computer simulation of the method as applied to a simply supported beam with a series of roller constraints. Initial studies indicate that the method can provide a better final mathematical model of a structure than can a conventional ground test of the structure.

This work was done by Ben K. Wada, Chin-Po Kuo, and Robert J. Glaser of Caltech for NASA's Jet Propulsion Laboratory. To obtain a copy of the report, "Multiple Boundary Condition Testing Used To Validate a Structural Dynamic Model of a Large Flexible Structure," Circle 39 on the TSP Request Card. NPO-16620

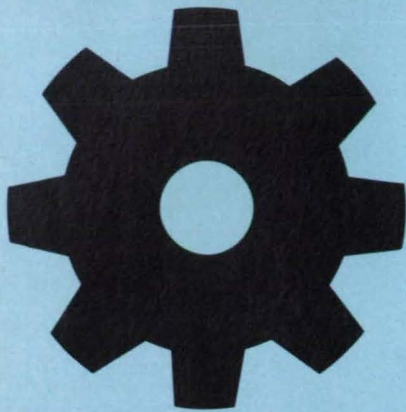
EcoSphere



A work of art, a scientific miracle, a carefree aquarium of 6" diameter sealed glass. Developed by NASA using live shrimp, algae, water and air in bioregenerative balance. Acrylic base and one-year life policy included. Delivered: \$250.00

Engineering & Research Associates, Inc.
500 N. Tucson Blvd., Tucson, AZ 85716
1-800-223-5369, Ext. 331

Machinery



Hardware, Techniques, and Processes

- 106 Modified Cobalt Drills With Oil Passages
- 107 Spiral-Groove Ring Seal for Counterrotating Shafts
- 109 Designing Power-Transmission Shafting
- 110 Locating Cracks Amid Pitting and Corrosion
- 111 Eliminating Thermal Cracks in Flange/Duct Joints
- 112 Adapting Inspection Data for Computer Numerical Control
- 112 Non-Back-Drivable, Freewheeling Coupling
- 114 Effects of Gear-Cutter Geometry on Performance
- 115 High-Speed Propeller for Aircraft
- 117 Pump for Saturated Liquids
- 117 Receptacle for Optical-Fiber Scraps
- 118 Thermally Integrated Fuel-Cell/Electrolyzer Systems
- 119 Hydraulic Actuator for Ganged Control Rods
- 120 Ignition System for Gaseous Propellants
- 121 Rigid/Compliant Helicopter Rotor
- 122 Helicopter Pitch-Control Mechanism Reduces Vibration
- 123 Controlled-Temperature Hot-Air Gun
- 124 Adjustable Tooling for Bending Brake

Books & Reports

- 125 Orbital Transfer Vehicle with Aerodynamic Braking
- 126 Algorithm for Calibrating Robot Arms
- 126 Overcoming Robot-Arm Joint Singularities
- 126 Theory and Tests of Two-Phase Turbines
- 127 Crash Tests of Protective Airplane Floors

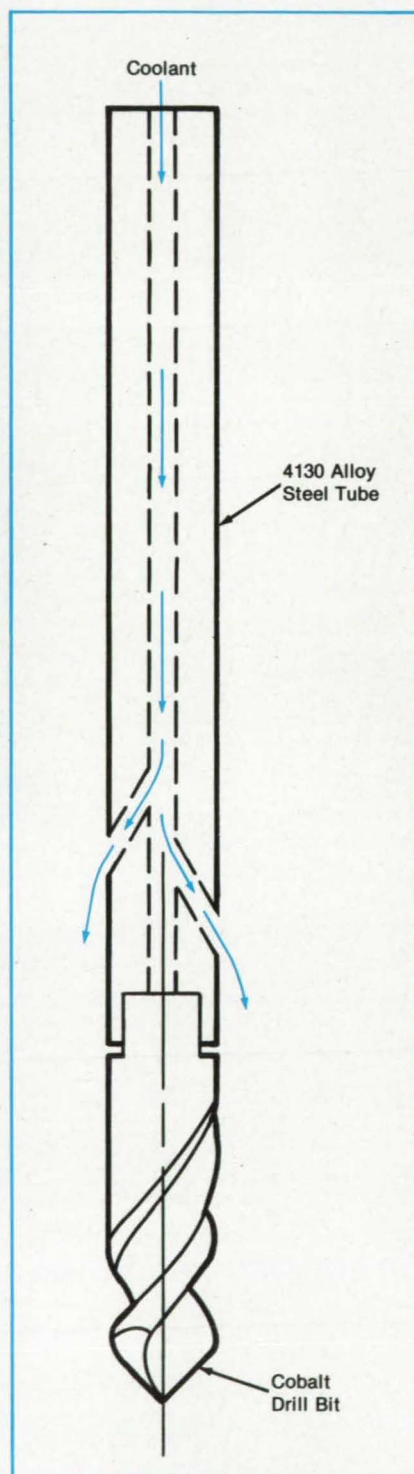
Computer Programs

- 82 Hytess-Hypothetical Turbofan-Engine Simplified Simulation
- 82 Aircraft Rollout Iterative Energy Simulation
- 83 Estimating Transient Pressure Surges in Cryogenic System
- 83 Computing Cooling Flows in Turbines
- 83 Four-Cylinder Stirling-Engine Computer Program

Modified Cobalt Drills With Oil Passages

Oil is forced through the drill shanks to lubricate the cutting edges.

Marshall Space Flight Center, Alabama



Drill bits have been cooled and lubricated by oil forced through the drill shanks and out holes adjacent to the bits. This cooling technique increases drill-bit life and allows increased drill feed rates.

The particular application involved the removal of inertia-weld nuggets from the bottoms of holes 10 in. (25.4 cm) long with 0.188 in. (0.47 cm) diameter. The nugget material is left after inertia welding of Haynes 188 (or equivalent) posts (containing the holes) to Inco 718 (or equivalent) stubs. The nuggets are irregularly shaped with inconsistent material properties.

Carbide drill bits tend to break from the surface irregularities, making cobalt a better cutting tool material. However, cobalt drill bits dull rapidly without adequate cooling. The drill diameter is only 0.010 in. (0.025 cm) less than that of the hole. The conventional cooling method fails to get coolant to the cutting surface of the drill at the bottom of the hole.

The solution to the problem is shown in the figure. The drill shank is joined with a tube having three exit holes 120° apart near the shank end. Cooling oil is forced through the tube and out the exit holes toward the bit.

This work was done by E. E. Hutchison and D. Richardson of Rockwell International Corp. for **Marshall Space Flight Center**. No further documentation is available.

MFS- 29137

During Drilling the Bit Is Cooled by oil forced through the shaft and out holes near the bit.

Spiral-Groove Ring Seal for Counterrotating Shafts

The self-lubricating seal tolerates high sliding speeds.

*Lewis Research Center,
Cleveland, Ohio*

The spiral-groove intershaft ring seal is a new seal concept that has potential application in sealing fan-bleed air between two counterrotating shafts in advanced gas-turbine engines. This is a difficult sealing application for any contacting-type seal because the counterrotating shafts set up very high sliding speeds for the seal. In addition to the high sliding speed, the seal must accommodate axial translation due to relative axial motion between the two shafts.

The intershaft ring-seal application is an excellent example of the need for applying self-acting, gas-lubricating bearing technology to contacting-type seals. Application of a self-acting geometry in the form of spiral grooves to the faces of the ring-seal housing will maintain a thin air film of relatively high stiffness between the seal ring and the housing, thereby enabling the seal to operate in a noncontacting mode over the entire engine-operating range. The seal could then operate at high sliding speeds, accommodate axial translations, and have leakage rates consistent with contacting-type seals.

When spiral grooves are employed in a seal as a film-generating mechanism, the following are generally required to calculate the axial-force equilibrium: (1) film load-capacity curves (lift force as a function of film thickness), (2) minimum film thickness over the operating range, and (3) optimization of the spiral-groove geometry to maximize the lift force for a given seal-envelope size and operating condition. Figure 1 shows the intershaft seal concept. The housing, which contains the carbon ring, rotates with the inner shaft. The carbon ring is bounded on its outside diameter by the outer shaft,

Do you know that Valcor makes all these fluid control products?



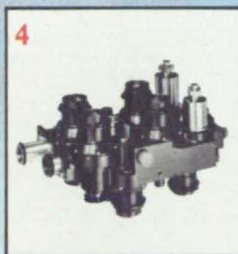
1
SELF-DISPLACING
HYDRAULIC
ACCUMULATORS



2
PRESSURE REGULATORS
& RELIEF VALVES



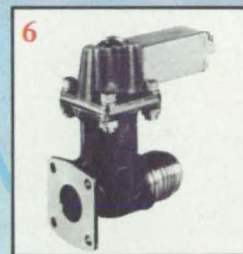
3
SOLENOID &
PRESSURE OPERATED
FUEL VALVES



4
PRESSURIZATION
SYSTEMS



5
MODULATING
VALVES



6
HOT GAS
SOLENOID VALVES

These aircraft companies do.

1. Northrop/McDonnell (F-18) • Grumman (X-29 FSW)
Boeing (AWACS E-34) • Lockheed (S3A & C5A)
2. Fairchild (F-27 & FH-227) • North American Rockwell (F-86)
McDonnell Douglas (F-4E) • Hughes Research • NASA Programs
3. Multiple Programs for:
Boeing • United Technologies • Rockwell • Northrop • Aircsearch
McDonnell Douglas • Grumman • Fairchild Republic • Lockheed
Woodward Governor • Saab • Allison • Sundstrand • Beech • Cessna
4. General Dynamics (C-131) • Lockheed (C5A)
Boeing (B-52, KC135, B-707, B-727, B-737, B-747)
5. Grumman (X-29 FSW & A6) • Electronic Fuel Controls Mfrs.
6. Fairchild (SF-240) • Bell Helicopters • Rockwell (A10) • GM

Get to know us better. Contact our Aerospace Applications Department for your copy of Valcor's Military/Aerospace Product Catalog.



VALCOR ENGINEERING CORPORATION

2 Lawrence Road, Springfield, New Jersey 07081
(201) 467-8400 TWX: 710-996-5976

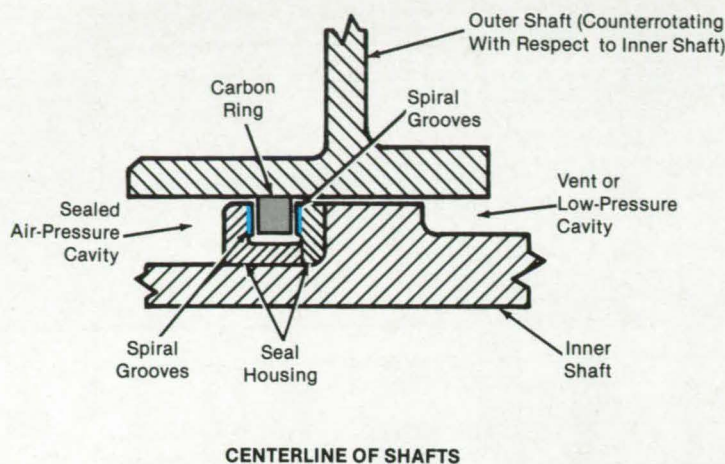


Figure 1. The **Intershaft Seal** includes spiral grooves that generate lubricating gas films.

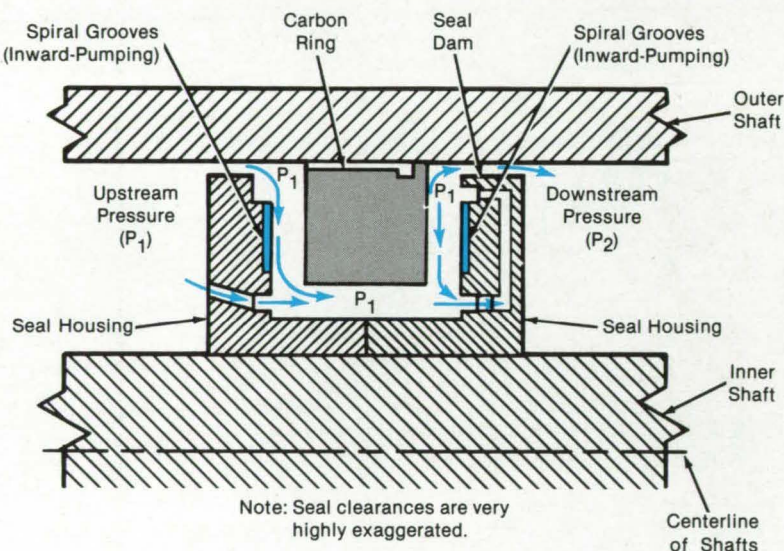


Figure 2. In the **Pressure-Balanced Spiral-Groove Concept**, the spiral-groove flow is isolated from the seal-leakage flow.

which counterrotates with respect to the inner shaft. As the shafts rotate, the carbon ring expands into the outer shaft and assumes the speed of the outer shaft. The relative sliding speed between the carbon ring and the inner shaft can approach 255 meters per second (835 feet per second).

It should be noted that the carbon ring may require a radial split line to limit hoop stresses due to rotation and to assure that the carbon ring will rotate with the outer shaft. Relative axial translations between the inner and outer shafts of up to 0.64 centimeter (0.25 inch) due to thermal expansion are possible over the design operating range. This translation causes the carbon ring to approach one of the two housing faces. The spiral grooves on the housing faces generate a very high lift force as the carbon ring ap-

proaches either face, thereby maintaining a fluid film between the carbon ring and the housing face.

Figure 2 is a schematic drawing of the seal showing it in a neutral position (equal clearance on either side of the carbon). The total axial clearance between the carbon ring and the housing face is only 0.0203 millimeter (0.0008 inch) or 0.0102 millimeter (0.004 inch) per side when the seal is centered in the housing. The air-flow through the seal is shown; P_1 is the high pressure, and the pressure drop from P_1 to P_2 occurs across the seal dam. The porting shown is designed such that the spiral grooves are bounded by the sealed pressure (P_1) at both the outside and inside diameters; hence, there is no pressure difference across the spiral grooves. This is known as a pressure-balanced spiral-groove concept. The

pressure-balanced concept isolates the spiral-groove flow from the seal-leakage flow so that the spiral-groove performance is not subject to any ill effects due to seal-leakage flow.

Transients such as pressure and thermal expansion that occur over the engine-operating range will change the axial-force equilibrium of the seal, thus causing the carbon seal ring to approach one of the housing faces. As the clearance between the carbon seal ring and one of the housing faces approaches zero clearance, the spiral grooves generate a very high lift force. The lift force increases exponentially with reduction in clearance until a clearance is achieved at which axial-force equilibrium is restored. The forces that enter into the axial-force equilibrium are pressure-area forces on the carbon ring, friction force between the carbon ring and the outer shaft (produced by relative axial translations of the shafts), and the lift force generated by the spiral grooves.

This work was done by Eliseo DiRusso of **Lewis Research Center**. Further information may be found in NASA TP-2142 [N83-25712/NSP], "Design Analysis of a Self-Acting Spiral Groove Ring Seal for Counter-Rotating Shafts" [57]. A copy may be purchased [prepayment required] from the National Technical Information Service, Springfield, Virginia 22161. LEW-14248

EMPLOYEES APPRECIATE THE PAYROLL SAVINGS PLAN. JUST ASK THE PEOPLE AT GEORGIA-PACIFIC.

"Besides being a good investment in my country, Bonds help me save for my two daughters."

—Craig Heimbigner



U.S. Savings Bonds now offer higher, variable interest rates and a guaranteed return. Your employees will appreciate that. They'll also appreciate your giving them the easiest, surest way to save.

For more information, write to: Steven R. Mead, Executive Director, U.S. Savings Bonds Division, Department of the Treasury, Washington, DC 20226.

U.S. SAVINGS BONDS
Paying Better Than Ever

A public service of this publication.

Designing Power-Transmission Shafting

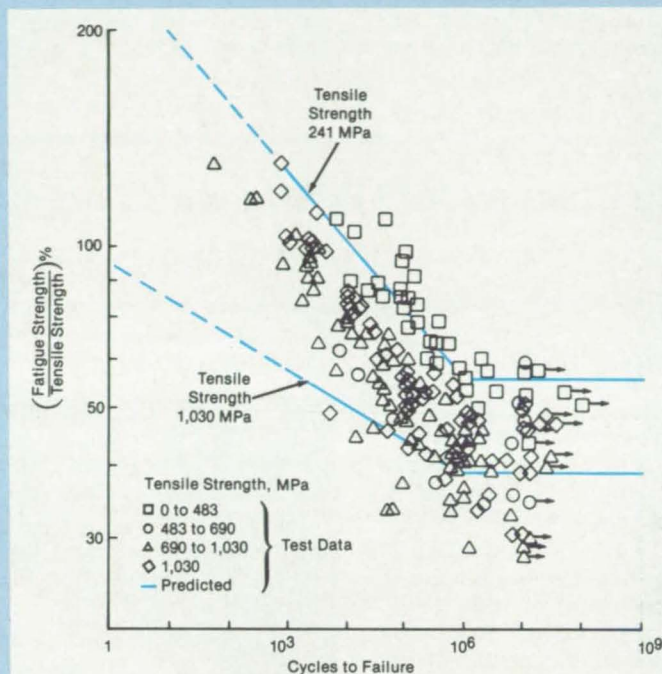
Consideration of stress and fatigue life gives better designs.

Lewis Research Center,
Cleveland, Ohio

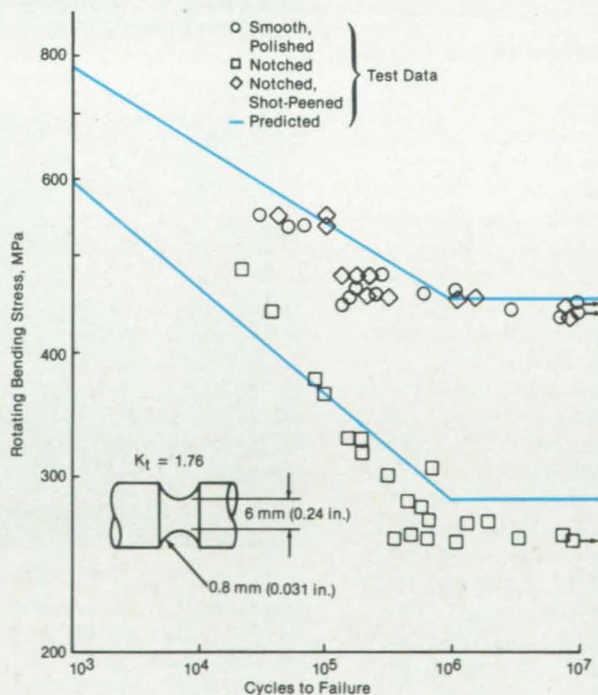
Power-transmission shafting is a vital element of all rotating machinery. A shafting-design procedure has been developed based on fatigue-strength considerations. This method not only accounts for the effects of static and constant-amplitude fluctuating loads but will provide shaft-diameter estimates for variable-amplitude-loading duty cycles.

A stress-life approach is adopted for limited-life designs, restricted to the intermediate-to-high cycle-fatigue-life region. A local notch strain-life analysis is recommended for short-lived designs. In the absence of actual component-fatigue data, the S-N (stress-life) characteristics of the shaft in bending can be approximated by a straight line connecting the true fracture-strength coefficient with the corrected fatigue limit of the shaft on log/log coordinates. The figure shows that this approximation works reasonably well for a variety of steels, based on fatigue data found in the open literature. The predictions appearing in these figures are an estimate of the fatigue limit based on the ultimate tensile strength of the steel. Knowledge of the true fatigue limit for the particular steels in question would be expected to enhance the accuracy of the prediction.

The method requires the use of the fatigue limit of the shaft to be designed, which is almost always different from the fatigue limit of the highly-polished, notch-free test specimen, commonly listed in material-property tables. Typical values of fatigue-life-modifying factors are used to correct the fatigue limit of the test specimen for service factors that are known to affect fatigue strength. These factors include surface condition, size, reliability, temperature, stress concentration, press-fitted collars, residual stress, and corrosion corrections. For example, residual stress due to certain manufacturing processes can have major effects (both beneficial and negative) on shaft fatigue life. This is clearly illustrated in the lower part of the figure, which shows that the introduction of compressive residual stress in the notched region of the test specimen through shot peening has essentially eliminated the notch effect almost entirely.



COMPARISON WITH TEST DATA FOR STEELS OF DIFFERENT TENSILE STRENGTH



COMPARISON WITH TEST DATA FOR NOTCHED SPECIMENS

The **Stress/Life Characteristic** of a shaft is approximated for design purposes by straight lines based on previously published data. The straight-line predictions shown here are estimates of the fatigue limit based on the ultimate tensile strength of steels.

Shafting material, rigidity, and critical speed are also considered, as are surface finish, dimensional tolerance, and material-strength properties of commonly-used commercial transmission-line shafting. Recommended gear and bearing maximum-shaft-misalignment values are also addressed. Critical speed considerations are used along with a Rayleigh-Ritz method to calculate, as a first approximation, the fundamental or first critical frequency of a shaft/bearing system using

either completely-rigid or laterally-flexible bearing supports.

A longstanding objective in the design of power-transmission shafting is to eliminate excess shaft material without compromising operational reliability. This shafting-design method allows the designer to assess the impact of key operating and design variables and shaft-material selection on fatigue life and shaft size. The method lends itself to the computer-aided design of both aerospace and in-

dustrial shafting.

This work was done by Stuart H. Loewenthal of **Lewis Research Center**. Further information may be found in NASA RP-1123 [N84-27041/NSP], "Design of Power-Transmitting Shafts." [\$8.50]. A copy may be purchased [prepayment required] from the National Technical Information Service, Springfield, Virginia 22161. LEW-14240

Locating Cracks Amid Pitting and Corrosion

Use of two fluorescent penetrants reveals cracks.

Lyndon B. Johnson Space Center, Houston, Texas

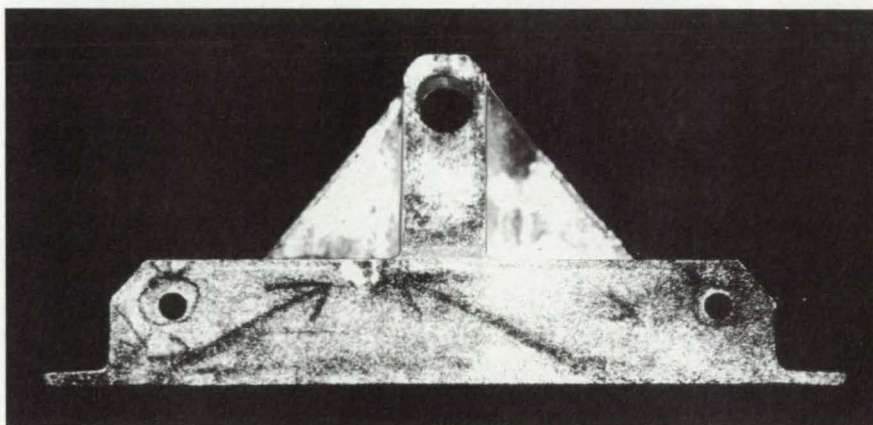
Two fluorescent oils are used in a new inspection technique for locating cracks in metal parts. Use of just one fluorescent oil is not always effective when a part is pitted or corroded. The pits and corroded areas absorb the dye along with the cracks, thus masking fluorescence from the cracks.

A part to be inspected by the two-penetrant technique is first degreased in a solvent vapor, then chemically etched to remove 0.0004 to 0.0006 in. (0.010 to 0.015 mm) of material from the surface. The part is then dried in warm, circulated air at a maximum temperature of 175°F (79°C).

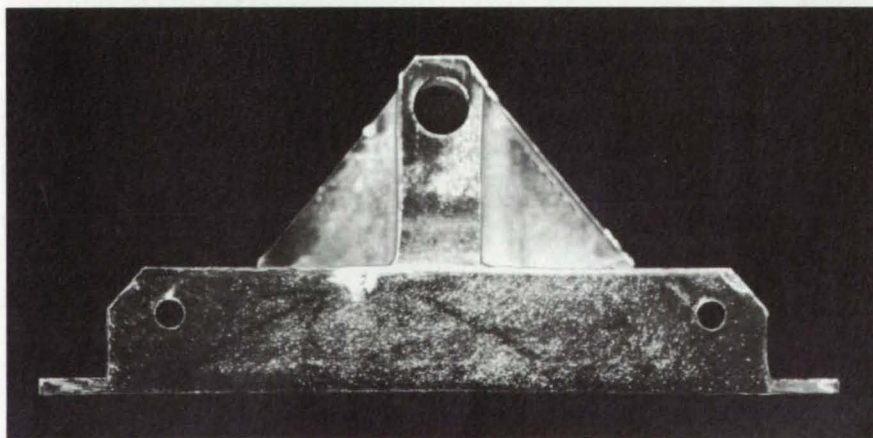
A postemulsifiable fluorescent oil, ZL-30 (or equivalent), is applied to the part and allowed to remain on the surface for 30 min. Then a water-washable fluorescent oil, ZL-17 (or equivalent) is applied and the excess allowed to drain off. The water-washable oil emulsifies the postemulsifiable oil on the surface so that it can be removed from the surface by a water rinse, even from the pitted and corroded areas. However, the postemulsifiable oil embedded in deep, fine cracks remains.

The water rinse is done under ultraviolet light. The part is then immersed in an aqueous solution of developer ZP-13A (or equivalent), drained, dried in air at 175°F (79°C) maximum, then cooled below 100°F (38°C). After waiting at least 15 min for development (but no longer than 75 min), the part is examined in ultraviolet light. Fluorescent dye retained by cracks is readily visible and distinguishable from the minimal fluorescence retained by pitted and corroded material (see figure).

The dual-dye technique has been used to inspect metal parts having surface-roughness-height ratings from 125 to 450 μ in. (3.2 to 11.4 μ m). The parts have included shot-peened machined aluminum extrusions; partially machined aluminum



AFTER TREATMENT WITH ONE FLUORESCENT OIL



AFTER THE DUAL-OIL TREATMENT

This Machined Aluminum Fitting has extensive pitting and areas of corrosion that retain fluorescent penetrating oil. In the upper photograph, the fluorescence from these areas obscures fluorescence from oil absorbed by cracks. After treatment with a second, emulsifying oil, much of the fluorescence from pitted and corroded areas disappears and, as shown in the lower photograph, fatigue cracks emanating from holes become evident.

castings; aluminum, steel, and titanium tubular weldments; aircraft landing-gear components; chemically milled aluminum sheet and extrusions; and rough-machined aluminum and steel forgings. It has also

been used on nonporous ceramic parts.

This work was done by Peter P. Fahey of Fairchild Republic Co. for **Johnson Space Center**. For further information, Circle 69 on the TSP Request Card. MSC-20311.

NASA Tech Briefs, May/June 1986

Eliminating Thermal Cracks in Flange/Duct Joints

Heat and pressure during bonding allow joints to accommodate expansion.

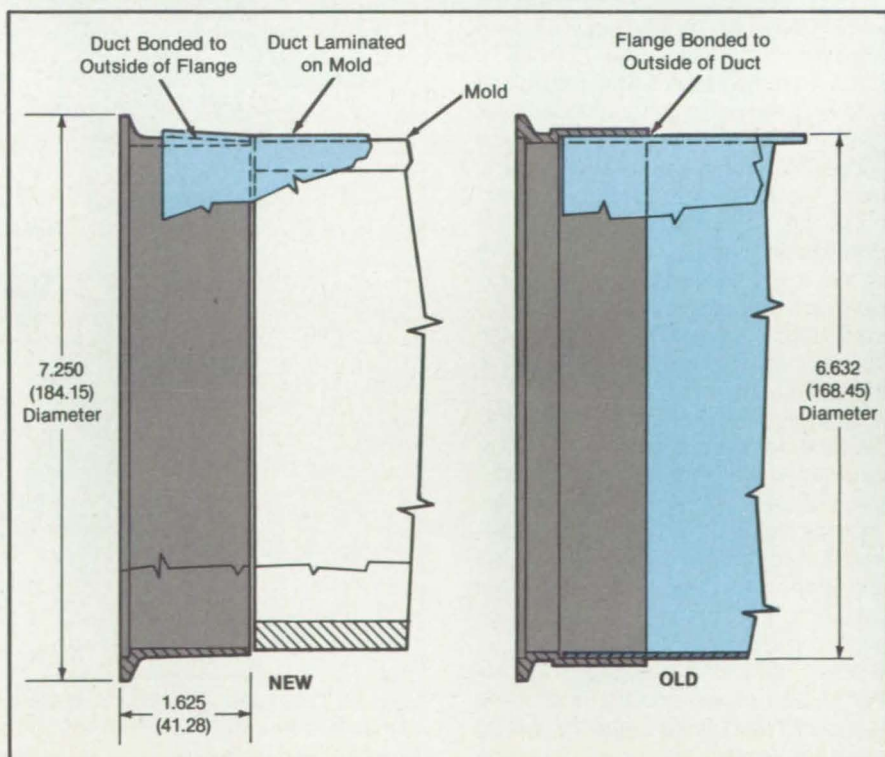
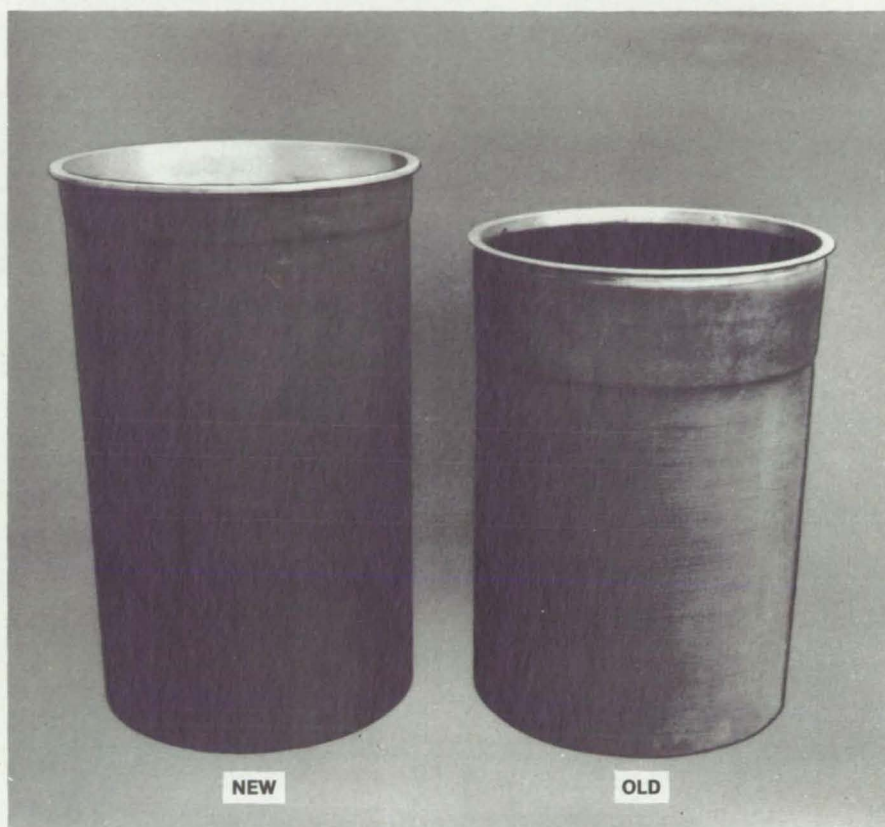
Lyndon B. Johnson Space Center, Houston, Texas

An improved technique for attaching an aluminum flange to an aramid/epoxy duct prevents the subsequent development of cracks in the joint during thermal stress. Previously, the flange was bonded to the outside surface of the duct (see Figure 1). In service, leaks occurred at the bond line when temperature and pressure rose. The attachment method made no allowance for the differing thermal expansion rates of aluminum and aramid/epoxy.

In the new method, the flange is butted against the cylindrical mold on which the duct is to be fabricated. The flange has a tapered neck so that it will nest in the duct opening. The epoxy-impregnated aramid tape is wrapped around the mold so that the tape overlaps the flange (see Figure 2). While the tape is being wrapped, pressure is applied to it and the inside of the flange as they are heated uniformly to the maximum expected operating temperature. The heat and pressure are maintained until the aramid/epoxy laminations have cured.

The new method produces reliable bonds. Flanged ducts have been tested at temperatures ranging from -150 to $+350^{\circ}\text{F}$ (-100 to $+180^{\circ}\text{C}$) and pressures of up to 100 lb/in.^2 gauge (790 kPa) through 100 cycles without flange/duct separation.

This work was done by James E. Adams of Rockwell International Corp. for **Johnson Space Center**. For further information, Circle 46 on the TSP Request Card. MSC-20833



Adapting Inspection Data for Computer Numerical Control

Machining time for repetitive tasks is reduced.

Marshall Space Flight Center, Alabama

A program for a computer-numerical-control jig boring machine ensures that holes are drilled and reamed with high accuracy in post stubs on the main injector body of the Space Shuttle main engine. Although the post stubs are positioned so that they may deviate from the design position by as much as 0.025 inch (0.635 millimeter), the program controls the hole positions to within 0.010 inch (0.254 milli-

meter) of the design positions. With modifications this approach should be applicable to the machining of many precise holes on large machine frames and similar objects.

The program converts measurements of stub post locations by a coordinate-measuring machine into a form that can be used by the numerical-control computer. The work time is thus reduced by

10 to 15 minutes for each post. Since there are 600 such posts on each injector, the time saved per injector is 100 to 150 hours.

This work was done by Everett E. Hutchison of Rockwell International Corp. for Marshall Space Flight Center. No further documentation is available. MFS-29117

Non-Back-Drivable, Freewheeling Coupling

Cables can be reeled in and out with less risk of tangling.

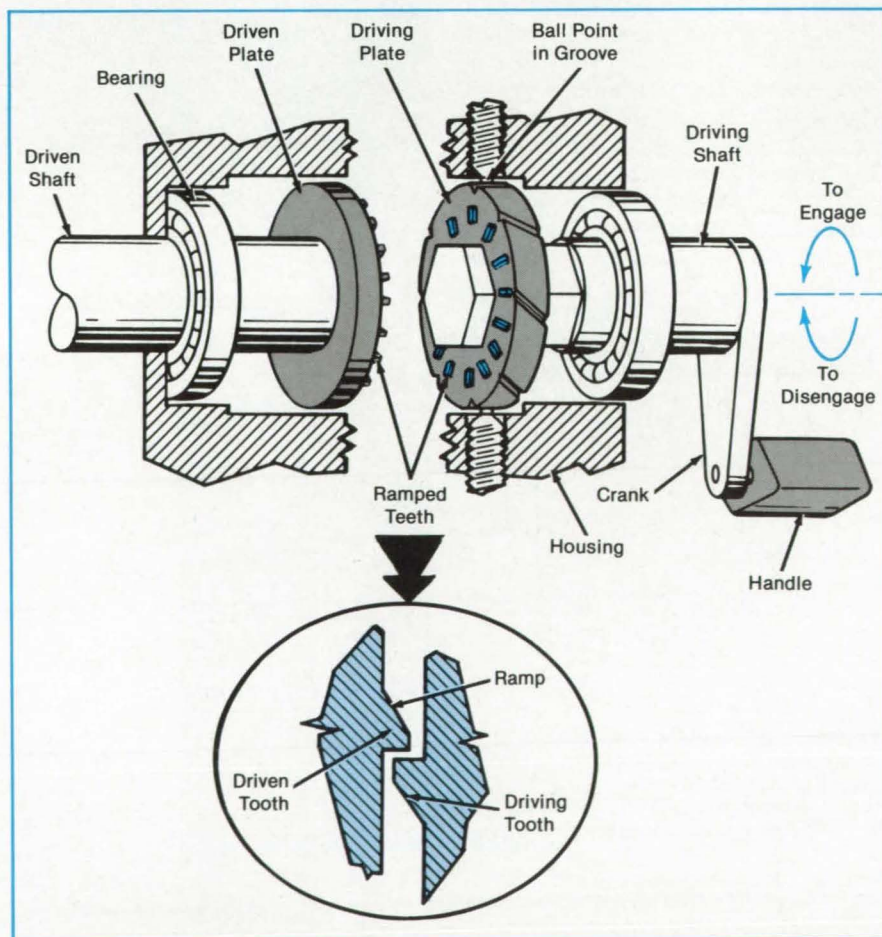
Lyndon B. Johnson Space Center, Houston, Texas

An overrunning clutch transmits forward rotary power from a driving unit (for example, a motor or a hand crank) but does not allow the driven unit to transmit power to the driver. The clutch allows the driven unit to turn freely forward faster than the driver; that is, to freewheel. If the driven unit reverses its direction of rotation, the clutch disengages the driving and driven units, allowing reverse free-wheeling.

The clutch contains a driving plate and a driven plate on separate coaxial shafts (see figure). The opposing faces of the plates hold ramp-shaped (ratcheting) teeth. The driven plate is fixed to its shaft, but the driving plate is splined on its inside circumference and is free to slide axially on the splined driving shaft. The driving plate has helical grooves in its outside circumference; ball-point screws in the housing around the driving plate ride in these grooves.

When the hand crank (or motor) turns the driving plate in the forward direction (counterclockwise in the figure) faster than the driven plate, the ball points engage the helical grooves, moving the driving plate against the driven plate and engaging the teeth. The driving plate then transmits power to the driven plate through the engaged teeth.

When the clutch is engaged, but not transmitting power, and the driven side rotates forward faster than the driving plate, the ramped teeth push the plates



Opposing Teeth Engage with clockwise rotation and disengage with clockwise rotation of the crank. The driving plate moves axially with respect to the driven plate on ball points to engage and disengage.

The Inland Motor Team Philosophy: Demanding Applications Require Servo Components That Are Complementary—And Uncompromising.



At Inland Motor we specialize in finding solutions to difficult motion control problems. That's why we have pioneered the development of servo systems comprised of fully compatible, complementary servo components. By supplying motors, amps and tachs that are designed to work together without compromise, we're able to deliver "systems" that are not only ideally suited for your application but remarkably obedient.

Building Smart One Block At A Time

The system illustrated in Figure 1 is a simplified example of a high-performance single axis dc servo system. The diagram illustrates our commitment to providing a tailored solution to each of your motion control requirements. Inland Motor designs and manufactures brushless and brush-type motors in both frameless and housed configurations, as well as a full line of PWM servo amplifiers. Once the dynamic and environmental constraints (such as torque, speed, duty cycle, envelope, ambient temperature, precision, etc.) have been identified, we can then specify or develop a motor suited to those requirements.

Once parameters are established, an amplifier is sized for your application. Motor control requirements, such as voltage and current, can be matched through winding changes to any of several pulse-width-modulated (PWM) amplifiers manufactured by Inland Motor. Finally, a power sup-

ply and transformer can be selected to complement your amplifier.

Our Frameless Motors Eliminate Backlash

Most of our existing motor and tachometer designs are "frameless, direct-drive" configurations. This means that unwanted backlash asso-

ciated with gears and belts is eliminated. You receive the full benefit of a motor (available peak torques range from 1 oz. in. to 1,000,000 oz. in.) that is an integral part of your machine, relying on existing bearings and shaft structure for support. And, because direct-drive is not suitable for every application, we offer housed motors and tachs as well.

Servo Amps With No Room For Compromise

Our PWM servo amps are available in many configurations to suit a variety of applications. Each model has an internal, high bandwidth current loop as its foundation. Current loops are what dc motors respond to best, so that's where we have concentrated our efforts. Around the inner current loop, we offer features such as velocity control (analog and digital), phase-locked loops and position loops. Our PWM servo amps operate at inaudible frequencies of 20 kHz or higher, are 90% efficient, need no cooling fans and come in a small modular package size.

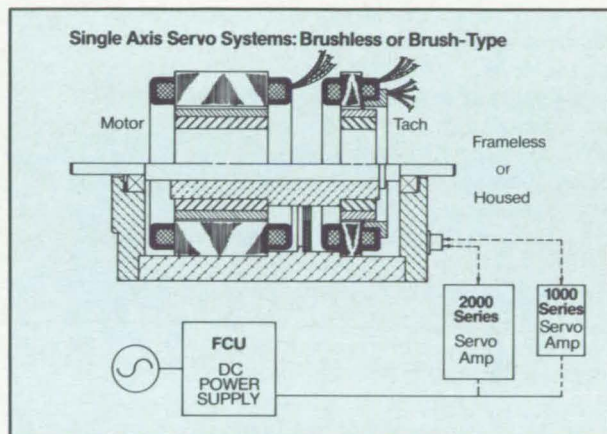
When you purchase a complementary motor and amp from Inland, we compensate the amp to the motor and deliver a current loop Bode plot for the combination.

In addition, we offer power supplies that provide the appropriate dc voltage and current to run our PWM amplifiers from a single-phase ac source. These units handle power sequencing and absorb regenerative energy as required.

Together, our servo amps and power supplies combine to maximize your motor's performance, not compromise it.

Send Us Your Most Un-Controllable Problems

We speak of the "Inland Motor Team Philosophy" because it's a team of people—not a particular product—that lies at the heart of our company. When you call the Specialty Products Group for assistance, you'll



be connecting with engineers committed to finding solutions for your one-of-a-kind application problems. That's why site visits are often arranged so we can discuss your project in detail. We think our team is quite talented. But, what most distinguishes the Group is our determination to be responsive—to be a team that adapts, tests and refines our components until we can deliver you true motion control solutions.

Inland Motor Specialty Products Group: a team of people committed to delivering solutions to your most challenging motion control problems.

INLAND MOTOR
KOLLMORGEN CORPORATION
SPECIALTY PRODUCTS GROUP
501 First St. Radford, VA 24141
703/639-9045 TWX: 710-875-3740



apart. The driven plate then turns independently.

When the clutch is engaged and the driven side starts to turn backward (clockwise in the figure), the teeth rotate the driving plate backward only briefly; the driving plate slides on its grooves until the teeth disengage. No further motion is transmitted from the driven plate to the driver.

The clutch was developed for reeling and unreeling a tether line used to link an astronaut to a space vehicle. It allows the line to be pulled out freely and helps to prevent the line from tangling in the reel housing when the crank is turned backward. The new clutch concept may also be applicable to fishing reels, toys, and safety-line mechanisms.

This work was done by W. R. Llewellyn

of Martin Marietta Corp. for **Johnson Space Center**. For further information, Circle 86 on the TSP Request Card.

This invention is owned by NASA, and a patent application has been filed. Inquiries concerning nonexclusive or exclusive license for its commercial development should be addressed to the Patent Counsel, Johnson Space Center [see page 29]. Refer to MSC-20475.

Effects of Gear-Cutter Geometry on Performance

Bending stress is reduced by improving tooth-fillet design.

Lewis Research Center, Cleveland, Ohio

Aircraft gas-turbine engines generally operate at shaft speeds ranging from 10,000 to 30,000 rpm. To harness this power and to reduce the engine speed to the desired rpm, the power-transmission industry has been developing high-performance power-transmission systems. A recently completed research addressed the gear-tooth geometry and explored how various design parameters affect gear-tooth bending strength, compressive strength, noise, and vibration.

It was demonstrated and verified, using mechanical and computer models, that gear-cutter geometry has a significant impact on the calculated bending stresses. Using the optimized gear-cutter design technology of this work, the gear designer can reduce the bending stresses by up to 20 percent. This reduction in bending stress is a result of the improved geometry of the tooth fillet, which, in turn, results in a significant improvement in horsepower-per-pound ratio. The results of this work can be summarized as follows:

- A definite relationship exists between the pitting resistance and bending strength of gear teeth. This relationship is controlled by the selected allowable compressive and bending stresses. For high-quality aircraft-type gearing, the various modifying factors used to calculate working stresses have no effect on the relationship between pitting resistance and bending strength, although they may affect the selection of the allowable stresses. The balancing of gear-tooth designs for pitting resistance and bending strength can thereby be accomplished by manipulation of the geometry factors "I" and "J" for pitting resistance and bending strength, respectively.
- Using the new AGMA Standard 218.01 as a guide, computer programs for cal-

PARAMETER VARIATIONS	I	J
Addendum $\frac{1.00}{P_d}$ to $\frac{1.50}{P_d}$	Increase 20%	Increase 45%
Dedendum $\frac{1.40}{P_d}$ to $\frac{1.15}{P_d}$	No Effect	Increase 15%
Pressure Angle 18.5° to 25°	Increase 20%	Increase 35%
Helix Angle 0° to 20°	Increase 50%	Increase 36%
Face-to-Diameter Ratio 0.4 to 1.1	Increase 21%	Increase 50%

The **Gear-Tooth Geometry Factors "I" and "J"** for pitting resistance and bending strength, respectively, are increased by changing the geometry of the tooth fillet.

culating gear-tooth geometry factors "I" and "J" and the mechanical model of the gear-tooth generating machine have been shown to be valid tools for determining geometry factors for modified gear-tooth forms.

- For AGMA standard long/short addendum; i.e., pinion addendum equal to 125 percent of standard and gear addendum equal to 75 percent standard, pitting resistance tends to control the design of external meshes, and bending strength tends to control the design of internal meshes.
- Significant changes in gear-tooth geometry factors "I" and "J" can result when certain gear-tooth design parameters are varied. Increases in the

values of "I" and "J" represent increased capacity for the gear mesh. During this work, one parameter was varied as others were held constant. At a gear ratio of 2.5 to 1, the table summarizes some approximate effects on pinion "I" and "J" as the noted parameters are varied. Improvements in "I" and "J" tend to peak in the range between 15° and 20° for helix-angle variation. Improvement in "I" as listed is for a 15° helix angle.

- In light of the increases which can be accomplished in geometry factors, a transmission design rated at 450 hp (340 kW) could be uprated to 525 hp (390 to 410 kW) using improved gear-tooth-geometry, high-contact-ratio

helical gears of the same size and weight. These gears should run quieter and smoother than the spur-gear system.

This work was done by Dezi Folenta of Transmission Technology Co., Inc., for **Lewis Research Center**. Further information may be found in "Study of Gear

Geometry/High Contact Ratio Affecting High Performance Helicopter Transmissions." To obtain a copy, Circle 16 on the TSP Request Card. LEW-14243

High-Speed Propeller for Aircraft

Engine efficiency will be increased.

Lewis Research Center, Cleveland, Ohio

The advanced high-speed propeller (propfan) extends the cruise speed of conventional turboprop systems from the 0.5- to 0.6-mach range to the mach-0.8 speed range of today's turbofan-powered aircraft. Compared to turbofans, however, the propfan offers a substantial improvement in propulsive efficiency. Fuel savings over advanced high-bypass-ratio turbofan systems are estimated to be 15 to 20 percent (30 to 50 percent over current turbofan systems). Had the domestic fleet of B727, B737, and DC-9 aircraft been replaced with propfan engines in 1981, a total of 3 billion gallons ($1 \times 10^7 \text{ m}^3$) of fuel would have been saved. Examples of propfan-powered transport-aircraft concepts are shown in Figure 1.

The major features of an advanced high-speed turboprop propulsion system are shown in Figure 2. The propeller blades themselves are required to be quite thin and highly swept to minimize compressibility losses and propeller noise during high-speed cruise. The use of 8 or 10 blades with a high-propeller-power loading allows overall propeller diameter to be kept relatively small.

An area-ruled spinner and integrated nacelle shape reduce compressibility losses in the propeller hub region. Finally, a large modern turboshaft engine and gearbox provide power to the advanced propeller.

The propfan system is adaptable to a number of applications, such as high-speed (subsonic) business and general-aviation aircraft, and military aircraft including V/STOL.

This work was done by David A. Sagerser of **Lewis Research Center** and Bernard S. Gatzert of Div. of United Technologies Inc. Further information may be found in NASA TM-83736, [N84-29878/NSP], "Fuel Savings Potential of the NASA Advanced Turboprop Program" [\$10]. A copy may be purchased [prepayment required] from the National Technical Information Service, Springfield, Virginia 22161. LEW-14241



Figure 1. **Typical Transport Airplanes** are shown equipped with the new high-speed propellers.

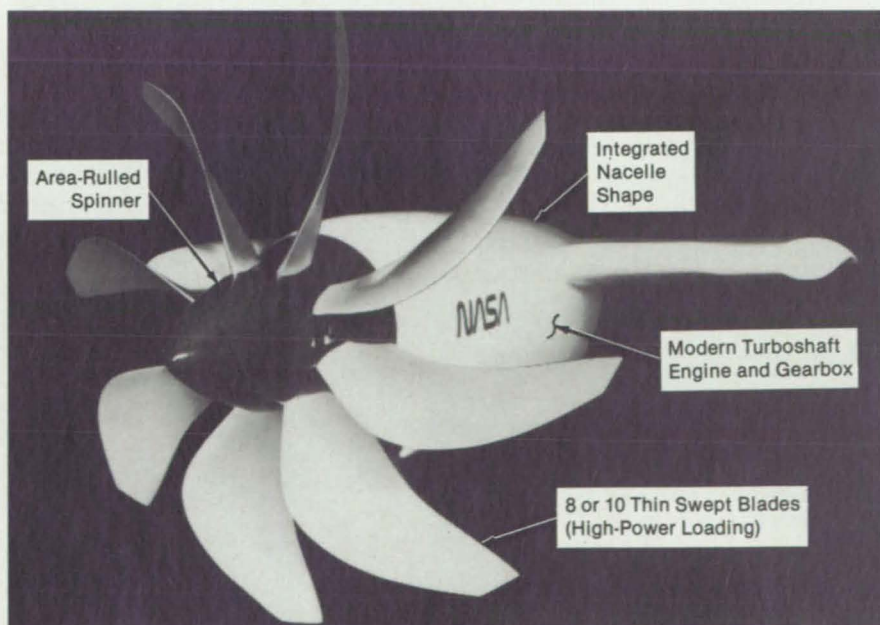


Figure 2. The **Advanced High-Speed Turboprop System**, with the design features indicated here, will increase efficiency. Fuel savings of 30 to 50 percent over present systems are anticipated.

In Mathematical and Statistical FORTRAN Programming **IMSL** Gets You to the Solution **Faster**

There is a faster way to get from problem to solution. A way to reduce development time, simplify maintenance, improve accuracy. A way to measurably increase productivity by selecting from hundreds of complete, fully tested mathematical and statistical FORTRAN subprograms:

IMSL subroutine libraries

Comprehensive, economical, and supported by the world's leading supplier of FORTRAN libraries for mathematics and statistics.

Calling a routine from an IMSL library is faster than writing it. It's a simple fact, but it can mean a big improvement in the productivity of both people and computers. It's why professional problem solvers in more than 60 countries have chosen IMSL libraries as their standard resource for FORTRAN programming. **IMSL libraries get you to the solution faster.**

Return this coupon to:

IMSL Sales Division
2500 ParkWest Tower One
2500 CityWest Boulevard
Houston, Texas 77042-3020, USA.

Telephone: (713) 782-6060
Telex: 791923 IMSL INC HOU

**In the U.S. (outside Texas) call toll-free
1-800-222-IMSL.**

- ☐ The IMSL Library ☐ MATH/PC-LIBRARY
☐ SFUN/LIBRARY ☐ STAT/PC-LIBRARY

Name _____

Department _____

Title _____

Organization _____

Address _____

City _____

State _____

Postal Code _____

Area Code/Phone _____

Telex _____

Computer Type _____

NTB8605

IMSL

Problem-Solving Software Systems

Broad Scope.

IMSL libraries provide the most comprehensive selection of mathematical and statistical FORTRAN subprograms available. In almost any numerical programming application, IMSL libraries will meet your current and future needs with over 700 high-quality subprograms.

Standard User Interface.

Uniform calling conventions and documentation for all supported computer environments make IMSL libraries easy to learn and easy to use. Programs developed using IMSL libraries are much simpler to de-bug and maintain than programs containing undocumented, non-standard or unverified code.

Wide Compatibility.

IMSL libraries are affordably priced and compatible with most computing environments, from supercomputers to personal computers. Making IMSL libraries available on all of your computer systems can expand development flexibility and enhance application portability in your multiple-computer environment.

Comprehensive Support.

IMSL product support includes expert consultation, regular software enhancement, and maintenance. These services are performed entirely by IMSL personnel to ensure quality and consistency. IMSL's systematic, comprehensive support is the best way to protect the value of your software investment.

Accuracy and Reliability.

IMSL subroutines are designed, and exhaustively tested, for accuracy and reliability—and continually verified through thousands of hours of computation by customers around the world. Using IMSL libraries not only increases productivity, but can also enhance the accuracy and robustness of your programs and applications.

The IMSL Library MATH/PC-LIBRARY

Over 500 mathematical and statistical subroutines
Subroutines for mathematical applications (for IBM personal computers)

STAT/PC-LIBRARY

Subroutines for statistical analysis (for IBM personal computers)

SFUN/LIBRARY

Subprograms for evaluating special functions

Pump for Saturated Liquids

Boiling liquids would be pumped by a device based on proven components.

NASA's Jet Propulsion Laboratory, Pasadena, California

A proposed pump is designed to handle boiling liquids. Conventional liquid pumps do not accept liquids at their saturation, or boiling, pressures. The proposed pump would make it unnecessary to pressurize cryogenic liquids in order to pump them. The problems of introducing a noncondensable pressurizing gas could be avoided.

According to the two-phase pumping concept, the saturated liquid flows from a tank to a two-phase nozzle, in which it flashes into a liquid/vapor mixture and impinges on an inclined-plate separator (see figure). The separated liquid flows through a diffuser to a discharge conduit. The separated vapor is compressed and returned to the tank.

If the nozzle, separator, and diffuser have high enough efficiencies and if the nozzle-exit pressure is low enough, the liquid will discharge at a higher pressure than it had in the tank. In addition, it will be cooled to the saturation temperature corresponding to the nozzle-exit pressure.

The two-phase pump, then, produces two important changes: It raises the pressure of the liquid from the tank pressure to a higher discharge pressure, and it creates a net positive-suction head equal to the difference between the discharge pressure and the nozzle-exit pressure. The suction head is a result of both the pressure rise and the temperature drop of the liquid.

Even though the liquid is discharged at a temperature lower than that in the tank, there is no net cooling in the pump: On the contrary, there is net heating. The vapor returned to the tank contains the heat removed from the discharged liquid

plus the heat from the compressor.

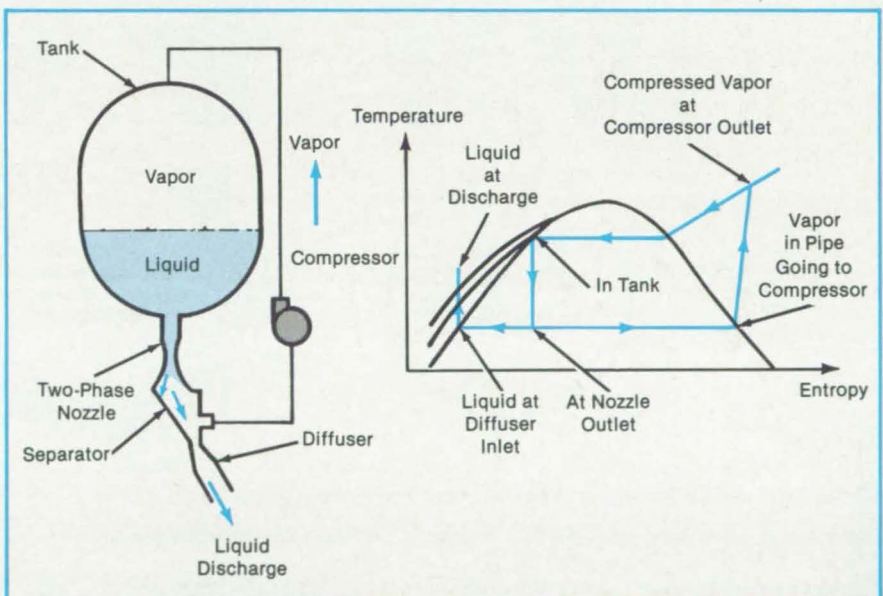
The pump would use the same combination of the two-phase nozzle, separator, and diffuser that were previously used in jet pumps and in liquid-metal magnetohydrodynamics. In those applications, the energy of the liquid leaving the separator was used to do pumping work or electrical work before the liquid entered the diffuser.

Calculations based on representative efficiencies for the nozzle, separator, diffuser, and compressor show that the two-phase pump would perform well. For example, with a tank pressure of 18 lb/in.² (124 kPa) and a nozzle-exit pressure of

5 lb/in.² (35 kPa), it would pump liquid hydrogen to a discharge pressure of 27 lb/in.² (186 kPa). (Pressures are absolute values.)

The two-phase pump is especially attractive for transferring cryogenic liquids from one tank to another. In such transfers, the combination of pressure rise and liquid cooling permits transferring the liquid without venting the receiver tank, thus preventing loss of fluid.

This work was done by David G. Elliott of Caltech for NASA's Jet Propulsion Laboratory. For further information, Circle 10 on the TSP Request Card. NPO-16152



Expanding a Saturated Liquid in a nozzle and diverting its phases along separate paths in a liquid/vapor separator raises the pressure of the liquid. The liquid is cooled in the process.

Receptacle for Optical-Fiber Scraps

Small pieces of glass are trapped by moving air.

John F. Kennedy Space Center, Florida

A safety device holds small scraps of glass optical fibers until disposal. The scraps are cleaved and broken pieces produced during splicing and other manufacturing operations. These scraps are hazardous:

Made of clear glass and typically only 125 μm in diameter, they penetrate the skin easily and are difficult to see to remove. Previously, the pieces were stored until disposal on the adhesive sides of tape

strips. However, the scraps are extremely light in weight and do not adhere well; after the tape becomes loaded, additional fibers do not contact the adhesive.

The device (see figure) traps the fibers in

a section of black air-conditioner filter material. The filter section rests on a metal screen above an axial fan, which pulls air down through the filter. The fan is a small, quiet unit of a type ordinarily used to cool electronic equipment.

The filter is held in a section of polyvinyl chloride (PVC) pipe having a diameter of 3 in. (7.6 cm). Air is exhausted through triangular gaps cut in the bottom of a similar piece of pipe below the motor. Phenolic transition gaskets are placed between the

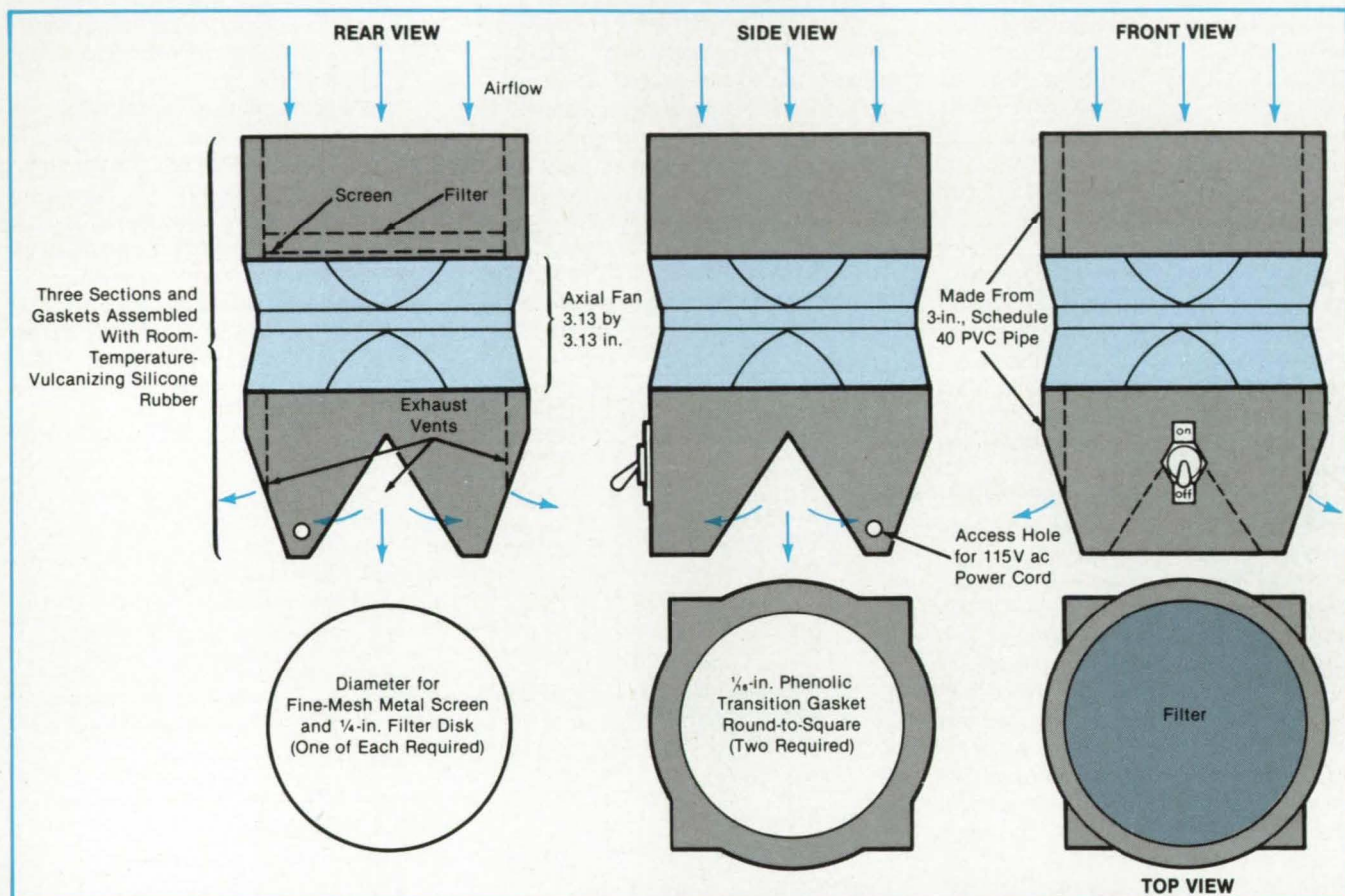
round pipe and the motor, which has a square outline. Although round pipe was used to construct the prototype units, square pipe could also be used, thereby eliminating the need for the transition gaskets.

During manufacturing operations, the fiber scraps are dropped on the filter with tweezers. The moving air retains the fibers in the filter. The filter is lifted out to dispose of the fiber scraps, then replaced in the unit. As an added benefit, the exhaust from

the bottom of the unit is convenient for drying fibers that have been cleaned in acetone.

This work was done by R. O. Nevin of Lockheed Space Operations Co. for Kennedy Space Center. No further documentation is available.

Inquires concerning rights for the commercial use of this invention should be addressed to the Patent Counsel, Kennedy Space Center [see page 29]. Refer to KSC-11326.



A Small Fan Pulls Air Through a Filter to trap broken pieces of glass fiber. The unit is inexpensive and assembled from readily available parts.

Thermally-Integrated Fuel-Cell/Electrolyzer Systems

The design is less complex and more reliable than prior designs.

Lewis Research Center, Cleveland, Ohio

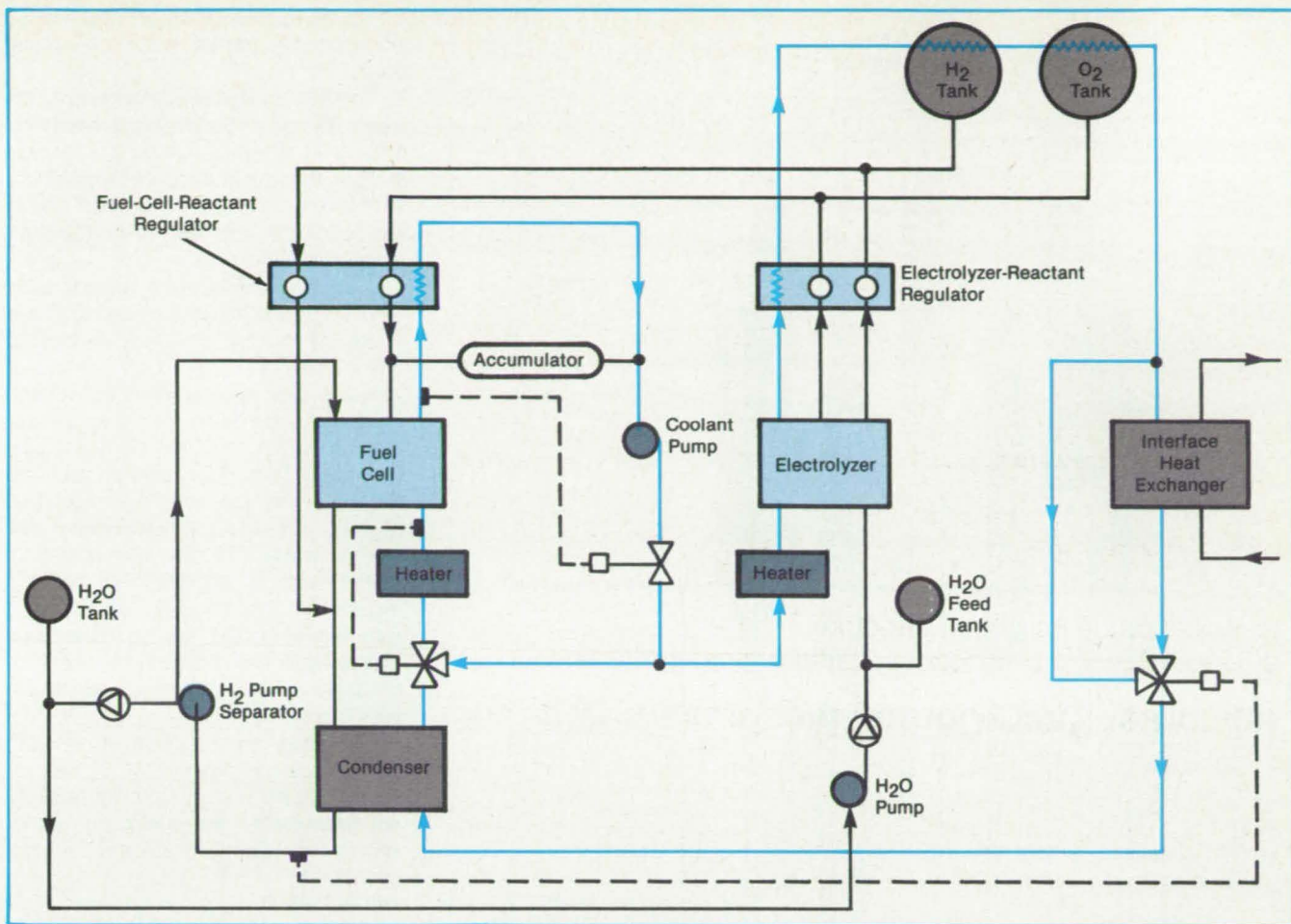
A new and more efficient method of thermally integrating a fuel cell and an electrolyzer has been designed. This design addresses the thermal integration of a fuel cell and a water electrolyzer in a regenerative fuel-cell system.

Since the operation of the regenerative fuel-cell system involves the alternate activation of the fuel cell and the electrolyzer, the individual cells must be cooled while they are operating, and then

heated, while idle, to maintain them at operating temperature. Previous system concepts had a coolant loop for each stack with a heat exchanger between them for the required heat transfer. This is a system configuration (see figure) that provides this thermal integration with a single coolant loop. This configuration does not have the thermal limitations associated with trying to transfer heat between two coolant loops.

A single-loop system has the benefit of fewer components than a two-loop system, and therefore is less complex and more reliable. This is adaptable to stand-alone power systems in conjunction with solar panels for remote-area applications.

This work was done by J. Garow, K. Michaels, and R. Martin of United Technologies Corp. for Lewis Research Center. No further documentation is available. LEW-14235



The **Thermally-Integrated Fuel-Cell/Electrolyzer System** uses a single coolant loop.

Hydraulic Actuator for Ganged Control Rods

One device moves multiple elements synchronously.

NASA's Jet Propulsion Laboratory, Pasadena, California

A proposed hydraulic actuator would move several nuclear-reactor control rods in unison. The actuator would be simpler than a single electric-motor mechanism for operating the ganged rods. It would not only be simpler, lighter, and more compact than individual rod actuators but would also be easier to synchronize. Conceived for use aboard spacecraft, the actuator principle could be applied to terrestrial hydraulic machinery involving the motion of ganged rods.

The actuator would ensure that the control rods are inserted in the reactor during launch, that they are withdrawn when the reactor is in space, and that they re-enter the reactor, when necessary, if the system malfunctions. The actuator thus would prevent the reactor from going critical if the spacecraft should

fall into a body of water after an aborted launch. It would then allow the reactor to start producing power when the spacecraft is safely started on its mission and would interrupt power generation in an emergency.

The conceptual actuator consists of an electromagnetic pump and a set of seven hexagonal tubes, one tube surrounding each of the hexagonal control rods (see figure). Depending on the direction of flow, liquid lithium forced through the tubes by the pump provides the pressure to push the tubes out of the reactor, to maintain them out of the reactor, and to return them to the reactor.

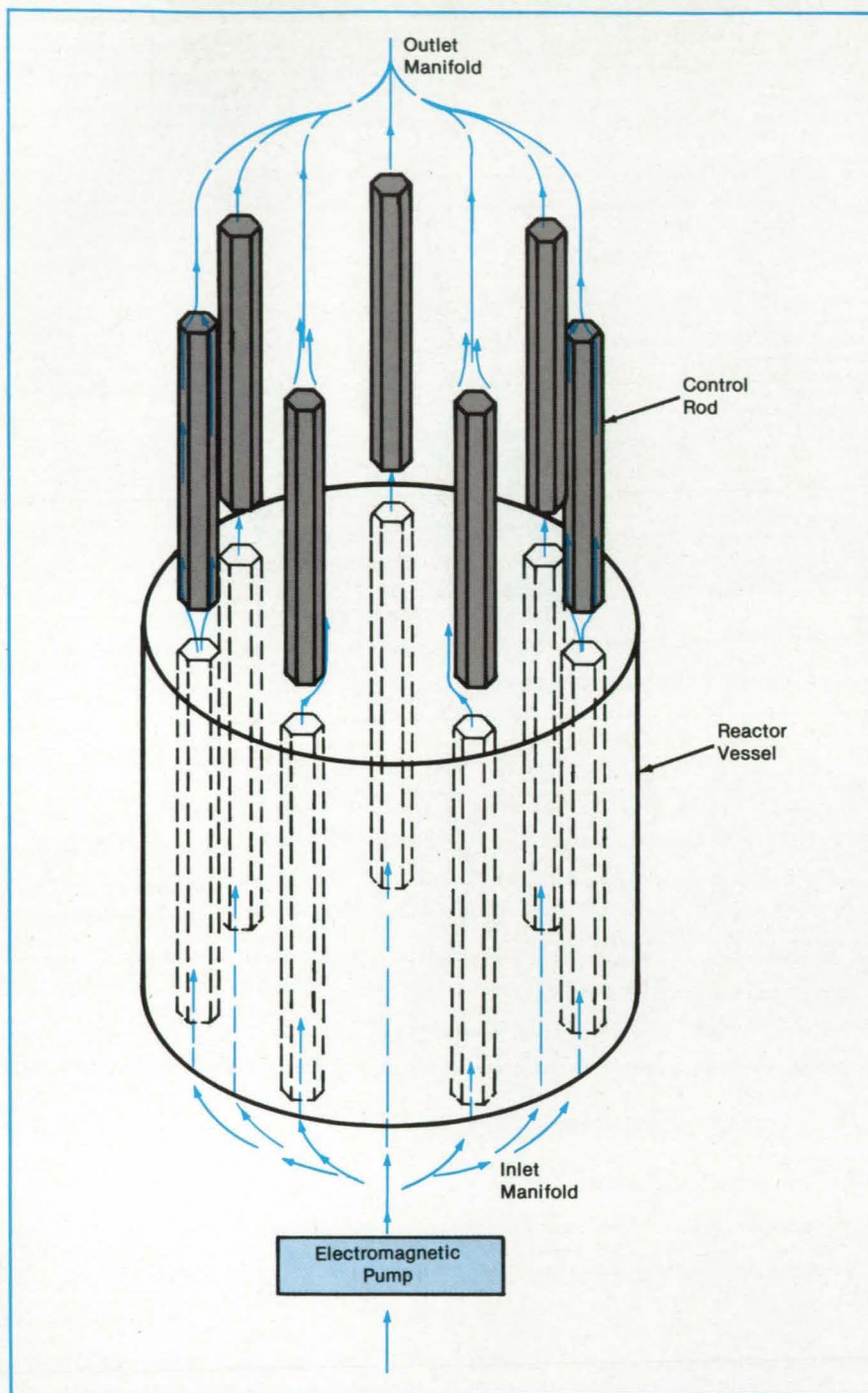
When the reactor is turned off, the rods are within the core and are mechanically held there against inertial forces. The electromagnetic pump does not operate at that time. The lithium in

the tubes and pump is kept liquid by the heat transferred to it from an auxiliary radioisotope thermoelectric generator.

When the time comes to start up the reactor, the auxiliary power source drives the electromagnetic pump, which builds up pressure against the ends of the rods in the reactor. The pressure overcomes the mechanical rod restraints and moves the rods out of the reactor. The reactor then develops a self-sustaining reaction.

The rods are held in their withdrawn position by the force of the flowing lithium. In zero gravity, this force could be low.

To shut the reactor, the direction of the electromagnetic pump is reversed. The lithium, now flowing in the opposite direction, pushes the rods back into the reactor and holds them there. The rods



inhibit the nuclear reaction and reduce the reactor output to below the critical level.

The flowing lithium performs an additional function: Besides operating the rods, it removes heat from the reactor, thereby helping to keep its temperature at the required value. The lithium cools the reactor in both the forward and reverse directions of flow.

The lithium enters the reactor by a single pipe and leaves it by a single pipe. Inside the reactor, a manifold divides the lithium flow into the seven control-rod tubes, and a second manifold recombines the tube flows into a single exit flow. The fact that the individual pipe flows may be slightly different and that the rods may therefore be moved at slightly different speeds, does not adversely affect the shutdown operation. The system is designed so that the slowest rod is fast enough. Moreover, as the rods seat, the flow in their tubes drops, and more pressure becomes available to drive the remaining moving rods more rapidly.

This work was done by Dennis C. Thompson and Robert M. Robey of Westinghouse Electric Corp. for NASA's Jet Propulsion Laboratory. For further information, Circle 14 on the TSP Request Card. NPO-16503

The **Electromagnetic Pump** pushes liquid lithium against the ends of control rods, forcing them out of or into the nuclear reactor. Color arrows show the lithium flow for reactor startup and operation. The flow is reversed for shutdown.

Ignition System for Gaseous Propellants

A spark plug in a fuel-injection manifold resists corrosion and allows efficient combustor cooling.

Marshall Space Flight Center, Alabama

Installation of the spark plug in the fuel-injection manifold of a coaxial injector (see figure) promotes a more efficient cooling of combustor walls in rocket and turbine engines. The spark plug is not subjected to the erosion and contamination

that occur in the combustion chamber.

Simple in concept and inexpensive, spark discharge reliably ignites gaseous fuels, especially gaseous hydrogen with gaseous or liquid oxygen. Normally a

spark plug is placed so that its tip is at the combustor wall far enough downstream of the injector face to be exposed to partially or fully mixed gases. The exposure to combustion temperatures causes erosion of the uncooled plug. When the com-

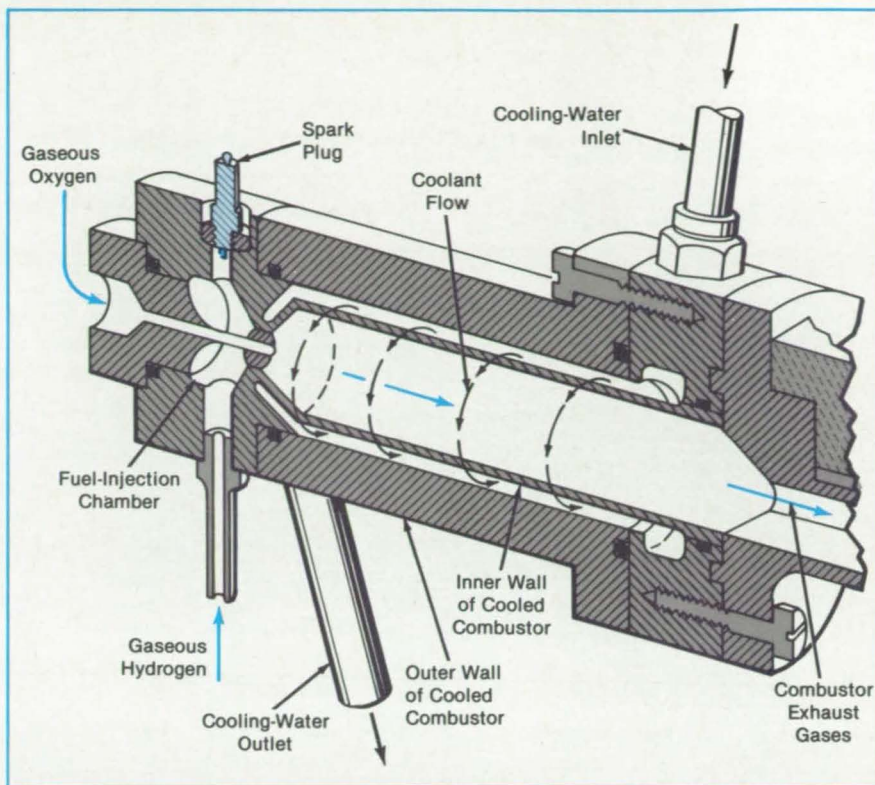
bustor walls must be cooled by a fluid, the presence of the spark-plug port impedes the effectiveness of the coolant.

With the spark plug located in the fuel-injection manifold, the ignition sequence begins with the introduction of gaseous oxygen through the central oxygen tube at the main operating flow rate, followed by sparking and the introduction of gaseous hydrogen through an entry port in the side of the fuel-injection manifold.

At first, gaseous oxygen fills both the combustor and the fuel-injection manifold. When the main fuel valve is opened, the hydrogen mixes with the oxygen and purges it from the fuel-injection manifold. During this expulsion, ignition occurs when an interface of mixed flammable gases passes across the spark discharge. Then the flaming interface of mixed gases, with gaseous oxygen being pushed ahead of it and with gaseous hydrogen following it, passes from the fuel-injection manifold, through the annular fuel-injection port and into the main combustor.

As the interface contacts the oxygen stream of the central oxygen tube, ignition occurs at the injector face and is sustained by the propelling hydrogen fuel. During the sustained combustion, the spark-plug tip remains cool and clean. Without a spark-plug port, the main combustor can be cooled efficiently.

Eighteen tests have proven this injector design; no ignition failures occurred in 8,000 seconds of operation with gaseous



After Ignition Occurs in the Fuel Injector, combustion is maintained in the cooled main combustor leaving the spark-plug tip in a cool, clean environment.

oxygen and hydrogen. The system can also be used with other propellants that are gaseous in the ignition phase.

This work was done by Richard A. Pieron of Rockwell International Corp. for

Marshall Space Flight Center. For further information, Circle 73 on the TSP Request Card.
MFS-29125

Rigid/Compliant Helicopter Rotor

The rotor structure ensures both effective aerodynamic support and efficient pitch changes.

Ames Research Center, Moffett Field, California

A conceptual helicopter rotor design includes blade-root structures that are rigid in flexure but compliant in torsion. The four blades are shells with rigid inner I-beam arms that are integrated with the rotor hub. Through each blade, a control arm extends from a pitch-control actuator in the hub (see figure). Elastomeric bearings allow the control arms to twist the blades and thus change the blade pitch without turning the I-beam arms. Centrifugal force is carried by a tension strap. Leading and lagging movements of the blades are restrained by dampers. Ducts inside the leading and trailing edges of the blade shells carry air for partial cyclic aerodynamic control of lift and pitch.

The pitch of the blades is varied collectively by synchronized rotation of the actuator arms on the hub at the blade roots,

which apply torsion to the blades. The tension straps offer negligible restraint to torsion and thus allow the actuator arms to twist the blades freely. If an actuator arm should fail, a redundant arm at the root of the same blade provides continued control and support. The redundant arm and bearings are normally separated by a small gap but make contact when a failure occurs.

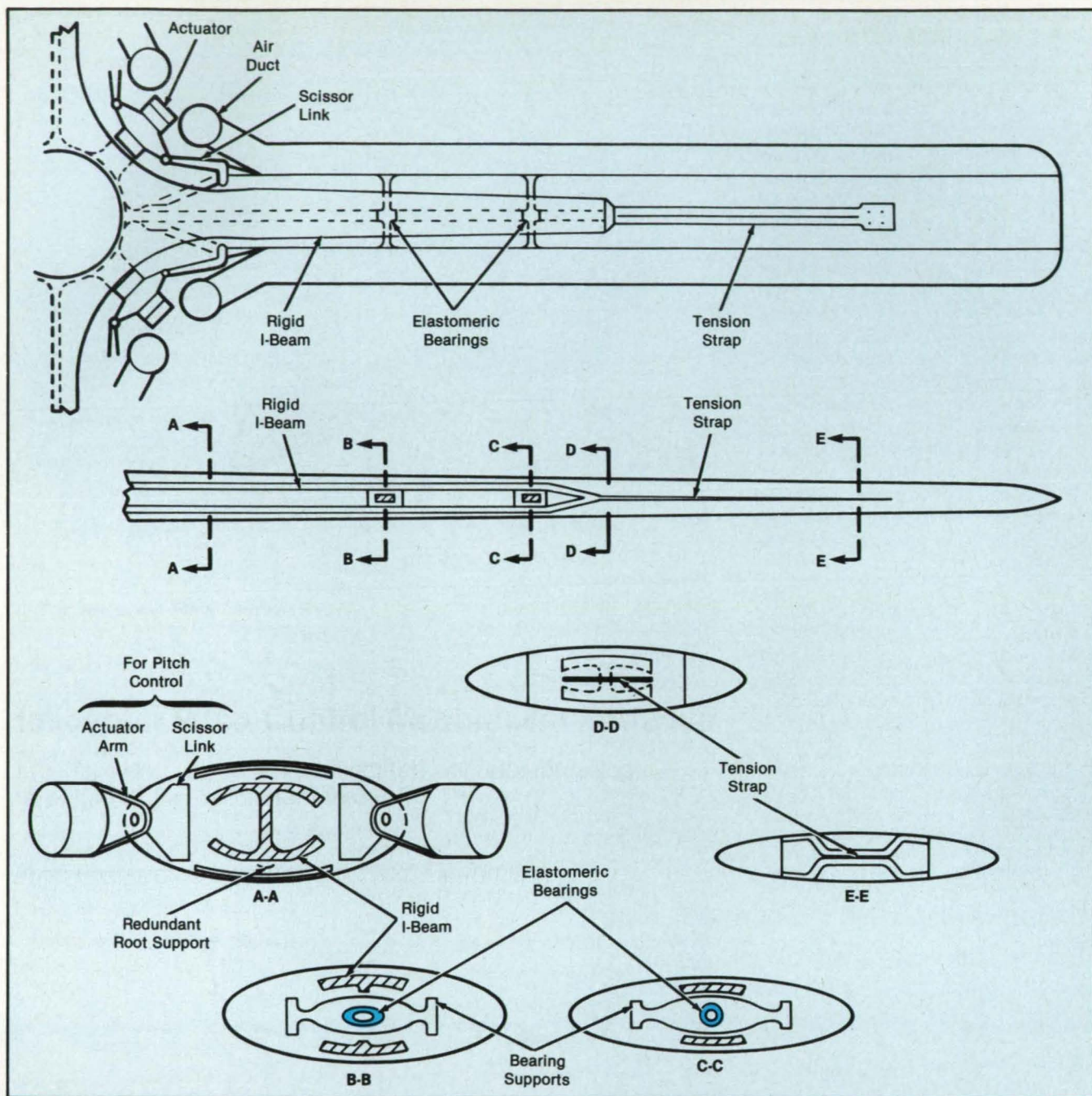
Because the control arms support the blades at their roots, root bearings are not needed. Neither are thrust bearings needed, because the tension straps resist the centrifugal force. Because the blades can be twisted without twisting their I-beam arms, control forces are reduced. Moreover, because root bearings are not used and more space is therefore available at the roots, the

I-beams can be designed to resist loads more efficiently.

This work was done by P. Jeffery of United Technologies Corp. for Ames Research Center. Further information may be found in NASA CR-166399 [N82-32341/NSP], "Rotosystems Research Aircraft Vertical Drag Test Report."

Copies may be purchased [prepayment required] from the National Technical Information Service, Springfield, Virginia 22161, Telephone No. (703) 487-4650. Rush orders may be placed for an extra fee by calling (800) 336-4700.

Inquiries concerning rights for the commercial use of this invention should be addressed to the Patent Counsel, Ames Research Center [see page 29]. Refer to ARC-11518.



The **Top, Sides, and Cross Sections** show details of the torsionally compliant, flexurally rigid rotor. The structure permits more efficient pitch control with less weight. At the same time, it improves reliability through redundancy in supports and control mechanisms.

Helicopter Pitch-Control Mechanism Reduces Vibration

Large forces could be accommodated without increasing the weight of the helicopter structure.

Ames Research Center, Moffett Field, California

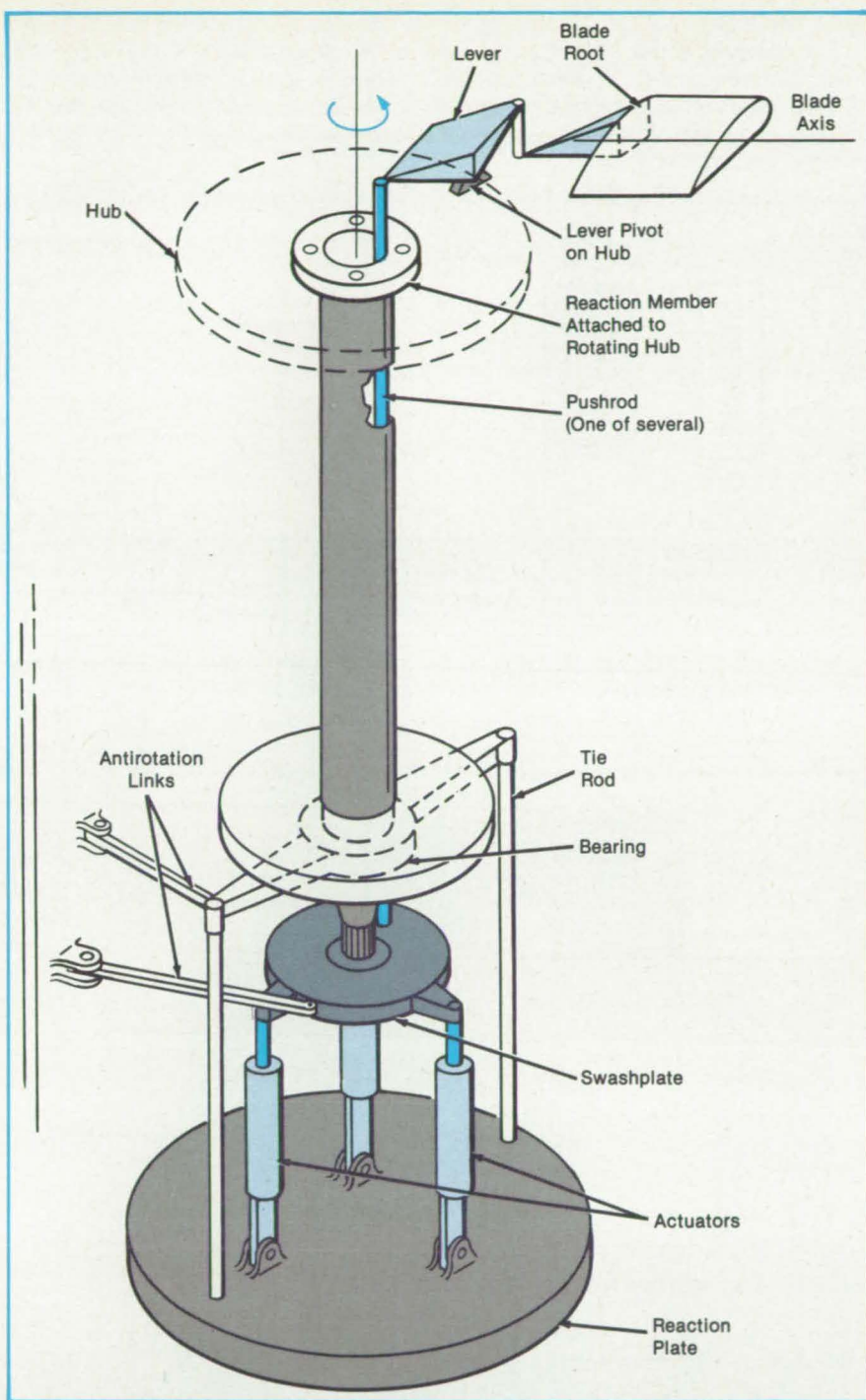
A proposed pitch-change mechanism for a helicopter rotor can prevent large control reaction forces from being applied to the gearbox or fuselage. The new mechanism would yield stiffer control and improve the accuracy of pitch changes under load. As a

result, a heavy casting would not be needed for the gearbox, nor extra reinforcing members would be needed for the fuselage bulkheads, stringers, skin, and other parts. Distortion of the gearbox and consequent gear deflections would be avoided. In addition,

the helicopter parts would be protected from the fatigue and early failures caused by the variable, cyclic nature of control forces.

The mechanism was developed for the "X-wing" aircraft, which employs a stiff rotor with four blades. Compressed air is blown

NASA Tech Briefs, May/June 1986



Reaction Forces for This Pitch Control Mechanism are provided in the rotor hub rather than in the fuselage or gearbox. Control forces are transmitted to the hub through the reaction plate and reaction member.

through slots in the leading and trailing edges of the blades for partial cyclic and collective pitch control. Additional mechanical collective pitch control is required for trimming the blades during hovering and high-speed fixed-wing flight. However, reaction loads for mechanical collective pitch control are quite high — about 60,000 lb (270,000 N). Without the new mechanism, the excess structural weight for resisting such loads would be prohibitive.

In the proposed mechanism, reaction forces are developed in the rotor hub. Long load paths to the gearbox and fuselage, as in previous helicopters, are eliminated. A reaction member is rigidly attached to the hub and rotates with it (see figure). At the lower end of the reaction member, a bearing forms a bridge to the fuselage through a stationary beam and an antirotation link. The beam is connected to a reaction plate through the rods.

Control actuators and a control swashplate, which can slide on the reaction member and tilt, are mounted on the reaction plate. An antirotation link secures the swashplate. Pushrods connect the swashplate through the reaction member to the rotor hub. At the hub, levers, links, and pitch arms connect the pushrods to the blades.

*This work was done by H. Lemont of United Technologies Corp. for **Ames Research Center**. Further information may be found in NASA CR-166399 [N82-32341/NSP], "Rotosystems Research Aircraft Vertical Drag Test Report."*

Copies may be purchased [prepayment required] from the National Technical Information Service, Springfield, Virginia 22161, Telephone No. (703) 487-4650. Rush orders may be placed for an extra fee by calling (800) 336-4700.

Inquiries concerning rights for the commercial use of this invention should be addressed to the Patent Counsel, Ames Research Center [see page 29]. Refer to ARC-11513

Controlled-Temperature Hot-Air Gun

Materials are tested before installation in wind tunnels.

Lyndon B. Johnson Space Center, Houston, Texas

Materials that may find applications in wind tunnels are first tested in the laboratory with the setup shown in the figure. Resembling an elaborate but carefully regulated hot-air gun, the setup is used to

NASA Tech Briefs, May/June 1986

apply blasts of air at temperatures above 1,500 °F (815 °C) to the test specimens.

A typical test sequence is the following:

- The shop air supply is turned on at

gauge 1.

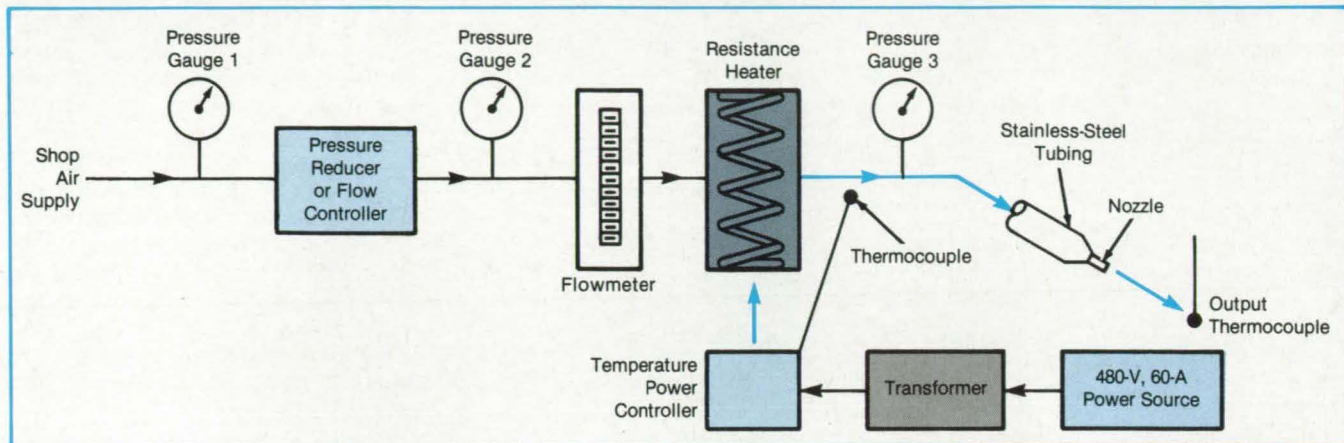
- The heater power is turned on and adjusted to obtain approximately the desired temperature at a thermocouple near the nozzle.

- The pressure is adjusted at gauge 2 to "fine tune" the output temperature.
- Further fine adjustments of the pressures, temperatures, and flow are made until the conditions in the air blast just outside the nozzle are those at which a

specimen is to be tested.

The specimen is mounted on a tripod-supported stand, the top of which can be slanted. The slant angle is adjusted for the required angle between the air blast and the specimen surface.

This work was done by Max C. Munoz of Rockwell International Corp. for Johnson Space Center. For further information, Circle 85 on the TSP Request Card.
MSC-20693



The **Hot-Air Gun** differs from commercial units in that the flow rate and temperature are monitored and controlled. With a typical compressed-air-supply pressure of 25 to 38 psi (170 to 260 kPa), the flow rate and maximum temperature are 34 stdft³/min (0.96 stdm³/min) and 1,090 °F (590 °C), respectively.

Adjustable Tooling for Bending Brake

Deep metal boxes and other parts are easily fabricated.

Lyndon B. Johnson Space Center, Houston, Texas

An adjustable tooling jig for a bending brake accommodates spacing blocks and either a standard male press-brake die or a bar die. By increasing the free space available for bending sheet-metal parts, the jig makes it easier to fabricate such items as deep metal boxes or brackets with right-angle bends.

As shown in Figure 1, the jig is interposed between the press brake and one of the press-brake dies — in this case, the male die. Spacer blocks are fabricated to the required dimensions as needed by cutting them from metal scraps.

To make deep metal boxes, the jig is used in the configuration of Figure 1 (spacer-block mode). A typical forming operation in this mode is shown at the top of Figure 2.

To fabricate smaller parts with multiple right-angle bends, the window-die mode is used. In this configuration, the press-brake die is removed from the bottom of the jig, and a round or square bar is clamped between the upper and lower 90° grooves. The bar then serves

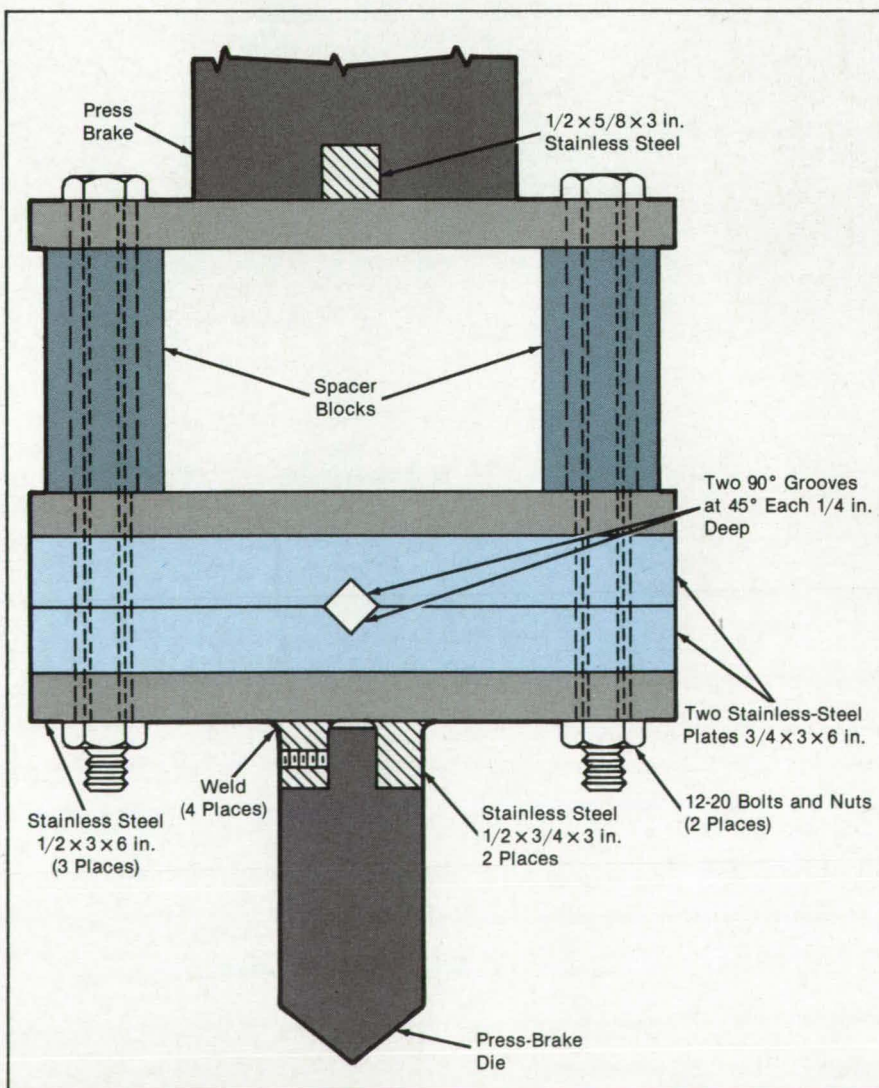
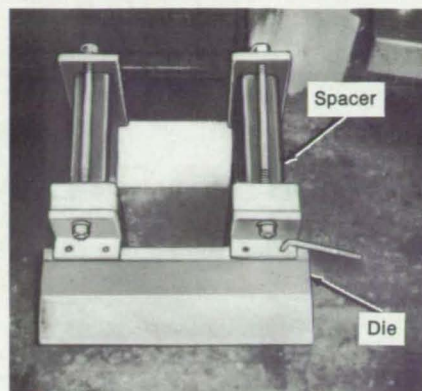


Figure 1. The **Adjustable Tooling Jig** holds spacer blocks, a press-brake die, a bar window die, or a combination of the three.

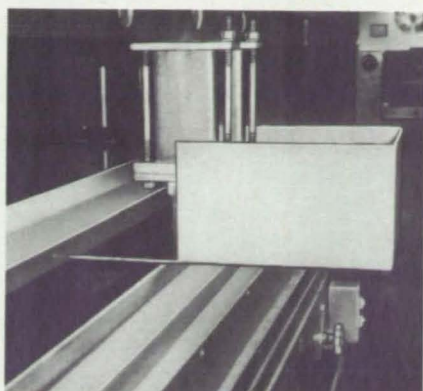
as the male bending die, cooperating with a female die consisting of a grooved block placed on the lower press-brake surface.

A forming operation in the window-die mode is shown in the lower half of Figure 2.

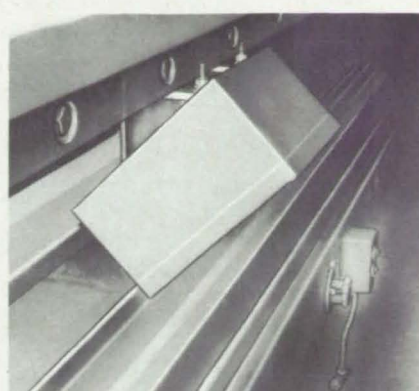
This work was done by James M. Ellis of Johnson Space Center. No further documentation is available. MSC-20730



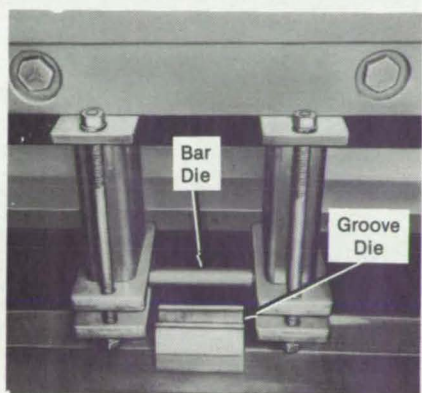
JIG BEFORE INSTALLATION



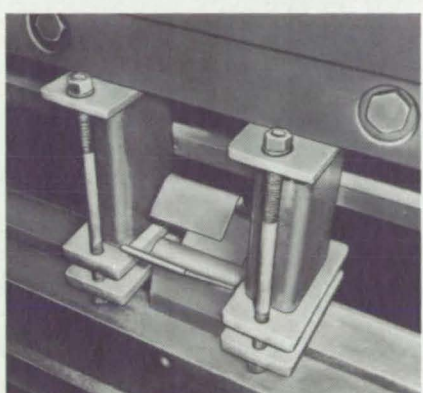
**JIG INSTALLED:
ABOUT TO MAKE A BEND**



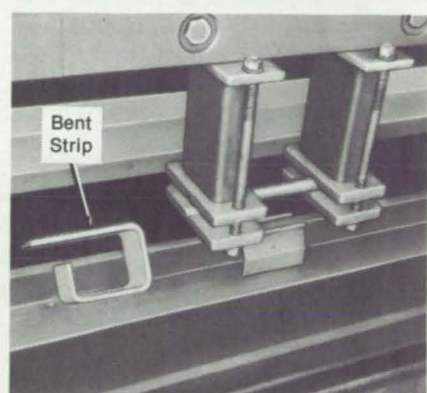
BEND COMPLETED



**JIG IN PLACE:
STRIP NOT YET INSERTED**



STRIP BEING BENT



**BENT STRIP REMOVED
FROM DIES**

Figure 2. **Typical Bending Operations** include the bending of a cut metal sheet into a box (above) and the bending of a metal strip into a bracket with multiple inward 90° bends (below).

Books and Reports

These reports, studies, and handbooks are available from NASA as Technical Support Packages (TSP's) when a Request Card number is cited; otherwise they are available from the National Technical Information Service.

Orbital-Transfer Vehicle With Aerodynamic Braking

The vehicle would include an airbrake for deceleration into a lower orbit.

A report describes a proposed vehicle for carrying payloads between low and high orbits around the Earth. The vehicle would use the thin, upper atmosphere for braking when returning to a low orbit. Since less propellant would be needed than would be required for full retrorocket braking, the vehicle could carry a larger

NASA Tech Briefs, May/June 1986

payload and therefore reduce the cost of space transportation.

Unlike previously proposed aerobraking orbital transfer vehicles (AOTV's), it would be an integrated structure in which supports for the aerobrake, the rockets, the fuel tanks, and other subsystems are shared to obtain more efficient use of structural elements and therefore smaller mass.

The aerobrake surface would be a wide-angle cone of elliptical cross section, with a toroidal skirt and an apex blunted to an ellipsoid. It would be made of aluminum with a rigid thermal-protection layer. During braking, it would shield the rockets, tanks, and payload like an umbrella in the wind. The structure would be assembled in space and could be used many times to carry payloads in both directions between low Earth orbit and space stations. Once assembled, the vehicle would not return to the surface of the Earth, but would exchange payloads with the Space Shuttle in orbit.

The report covers such topics as aerodynamics, propulsion, structural mass,

aerobrake heating, thermal protection, and vehicle performance. In a section on technology improvements, the report notes that certain advances would lead to improved design and performance. Engines with greater specific impulse, for example, would reduce the masses of the tank and propellant. The development of composite structural elements would reduce mass without decreasing strength and rigidity. The use of fabric or soft insulation would reduce mass while improving strength and heat resistance.

This work was done by Carl D. Scott, Kornel Nagy, Barney B. Roberts, Robert C. Ried, Kenneth Kroll, and Joe Gamble of Johnson Space Center. To obtain a copy of the report, "Design Study of an Integrated AOTV Concept," Circle 77 on the TSP Request Card.

This invention is owned by NASA, and a patent application has been filed. Inquiries concerning nonexclusive or exclusive license for its commercial development should be addressed to the Patent Counsel, Johnson Space Center [see page 29]. Refer to MSC-20921.

Algorithm for Calibrating Robot Arms

Robots can be made to less demanding specifications and yet be more accurate.

A software-based calibration method for robots increases the accuracy with which manipulators are positioned. The method, described in a published paper, can be used on any serial-link robot with any combination of revolute and prismatic joints.

The method increases the accuracy of positioning the manipulator at any point in the workspace relative to a fixed coordinate system. Accurate absolute positioning capability is particularly useful for those tasks where the robot is issued a target location by external sensory devices, such as a vision system. With the new method, ultraprecise manufacturing and high-resolution measurements of robot components are unnecessary. The method therefore reduces the cost of robots in addition to increasing robot accuracy.

This method is based on a study of the geometric relationships among the robot joints and links, error parameters, and position-sensor measurements. Matrix/vector equations are derived to express the transformations between the robot-link and stationary reference frames. The resulting algorithm and computer program provide a means with which the geometric link parameters are estimated. The singularities which arise from using the Denavit-Hartenberg parameters for parallel or near parallel consecutive joint axes are avoided by definition of a new set of link parameters.

The simulation part of the program sets up a mathematical model of the robot to be calibrated and tests the performance of the calibration method. The inputs to the simulation part include the link-parameter biases, joint-state variable-measurement errors, and end-point measurement-error statistics. The program then causes the computation of the nominal and actual end-point positions for several joint-state configurations. The eventual result of the simulation is a comparison of how well the biases are estimated. The simulation part of the program can also be used to interpret the results of a calibration.

The calibration part is similar to the simulation part. The manipulator is moved to a designated point, and the state variables and end-point position are measured. The computer calculates new bias values from these measurements. The program causes this procedure to be

repeated until there is no further improvement in the accuracy of the estimates of the end-point positions.

After deriving the calibration equations and algorithm, the paper describes the software and gives examples of its use with two types of robots: the Puma 600 and the Stanford Arm. The numerical results of simulations on these robots show that the calibration technique can improve the absolute positioning accuracy of serial-link manipulators using only end-point measurements.

This work was done by Samad A. Hayati of Caltech and Majdedin Mirmirani of California State University, Los Angeles for NASA's Jet Propulsion Laboratory.

To obtain a copy of the paper, "A General Software for Robot Geometry Calibration," Circle 53 on the TSP Request Card.
NPO-16569

Overcoming Robot-Arm Joint Singularities

Kinematic equations allow an arm to pass smoothly through a singular region.

A report discusses mathematical singularities in the equations of robot-arm control. An operator commands a robot arm to move in a direction relative to its own axis system by specifying a velocity in that direction. This velocity command is then resolved into individual-joint rotational velocities in the robot arm to effect the motion. However, the usual resolved-rate equations become singular when the robot arm is straightened.

One solution is simply to avoid the singular position of the robot arm; but in using resolved-rate equations, the operator's commands to move the arm as desired may cause the arm to pass inadvertently through a singularity. Erratic motion may result until the arm moves sufficiently far from the singularity. To overcome this elbow-joint singularity, a new set of kinematic rate equations has been developed to allow continued translational control of the robot hand, even though the robot arm is fully, or almost fully, extended.

These kinematic equations, instead of the regular resolved-rate equations, can be used to translate the robot hand in the neighborhood of the singularity. The kinematic equations give the operator the option to bend the robot arm at the elbow in either the up or down position. The operator simply extends the arm and backs it up again to reverse automatically the direction of the elbow bend (a difficult maneuver for the usual resolved-rate equations).

The equations were applied to move a

graphically-simulated robot arm, and the desired motions were successfully obtained. Finally, two integration methods (Euler and Adams-Bashforth second-order predictor) were compared for three integration-step sizes (1/16-, 1/32-, and 1/64-s) with little or no differences seen in either set of tests. It therefore appears that a user constrained in the area of computer power could take advantage of the simpler Euler-integration scheme with a step size of 1/16 s, but this decision would depend on the specific situation.

This work was done by L. Keith Barker and Jacob A. Houck of Langley Research Center and Susan W. Carzoo of Sperry Corp. Further information may be found in NASA TP-2376 [N85-15446/NSP], "Translational Control of a Graphically Simulated Robot Arm by Kinematic Rate Equations That Overcome Elbow Joint Singularity" [\$8.50]. A copy may be purchased [prepayment required] from the National Technical Information Service, Springfield, Virginia 22161.
LAR-13415

Theory and Tests of Two-Phase Turbines

New turbines open the possibility of new types of power cycles.

A report describes the theoretical analysis and experimental testing of two-phase impulse turbines. Such turbines open the possibility of new types of power cycles operating with extremely wet mixtures of steam and water, organic fluids, or immiscible liquids and gases. Possible applications are geothermal power, waste-heat recovery, refrigerant expansion, solar conversion, transportation, and engine-bottoming cycles. Potential advantages over conventional vapor cycles in these applications are the more effective use of the energy in such hot liquids as geothermal fluids, better matching to sensible-heat sources, lower shaft speeds, and the flexibility of operating without the restriction of dry-vapor expansion.

The two-phase turbines were tested with water-and-nitrogen mixtures and with Refrigerant 22 (CHClF₂). Nozzle efficiencies were 0.78 (measured) and 0.72 (theoretical) for water-and-nitrogen mixtures at a water/nitrogen mixture ratio of 68 by mass and were 0.89 (measured) and 0.84 (theoretical) for Refrigerant 22 expanding from 0.02 quality to 0.28 quality, where "quality" is defined as the ratio of vapor mass to total mass in a local fluid sample. The theoretical velocities are lower than those measured, probably because of an overestimation of drop size.



Blade efficiencies (shaft power before windage and bearing loss divided by nozzle jetpower) were 0.63 (measured) and 0.71 (theoretical) for water-and-nitrogen mixtures and 0.62 (measured) and 0.63 (theoretical) for Refrigerant 22 with a single-stage turbine and were 0.70 (measured) and 0.85 (theoretical) for water-and-nitrogen mixtures with a two-stage turbine. The measured rotor efficiencies are 10 to 15 percent below the calculated values because of sideways spreading of the liquid on the blades and retention of a liquid film by the blades. It is not known whether these losses can be reduced or whether they are fundamental limitations.

Although the efficiency of single-stage two-phase turbines will be only about 50 percent, this is sufficient for replacing the throttling steps in geothermal plants, refrigeration systems, and other systems that use irreversible flashing processes. However, it is problematic whether the value of the added energy output will offset the cost of the turbine and associated equipment. To compete with vapor turbines, a two-phase turbine must have an efficiency of more than 65 percent — about the upper limit of efficiency for two-phase turbines, and probably attainable only with organic working fluids.

In sum, two-phase turbines appear promising in organic-fluid waste-heat or geothermal binary cycles where there is a significant thermodynamic advantage in using saturated-liquid expansion and where the flow conditions are conducive to the best two-phase turbine efficiency. Two-phase turbines using steam and water expanding to the low pressures required in most applications, such as geothermal, may be ruled out by low efficiency and possibly erosion.

This work was done by David G. Elliott of Caltech for **NASA's Jet Propulsion Laboratory**. Further information may be found in NASA CR-168834 [DE82013037], "Theory and Tests of Two-Phase Turbines" [\$14.50]. A copy may be purchased [prepayment required] from the National Technical Information Service, Springfield, Virginia 22161. NPO-16039

Crash Tests of Protective Airplane Floors

Energy-absorbing floors reduce structural buckling and the impact forces on occupants.

A 56-page report discusses crash tests of energy-absorbing aircraft floors. It describes the test facility and procedures; the airplanes, structural modifications, and seats; the crash dynamics; the floor

NASA Tech Briefs, May/June 1986

and seat behavior; and the responses of anthropometric dummies seated in the airplanes. The report also presents plots of the accelerations, photographs and diagrams of the test facility, and photographs and drawings of the airplanes before, during, and after testing.

Three six-place, low-wing, twin-engine airplanes were crashed under controlled free-flight conditions. One airplane had a conventional floor. Each of the other two airplanes was modified to incorporate one of two load-limiting (energy-absorbing) subfloors.

The modified portion of the subfloor structure extended from the main wing spar to aft of the rear cabin door. The upper floor panel was not changed, but the keel beams, bulkheads, stringers, and lower contour skin were removed. These were replaced, in one case, by a corrugated-beam, notched-corner subfloor structure, in the other, by a flat-beam, notched-corner subfloor structure.

All airplanes were allowed to strike a concrete surface at a speed of about 37 meters per second and at an angle of 15°. In each case, the airplane struck the ground squarely on its bottom (at a pitch angle of 0°) with the landing gear retracted.

The lowest floor accelerations and the least seat crushing — as well as the greatest subfloor crushing — occurred in

the modified airplanes. The most effective of the two energy-absorbing subfloors was the corrugated-beam, notched-corner structure. This subfloor reduced the peak deceleration at the seats to the range of 25 to 30 times the gravity, as compared with a range of 40 to 55 times the gravity for the unmodified airplane. The structural crushing of the energy-absorbing subfloors minimized the upward heave of the cabin floor.

Crash pulses — the normal transverse and longitudinal acceleration histories — were recorded on five seated dummies and at various points on the structure. The accelerations on the dummies generally reflected the same trends as the accelerations on the structures. Lower accelerations occurred on the modified-subfloor airplanes.

This work was done by Huey D. Carden of **Langley Research Center**. Further information may be found in NASA Technical Paper 2380 [N85-13267/NSP], "Full-Scale Crash Test Evaluation of Two Load-Limiting Subfloors for General Aviation Airframes."

Copies may be purchased [prepayment required] from the National Technical Information Service, Springfield, Virginia 22161, Telephone No. (703) 487-4650. Rush orders may be placed for an extra fee by calling (800) 336-4700. LAR-13414

Spacecraft/Satellite Communications Systems

CONTEL SPACECOM, a division of CONTEL Federal Systems, is continuing our tradition of excellence in space communications. In addition to our involvement in the development and implementation of the communications segment for CSOC, we are further extending our expertise with growth in such areas as the Strategic Defense Initiative program, Space Station development, and exciting IR&D.

We are looking to expand our staff of exceptional people and have multiple positions available at our headquarters facilities as well as our other facilities, nationwide:

- COMPUTER SYSTEMS**
- Real-Time Control
 - Simulation & Analysis
 - Management Information Systems
 - C3I
 - Telemetry & Networks
 - Systems Management

- SYSTEMS ENGINEERING**
- Spacecraft Engineering
 - Facilities Engineering
 - Advanced Systems
 - Communications Systems
 - Systems Integration and Testing
 - IR&D
 - Battle Management/C3I

Your technical expertise, creative ability, and appropriate experience (in addition to a BS, MS or PhD degree) will earn an excellent career opportunity for involvement in meaningful and far-reaching technologies.

Send your resume for a confidential review to: Charlie Virtue, Management of Employment, Dept. NA-MJ86, CONTEL SPACECOM, 1300 Quince Orchard Blvd., Gaithersburg, MD 20878.



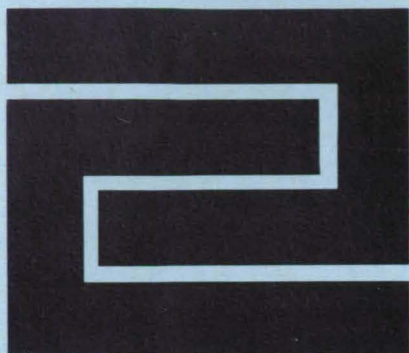
**CONTEL
SPACECOM**

A Division of CONTEL Federal Systems

U.S. Citizenship Required

We are an Equal Opportunity Employer

Circle Reader Action No. 398



Hardware, Techniques, and Processes

- 128 Thermally Activated Metal-to-Glass Bonding
- 135 Electrochemical Process Makes Fine Needles
- 136 Filters for Submillimeter Electromagnetic Waves
- 137 Weld Repair of Thin Aluminum Sheet
- 138 Repairing Hard-to-Reach Cracks in Heat-Exchanger Tubes
- 139 Depositing Diamondlike Carbon Films
- 140 Masking Technique for Ion-Beam Sputter Etching
- 141 Unitized Nut-and-Washer Assembly
- 144 Acoustic Translation of an Acoustically Levitated Sample
- 145 Acoustic Levitator Maintains Resonance
- 145 Xenon-Ion Drilling of Tungsten Films
- 146 Laser Cutting of Thin Nickel Bellows

Books & Reports

- 147 Theoretical Foundation for Weld Modeling

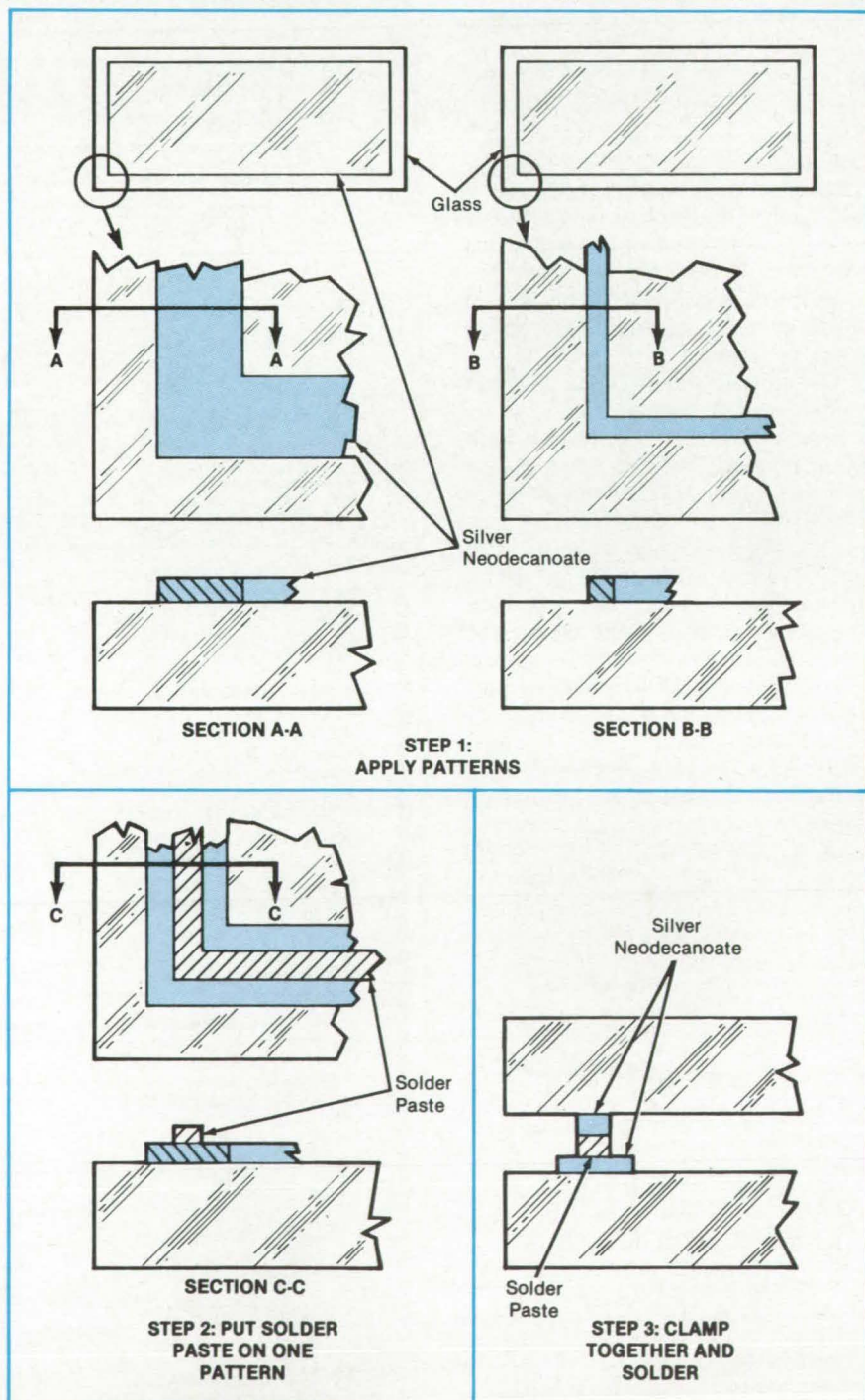
Thermally-Activated Metal-to-Glass Bonding

Hermetic seals are formed easily by use of a metallo-organic film.

NASA's Jet Propulsion Laboratory, Pasadena, California

A metallo-organic film is thermally bonded to glass and soldered or welded to form a hermetic seal. The film is applied as an ink consisting of silver neo-

decanoate in xylene. The relative amounts of the ingredients are selected to obtain the desired viscosity. The material can be applied by printing or even by



A Metallo-Organic Film is deposited on two pieces of glass, then soldered to make a hermetic seal.

Multiple Pages Intentionally Left
Blank

scribing with a pen.

The figure illustrates a representative procedure for making a hermetic seal between two flat pieces of glass. First, the ink is deposited on the two pieces in matching patterns. The pattern on the lower piece has slightly wider lines. The glass pieces then are heated in air to 260°C to evaporate the xylene and decompose the silver neodecanoate, leaving adherent patterns on the glass.

Solder paste is deposited on the wider lines and dried normally. The upper glass

is placed over the lower glass with its metal pattern resting on the solder paste. The pieces are clamped together and soldered, using the standard thermal cycle specified for the solder.

In semiconductor packaging, the customary line width for hermetic seals is about 1 mm. If the seal is to encapsulate electronic circuitry that must not be overheated, the heat for decomposition and soldering can be supplied by a laser to confine the high temperature to the seal region. This sealing technique should be

useful in making solar-cell modules, microelectronic packages, and other hermetic silicon devices.

This work was done by Brian D. Gallagher of Caltech for NASA's Jet Propulsion Laboratory. For further information, Circle 58 on the TSP Request Card.

Inquires concerning rights for the commercial use of this invention should be addressed to the Patent Counsel, NASA Resident Office-JPL [see page 29]. Refer to NPO-16423.

Electrochemical Process Makes Fine Needles

The improved process is less tedious than manual dipping and can be left unattended.

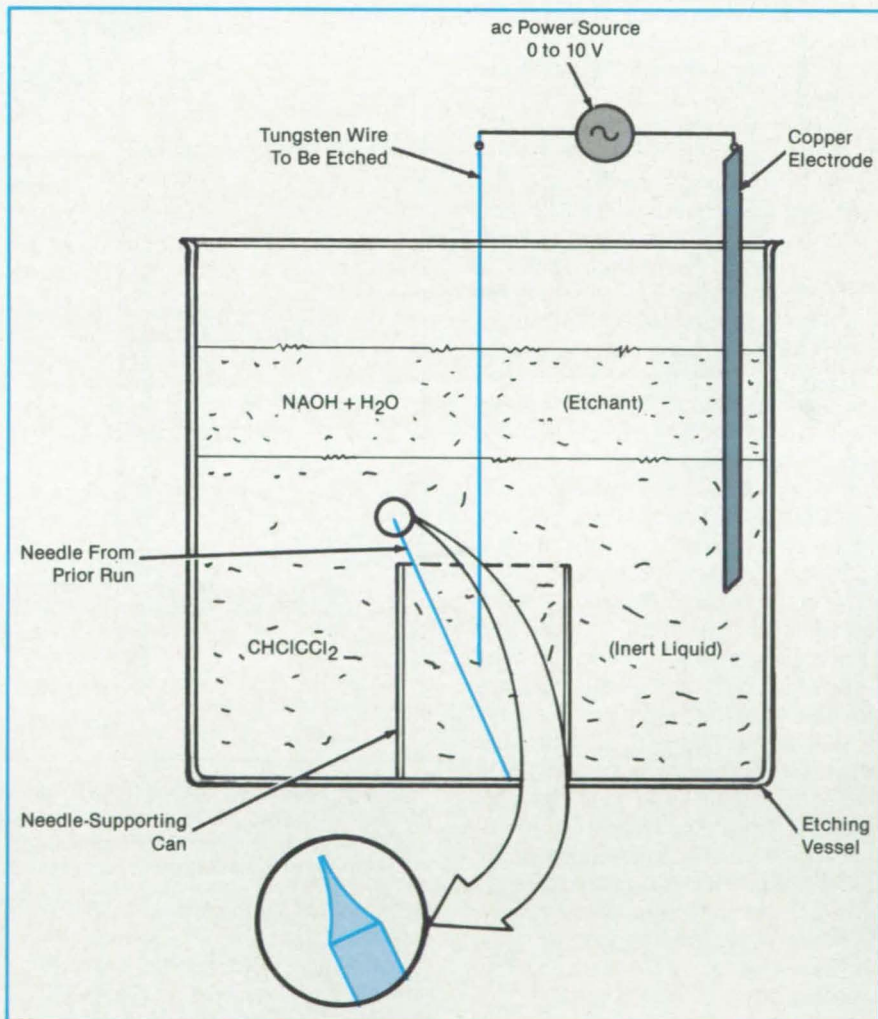
NASA's Jet Propulsion Laboratory, Pasadena, California

An electrochemical process makes fine tungsten needles for use as microscopic probes or field-emission cathodes. Until now, fine needles were produced from tungsten wire by tedious manual dipping in an etching solution, with careful minute-by-minute inspection to determine when the etching should be stopped. The improved process does not require close monitoring and can be left unattended for an indefinite time.

The process uses sodium hydroxide in water as a caustic etching liquid and trichloroethylene, a denser, immiscible, inert fluid underneath the etchant. As shown in the figure, the tungsten wire is suspended from above the etching vessel; the lower end of the wire is in the trichloroethylene. A copper electrode is placed elsewhere in the vessel. An alternating voltage — usually 6 to 7 V — is applied between the wire and the electrode.

Wires of 0.010- to 0.015-in. (0.25- to 0.38-mm) diameter are etched in 5 to 10 min. The portion of the wire in the etchant gradually thins to a filament, then breaks into two segments having pointed ends. The lower segment sinks into the trichloroethylene and is not etched any further. A can or other support may be placed at the bottom of the vessel to catch the sinking needle and protect the tip.

The newly formed needle can be lifted out with forceps or left at the bottom of the vessel while new segments of wire are etched. If the apparatus is left unattended as a needle is formed, no harm is done: The needle falls to the bottom as usual, and the upper wire segment in the caustic solution eventually dissolves completely, interrupting the electrical current. In principle, the process can accommodate dozens of wires connected electrically in parallel, so that many



The **Etching Vessel** is filled with a dense, inert lower liquid covered by a less-dense, caustic etching solution. The newly formed needle breaks off the upper part of the wire in the etchant and falls into the can in the inert liquid below.

needles can be formed in one batch.

This work was done by John L. Watkins of Caltech for NASA's Jet Propulsion

Laboratory. For further information, Circle 9 on the TSP Request Card. NPO-16311

Filters for Submillimeter Electromagnetic Waves

Stacked square wires are plated, fused, and etched to form arrays of holes.

NASA's Jet Propulsion Laboratory, Pasadena, California

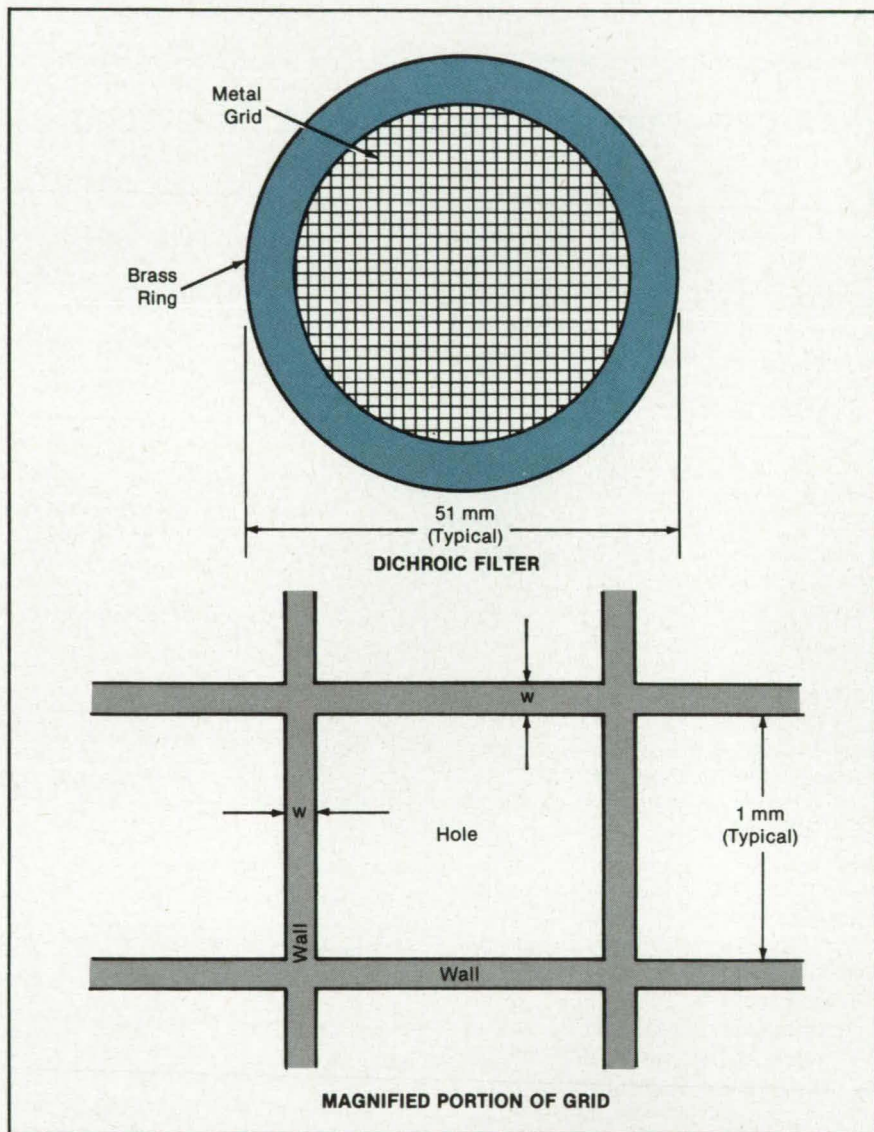
A new manufacturing process is expected to produce filters that are strong, yet have the small, precise dimensions and smooth surface finish essential for dichroic filtering at submillimeter wavelengths. Many filters, each one essentially a wafer containing a fine metal grid (see figure), can be made at the same time.

The starting material is the wires. They should be square in cross section and straight with sharp corners and smooth sides. The square-cross-section wires can be made by drawing round wires through a die. A die composed of four silicon carbide side plates held in a clamping block would ensure the sharp edges needed for accurate filtering.

The wires are cut to lengths of about 24 inches (61 centimeters), suitable for the depth of the available plating tank. The wires are suspended in an electroless nickel-plating bath, and a coating of nickel is formed on them. (Electroless plating is used because it gives a fairly even nickel coat, whereas electroplating builds up undesired thickness along the wire edges.) Optionally, the wires may then be coated with a thin layer of pure tin to facilitate subsequent soldering. The combined thickness of nickel and tin should be less than one-twentieth the thickness of a wire. The nickel-plated, tinned wires are cut to a length of 2 inches (5 centimeters). Two semicylindrical bundles of the cut wires are stacked in a semicylindrical aluminum trough and clamped in the trough by a flat plate on the open diameter so that the wires are oriented uniformly with flat surfaces parallel to the plate. The trough and strips are placed in a furnace and heated to melt the tin. (The tin does not adhere to the aluminum.)

In a faster and easier version of the process, the wires are packed directly into brass semicylinders. With the semicylinders clamped together, the assembly is fused or subjected to capillary sweating with G35n/37Pb solder.

After cooling, the two bundles in their solid tin matrix are clamped between tinned brass half cylinders, having an outside diameter equal to the required outside diameter of the finished filter. They are placed in the furnace and fused together. The cylinder thus formed is sawed into wafers, then lapped and



A Grid of Nickel and Tin is held in a brass ring. The wall thickness, the thickness of the filter (hole depth), and the lateral hole dimensions all depend upon the operating frequency and filter characteristics. The dimensions shown are for a filter with a center wavelength of 1.4 millimeters. The thickness of the filter is 1.2 millimeters.

polished to the thickness required for the cutoff frequency. The wire cores are electrolytically etched from the wafers, leaving a grid of nickel in the solder or tin matrix. A subsequent thin gold plate of the etched wafer will assure good electrical performance.

The wire may be aluminum, copper, brass, silver, or other material. The etching electrolyte contains ions of the wire metal only. With the wire cores connected as anodes, the cores are etched away. With

the proper choice of etching conditions, the nickel plate and solder should not be attacked significantly.

This work was done by C. Martin Berdahl of Caltech for NASA's Jet Propulsion Laboratory. For further information, Circle 57 on the TSP Request Card.

Inquiries concerning rights for the commercial use of this invention should be addressed to the Patent Counsel, NASA Resident Office - JPL [see page 29]. Refer to NPO-16498.

Weld Repair of Thin Aluminum Sheet

A shield and heat sinks protect the area adjacent to the weld.

Lyndon B. Johnson Space Center, Houston, Texas

Weld repairing of thin aluminum sheets is now possible, using a niobium shield and copper heat sinks. In the past, weld repairing of thin aluminum sheets has not been possible, because of high-frequency-induced surface cracks and heat checks. The refractory niobium shield protects the aluminum adjacent to the hole, while the copper heat sinks help conduct heat away from the repair site. This technique limits the tungsten/inert-gas (TIG) welding bombardment zone to the melt area, leaving surrounding areas around the weld unaffected.

The figures illustrate the application of the new technique to the face sheet of a cold-plate assembly. Before welding, the fracture, dent, or puncture in the face sheet is machined away, leaving a smooth hole so that the rough edges and cracks are removed. After cleaning, the face-sheet edge at the hole is then depressed into the core cavity. As shown in Figure 1, the niobium heat shield and copper tooling are clamped over the area to be repaired.

As welding is initiated, the high-frequency-induced surface cracks are taken into the weld melt. The undercut (or countersink) on the back side of the niobium heat shield allows the molten weld to flow outward and away from the bombardment zone. Thus, the weld and its peripheral areas are free of high-frequency-induced surface cracks and heat checks. Figure 2 shows the resulting weld configuration.

This technique has been used successfully to repair aluminum cold plates on the Space Shuttle, resulting in a substantial cost saving and reducing delays. It also will have commercial applications, especially in sealing fractures, dents, and holes in thin aluminum face sheets or clad brazing sheet in cold plates, heat exchangers, coolers, and Solar panels. While particularly suited to thin aluminum sheet, this process also can be used in thicker aluminum material to prevent surface damage near the weld area.

This work was done by Charles S. Beuyukian and Mike J. Mitchell of Rockwell International Corp. for Johnson Space Center. No further documentation is available.
MSC-20902

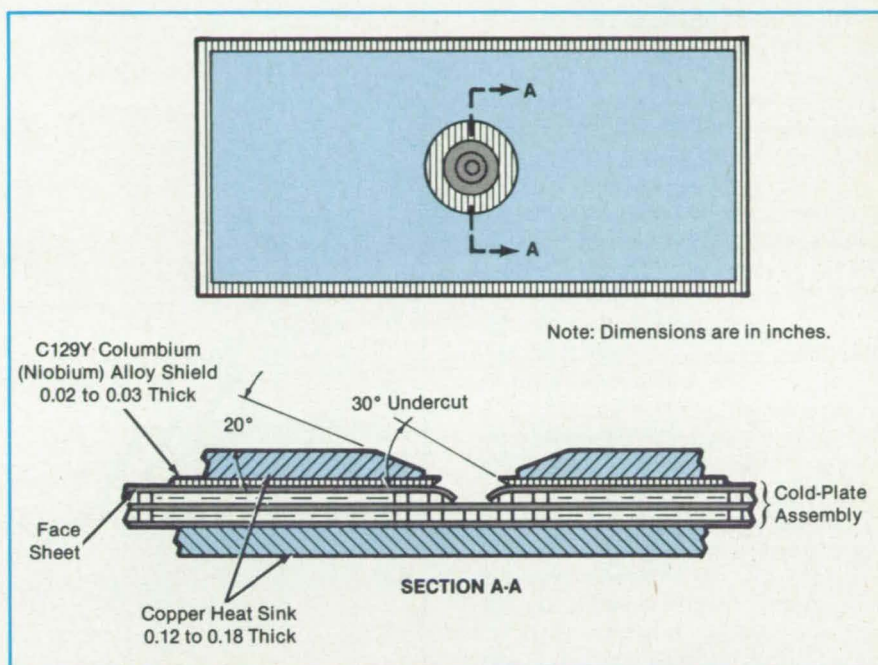


Figure 1. **Before Welding**, the edge of the hole in the face sheet is depressed into the cavity, and the shield and heat sink are clamped in place.

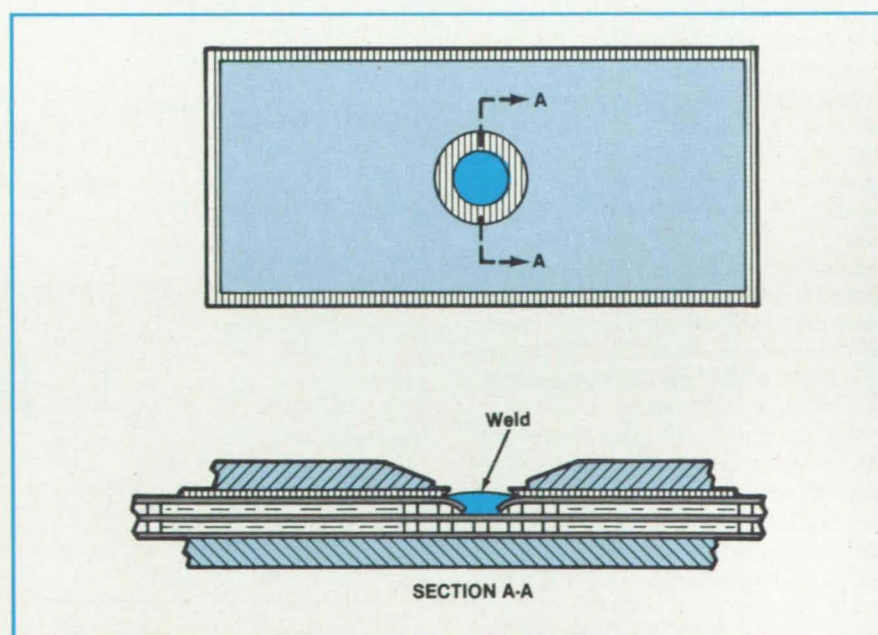


Figure 2. The **Weld Melt** flows beyond the edge of the undercut, where heat checking and cracking do not take place. Thus, the entire weld is free of cracks and heat checks.

Repairing Hard-to-Reach Cracks in Heat-Exchanger Tubes

Inaccessible leaks are repaired from accessible side of the tube.

Marshall Space Flight Center, Alabama

Tubes springing leaks on inaccessible surfaces can be repaired by a "fish-mouth" insert and two closeout patches. This method was developed for repairing leaks in the nozzle coolant tubes of the Space Shuttle main engine. Such a leak can occur on the side of a tube that touches the cold wall. Cutting through the wall to reach the cracked part of the tube is not feasible, but with the new method, the crack can be reached from the accessible opposite side. The method can also be used on other types of tubular heat exchangers.

A portion of the tube on the side opposite the crack is cut and removed (see figure). The opening should extend around one-half the circumference of the tube so that the insert can be slipped over the crack. The insert has an outside diameter equal to the inside diameter of the cracked tube. The insert is slightly shorter than the opening, and its slanted ends face the hot side, resembling a fish's mouth. These slanted ends are easily accessible for brazing or welding.

The insert is brazed or welded around its entire perimeter adjoining the cracked tube by tungsten/inert-gas apparatus. This seals off the crack. Longitudinal bonding of the insert to the tube wall further secures the insert and isolates the cracks.

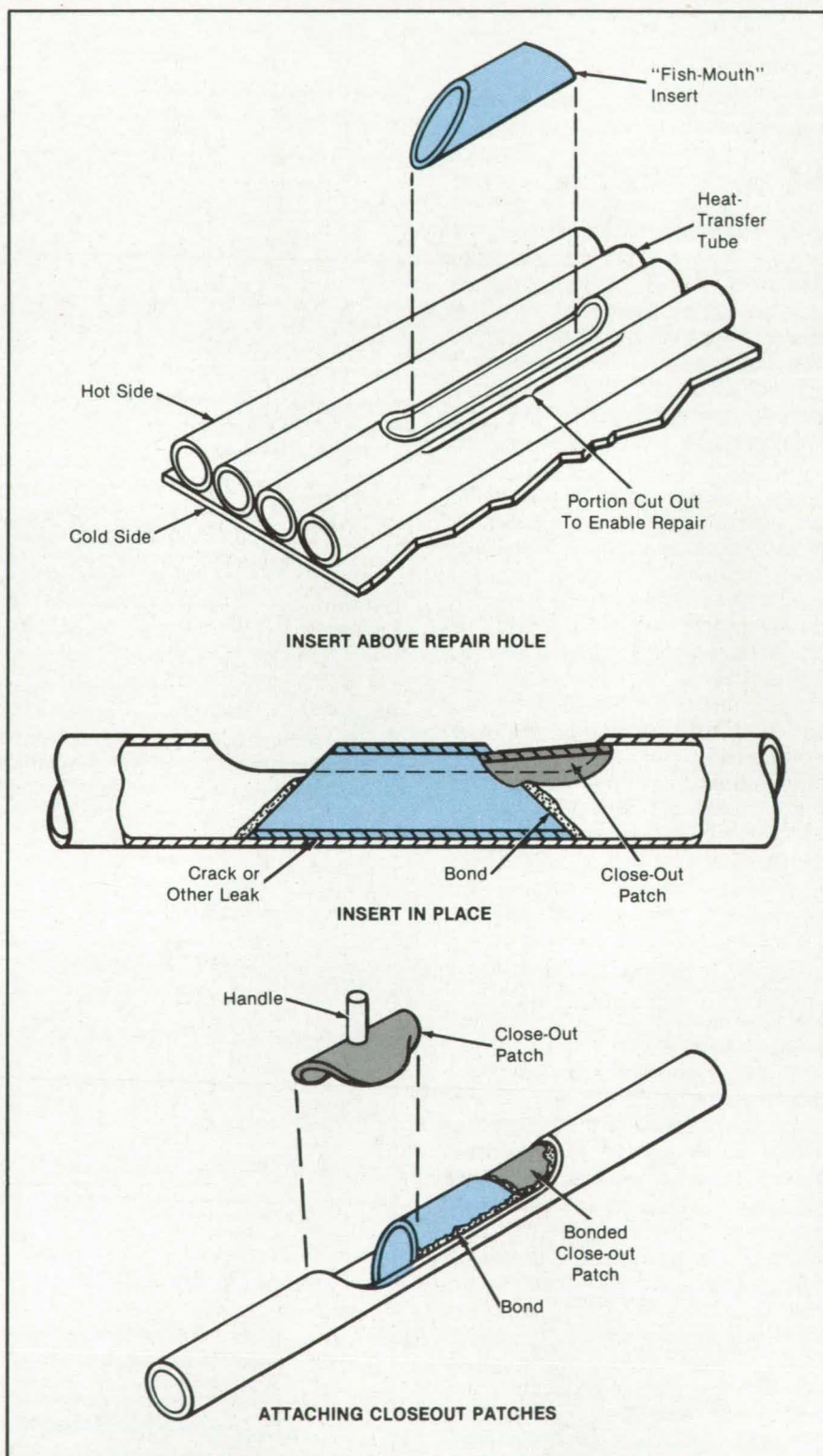
After the insert is secured, two closeout patches are positioned over what remains of the opening. The patches, which are cut to match the edge contours of the tube opening and the insert ends, are welded to the assembly. Rod-shaped handles on the patches allow the welding-machine operator to grasp and manipulate them; the handles are cut off after the patches are secured.

The insert should be long enough to cover the cracked area. When adjacent tubes are repaired, the repaired tubes may have to be alternated with short ones so that the welding can be staggered to prevent side-by-side welds.

The insert not only seals cracks but also strengthens the tube structurally. It does not interfere with the flow of the heat-exchange medium and does not significantly degrade the heat transfer.

This work was done by R. C. Mills, Sr., and J. Duesberg of Rockwell International Corp. for **Marshall Space Flight Center**. For further information, Circle 5 on the TSP Request Card.

MFS-29128



A Fish-Mouth Insert is placed in a cut in a leaky heat-exchanger tube. The insert is welded or brazed to the tube, and the remaining open area of the cut is patched.

Depositing Diamondlike Carbon Films

Radio-frequency, plasma, and ion-beam techniques are used.

Lewis Research Center, Cleveland, Ohio

A new process has been demonstrated to make thin films (usually thousands of angstroms to a few microns thick) that have the properties of diamonds. These diamondlike properties include high scratch resistance, high electrical resistivity, high thermal conductivity, insolubility in concentrated $\text{H}_2\text{SO}_4/\text{HNO}_3$, and optical properties that include high transmittance at visible wavelengths.

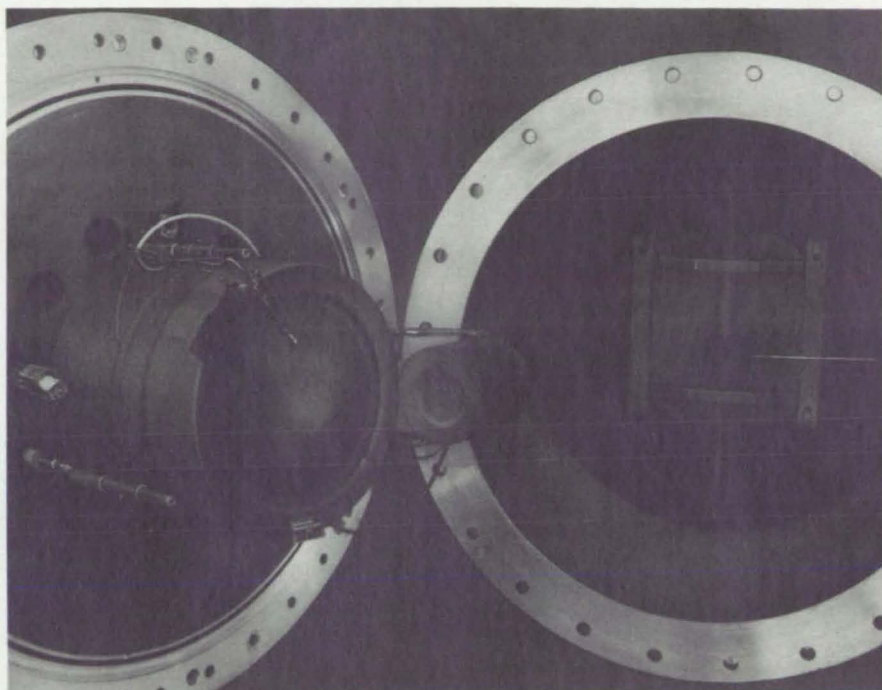
There have been many publications reporting efforts to produce carbon thin films with diamondlike properties. Various plasma and ion-beam techniques have been employed to generate the films. The films can be made by radio-frequency plasma decomposition of a hydrocarbon gas or other alkanes, by low-energy carbon-ion-beam deposition, or by ion plating and a dual ion technique using a carbon target.

Disadvantages of this prior art include the following:

- The quality of the films produced is such that the films appear to have a low electrical conductivity (1 to $10\ \Omega\text{-cm}$), greater optical absorption ($10^5\ \text{cm}^{-1}$), less resistance to chemical attack ($3\text{H}_2\text{SO}_4/1\text{HNO}_3$), and the films are softer and less dense.
- In some of the other techniques used to produce diamondlike films, the size of the substrate to be coated is limited. Also, the deposition rates are not as high.
- Another disadvantage is that because of the inability to control enough independent parameters, the films produced are stressed.

This unique process was developed to achieve films of superior quality; i.e., thin films that have the properties of diamonds. These thin films can be achieved by the following four processing steps:

1. Two ion sources, shown in the configuration in the figure, were used to generate the films.
2. The substrate (quartz, silicon, metals) is first exposed to an argon ion beam to clean absorbed gases and contaminants from its surface at energy levels between 500 and $1,000\ \text{eV}$ and current densities of 0.5 to $2\ \text{mA/cm}^2$.
3. A 30-cm hollow-cathode ion source with its optics masked to $10\ \text{cm}$ (as in the figure) is then used to deposit diamondlike films directly on a substrate.



This **Dual-Beam Ion Source** deposits films with properties like those of diamonds.

Argon gas is used in a hollow cathode to establish a discharge, and then CH_4 (methane) or other hydrocarbons are introduced into the discharge chamber as the main flow. The ideal ratio of CH_4 molecules to Ar atoms necessary to generate the films is 28 percent with energy levels between 80 and $150\ \text{eV}$. Ideal energy levels for generation of the films are $100\ \text{eV}$. With this energy level, it is necessary to have an accelerator voltage of $-600\ \text{V}$ to extract a beam.

4. To initiate a film, it is absolutely necessary for the current density to be low during initial deposition at the substrate (a typical value is one-half or less of the current density during full deposition) for periods of time varying from 3 to $30\ \text{min}$, depending on the substrate material. After this initial low-current condition, the 30-cm hollow-cathode ion source is set at the full-power current conditions, and then the 8-cm ion source using Ar gas at 200 to $500\ \text{eV}$ is turned on with a current density at the substrate of $25\ \mu\text{A/cm}^2$. This addition of energy to the system increases mobility of the condensing atoms and also serves to

remove lesser bound atoms. Typical deposited rates at these conditions are 70 to $80\ \text{\AA/min}$. Liquid nitrogen was used in cold traps of the diffusion pumps and the cryoliner of the vacuum system during the deposition process.

The advantages of this new process over others are that the films produced, though amorphous, are clear, extremely hard, chemically inert, of high resistivity, and have an index of refraction of 3.2 — properties that are similar to those of single-crystal diamonds. These films have possible uses in microelectronic applications, high-energy-laser and plastic windows, corrosion protection for metals, and other applications where the desired properties of the film can be shaped during the film-formation process.

This work was done by Michael J. Mirtich, James S. Sovey, and Bruce A. Banks of **Lewis Research Center**. Further information may be found in NASA TM-83743 [N84-31512/NSP], "Dual Ion Beam Deposition of Carbon Films with Diamond Like Properties" [\$7]. A copy may be purchased [prepayment required] from the National Technical Information Service, Springfield, Virginia 22161.

Masking Technique for Ion-Beam Sputter Etching

Integrated-circuit surface structures have high aspect ratios.

Lewis Research Center, Cleveland, Ohio

An improved process for the fabrication of integrated circuits has been developed. Previous organic resists, metal, and metal-oxide masks limited the aspect ratio of surface structures, because the sputter mask has a finite sputter-etch rate. As the mask material etches away, the walls of the etched substrate become sloped or faceted rather than having ideal vertical walls.

Utilizing a technique that allows for the codeposition of carbon, the sputter mask can be made to have no net loss or even a slight gain in thickness with time. This allows very-high-aspect-ratio surface features to be ion-beam sputtered without concern for sputter-mask life. The sputter mask is replenished in a manner that allows a very thin sputter mask to be used. The ability to use thin masks that do not become thinner or narrower allows high-resolution sputter etching and straight walled features to be produced. Use of a carbon film for a sputter mask allows high rates of sputter etching because the sputter mask would not be heat-sensitive and a high ion-beam power density could be used.

This technique utilizes simultaneous ion-beam sputter etching and carbon sputter deposition in conjunction with a carbon sputter mask or an organic mask that can be decomposed (thermally or by ion-bombardment scission fragmentation) to produce a carbon-rich sputter-mask surface. This carbon surface can be extremely thin (a few hundred to a few thousand angstroms). The mask along with the unmasked portion of the substrate are bombarded typically with 200 to 3,000-eV inert-gas ions while simultaneous carbon deposition is occurring. The arrival of sputter- or vapor-deposited carbon can easily be adjusted to allow the sputter mask to have a nearly zero or even slightly positive increase in thickness with time, while at the same time the unmasked portion of the substrate has a high net sputter-etch rate. The reason for this disparity of etch rates is the large difference in sputter yield between carbon and all other materials.

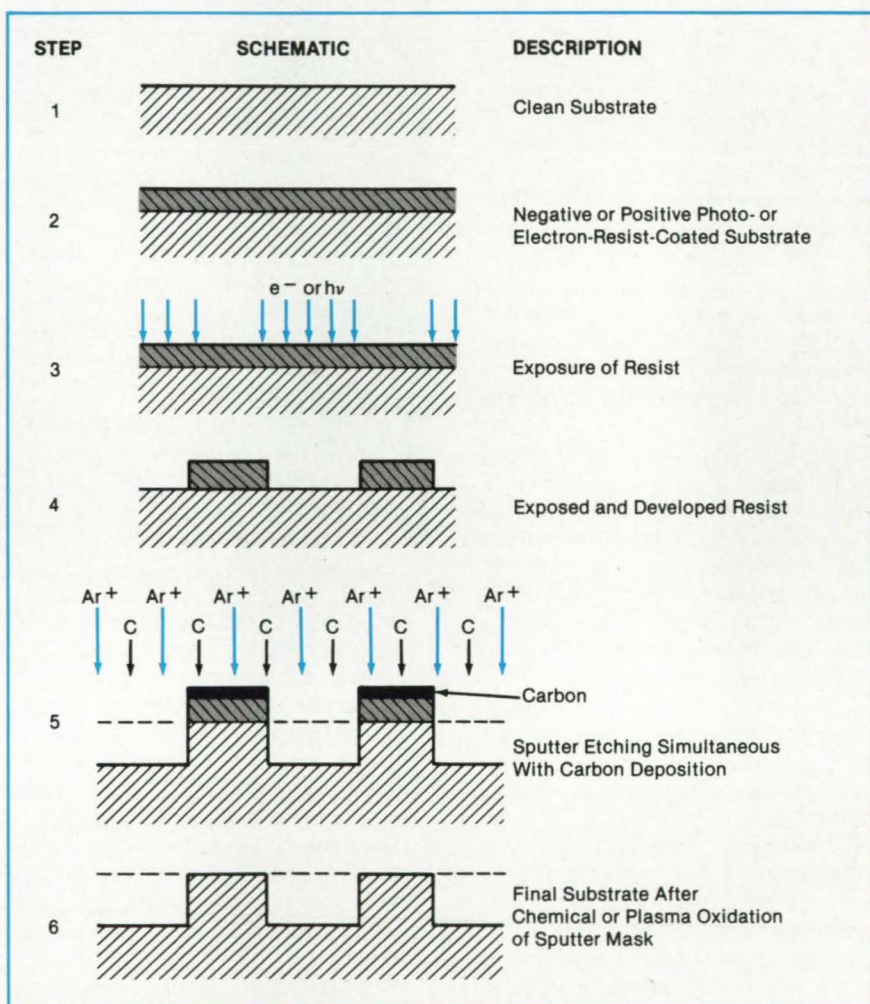


Figure 1. This **Sputter-Etching Process** replenishes the sputter mask with carbon to prevent premature mask loss.

The high sputter yield of the unmasked portion of the substrate prevents any net carbon-film buildup as does occur on the carbon-coated mask. After the sputter etching is completed, the remaining mask can be removed by conventional chemical resist-removal techniques or by oxygen RF plasma oxidation. Figure 1 shows the general sequence of steps as they modify the substrate to be sputter-etched. Figure 2 shows several configurations of ion sources that provide ion-beam sputter etching simultaneously

with carbon sputter or vapor deposition.

Variations can be made to the described process such as the following seven:

1. An alternate sequence can be used to make a negative of the Figure 1 sequence by changing the sequence after step 4. The substrate and the developed mask could be sputter- or evaporation-coated with a very thin carbon film. The resist (plus its carbon coating) could then be chemically dissolved leaving a carbon film

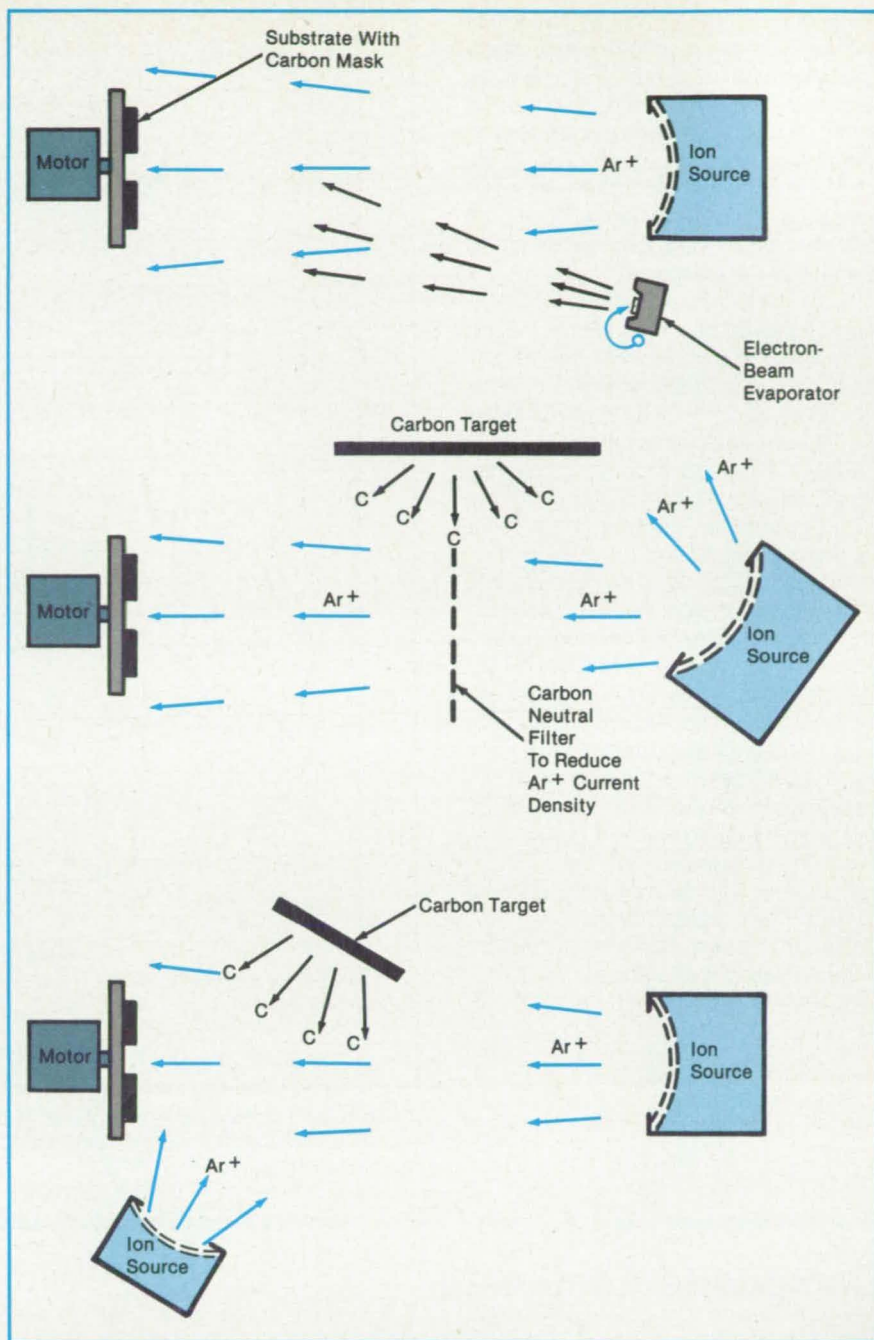
where the resist was not present, and an uncoated substrate where the resist used to be, then continuing starting with step 5.

2. The sputtering ions can be other inert or noninert gases or free radicals.
3. The substrate can be rotated.
4. The arrival angle and energy of the bombarding ions and/or the carbon can be varied.
5. The resist can be either negative or positive and can be exposed by electrons, ions, visible light, or X-rays.
6. Sputter etching can be RF or ion-beam.
7. The ratio of carbon-atom arrival to removal from the substrate can be varied to control the rate of mask replacement from net etching to net deposition. This ratio can be varied during ion-beam sputter etching to achieve desired substrate or sputter-mask characteristics.

This work was done by Bruce A. Banks and Sharon K. Rutledge of **Lewis Research Center**. Further information may be found in NASA TM-82873 [N82-28445/NSP] "Ion Beam Sputter Etching of Integrated Circuits and other Micro-electronic Components" [\$7]. A copy may be purchased [prepayment required] from the National Technical Information Service, Springfield, Virginia 22161.

Inquiries concerning rights for the commercial use of this invention should be addressed to the Patent Counsel, Lewis Research Center [see page 29]. Refer to LEW-13899.

Figure 2. These **Ion-Source Configurations** can each be used to perform ion-beam sputter etching simultaneously with carbon sputter or vapor deposition.



Unitized Nut-and-Washer Assembly

A proposed fastener would be nonscratching and easy to install.

Lyndon B. Johnson Space Center, Houston, Texas

A combination nut, washer, and lock-washer would secure parts quickly without damaging metal finishes. The proposed fastener is intended for attaching leads and buses to studs on electronic equipment.

The conventional way of securing a lead is to attach it to a stud with a flat washer, a lockwasher, and a nut. The flat washer is placed between the lead terminal and the lock washer to prevent the latter from cutting into the plated finish of the terminal.

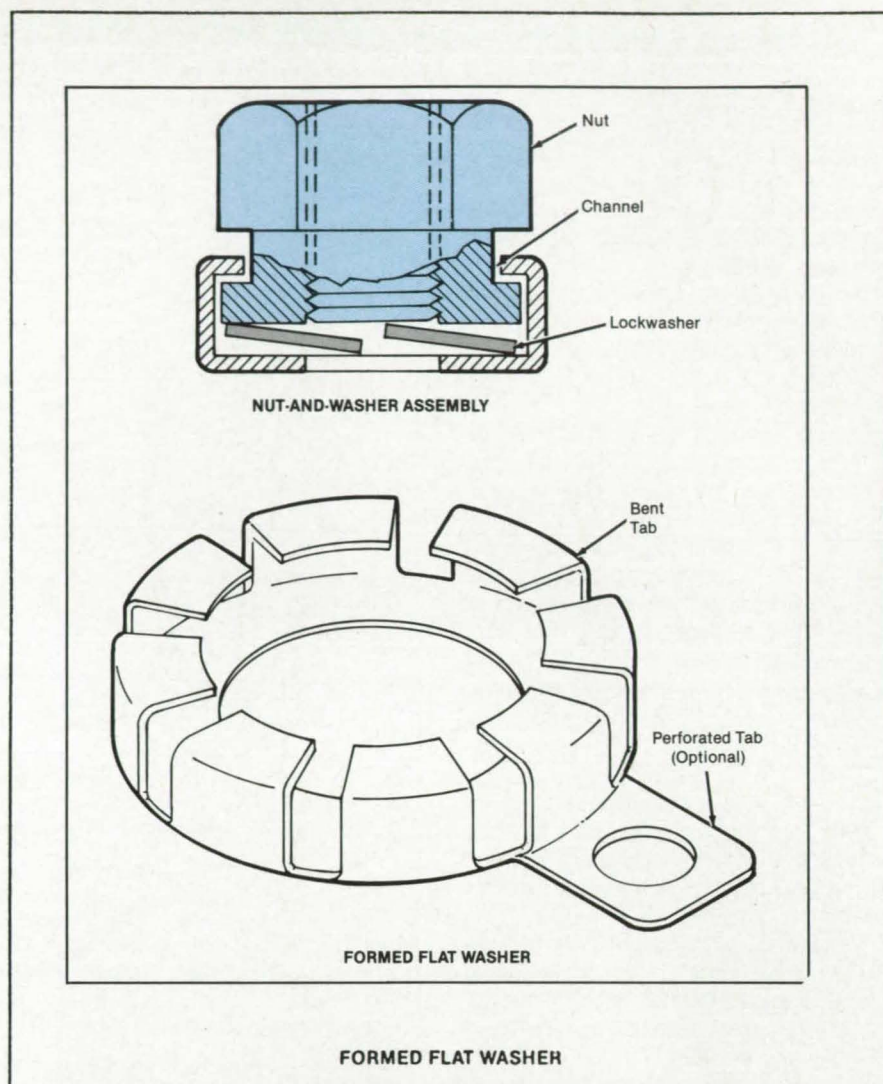
The manual assembly of the three parts is tedious, especially with small-diameter studs. It is also prone to error when the flat washers are made of corrosion-resistant steel (CRES) and are used in conjunction with shim washers

made of nickel-plated copper. The shims are used as spacers between multiple connections on the same stud or to bring terminals on adjacent studs to the same level. They can easily be confused with CRES washers, which have lower electrical conductivity. Thus, the accidental substitution of a CRES washer for a copper shim could cause overheating and damage to the equipment.

Since the proposed fastener would be attached as a unit they would reduce assembly time and eliminate the need to stock separate CRES washers, thereby also eliminating erroneous substitution for the lower resistance shims.

The nut on the proposed fastener would be made by machining a circumferential channel on hexagonal, non-locking nut (see figure). The outer portion of the flat washer would be cut away in a pattern to make tabs. The washer would be attached to the nut by bending the tabs into the channel. The width of the channel would have to be equal to the free height of the lockwasher, which would be sandwiched between the nut and the flat washer. Tightening the nut on a stud would automatically compress the lockwasher, which may be a helical locking spring or internal-tooth type.

This work was done by Peter J. Rossi of Rockwell International Corp. for Johnson Space Center. No further documentation is available.
MSC-20903



The **Nut and Lockwasher Are Captured** by the bent tabs of a flat washer in this concept for a unified fastener. The optional perforated tab on the flat washer would allow easy tagging and storage.

Composite Fasteners

Flexible fasteners are easily installed and removed by hand.

Langley Research Center, Hampton, Virginia

Flexible composite fasteners made of polyvinyl chloride or other resilient synthetic material are designed for joining together various materials which may vary slightly in thickness during use. The fasteners are easily installed and removed by hand and maintain approximately the same tension in bonding the materials together, regardless of the subsequent movements of the materials.

A fastener of this type is designed to join or bind structures requiring only a snug all-around fit in the lateral and longitudinal directions of the fastener

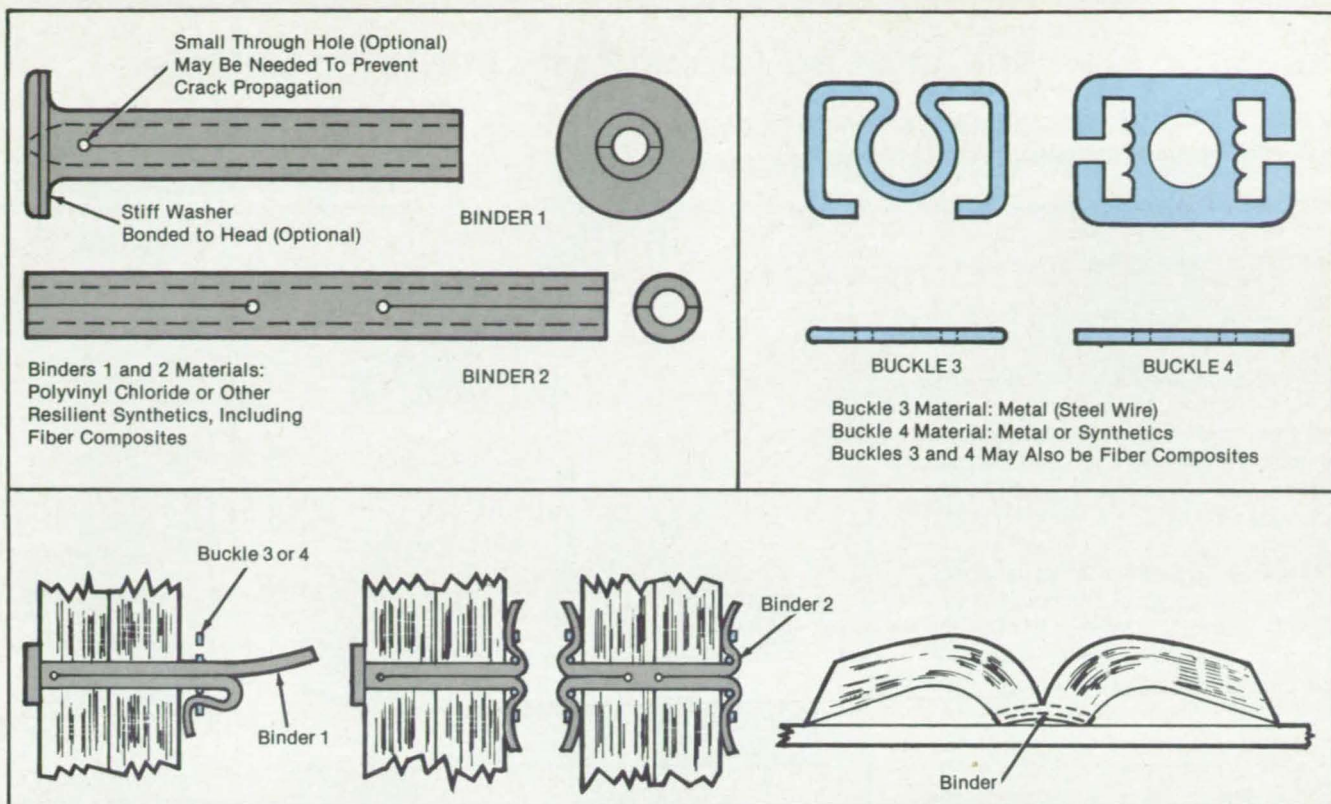
shaft. The fastener, being flexible, is also capable of yielding under loading in all directions but will still bind the structures with initial tightness and will maintain its circular shape in the shaft before and after structural movement.

One application of this fastener concept is the binding together of paper to make a book (see figure). The flexibility of the fastener allows the book to open wider, and the snug fit between the fastener shaft and the circular holes at the edge of the book will keep the pages evenly spaced and aligned. Also, more

bearing area is provided between the paper and the fastener shaft to resist page tearout. The fastener shaft can be cut easily with scissors or a knife and can be produced in different sizes.

Another application of this fastener is as a hole sealer. Binder 1 and buckle 3 or 4, if produced in various sizes, can be used as a fluid sealer. The head and the shaft of the binder could block a hole in a structure completely to form an airtight seal.

With the proper selection of dimensions and materials, the fastener can also



The **Design and Choice of Material** of the new fasteners enables a variety of uses; for example, as book binders, hole sealers, insulating fasteners for electronic circuitry, or break-away energy-absorbing fasteners for vehicles in crashes.

be used as an energy-absorbing break-away fastener for fail-safe vehicles in crashes. The fastener shaft could be designed to yield and breakaway at a given load. It can be used also as an insulating fastener in electronics or as a fastener with minimal heat flow for transistor devices or other devices requiring such properties.

This work was done by Gim Shek Ng of Langley Research Center. No further documentation is available.
LAR-13058

NASA WANTS YOU

to tell your fellow citizens how you have applied NASA research in your products or processes.

For more information, call:
Linda Watts (301) 621-0241
NASA Spinoffs



YSI Space-Qualified Thermistors

...with performance and traceability documentation

YSI 44900 Series Precision Thermistors, with interchangeability to $\pm 0.1^\circ\text{C}$, meet the requirements of GSFC S-311-P-18 for precise temperature compensation, measurement and control during extended space flight. NASA-monitored procedures for qualification testing and acceptance screening make YSI 44900 Series Thermistors ideal for a wide range of critical scientific and high-reliability industrial applications.

from Yellow Springs



Industrial Division
Yellow Springs Instrument Co., Inc.
Yellow Springs, Ohio 45387 USA • Phone 513 767-7241

Acoustic Translation of an Acoustically Levitated Sample

A sample can be moved quickly from hot to cold regions in the levitation chamber.

NASA's Jet Propulsion Laboratory, Pasadena, California

An acoustic-levitation apparatus uses only one acoustic mode to move a sample from one region of a chamber to another. The sample can be heated and cooled quickly by translation between hot and cold regions of the levitation chamber.

Thus far, acoustic levitators have been tested successfully in chambers of uniform temperature. Because of the large mass of the furnace surrounding levitation cells, these chambers require a considerable amount of time to change their temperatures. Hence, they are unsuitable for containerless experiments requiring quick cooling of the processed sample.

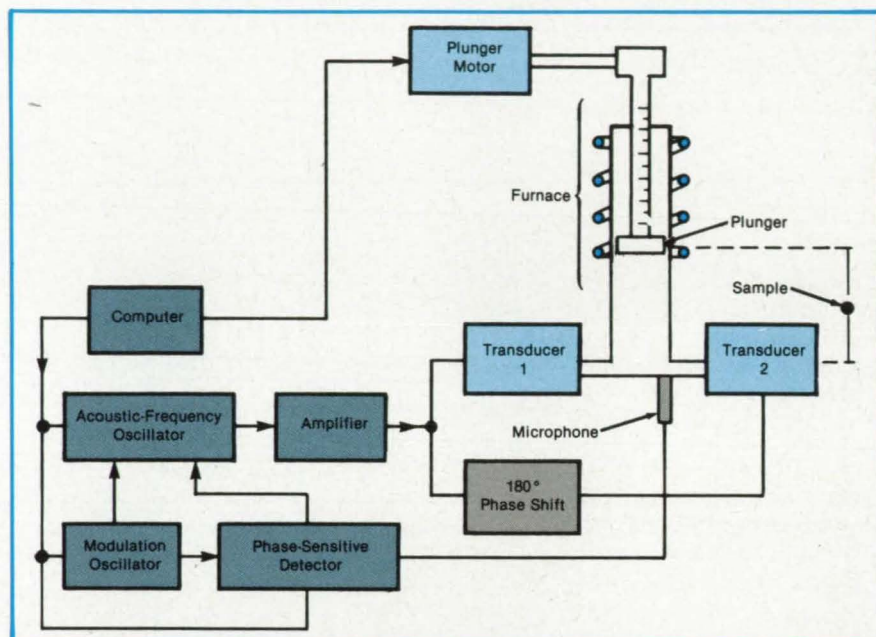
Samples can be cooled quickly in the system shown in the figure. A long, round cylindrical acoustic resonator is excited by two transducers positioned 180° apart at the cold end. For a uniform-temperature system, the resonance frequency decreases as the length of the chamber increases, according to the following equation for the normal-mode resonant frequency:

$$f(mn\pi) = (c/2a)[\alpha_{mn}^2 + (n_z a/l_z)^2]^{1/2}$$

where c is the speed of sound, a and l_z equal the radius and length of the resonator, respectively, and α_{mn} is a constant depending on the values of m and n . For a real levitation system, this equation will be modified slightly by such perturbation effects as those due to the acoustic ports, waveguides, and temperature gradients.

By driving the transducers out of phase, one obtains maximum acoustic power coupled to the (102) resonant mode and nearly zero power coupled to various plane-wave modes that would interfere with the levitation forces. The (102) mode produces acoustic forces that position a sample at the center of the chamber. Thus, as the chamber is lengthened by raising the plunger, the central levitation position is raised, carrying the sample along with it.

The feedback system shown in the figure continuously adjusts the acoustic frequency to track the resonant mode as the chamber length changes and to compensate for the perturbations. The



A Levitated Sample Is Raised into the furnace region by raising the plunger: The frequency of the sound produced by the transducers is adjusted by the feedback system to maintain the (102) resonant mode, which levitates the sample midway between the transducers and the plunger regardless of the plunger position.

acoustic-oscillation frequency is modulated at a low frequency about the resonance value. A microphone measures the chamber acoustic-pressure signal, and a phase-sensitive detector measures the magnitude and sign of the received modulated signal. For a properly calibrated system, this detected modulation signal will be zero at the chamber resonance.

When the resonance frequency changes due to the plunger motion or other causes, the detected modulation-error signal can be used to change the frequency of the oscillator to maintain continuously chamber resonance. The detected modulation signal can be fed back to the oscillator by analog or digital means.

With this system the sample would be heated and then cooled quickly by being inserted into the cool (lower) region of the resonator, raised into the heated region by the rising plunger, and then, after it had been processed at the desired temperature, quickly lowered to the cold region by the descending plunger. After the sample has cooled, it can be removed and replaced by a new sample.

In one of the variations of this system, the plunger would remain above the furnace to eliminate delays caused by the heating and cooling of the plunger. Another version uses a telescoping chamber instead of a plunger. When temperature uniformity of the sample is extremely important, the cylinder could be curved through the furnace region so that the sample will be almost completely surrounded by uniform radiant heat. Sample quick cooling can also be accomplished using other $(10n_z)$ modes with $n_z > 2$. As n_z increases, the sample movement relative to the plunger motion can be increased, thus enhancing the quick-cooling process.

This work was done by Martin B. Barmatz and James L. Allen of Caltech for NASA's Jet Propulsion Laboratory. For further information, Circle 50 on the TSP Request Card.

This invention is owned by NASA, and a patent application has been filed. Inquiries concerning nonexclusive or exclusive license for its commercial development should be addressed to the Patent Counsel, NASA Resident Office-JPL [see page 29]. Refer to NPO-16675.

Acoustic Levitator Maintains Resonance

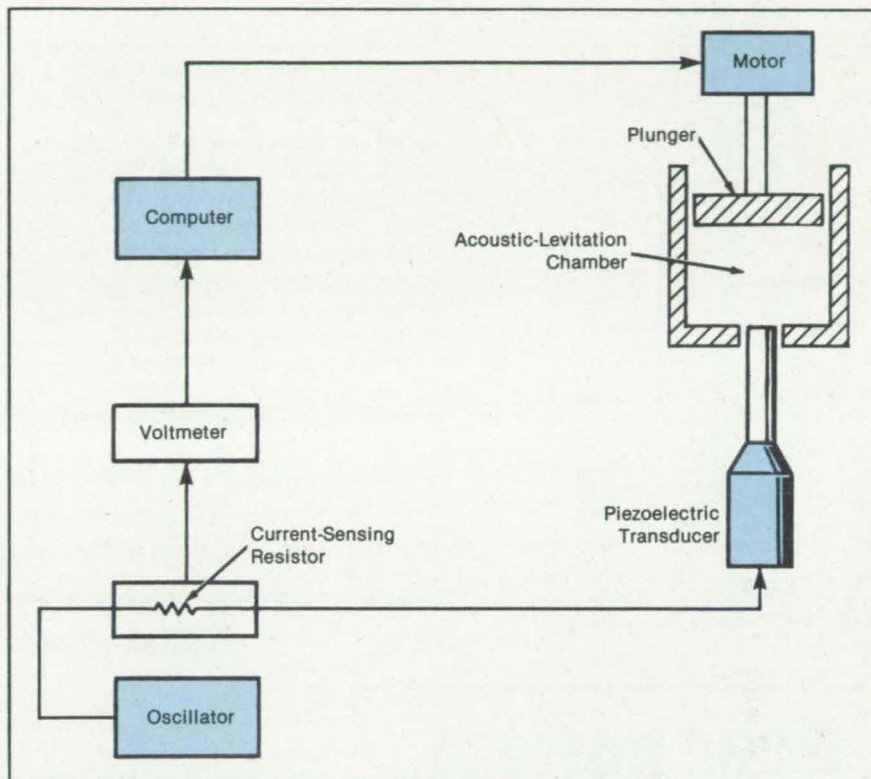
Transducer loading characteristics allow resonance to be tracked at high temperature.

NASA's Jet Propulsion Laboratory, Pasadena, California

An acoustic-levitation system automatically adjusts the sound frequency or chamber length to maintain the resonance necessary for levitation. Developed for containerless processing of materials at high temperatures, the system does not rely on microphones as resonance sensors, since microphones are difficult to fabricate for use at temperatures above 500 °C. Instead, the system uses the acoustic transducer itself as a sensor.

The resonance in the acoustic-levitation chamber affects the mechanical load on the transducer. This load, in turn, affects the electrical behavior of the device. Near the acoustic resonance, the transducer current reaches a minimum, and the voltage and impedance reach a maximum. By monitoring any of these parameters and adjusting the sound frequency (in a constant-length levitator) or the chamber length (in a constant-frequency levitator) accordingly, one can keep the chamber resonating as the temperature changes.

In a constant-frequency system, for example, a piezoelectric transducer is coupled to a cylindrical chamber (see figure). The chamber length is set by a plunger, the position of which is controlled by a computer. The transducer current is monitored via the voltage across a series resistor. The computer finds the resonant plunger position by searching among the currents measured throughout a small range of recent positions. The computer commands the



The **Acoustic-Levitation Chamber** length is automatically adjusted to maintain resonance at a constant acoustic frequency as the temperature changes.

plunger to dither about the new resonant (minimum current) position. This process repeats continuously. Therefore, as the chamber temperature changes during processing, the chamber length is continuously adjusted to maintain resonance

and levitation.

This work was done by Martin B. Barmatz and Mark S. Gaspar of Caltech for NASA's Jet Propulsion Laboratory. For further information, Circle 49 on the TSP Request Card. NPO-16649

Xenon-Ion Drilling of Tungsten Films

Many small, precise holes are produced simultaneously.

NASA's Jet Propulsion Laboratory, Pasadena, California

High-velocity xenon ions are used to drill holes of controlled size and distribution through the tungsten layer that sheaths the surface of a controlled-porosity dispenser cathode of a traveling-wave-tube electron emitter. This rapid, precise drilling technique could be ap-

plied to films of other metals and used in other applications where micron-scale holes are required. The method requires only a few hours, as opposed to tens of hours by prior methods.

A controlled-porosity dispenser cathode employs a barium/calcium/aluminum

oxide mixture that migrates through pores in the cathode surface, thus coating it and reducing its work function. Present cathode-fabrication techniques result in non-uniform hole sizes and spacing and in poor hole quality. This causes the coating to become uneven, reducing the efficiency

of the electron emitter.

The first step of the new drilling technique is the fabrication of an electroformed nickel mesh or silicon mask containing holes matching those desired in the cathode. This mask then receives an outer carbon coating through bombardment by carbon struck from a graphite block by a beam of high-velocity ions formed from xenon gas (see Figure 1).

The coated mask is placed on the cathode. The mask is then bombarded by

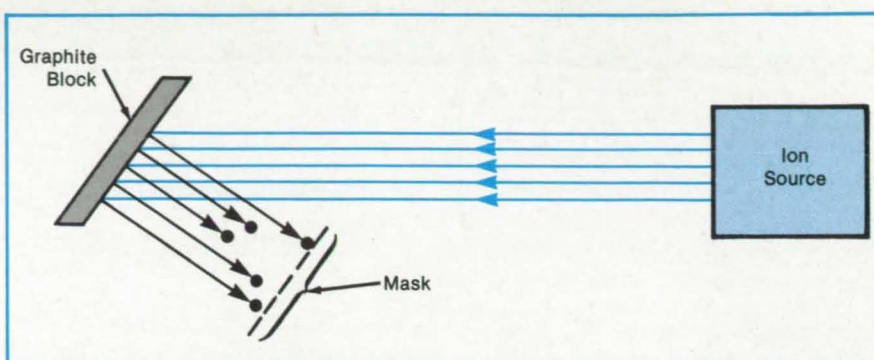


Figure 1. A **Hard Carbon Coating** is deposited on a mask. The mask is struck by carbon atoms dislodged from a graphite block by a beam of high-velocity xenon ions.

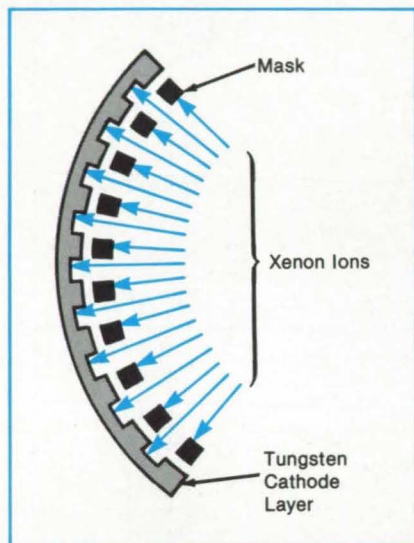


Figure 2. A **Tungsten Cathode Layer** is Etched through the carbon-coated mask by xenon ions.

xenon ions (see Figure 2). Although these ions etch both the mask and the portions of the cathodes exposed through the holes in the mask, the portions of the cathode protected by the mask are not etched. The use of xenon increases the tungsten/carbon etch ratio over that attainable with other ions. The holes made in the cathode surface faithfully repro-

duce the pattern in the mask. In the initial application of this technique, 5- μ m holes were produced in 12- μ m-thick tungsten.

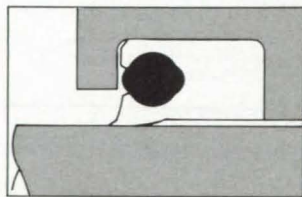
This work was done by Charles E. Garner of Caltech for NASA's Jet Propulsion Laboratory. For further information, Circle 54 on the TSP Request Card. NPO-16626

Laser Cutting of Thin Nickel Bellows

The technique avoids the damage caused by the trimming of thin material on a lathe.

Marshall Space Flight Center, Alabama

Near perfect contamination exclusion! Fits "snap-in" O-ring glands.



RSA Scraper.

- Compression-actuated for tight seal at both dynamic and static interfaces.
- Operates at temperatures from -40° to 250°F .
- Functions at high linear speeds and with heavy side loading.
- Can be incorporated into bearing-retaining nut. Proven in hydraulic actuators, piston rods, etc. Call, or write for Bulletin RSAS.

GT GREENE, TWEED & CO
North Wales, PA 19454 • USA • (215)256-9521

A laser cutting technique produces narrow, precise, fast, and repeatable cuts in thin nickel-alloy bellows material. This technique avoids the distortion, dents, and nicks produced in delicate materials during lathe trimming operations, which require high cutting-tool pressure and holding-fixture forces.

The laser cutting operation uses an intense focused beam to melt the material and an assisting gas to force the melted material through the part thickness, creating a void. When the part is rotated or moved longitudinally, the melting and material removal is continuous and creates a narrow, fast, precise, and repeatable cut. This technique can be used to produce cuts of specified depths less than the material thickness.

With argon as the assisting gas, a 400-W Nd: YAG laser has been used in three cutting operations on the multiple plies of a thin [0.014 to 0.018 in. (0.36 to 0.46 mm)] nickel-base alloy 718 used to fabricate the Space Shuttle main engine flex duct bellows. The operations were marking pass, seal weld trim, and ending trim. A "marking pass" operation places a narrow, shallow line on the outer bellows ply, running parallel to and at a specified distance from the bellows first convolution wall. A "seal weld trim" operation cuts through an existing electron-beam weld approximately 0.028 in. (0.71 mm) deep and 0.040 in. (1.0 mm) wide. This trim is a critical operation, because all nonfused ply material must be removed from one side of the weld while leaving a sufficient amount of weld nugget on the part for subsequent electron-beam welding without fusion of the remaining bellows plies. An "end ring trim" operation cuts through a one-ply end ring approximately 0.060 in. (1.5 mm) thick. This trim operation removes excess manufacturing stock from the bellows end ring and generates a surface that must comply with four drawing requirements.

This work was done by Craig L. Butler of Rockwell International Corp. for Marshall Space Flight Center. No further documentation is available. MFS-29133

Books and Reports

These reports, studies, and handbooks are available from NASA as Technical Support Packages (TSP's) when a Request Card number is cited; otherwise they are available from the National Technical Information Service.

Theoretical Foundation for Weld Modeling

Differential equations describe the physics of tungsten/inert-gas and plasma-arc welding in aluminum.

A report collects and describes the necessary theoretical foundation upon which a numerical welding model could be constructed for tungsten/inert gas or plasma-arc welding in aluminum without a keyhole. The governing partial differential equations for the flow of heat, metal, and current are given, together with boundary conditions relevant to the welding process. Numerical estimates for the relative importance of various phenomena and the required properties of 2219 aluminum are included.

This is apparently the first attempt to construct a single model that simultaneously incorporates realistic three-dimensional geometries and boundary conditions, while also predicting the moving phase-change boundary as determined by latent-heat considerations and calculated velocities in the weld puddle. Concentrating on the weld puddle, the report provides the necessary governing equations and associated boundary conditions that determine the temperatures and the flow of heat in the heat-affected zone of the workpiece, the shape of the puddle, and the flow of metal and current in the puddle.

The resulting model did not cover all aspects of welding in complete generality. At present, it would be premature to attempt to incorporate metal transfer from a consumable electrode, or welding rod or wire, plasma flow and heat transfer in the arc, and the much more complex aspects of weld-puddle shape for high-power-density welding practices that produce vapor cavities. Instead, the report is aimed at the modeling of autogenous, nonconsumable (tungsten) electrode gas- or plasma-arc welding without a keyhole — the kind of welding of particular importance in aluminum structures. While not all inclusive, the theory can be used to produce quantitative answers to

questions that have not yet been addressed. These include the relative roles of stirring due to the variation of surface tension with temperature versus magnetohydrodynamic stirring in determining puddle shape and the effects of changes in arc pressure, velocities, and shear.

Because of the multiplicity of phenomena contained in the general case, the numerical modeling results will be difficult to interpret. Therefore, the value of such computations would be greatly enhanced by examining separate, simplified cases in which the various phenomena are treated in isolation. Results for such special cases will enhance general un-

derstanding and the interpretation of more general results. These results may reveal that some of the effects and phenomena included in the very general description may be of minor practical consequence and thus do not need to be included and that others are of greater importance than presently realized.

This work was done by S. C. Traugott of Martin Marietta Corp. for Marshall Space Flight Center. To obtain a copy of the report, "Discrete Element Weld Model. Phase I: General Model of a Weld Puddle Without a Cavity," Circle 48 on the TSP Request Card.
MFS-27095

Cost effective fabrics for people who can't afford failures.



Aerospace...Defense...Composites... Safety Apparel...Filtration

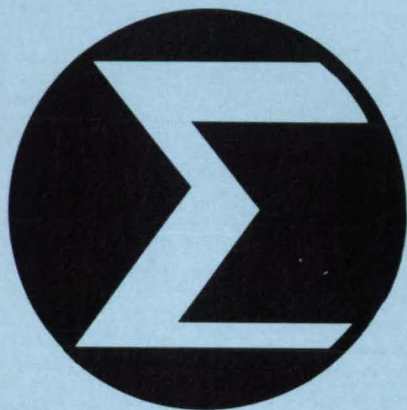
More than 300 fabrics engineered to exacting performance specifications are being used to insulate, dampen, seal, filter, suppress noise, retard fire, protect people and resist hostile environments. Tex-Tech Industries has the problem-solving experience and manufacturing capabilities to produce fabrics that exceed your expectations of performance.

We can help shape your ideas from concept to production with the "material difference".

Contact Tex-Tech Industries, Inc., Main Street, P.O. Box 8, North Monmouth, ME 04265. Call (207) 933-4404.

**TEX
TECH
INDUSTRIES, INC.**

Mathematics and Information Sciences



Hardware, Techniques, and Processes

- 148 Digital Filter Separates Signal from Noise
- 149 Adaptive Quantizer for Burst Synthetic-Aperture Radar

Books & Reports

- 150 Autonomous Orbital Calculation for Satellites
- 151 Decluttering Methods for Computer-Generated Graphic Displays

Computer Programs

- 86 Graphics Programs for the Dec Vax Computer
- 86 Computing Benefits and Costs for Propulsion Systems
- 86 Analyzing Multidimensional Image Data
- 88 High-Level Data-Abstraction System
- 88 Constant-Elasticity-of Substitution Simulation
- 90 An Expert-System Engine with Operative Probabilities

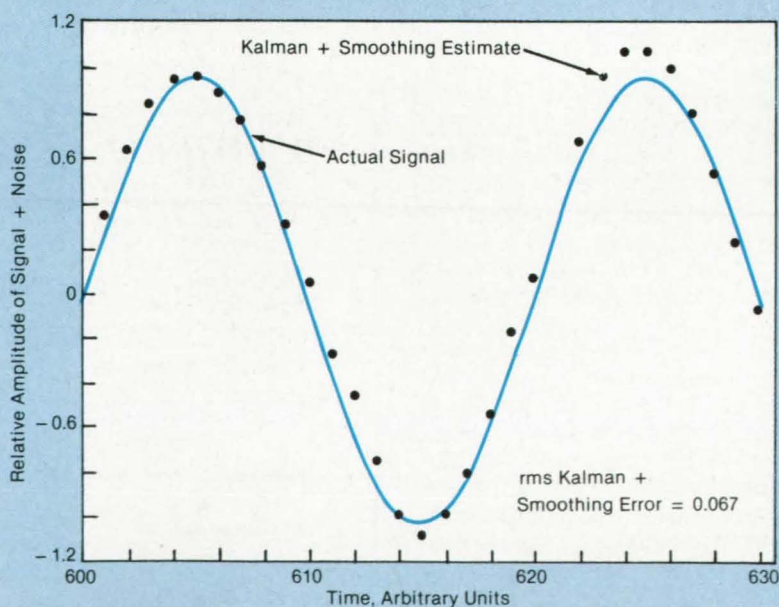
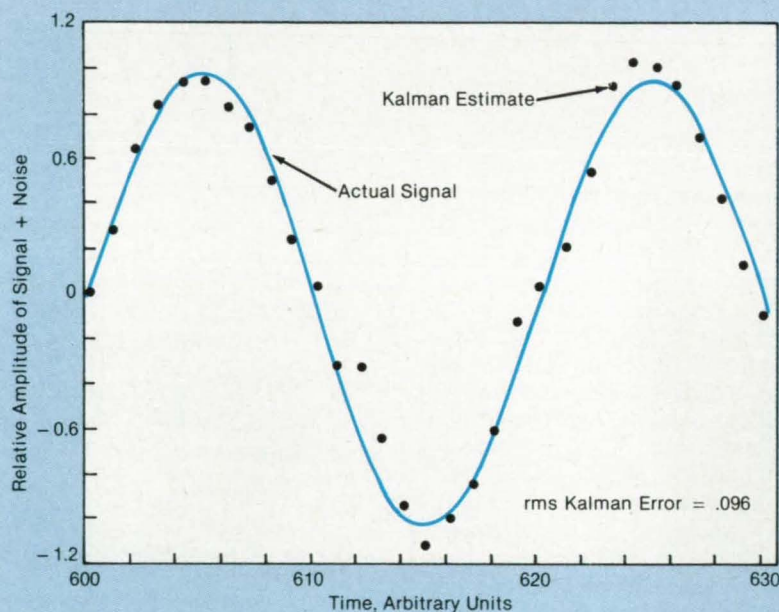
Digital Filter Separates Signal From Noise

The variance of the signal-estimation error is minimized.

Lyndon B. Johnson Space Center, Houston, Texas

A mathematical technique extracts best estimates of a signal component from periodic digital samples of a signal plus noise. The technique combines Kalman- and smoothing-filter algorithms

to minimize the mean-square estimation error based on past, present, and predicted samples of the signal plus noise. The technique will be useful in image analysis and other applications involving



Estimates of a Signal extracted from signal plus noise were made by Kalman filtering alone (above) and by Kalman-plus-smoothing filtering (below). The rms error is smaller with smoothing, signifying a better estimate.

the processing of noisy signals.

The objective is to find the signal $x(t)$ in a received or measured waveform $z(t) = x(t) + s(t)$, where t = time and $s(t)$ = the noise component. In Kalman filtering, samples of the waveform are taken at the present and at past times t_i, t_{i-1}, t_{i-2} , etc. A Kalman filter provides an optimal estimate of the signal components of the samples, provided that the autocorrelation functions of the signal and additive noise are known. The task in Kalman filtering is to obtain the difference equations for the signal and noise dynamics that give the correct autocorrelation

functions for the signal and noise.

The difference equations generally involve polynomials of finite order, the coefficients of which yield the Kalman-filter coefficients. The Kalman-filter equations provide the best estimate for $x(t_i)$ based on all the data $z(t_j)$ received prior to the present time, t_i . It is possible, however, to improve the estimate by using predicted data for times beyond t_i . These estimates are provided by the smoothing equations, which use the initial output of the Kalman filter to make the predictions.

Difference equations have been derived for the first through fourth orders. In

one test of the technique, second-order difference equations were used on a signal with an autocorrelation function consisting of a cosine multiplied by an exponential and an exponential noise autocorrelation function. The figure shows the Kalman (alone) and Kalman-plus-smoothing estimates for this case. The rms error was 30 percent less with smoothing.

This work was done by William M. Lear of TRW, Inc., for Johnson Space Center. For further information, Circle 4 on the TSP Request Card.
MSC-20914

Adaptive Quantizer for Burst Synthetic-Aperture Radar

Unneeded bits are discarded to facilitate computation.

NASA's Jet Propulsion Laboratory, Pasadena, California

An adaptive quantizer for burst-mode synthetic-aperture radar reduces the data rate of the return signal. The device, called a block floating-point quantizer (BFPQ) is basically an analog-to-digital converter that covers a wide dynamic range and discards appropriate lower order bits. The BFPQ is, in effect, a digital approximator with automatic gain control.

The BFPQ moves the floating-point marker (i.e., the decimal point) in the binary representation of signal data in accordance with the perceived dynamic range. The available step sizes are thus limited to multiples of the underlying

smallest quantization step (represented by the lowest order bit). The BFPQ retains only the first K most significant bits of the signal; an (L, K) BFPQ is one that does K -bit quantization of a signal that is originally quantized to L bits. For example, an $(8, 2)$ BFPQ that receives a signal near the middle of its dynamic range might retain the 3rd and 4th or the 4th and 5th bits.

To design a BFPQ, it is necessary to select optimally the dynamic range $2X_{\max}$ and the number, K , of quantization bits of the L available. This requires consideration of the quantization error and its contribution to noise. Of course, the thermal

noise contribution must also be considered, and the combined effects of both noise sources on the overall signal-to-noise ratio must be determined.

The quantization error is simply the difference between the actual signal level and its binary approximation. The BFPQ selects the K contiguous bits for the present burst on the basis of the signal received during the previous burst. The selection does not change during a burst, even when the signal goes above or below the present K -bit range. When the signal changes drastically in this way during a burst, an incorrect gain is selected.

The BFPQ concept has been tested



Burst-Mode Synthetic-Aperture-Radar Images were made of the Pissgah lava flow at Pissgah, California. The left image was made with a 1-bit (nonadaptive) quantizer. The right image was made with an $(8, 1)$ block floating-point quantizer.

numerically and experimentally. The figure shows a burst-mode synthetic-aperture-radar image processed by 1-bit uniform (that is, nonadaptive) quantization and by (8,1) adaptive quantization. The adaptively processed image shows

an improvement in dynamic range. Other potential applications for the BFPQ include speech compression and picture-data compression.

This work was done by Tae H. Joo, Daniel N. Held, Rolando L. Jordan, and

Fuk K. Li of Caltech for NASA's Jet Propulsion Laboratory. For further information, Circle 98 on the TSP Request Card. NPO-16582

Books and Reports

These reports, studies, and handbooks are available from NASA as Technical Support Packages (TSP's) when a Request Card number is cited; otherwise they are available from the National Technical Information Service.

Autonomous Orbital Calculation for Satellites

An onboard orbital navigation system would reduce dependence on Earth-to-satellite links.

A report discusses the mathematics of a proposed navigation subsystem that would keep a geostationary satellite in its proper orbit without ground control. The subsystem uses data from Earth and Sun

sensors to activate thrusters for station-keeping maneuvers. With sensors already on satellites for determining attitude, the subsystem should be able to maintain the satellite within 3° of a specified equatorial longitude for up to 6 months. With more accurate sensors, the subsystem should be able to maintain the orbit within 0.1°.

The key parameter for maintaining the orbit is the angle formed between two lines extending from the satellite, one to the center of the Earth, the other to the center of the Sun. This angle is independent of the satellite attitude and therefore

is not perturbed by errors in the attitude-sensing and attitude-control subsystems. The angle is computed from the inner product of the satellite-to-Earth and satellite-to-Sun vectors measured by the satellite Earth and Sun sensors and the solar-array drive potentiometer.

A time series of measurements is required to determine the orbit, especially since errors need to be averaged or filtered out as much as possible. Position information at different times is related through the orbital equations of motion. As they are acquired, the measurements

ARAC Finds Answers To Questions You Never Knew You Had!!

1. **IMAGINE** A resource that could provide total access to disclosed technology data worldwide.
2. **IMAGINE** That this resource is staffed with the finest scientific and engineering minds to assist you in acquiring these data.

An ARAC Technology Transfer Process Provides:

- An edited search of all relevant published technologies.
- Full texts highlighting the most significant information.
- Contacts with identified technical experts.
- Overall analysis and discussion of key findings by experienced ARAC engineers.

3. **UTILIZE ARAC** services and find the best possible answers to your technical questions at the best possible prices.

For Those Answers Contact:

Ms. Chris Schell
ARAC
611 N. Capitol Avenue
Indianapolis, IN 46204
317/262-5003

A NASA Supported Industrial Applications Center

There is a Solution.

- ✓ memory loss
- ✓ board failure
- ✓ read-write errors
- ✓ "hung" equipment
- ✓ costly downtime

The above headaches, caused by spikes, surges, transients, common and normal mode noise, effect all micro-processor based equipment.

A word of caution:

The industry today is being inundated with filters and surge suppressors of all types, shapes and prices. Do not be misled by grossly exaggerated performance claims. TyCOR® has been the leader in the AC Power Line Filter Industry for 10 years and its products continue to meet and exceed the rigid performance tests imposed by the industry.

The New Improved High Efficient...



Circle Reader Action No. 308

are processed by a sequential, extended Kalman filtering algorithm; therefore, the measurements need not be stored. The equations assume that errors can be modeled as Gaussian noise so that the system is modeled as a whole by a stochastic differential equation.

Assuming a set of typical orbital parameters and angle measurements every 30 minutes, the authors conclude that station-keeping maneuvers are likely to be the major contributors to error. Such maneuvers are infrequent, however. The numerical integrator should be the next largest source of error. This type of error is a result of the rounding off imposed by the limitations of the onboard computer and could be reduced by improving the integration algorithm. Two additional ways of improving performance include adaptive filtering and data compression.

This work was done by Kenneth D. Mease, Mark S. Ryne, and Lincoln J. Wood of Caltech for NASA's Jet Propulsion Laboratory. To obtain a copy of the report, "An Approach to Autonomous Onboard Orbit Determination," Circle 79 on the TSP Request Card.
NPO-16532

Decluttering Methods for Computer-Generated Graphic Displays

Symbol simplification and contrasting enhance the viewer's ability to detect a particular symbol.

A report describes the experiments designed to indicate how various decluttering methods affect the viewer's abilities to distinguish essential from nonessential features on computer-generated graphic displays. The results indicate that partial removal of nonessential graphic features through symbol simplification was as effective in decluttering as the total removal of nonessential graphic features.

It had been hypothesized that search time is proportional to the number of visual features present in a display. Based on this hypothesis, the total removal of nonessential features would yield the most rapid search. The search would take longer if decluttering is done by contrasting (in which nonessential features remain on the display but are reduced in line width and intensity) than if it is done by simplification (partial removal of nonessential features). Similarly, search time would be greater when graphic products are displayed against a map background than without this background. This hypothesis was tested in a study in which the participants' task was to count the number of a particular class of displayed symbols as decluttering methods and map backgrounds were varied.

The hypothesis was supported in part: The total removal of extraneous symbols and simplification of these symbols facilitated search speed and accuracy relative to contrasting and no decluttering, while contrasting facilitated performance relative to no decluttering. In these cases, fewer graphic features were present after removal and simplification than after contrasting.

However, the hypothesis is contradicted by several aspects of the data:

- Removal, which produced the greatest reduction in visual features, did not significantly reduce the response time in comparison to simplification.
- Map backgrounds, which contained high levels of graphic features, did not yield a main effect upon response time; instead, they caused an increase in performance after contrasting and a decrease in performance after simplification. These results therefore indicate that the hypothesis is only partially true.

NASA Tech Briefs, May/June 1986

The degree to which decluttering makes essential graphic information distinctive, rather than the absolute number of visual features per se, appears to be critical in determining response time. Thus, even though more graphic information remains after simplification than after removal, both decluttering operations produce a small set of highly distinctive symbols that can be readily located. The presence of another set of smaller, simplified symbols after simplification does not increase the response time relative to removal because these simplified symbols readily stand out against the essential symbol set and vice-versa. Similarly, map backgrounds appear to increase the color contrast between essential and nonessential symbols. Thus, in contrasting, the presence of additional graphic features (for example, terrain markings and road symbols) enhances the discrimination between single-line and double-line-width symbols.

These results not only suggest a theoretical framework for studying decluttering, but also demonstrate the viability of simplification and contrasting as decluttering methods. Both of these methods still allow users to perceive interrelationships among the various graphic display elements, yet enable essential graphic elements to be perceptually distinct. Although simplification is the more effective of these two methods, contrasting is preferred by users. If users are given the option to declutter hierarchically, the first level of decluttering could be contrasting, followed by simplification or removal or both at the second level.

This work was done by E. Eugene Schultz, Jr., of Caltech for NASA's Jet Propulsion Laboratory. To obtain a copy of the report, "Decluttering Methods for High Density Computer-Generated Graphic Displays," Circle 40 on the TSP Request Card.

NPO-16733

Tycor AC Power Line Filters . . .

the **POWERful** Solution. ✓

Tycor filters eliminate the need for dedicated lines, costly re-boots, decrease down-time, service calls, board replacement, and the need for large spare parts inventory. They have proven to be cost effective in less than 3 days on problem sites and 90 days on typical sites.

(actual field evaluations by national companies show an 81% decrease in service calls)

TYCOR ELECTRONIC PRODUCTS LTD.

Head Office:
6107 - 6th Street S.E.
Calgary, Alberta, Canada
T2H 1L9

**FOR A DISTRIBUTOR
NEAREST YOU CALL
TOLL FREE:
1-800-661-9263**



Circle Reader Action No. 309

151



Hardware, Techniques, and Processes

152 Small-Portion Water Dispenser
152 Rotating Apparatus for Isoelectric Focusing

Small-Portion Water Dispenser

Pressure is regulated and flow is timed to control the amount dispensed.

Lyndon B. Johnson Space Center, Houston, Texas

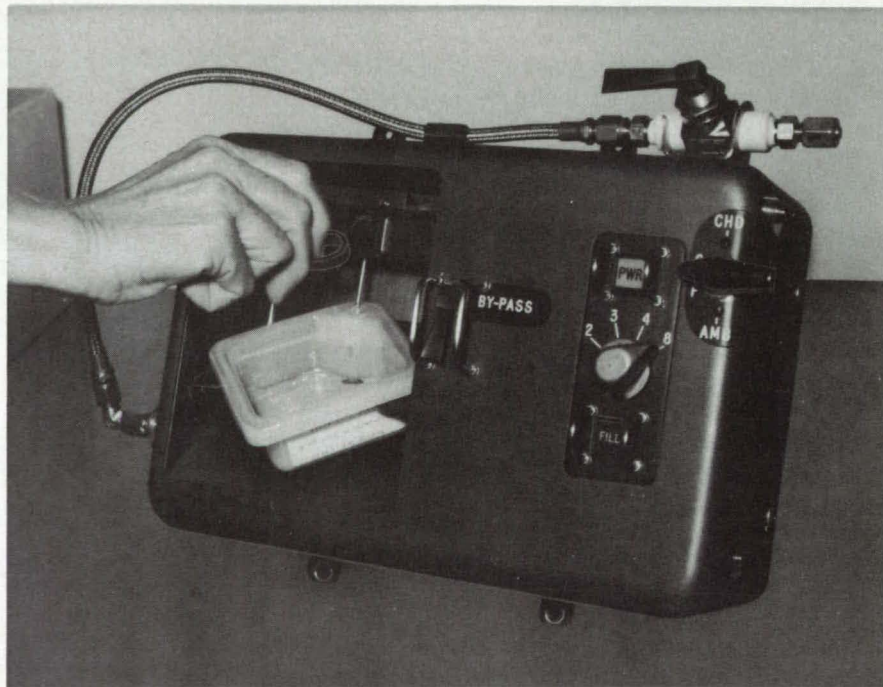
A dispenser provides a measured amount of water for reconstituting dehydrated foods and beverages. The dispenser holds the food or beverage package while it is being filled with either cold or room-temperature water (see figure). Other uses might include the dispensing of fluids or medicine.

A pressure regulator in the dispenser reduces the varying pressure of the water supply to a constant pressure. An electronic timer stops the flow after a predetermined length of time. The timed flow at regulated pressure ensures that a controlled volume of water is dispensed.

The user inserts a package to be filled in a nest in the dispenser and adjusts the

dispensing needle to pierce the septum of the package. The "power" button is then depressed and a selector valve is turned to the cold ("CHD" in the figure) or room-temperature ("AMB" in the figure) position. After choosing the amount of water — 2, 3, 4, or 8 ounces (59, 89, 118, or 237 milliliters) — the user depresses the "fill" button. When the dispenser has filled the package, the user disengages the needle and removes the package.

This work was done by Jack C. Joerns of Technology Inc., for Johnson Space Center. For further information, Circle 74 on the TSP Request Card.
MSC-20534



The **Dispensing Unit** is shown here in operation with the dispensing needle about to penetrate a plastic food package.

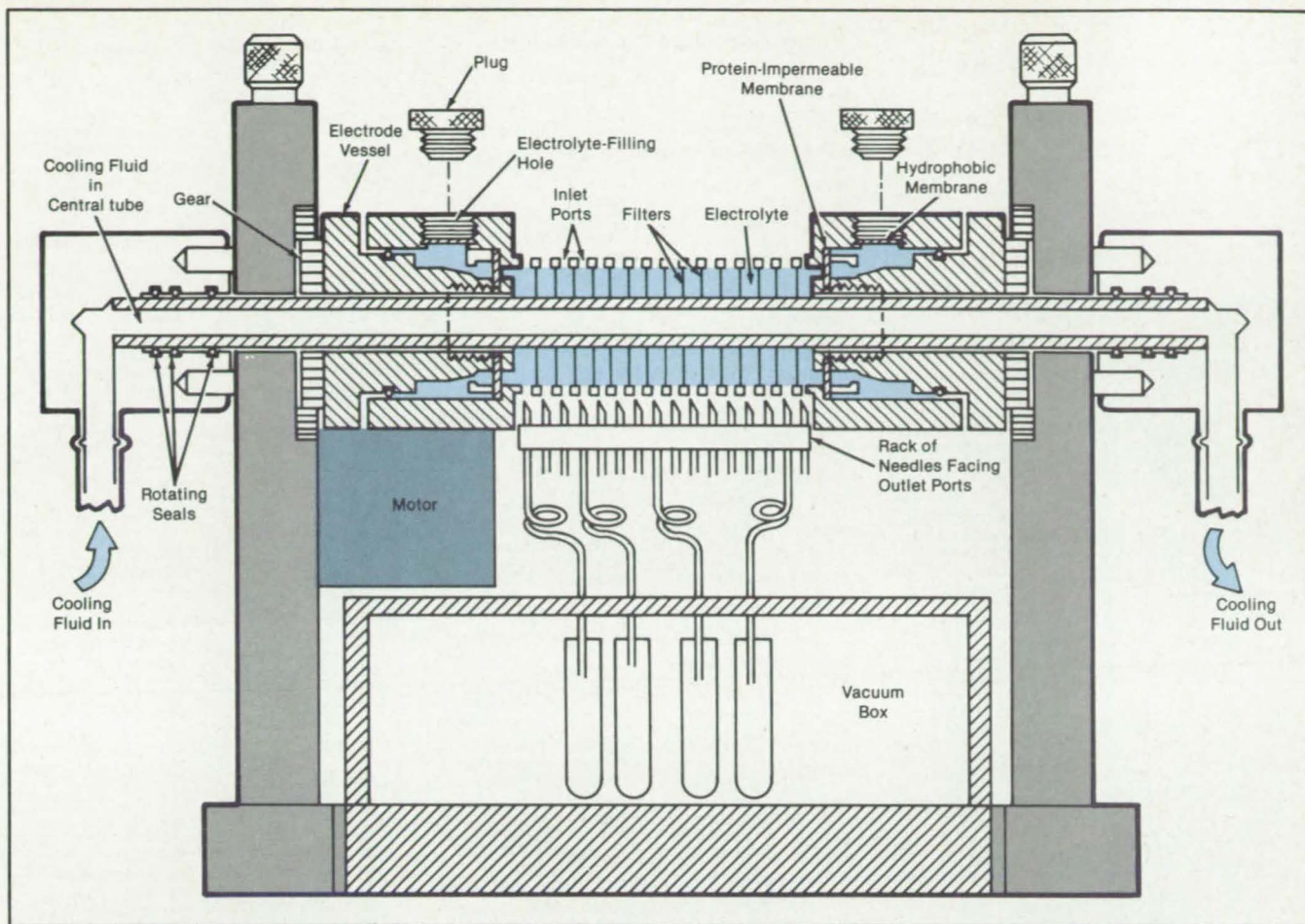
Rotating Apparatus for Isoelectric Focusing

The remixing of separated fractions is prevented.

Marshall Space Flight Center, Alabama

An improved isoelectric focusing apparatus helps to prevent electro-osmosis and convection, both of which cause the remixing of separated fractions. The frac-

tionating column is segmented and rotated about a horizontal axis: Only the combined effects of both features are fully effective in making good separations.



The Improved Isoelectric Focusing Column is rotated and segmented to prevent the remixing of separated protein fractions.

Isoelectric focusing is an electrophoretic process in which mixtures of proteins in an electrolyte are separated into components, each of which migrates to an equipotential surface or region in which it comes to rest. The separated fractions are then withdrawn individually for further analysis.

The improved apparatus (see figure) is slowly rotated continuously or rocked (at a rotational amplitude of at least 180°) about its horizontal axis so that the average gravitational vector experienced by the fluid is zero and convection is therefore suppressed. Electro-osmosis is suppressed and convection is further suppressed by separating the column into disklike compartments along its length with filters.

The filters may be, for example, monofilament nylon screens of fine porosity offering some resistance to bulk fluid convection but allowing the free passage of electric currents and protein molecules. Each protein can therefore move into one

or more compartments, the contents of which are closest to its isoelectric point (the electric potential at which it comes to rest).

Each compartment has an inlet and an outlet port. The column is filled by taping the outlet ports closed, then manually injecting the fluid to be fractionated through the inlet ports. The inlet ports are taped closed before beginning rotation and applying the axial electric field.

The column would normally be made of glass or a transparent plastic like poly(methyl methacrylate). If the proteins are colored, the separation process can be viewed. The process can also be observed by an increase in the electrical resistance of the fluid along the column. Isoelectric focusing is preferably done at constant power, with the electric field gradually increasing from 5 to 10 V/cm up to 100 to 200 V/cm as the resistance increases.

The electric field is introduced by platinum electrodes at each end of the col-

umn and conducted by an electrolyte to the end compartments. Protein-impermeable membranes separate the protein-containing electrolyte of the column from the electrode electrolyte. A hydrophobic membrane allows the venting of electrolytically generated gases without spilling fluid.

Experiments have shown that the dimensions of the apparatus are not critical. Typical compartment and column volumes are 2 and 40 ml, respectively. Rotation speeds can lie between 3 and 30 rpm.

This work was done by Milan Bler of the University of Arizona for Marshall Space Flight Center. For further information, Circle 76 on the TSP Request Card.

Title to this invention, covered by U.S. Patent Nos. 4,204,929 and 4,362,612, has been waived under the provisions of the National Aeronautics and Space Act [42 U.S.C. 2457(f)], to the University of Arizona, Tucson, AZ 85721.
MFS-26012

Subject Index



A

ACOUSTIC IMPEDANCE

Acoustic-liner admittance in a duct page 101 LAR-13399

ACOUSTIC LEVITATION

Acoustic levitator maintains resonance page 145 NPO-16649

Acoustic translation of an acoustically levitated sample page 144 NPO-16675

ACTIVATION

Wireless jump starts for partly disabled equipment page 49 MSC-21010

AERODYNAMIC BRAKES

Orbital-transfer vehicle with aerodynamic braking page 125 MSC-20921

AERODYNAMIC DRAG

Two-axis, self-nulling skin-friction balance page 98 LAR-13294

AERODYNAMIC NOISE

Acoustic-liner admittance in a duct page 101 LAR-13399

AEROSPACE ENVIRONMENTS

Predicting the cosmic-ray environment near Earth page 78 NPO-16617

AGRICULTURAL AIRCRAFT

Predicting aircraft spray patterns on crops page 78 LAR-13432

AIR COOLING

Computing cooling flows in turbines page 83 LEW-13999

AIRCRAFT

Crash tests of protective airplane floors page 127 LAR-13414

AIRCRAFT BRAKES

Aircraft rollout iterative energy simulation page 82 MSC-20816

AIRCRAFT ENGINES

High-speed propeller for aircraft page 115 LEW-14241

HYTESS — hypothetical turbofan-engine simplified simulation page 82 LEW-14020

AIRCRAFT INSTRUMENTS

Sensing horizontal heading in aircraft maneuvers page 100 FRC-11043

ALUMINUM

Weld repair of thin aluminum sheet page 137 MSC-20902

ANALOG CIRCUITS

Analog video image-enhancing device page 46 LAR-13336

ANALOG TO DIGITAL CONVERTERS

Adaptive quantizer for burst synthetic-aperture radar page 149 NPO-16582

ANNULAR FLOW

Equations for annular-heat-transfer coefficients page 96 MFS-29074

ANTENNA RADIATION PATTERNS

Passive element shapes antenna radiation pattern page 41 NPO-16632

ANTENNAS

Passive element shapes antenna radiation pattern page 41 NPO-16632

ATTITUDE INDICATORS

Sensing horizontal heading in aircraft maneuvers page 100 FRC-11043

AXIAL FLOW TURBINES

Computing cooling flows in turbines page 83 LEW-13999

B

BINARY ALLOYS

Separation in binary alloys page 72 MFS-27074

BONDING

Thermally activated metal-to-glass bonding page 128 NPO-16423

BOUNDARY LAYER TRANSITION

Continuous, multielement, hot-film transition gage page 97 LAR-13319

BRAKES (FORMING OR BENDING)

Adjustable tooling for bending brake page 124 MSC-20730

BULK ACOUSTIC WAVE DEVICES

Measuring acoustic-radiation stresses in materials page 101 LAR-13440

BURSTS

Predicting failures of composite, spherical pressure vessels page 82 MFS-27050

C

CALIBRATING

Vacuum-ultraviolet intensity-calibration standard page 56 NPO-16621

CAPACITANCE

Variable synthetic capacitance page 36 GSC-12961

CERAMICS

Lightweight ceramic insulation page 65 MSC-20831

CHARACTERIZATION

A method for characterizing PMR-15 resin page 67 LEW-14253

CIRCUITS

Unbalanced-to-balanced video interface page 40 MSC-20950

CLUSTER ANALYSIS

Analyzing multidimensional image data page 86 GSC-12935

CLUTCHES

Non-back-drivable, freewheeling coupling page 112 MSC-20475

CMOS

Radiation hardening of computers page 50 NPO-16767

COATINGS

Depositing diamondlike carbon films page 139 LEW-14080

Effects of radiation on coatings page 71 NPO-16533

Measuring thickness of coatings on metals page 94 MFS-28126

COMMUNICATION SATELLITES

Economic-analysis program for a communication system page 74 NPO-16606

COMMUNICATION THEORY

Automated signal-to-noise ratio measurement page 48 MSC-21021

COMPUTER GRAPHICS

Decluttering methods for computer-generated graphic displays page 151 NPO-16733

Flutter- and vibration-animation program page 80 MSC-20895

Graphics programs for the DEC VAX computer page 86 NPO-16666

COMPUTER TECHNIQUES

Analyzing multidimensional image data page 86 GSC-12935

COMPUTERIZED SIMULATION

Aircraft rollout iterative energy simulation page 82 MSC-20816

Constant-elasticity-of-substitution simulation page 88 NPO-16524

HYTESS — hypothetical turbofan-engine simplified simulation page 82 LEW-14020

CONTROL RODS Hydraulic actuator for ganged control rods page 119 NPO-16503

CONTROL THEORY

Research program for vibration control in structures page 80 NPO-16615

CONTROL VALVES

Spring-loaded Joule-Thomson valve page 101 NPO-16546

COSMIC RAYS

Predicting the cosmic-ray environment near Earth page 78 NPO-16617

COST ANALYSIS

Computing benefits and costs for propulsion systems page 86 LEW-14129

COSTS

Constant-elasticity-of-substitution simulation page 88 NPO-16524

COUPLINGS

Non-back-drivable, freewheeling coupling page 112 MSC-20475

Self-aligning electrical connector page 33 MFS-26022

CRACK PROPAGATION

Crack growth in single-crystal silicon page 73 NPO-16757

CRACKS

Locating cracks amid pitting and corrosion page 110 MSC-20311

CRASH LANDING

Crash tests of protective airplane floors page 127 LAR-13414

CROP DUSTING

Predicting aircraft spray patterns on crops page 78 LAR-13432

CRYOGENIC ROCKET PROPELLANTS

Estimating transient pressure surges in cryogenic systems page 83 KSC-11312

CRYOPUMPING

Pump for saturated liquids page 117 NPO-16152

CRYSTAL GROWTH

Electron-diffraction analysis of growth of GaAs page 59 NPO-16755

CRYSTAL OSCILLATORS

Temperature-sensitive oscillator page 39 GSC-12958

Variable synthetic capacitance page 36 GSC-12961

CUTTING

Material for fast cutting page 70 MFS-29130

D

DATA LINKS

High-level data-abstracting system page 88 LAR-13244

DATA PROCESSING

Adaptive quantizer for burst synthetic-aperture radar page 149 NPO-16582

DECISION THEORY

An expert-system engine with operative probabilities page 90 LAR-13382

DEHYDRATED FOOD

Small-portion water dispenser page 152 MSC-20534

DELAMINATING

Preventing delamination of silvered FEP films page 64 MSC-20460

DIAMONDS

Depositing diamondlike carbon films page 139 LEW-14080

DICHROISM

Filters for submillimeter electromagnetic waves page 136 NPO-16498

DIGITAL COMPUTERS

Graphics programs for the DEC VAX computer page 86 NPO-16666

DIGITAL FILTERS

Digital filter separates signal from noise page 148 MSC-20914

DIRECTIONAL SOLIDIFICATION (CRYSTALS)

Separation in binary alloys page 72 MFS-27074

DISPENSERS

Small-portion water dispenser page 152 MSC-20534

DISPLAY DEVICES

Adjustable work station for video displays and keyboards page 44 MFS-26009

Decluttering methods for computer-generated graphic displays page 151 NPO-16733

DRAFTING

Parallel-end-point drafting compass page 103 MFS-29070

DRAFTING MACHINES

Parallel-end-point drafting compass page 103 MFS-29070

DRILL BITS

Modified drills with oil passages page 106 MFS-29137

DRILLING

Adapting inspection data for computer numerical control page 112 MFS-29117

DUCTS

Eliminating thermal cracks in flange/duct joints page 111 MSC-20833

Eliminating thermal cracks in flange/duct joints page 111 MSC-20833

Eliminating thermal cracks in flange/duct joints page 111 MSC-20833

Eliminating thermal cracks in flange/duct joints page 111 MSC-20833

Eliminating thermal cracks in flange/duct joints page 111 MSC-20833

Eliminating thermal cracks in flange/duct joints page 111 MSC-20833

Eliminating thermal cracks in flange/duct joints page 111 MSC-20833

Eliminating thermal cracks in flange/duct joints page 111 MSC-20833

in structural dynamic testing page 104 NPO-16620

E

ECHLETTE GRATINGS

Echelle/grism spectrograph page 54 GSC-12977

ECONOMIC ANALYSIS

Constant-elasticity-of-substitution simulation page 88 NPO-16524

Economic-analysis program for a communication system page 74 NPO-16606

ELECTRIC BATTERIES

Multikilowatt bipolar nickel/hydrogen battery page 39 LEW-14244

Reinforcing the separators for lithium/carbon cells page 70 NPO-16619

ELECTRIC CONNECTORS

Self-aligning electrical connector page 33 MFS-26022

ELECTRIC IGNITION

Ignition system for gaseous propellants page 120 MFS-29125

ELECTROMAGNETIC WAVE FILTERS

Filters for submillimeter electromagnetic waves page 136 NPO-16498

ELECTROPHORESIS

Rotating apparatus for isoelectric focusing page 152 MFS-26012

ENCAPSULATING

Tests of solar-array encapsulants page 71 NPO-16387

ENGINE DESIGN

Four-cylinder Stirling-engine computer program page 83 LEW-14155

EQUATIONS OF MOTION

Overcoming robot-arm joint singularities page 126 LAR-13415

ETCHING

Electrochemical process makes fine needles page 135 NPO-16311

Etching silicon films with xenon difluoride page 62 NPO-16527

F

FASTENERS

Composite fasteners page 142 LAR-13058

Unitized nut-and-washer assembly page 141 MSC-20903

FIBER OPTICS

Receptacle for optical-fiber scraps page 117 KSC-11326

FILM THICKNESS

Measuring thickness of coatings on metals page 94 MFS-28126

FLANGES

Eliminating thermal cracks in flange/duct joints page 111 MSC-20833

FLOORS

Crash tests of protective airplane floors page 127 LAR-13414

FLUTTER

Flutter- and vibration-animation program page 80 MSC-20895

FRACTIONATION

Rotating apparatus for isoelectric focusing page 152 MFS-26012

FRACTURES (MATERIALS)
Locating cracks amid pitting and corrosion
page 110 MSC-20311

FREQUENCY CONTROL
Acoustic levitator maintains resonance
page 145 NPO-16649

FRICIONLESS MEASUREMENT
"Two-axis, self-nulling skin-friction balance"
page 98 LAR-13294

FRICIONLESS ENVIRONMENT
Acoustic translation of an acoustically levitated sample
page 144 NPO-16675

FUEL CELLS
Thermally-integrated fuel-cell/electrolyzer systems
page 118 LEW-14235

G

GALLIUM ARSENIDES
Electron-diffraction analysis of growth of GaAs
page 59 NPO-16755

GAS PRESSURE
Feedback-controlled regulation of gas pressure
page 102 GSC-12990

GAS STREAMS
Controlled-temperature hot-air gun
page 123 MSC-20693

GAS TUNGSTEN ARC WELDING
Theoretical foundation for weld modeling
page 147 MFS-27095

GAS TURBINE ENGINES
Effects of gear-cutter geometry on performance
page 114 LEW-14243

GEOTHERMAL TECHNOLOGY
Theory and tests of two-phase turbines
page 126 NPO-16039

GLASS
Thermally activated metal-to-glass bonding
page 128 NPO-16423

GLAZES
Fast glazing of alumina/silica tiles
page 66 MSC-20976

GLOBAL POSITIONING SYSTEM
Autonomous orbital calculation for satellites
page 150 NPO-16532

H

HEAT EXCHANGERS
Repairing hard-to-reach cracks in heat-exchanger tubes
page 138 MFS-29128

HEAT TRANSFER COEFFICIENTS
Equations for annular-heat-transfer coefficients
page 96 MFS-29074

HELICOPTER CONTROL
Helicopter pitch-control mechanism reduces vibration
page 122 ARC-11513

HELICOPTERS
Helicopter pitch-control mechanism reduces vibration
page 122 ARC-11513

HERMETIC SEALS
Thermally activated metal-to-glass bonding
page 128 NPO-16423

HIGH TEMPERATURE AIR
Controlled-temperature hot-air gun
page 123 MSC-20693

HIGH VOLTAGES
Self-aligning electrical connector
page 33 MFS-26022

HOLDERS
Composite fasteners
page 124 LAR-13058

HOT-WIRE TURBULENCE METERS
Continuous, multielement, hot-film transition gage
page 97 LAR-13319

HUMAN FACTORS ENGINEERING
Adjustable work station for video displays and keyboards
page 44 MFS-26009

HYDRAULIC ACTUATORS
Hydraulic actuator for ganged control rods
page 119 NPO-16503

HYDROGEN OXYGEN FUEL CELLS
Thermally-integrated fuel-cell/electrolyzer systems
page 118 LEW-14235

I

IGNITION SYSTEMS
Ignition system for gaseous propellants
page 120 MFS-29125

IMAGE ANALYSIS
Digital filter separates signal from noise
page 148 MSC-20914

IMAGE ANALYSIS
Analyzing multidimensional image data
page 86 GSC-12935

IMAGE ENHANCEMENT
Analog video image-enhancing device
page 46 LAR-13336

IMAGE TRANSDUCERS
Two-element transducer for ultrasound
page 38 NPO-16591

INCOMPRESSIBLE FLOW
Evaluation of mathematical turbulence models
page 104 MFS-27118

INERTIAL NAVIGATION
Laser inertial navigation system
page 53 ARC-11473

INSPECTION
Locating cracks amid pitting and corrosion
page 110 MSC-20311

INSULATION
Lightweight ceramic insulation
page 65 MSC-20831

INTEGRATED CIRCUITS
Masking technique for ion-beam sputter etching
page 140 LEW-13899

INTERFACES
Unbalanced-to-balanced video interface
page 40 MSC-20950

IONIZING RADIATION
Predicting the cosmic-ray environment near Earth
page 78 NPO-16617

J

JET ENGINES
Acoustic-liner admittance in a duct
page 101 LAR-13399

JET PUMPS
Computing cooling flows in turbines
page 83 LEW-13999

JETS
Pump for saturated liquids
page 117 NPO-16152

JIGS
Adjustable tooling for bending brake
page 124 MSC-20730

JOINTS (JUNCTIONS)
Eliminating thermal cracks in flange/duct joints
page 111 MSC-20833

K

KALMAN FILTERS
Analyzing Shuttle orbiter trajectories
page 80 MSC-20786

L

LAMINATES
Preventing delamination of silvered FEP films
page 64 MSC-20460

LAND MOBILE SATELLITE SERVICE
Tougher addition of polyimides containing siloxane
page 65 LAR-13304

LAND MOBILE SATELLITE SERVICE
Economic analysis program for a communication system
page 74 NPO-16606

LANDING SIMULATION
Aircraft rollout iterative energy simulation
page 82 MSC-20816

LARGE SPACE STRUCTURES
Research program for vibration control in structures
page 80 NPO-16615

LASER CUTTING
Research program for vibration control in structures
page 80 NPO-16615

LASER CUTTING
Laser cutting of thin nickel bellows
page 146 MFS-29133

LASER DRILLING
Xenon-ion drilling of tungsten films
page 145 NPO-16626

LASER GYROSCOPES
Laser inertial navigation system
page 53 ARC-11473

LEVITATION
Acoustic levitator maintains resonance
page 145 NPO-16649

LIQUID COOLING
Acoustic translation of an acoustically levitated sample
page 144 NPO-16675

LIQUID COOLING
Modified drills with oil passages
page 106 MFS-29137

LIQUID OXYGEN
Estimating transient pressure surges in cryogenic systems
page 83 KSC-11312

LIQUID-GAS MIXTURES
Pump for saturated liquids
page 117 NPO-16152

M

MACHINE TOOLS
Modified drills with oil passages
page 106 MFS-29137

MACHINING
Adapting inspection data for computer numerical control
page 112 MFS-29117

MAINTENANCE
Repairing hard-to-reach cracks in heat-exchanger tubes
page 138 MFS-29128

MAN MACHINE SYSTEMS
An expert-system engine with operative probabilities
page 90 LAR-13382

MANIPULATORS
Algorithm for calibrating robot arms
page 126 NPO-16569

MASKING
Masking technique for ion-beam sputter etching
page 140 LEW-13899

MATHEMATICAL MODELS
Evaluation of mathematical turbulence models
page 104 MFS-27118

MEASURING INSTRUMENTS
Measuring thickness of coatings on metals
page 94 MFS-28126

MECHANICAL DRIVES
Designing power-transmission shafting
page 109 LEW-14240

MECHANICAL DRIVES
Effects of gear-cutter geometry on performance
page 114 LEW-14243

MESH
Non-back-drivable, freewheeling coupling
page 112 MSC-20475

MESSAGING
Filters for submillimeter electromagnetic waves
page 136 NPO-16498

MESSAGE PROCESSING
High-level data-abstracting system
page 88 LAR-13244

METAL BONDING
Preventing delamination of silvered FEP films
page 64 MSC-20460

METAL FILMS
Xenon-ion drilling of tungsten films
page 145 NPO-16626

METAL SHEETS
Weld repair of thin aluminum sheet
page 137 MSC-20902

METAL WORKING
Adjustable tooling for bending brake
page 124 MSC-20730

MICROELECTRONICS
Guidelines for SEU-resistant integrated circuits
page 42 NPO-16596

MILLING (MACHINING)
Material for fast cutting
page 70 MFS-29130

MONOTECTIC ALLOYS
Separation in binary alloys
page 72 MFS-27074

N

NASTRAN
Combining structural and substructural mathematical models
page 80 MSC-20897

NEEDLES
Electrochemical process makes fine needles
page 135 NPO-16311

NICKEL ALLOYS
Laser cutting of thin nickel bellows
page 146 MFS-29133

NICKEL HYDROGEN BATTERIES
Multikilowatt bipolar nickel/hydrogen battery
page 39 LEW-14244

NOISE REDUCTION
Digital filter separates signal from noise
page 148 MSC-20914

NONLINEARITY
Measuring acoustic-radiation stresses in materials
page 101 LAR-13440

NUCLEAR REACTOR CONTROL
Hydraulic actuator for ganged control rods
page 119 NPO-16503

NUMERICAL CONTROL
Adapting inspection data for computer numerical control
page 112 MFS-29117

NUSSELT NUMBER
Equations for annular-heat-transfer coefficients
page 96 MFS-29074

NUTS (FASTENERS)
Unitized nut-and-washer assembly
page 141 MSC-20903

O

O RING SEALS
Spiral-groove ring seal for counterrotating shafts
page 107 LEW-14248

OPERATOR PERFORMANCE
Variable-friction secondary face seals
page 92 LEW-14170

ORBIT CALCULATION
Autonomous orbital calculation for satellites
page 150 NPO-16532

ORBIT TRANSFER VEHICLES
Adjustable work station for video displays and keyboards
page 44 MFS-26009

ORBIT TRANSFER VEHICLES
Orbital-transfer vehicle with aerodynamic braking
page 125 MSC-20921

P

PACKINGS (SEALS)
Spiral-groove ring seal for counterrotating shafts
page 107 LEW-14248

PARSING ALGORITHMS
High-level data-abstracting system
page 88 LAR-13244

PAYLOAD DELIVERY (STS)
Computing benefits and costs for propulsion systems
page 86 LEW-14129

PHASE DETECTORS
Phase-measuring system
page 49 LAR-13439

PHOTOGRAPHIC PROCESSING
Analog video image-enhancing device
page 46 LAR-13336

PHOTOVOLTAIC CELLS
Reliability research for photovoltaic modules
page 42 NPO-16595

PISTON ENGINES
Four-cylinder Stirling-engine computer program
page 83 LEW-14155

PLAN POSITION INDICATORS
ROM-based plan-position-indicator sweep driver
page 34 LAR-13328

PLASMA ARC WELDING
Theoretical foundation for weld modeling
page 147 MFS-27095

POLYIMIDES
Tougher addition of polyimides containing siloxane
page 65 LAR-13304

POSITION INDICATORS
ROM-based plan-position-indicator sweep driver
page 34 LAR-13328

POTTING COMPOUNDS
Tests of solar-array encapsulants
page 71 NPO-16387

PRESSURE REGULATORS
Feedback-controlled regulation of gas pressure
page 102 GSC-12990

PRESSURE VESSELS
Spring-loaded Joule-Thomson valve
page 101 NPO-16546

PRESSURE VESSELS
Predicting failures of composite, spherical pressure vessels
page 82 MFS-27050

PRISMS
Echelle/grism spectrograph
page 54 GSC-12977

PROPELLERS
High-speed propeller for aircraft
page 115 LEW-14241

PROTECTIVE COATINGS
Depositing diamondlike carbon films
page 139 LEW-14080

PROTEINS
Effects of radiation on coatings
page 71 NPO-16533

PROTEINS
Rotating apparatus for isoelectric focusing
page 152 MFS-26012

Q

QUARTZ CRYSTALS
Temperature-sensitive oscillator
page 39 GSC-12958

R

RADARSCOPES
ROM-based plan-position-indicator sweep driver
page 34 LAR-13328

RADIATION DAMAGE
Guidelines for SEU-resistant integrated circuits
page 42 NPO-16596

RADIATION DETECTORS
Fabrication of an X-ray imaging detector
page 30 GSC-12956

RADIATION EFFECTS
Effects of radiation on coatings
page 71 NPO-16533

RADIATION HARDENING
Radiation hardening of computers
page 50 NPO-16767

RADIATION MEASURING INSTRUMENTS
High-resolution thermal X-ray detector
page 37 GSC-12953



REGENERATIVE FUEL CELLS

Thermally-integrated fuel-cell/electrolyzer systems
page 118 LEW-14235

RELIABILITY ANALYSIS

Reliability research for photovoltaic modules
page 42 NPO-16595

REMOTE CONTROL

Wireless jump starts for partly disabled equipment
page 49 MSC-20100

RESINS

A method for characterizing PMR-15 resin
page 67 LEW-14253

RESINS MATRIX COMPOSITES

A method for characterizing PMR-15 resin
page 67 LEW-14253

RESONATORS

Variable synthetic capacitance
page 36 GSC-12961

ROBOTS

Algorithm for calibrating robot arms
page 126 NPO-16569

Overcoming robot-arm joint singularities
page 126 LAR-13415

ROCKET ENGINES

Ignition system for gaseous propellants
page 120 MFS-29125

ROTARY WINGS

Rigid/compliant helicopter rotor
page 121 ARC-11518

ROTATING SHAFTS

Designing power-transmission shafting
page 109 LEW-14240

S

SAFETY DEVICES

Receptacle for optical-fiber scraps
page 117 KSC-11326

SATELLITE NAVIGATION SYSTEMS

Autonomous orbital calculation for satellites
page 150 NPO-16532

SCRAP

Receptacle for optical-fiber scraps
page 117 KSC-11326

SEALS (STOPPERS)

Variable-friction secondary face seals
page 92 LEW-14170

SEPARATORS

Reinforcing the separators for lithium/carbon cells
page 70 NPO-16619

SERVOCONTROL

Overcoming robot-arm joint singularities
page 126 LAR-13415

SERVOMECHANISMS

Algorithm for calibrating robot arms
page 126 NPO-16569

SHAFTS (MACHINE ELEMENTS)

Designing power-transmission shafting
page 109 LEW-14240

SIGNAL DETECTION

Phase-measuring system
page 49 LAR-13439

SIGNAL TO NOISE RATIOS

Automated signal-to-noise ratio measurement
page 48 MSC-21021

SILICON

Crack growth in single-crystal silicon
page 73 NPO-16757

SILICON FILMS

Etching silicon films with xenon difluoride
page 62 NPO-16527

SILICON NITRIDES

Material for fast cutting
page 70 MFS-29130

SILOXANES

Tougher addition polyimides containing siloxane
page 65 LAR-13304

SINGLE CRYSTALS

Crack growth in single-crystal silicon
page 73 NPO-16757

SINGLE EVENT UPSETS

Guidelines for SEU-resistant integrated circuits
page 42 NPO-16596

Radiation hardening of computers
page 50 NPO-16767

SKIN FRICTION

Two-axis, self-nulling skin-friction balance
page 98 LAR-13294

SOLAR CELLS

Etching silicon films with xenon difluoride
page 62 NPO-16527

Reliability research for photovoltaic modules
page 42 NPO-16595

Sunlight simulator for photovoltaic testing
page 58 NPO-16696

Tests of solar-array encapsulants
page 71 NPO-16387

SOLAR SIMULATION

Sunlight simulator for photovoltaic testing
page 58 NPO-16696

Solid state devices
page 30 GSC-12956

SPACE FLIGHT FEEDING

Small-portion water

SPRAYING

Predicting aircraft spray patterns on crops
page 78 LAR-13432

Dispenser
page 152 MSC-20534

SPACE SHUTTLE ORBITERS

Analyzing Shuttle orbiter trajectories
page 80 MSC-20786

SPACE TRANSPORTATION SYSTEM

Computing benefits and costs for propulsion systems
page 86 LEW-14129

SPACECRAFT DESIGN

Orbital-transfer vehicle with aerodynamic braking
page 125 MSC-20921

SPACECRAFT MODELS

Combining structural and substructural mathematical models
page 80 MSC-20897

SPACECRAFT REENTRY

Estimating average wind velocity along a trajectory
page 78 MSC-20792

SPECTROGRAPHS

Echelle/grism spectrograph
page 54 GSC-12977

SPECTROMETERS

Vacuum-ultraviolet intensity-calibration standard
page 56 NPO-16621

SPECTRUM ANALYSIS

Automated signal-to-noise ratio measurement
page 48 MSC-21021

SPHERICAL TANKS

Predicting failures of composite, spherical pressure vessels
page 82 MFS-27050

SPUTTERING

Masking technique for ion-beam sputter etching
page 140 LEW-13899

STARTING

Wireless jump starts for partly disabled equipment
page 49 MSC-20100

STIRLING CYCLE

Four-cylinder Stirling-engine computer program
page 83 LEW-14155

STORAGE BATTERIES

Multikilowatt bipolar nickel/hydrogen battery
page 39 LEW-14244

STRAPS

Composite fasteners
page 142 LAR-13058

STRESS MEASUREMENT

Measuring acoustic-radiation stresses in materials
page 101 LAR-13440

STRUCTURAL ANALYSIS

Combining structural and substructural mathematical models
page 80 MSC-20897

STRUCTURAL VIBRATION

Flutter- and vibration-animation program
page 80 MSC-20895

SUNLIGHT

Sunlight simulator for photovoltaic testing
page 58 NPO-16696

SYNCHROSCOPES

Phase-measuring system
page 49 LAR-13439

SYNTHETIC APERTURE RADAR

Adaptive quantizer for burst synthetic-aperture radar
page 149 NPO-16582

T

TEMPERATURE GRADIENTS

Measuring Seebeck coefficients with large thermal gradients
page 57 NPO-16667

TEMPERATURE MEASUREMENT

Measuring Seebeck coefficients with large thermal gradients
page 57 NPO-16667

THERMAL EMISSION

High-resolution thermal X-ray detector
page 37 GSC-12953

THERMAL INSULATION

Fast glazing of alumina/silica tiles
page 66 MSC-20976

Lightweight ceramic insulation
page 65 MSC-20831

THERMOCOUPLES

Measuring Seebeck coefficients with large thermal gradients
page 57 NPO-16667

THERMODYNAMIC EFFICIENCY

Theory and tests of two-phase turbines
page 126 NPO-16039

THERMOMETERS

Temperature-sensitive oscillator
page 39 GSC-12958

TILES

Fast glazing of alumina/silica tiles
page 66 MSC-20976

TRAJECTORY ANALYSIS

Analyzing Shuttle orbiter trajectories
page 80 MSC-20786

Estimating average wind velocity along a trajectory
page 78 MSC-20792

TRANSDUCERS

Two-element transducer for ultrasound
page 38 NPO-16591

TRANSIENT PRESSURES

Estimating transient pressure surges in cryogenic systems
page 83 KSC-11312

TUBE HEAT EXCHANGERS

Repairing hard-to-reach cracks in heat-exchanger tubes
page 138 MFS-29128

TUNGSTEN

Electrochemical process makes fine needles
page 135 NPO-16311

TURBINES

Theory and tests of two-phase turbines
page 126 NPO-16039

TURBOFAN ENGINES

HYTSS — hypothetical turbofan-engine simplified simulation
page 82 LEW-14020

TURBOPROP ENGINES

High-speed propeller for aircraft
page 115 LEW-14241

TURBULENCE METERS

Continuous, multielement, hot-film transition gage
page 97 LAR-13319

TURBULENCE FLOW

Evaluation of mathematical turbulence models
page 104 MFS-27118

U

ULTRASONIC WAVE TRANSDUCERS

Two-element transducer for ultrasound
page 38 NPO-16591

V

VALVES

Spring-loaded Joule-Thomson valve
page 101 NPO-16546

VAX-11 SERIES COMPUTERS

Graphics programs for the DEC VAX computer
page 86 NPO-16666

VIBRATION DAMPING

Research program for vibration control in structures
page 80 NPO-16615

Variable-friction secondary face seals
page 92 LEW-14170

VIDEO SIGNALS

Unbalanced-to-balanced video interface
page 40 MSC-20950

W

WASHER (SPACERS)

Unitized nut-and-washer assembly
page 141 MSC-20903

WAVEGUIDES

Passive element shapes antenna radiation pattern
page 41 NPO-16632

WELDING

Theoretical foundation for weld modeling
page 147 MFS-27095

WIND PROFILES

Estimating average wind velocity along a trajectory
page 78 MSC-20792

WIND TUNNELS

Controlled-temperature hot-air gun
page 123 MSC-20693

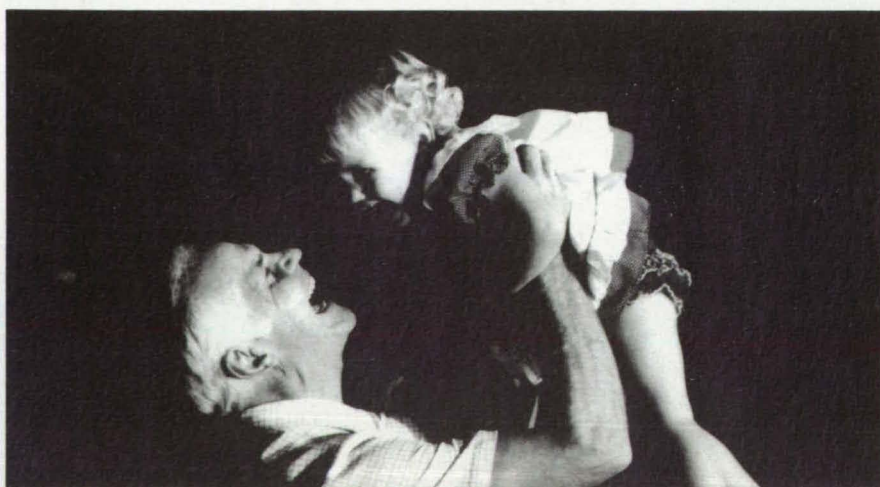
X

X-RAY IMAGERY

Fabrication of an X-ray imaging detector
page 30 GSC-12956

X-RAY FLUORESCENCE

High-resolution thermal X-ray detector
page 37 GSC-12953



WE'RE
FIGHTING FOR
YOUR LIFE

American
Heart
Association



A FRAMEWORK FOR ACTION: Improving Quality and Productivity in Government and Industry

The following recommendations were drafted at the 1984 NASA-sponsored "Symposium on Quality and Productivity: Strategies to Improve Operations in Government and Industry." They represent the collective wisdom of the more than 650 top executives from major American corporations, government agencies and universities who attended the symposium, which focused on the challenge of improving quality and productivity through effective managerial practices.

The major findings of the symposium are organized into nine themes, six of which were presented in the Fall and Winter 1985 issues of NASA TECH BRIEFS. In this issue, we conclude our presentation with themes seven through nine.

Each theme encompasses a set of recommended actions and management practices that have been shown to contribute to high quality and productivity—organizational imperatives in this era of the increasingly competitive global marketplace.

THEME 7: Modernization for Survival: Encouraging New Technology

Being a leader in research and development has been the key to keeping America competitive and in the forefront of technology. Although modernization involving new equipment and techniques is often difficult to justify on a return-on-investment criterion, management needs to have a philosophy that encourages new technology. Management also needs to have training plans for introducing new technology, to lessen the social impact on individuals.

"Effects of technology are not instantaneous, but there is a competitive imperative to use the most productive technology available. . . most of foreign competition strength is application of the newest technology." (Fred Garry, General Electric Company)

New technology is making inroads on all fronts—office automation, new manufacturing equipment and innovative processes. New products appear daily and one company's new product becomes part of the next company's new process.

Office automation, the technology with the greatest impact on white collar productivity, has taken hold in the United States at a much faster pace than factory automation. In general, the equipment costs less, it can be introduced piecemeal and, most important, the fundamental technologies are already available. Any organization with a desire to automate office procedures can find a reasonable selection of affordable equipment on the market. Experience has indicated sizable savings. F. Giannantonio, Avon Products, noted a positive return on investment in just one year:

"We measured indirect savings on productivity gains of 23 percent for management/professional staff and 53 percent for our secretarial/administrative staff."

But new technology means more than a way to do something faster or cheaper. It means social change and changes in the way work is organized and managed. Obtaining the full benefits of technology requires cooperation.

"Once the employees, their unions, and our management team joined hands, that new technology really began to pay off." (Garry)

Recommendation 7.1 Plan for the Technical and Social Impact of Technology

Careful planning is necessary to insure that the potential benefits of new technology are realized. These plans must not only address changes in work methods and procedures, but also in how work is organized and managed, and how employees who operate and maintain equipment will be affected.

In older plants, according to Garry, successful introduction of new technology requires open, honest, two-way communication between management and employees and a commitment to retraining. In G.E.'s experience, many low-skilled workers have been successfully trained to handle high-technology jobs, thereby minimizing worker dislocation.

In white collar organizations, information technology will dramatically alter patterns of social interaction and access to information. This will lead to power shifts in the organization that could have profound consequences if not anticipated. William Pfeiffer of ITT discussed the "electronic cottage" concept, an extreme case of decentralization. Stimulated by the increased power and portability of computers, people will be able to work in their homes or other locations physically separated from the central organization. Widespread application of this concept will not only alter work practices but will create major organizational and even social changes.

"Clearly, we're in for some profound changes, in both technology and office life. . . We must rethink our procedures and organizations." (Pfeiffer)

Recommendation 7.2 Stimulate Modernization Through Government Support and Incentives

Government has played an important role in the technology introduction process and should continue to do so. John Mittino described DoD's manufacturing technology program aimed at introducing new technology into the production environment. He stressed the importance of current DoD initiatives designed to share dollar savings resulting from a defense contractor's productivity-oriented capital investment, through efforts such as its Industrial Modernization Incentives Program.

The impact of such programs can be seen in success stories like that of General Dynamics, manufacturer of the F-16 fighter.

Willie Livingston of General Dynamics cited technology-based productivity improvements that have reduced the number of man-hours required to build an F-16 from 110,000 in 1979 to less than 30,000 in 1983. Overall, the F-16 program, stimulated by government incentives, will produce savings to DoD in excess of \$1 billion.

Robert Walquist of TRW, Inc. gave another example of government/industry cooperation. He described the joint efforts of NASA and TRW to make the Gamma Ray Observatory spacecraft program a model for more productive ways of doing business. The program has already implemented a series of productivity macro-goals to lead company, sub-contractor and individual employee productivity increases. TRW's efforts cover both team building and the use of new technology. With the use of mini computers they have developed a common government-contractor database which has reduced the need for reporting. Through video conferencing they have increased communications and reduced travel costs.

Recommendation 7.3 Maximize Computer-Related Technology

White collar operations in industry and government are benefitting from computer/communications technologies. In aerospace firms such as Lockheed Missiles and Space Company, computer-aided design and manufacturing (CAD/CAM) are increasingly viewed as a means of reducing the labor content of products and improving product quality. In the future, these technologies will provide a way to cope with a projected shortage of skilled engineers and technicians. Lockheed's Fred Oder reported productivity savings from CAD ranging from 36 to 73 percent when compared to the cost of manual design.

While advances in office automation are occurring daily, the major office productivity breakthroughs have not yet occurred. Major gains await improved component compatibility and the convergence of computer and telecommunications technol-

ogies. William Pfeiffer of ITT points to three main concerns and needs of users that must be satisfied if office automation is to fulfill its promise. First, there is a need for easily understandable software triggered by English language commands. Second, the user needs an integrated package of hardware, software and communications technology. And finally, the most difficult need to satisfy is the standardization of system architecture. Knowledgeable managers can influence hardware and system vendors by communicating these requirements. Until these needs are met, the office automation contribution to quality and productivity improvements will continue to be less than optimum.

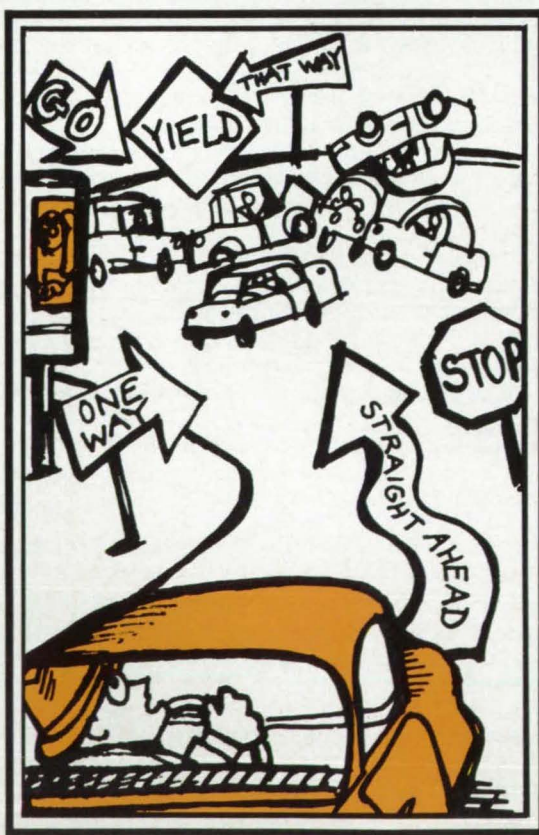
"The office of the future has not yet arrived. . . the technologies necessary to create it have been around for about ten years. . . what's missing is the 'glue'—the systems architecture that allows equipment from different vendors to work together. . . In other words, we have an electronic Tower of Babel." (Pfeiffer)

THEME 8: Maximize Human Capital: Developing Strategies to Improve Education and Training

Basic to productivity is education and training; it defines and develops the quality of human resources for the future. We have fallen behind in educational achievements and in the number of engineers graduating on a per capita basis. Improvement in national productivity and competitiveness depends on new strategies for the training, education and social conditioning of our most important natural resources—our people.

"Human capital is our most valuable national resource. It is insufficient to try to discuss productivity without discussing education which defines and develops the quality of human resources for the future." (Owen B. Butler, Procter & Gamble)

DON'T LET YOUR TECHNOLOGY COME TO A STANDSTILL



STAC has untangled some tough technological jams.

For people like you—who are ready to take your ideas from the drawing board to the marketplace . . . STAC can tackle your problems using worldwide resources.



- Conducts information research utilizing over 500 computer data bases
- Locates experts in federal labs, NASA, universities and private industries
- Analyzes new product potential
- Assesses patentability
- Assists SBIR proposers

Call the experts at NASA-Southern Technology Applications Center (STAC)
at (904) 392-6626.
In Florida call 1-800-FL-HI-TEC.



Over the past several years, business and government leaders have noted a decline in the basic preparation of our young people to meet the diverse challenges and complexities of our fast-changing society. Blame is commonly put on the public school system, but family, school, the community, government and industry must all share responsibility.

According to Butler, industry spends approximately \$30 billion annually on remedial and continuing education to make up for educational deficiencies in its work force. Schools, from the primary grades through college, must consider how to adapt their curricula, not just to the ever-changing job market but, equally important, to an ever-changing society. In this effort, the family, community, government and industry each have roles and responsibilities in guiding schools and motivating and educating young people for more productive lives. Each group must bear the responsibility and give it high priority.

Recommendation 8.1 Inform Educators of Required Job Skills

In the past, new employees entering the work force generally worked at low skill tasks on narrowly defined jobs that were relatively easy to learn. Today, employees are required to perform a broad range of tasks. They are expected to operate and maintain equipment, perform administrative tasks, participate in goal-setting and budgeting, and work in groups and teams that are self-directed and guided by principles rather than detailed procedures. Even people with strong educational backgrounds require a large amount of training to perform in this situation.

However, employees who lack a strong foundation in literacy, numbers skills and, above all, the ability to learn require even more training. Industry should bear the responsibility for specific job training, but our educational system must provide students with the basic skills required for employability in today's business environment.

Recommendation 8.2 Encourage Increases in the Number of New Scientists and Engineers

Industry should work closely with colleges to insure that scientists and engineers receive broad training, and should provide incentives that will attract them to manufacturing careers. The United States is falling behind in the number of new scientists and engineers compared with our competition.

"In 1982, engineering and science accounted for only 20 percent of all bachelors degrees earned in the United States. This compares with 25 percent of all such degrees earned in Japan, 34 percent in West Germany and more than 50 percent in the Soviet Union." (James M. Beggs)

Robert Cole of the University of Michigan notes that we not only have fewer technical people, but we deploy them in ways that may be adverse to our overall economic competitiveness.

"... Many of our most talented researchers and engineers have been siphoned off into the defense and aerospace industries... As I visit Japanese companies, I am struck by just how many engineers they have to throw at fairly mundane technical problems... Japanese technical personnel working directly in consumer products industries have

been able to generate improvement after improvement, resulting in reduced costs, higher quality and productivity."

Cole also points out that the training and career progression of engineers and technical support personnel in Japan give them a competitive edge. In particular, our nation is weak in the area of technical support people. In Japan, high school graduates are given extensive in-house technical training, allowing them to assume many engineering tasks. This frees up graduate engineers to work on more complex tasks. Our nation's weak-

FAIRCHILD WESTON... The Name To Know For Quality Instrumentation Data Recorders

Unrivalled Range and Versatility



Fairchild Weston products illustrated above include:

- MODEL 10 - Microprocessor controlled, 16" reel laboratory recorder/reproducer.
- EDCS - Error Detection and Correction System with Monitor.
- MODEL 12-B (AN/USH-33(V)) - High Environmental 10 1/2" reel recorder/monitor/reproducer.
- MODEL 9 - Transportable 15" reel, microprocessor controlled, very high versatility recorder/reproducer.
- ANALOG MULTIPLEXER/DEMULTIPLEXER - 16 Channels of Analog Data on 1 Channel of any tape recorder.
- MODEL 15 - High environmental 15" reel, microprocessor controlled, high versatility recorder/reproducer.
- MODEL 80 - Portable 14" reel, low cost recorder/reproducer.
- MODEL 80TA - Tempest qualified 14" reel, microprocessor controlled high versatility recorder/reproducer.
- MODEL 85 - Portable 14" reel, microprocessor controlled, high versatility recorder/reproducer.
- All models to IRIG (RCC) specifications.



FAIRCHILD WESTON SYSTEMS INC.

DATA SYSTEMS DIVISION
P.O. Box 3041, Sarasota, Florida 33578
(813) 371-0811 • Telex: 4947160

ness reflects the weak technical background of high school graduates and inadequate training and career path planning in industry. As a result, we are not developing and retaining individuals with the required competencies as well as we should.

Recommendation 8.3 Continue Training Employees for New Technology

Changes in process technology are occurring at an accelerated pace as industries attempt to remain competitive. This means that employees must continually learn new skills in order to keep

pace. As one example, Butler observed that the only thing in its disposable diaper line that hasn't changed in the past 20 years is the name of the product! Manufacturing technology has changed and computers have replaced electrical relays for process control. In another area, employees who used to stack paper towel products now program a robot that performs the stacking. Office employees are experiencing changes in technology that are almost as dramatic.

An organization that values its work force and seeks to maintain stable employment must devote considerable time and effort to training.

"To keep pace with these changing work place demands we must invest 7-10 percent of employees' time in training. That's an investment of up to \$3,000 per year per employee in wage dollars alone. Clearly, when we invest that kind of money, we want to make sure we get a proper return. We have to have employees who have the ability to learn and use their training." (Butler)

THEME 9: Improve Quality and Productivity Practices: Building a Quality Ethic

High quality goes hand-in-hand with high productivity. In many organizations, total defect costs range from 15 to 40 percent of budgets. For maximum organizational effectiveness, continuous improvement goals are needed and must have total commitment by management. Every function has customer and quality objectives that have to be translated into specifics that are meaningful to each organizational effort. All levels of management must assess organizational activities and processes on the basis of their impact on quality and productivity—not just on bottom-line results.

"The whole measure of our success . . . will boil down to quality performance. Shoddy workmanship, defective materials, inadequate quality control, cash overruns—all can be improved or eliminated." (James M. Beggs.)

For industry, the stakes in building a quality ethic are customer satisfaction, cost competitiveness and, ultimately, survival. At IBM, no level of defect is acceptable. John Jackson of IBM states: "More than anything else, quality or excellence stems from the people of an organization . . . and quality is everyone's job . . . Our total quality costs are roughly 15 to 40 percent of the revenue stream." For government, the penalties for failed quality are cost overruns and missed supplier milestones. A quality ethic should permeate every aspect of an organization, starting with hiring the best people and then challenging them to top performance.

"In contrast to just the traditional emphasis on profits, costs and production goals, leadership has to become obsessed with making sure all decisions are driven by quality improvement, customer satisfaction and building an innovative team environment." (David Braunstein, NASA)

In these comments from his welcoming address to symposium attendees, David Braunstein, Director of NASA Productivity Programs, stressed the underlying mandate to instill the quality ethic in any organization. As such, the pursuit

From DARPA to DOT

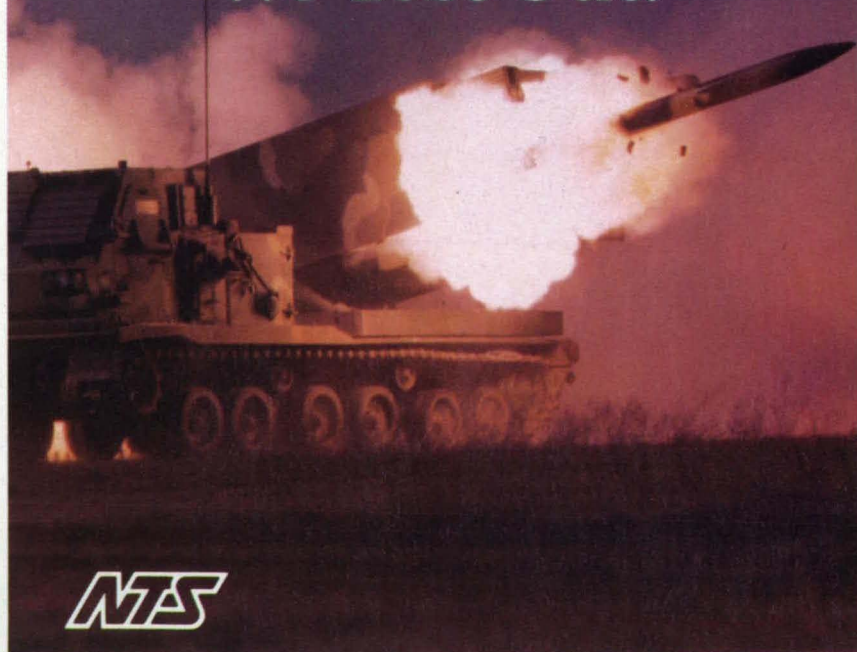
Whether it's the most esoteric DARPA project, or evaluating bumpers for DOT, the challenge is the same—to make the unknown not only knowable, but usable.

National Technical Systems does it in design, engineering, analysis and testing in many worlds: space shuttles and space stations, laboratories charting technology's distant future, and on the highways of America

where DOT'S safety rating program is based in part on work done in the world's largest independent auto crash laboratory.

To all our projects we bring unbeatable technical resources and the prideful dedication of our people. Our customers know that in aerospace, avionics, energy, transportation, communications and defense, we've been there before and have done it all.

We Test Out.



NTS

**National
Technical
Systems**

Call National Technical Systems.

In the west (714) 879-6110.

In the east (617) 263-2933.

Or write NTS, 533 Main St., Acton, Ma. 01720
or 1536 E. Valencia Dr., Fullerton, Ca. 92631.

Circle Reader Action No. 358

of quality and productivity is more an attitude, and not a program goal per se.

Recommendation 9.1 Make Quality a Total Management, Employee and Supplier Commitment

As top management sets organizational goals, so the quality ethic is driven by these goals. Leadership must transcend the narrow perspective of quality in technical terms to one which perceives quality as tantamount to organizational survival. Management must translate quality goals from the abstract, slogan level and relate them to all aspects of employee performance. Quality and productivity are consistently described as different sides of the same coin. This means that employees have to see their jobs not only in terms of "getting the product out" but also in terms of meeting top quality goals. Within an organization this involves how organizational elements cooperate and satisfy each other. Outside the organization it involves the relationship and dealings between customers and suppliers.

"Our managers, supervisors and foremen are thoroughly educated in the policy that quality is the very life of Sony products. . . They are trained in the field to understand how important quality is for sales and after-sales service."

(Sadami Wada, Sony Corporation)

Cooperation between a company and its vendors and suppliers is viewed as a major contributing factor to the high quality levels attained by Japanese manufacturers. Instead of responding to peremptory demands for higher quality, Japanese vendors establish mutually agreed-on targets for improvement as part of a quality plan. This features rapid, two-way feedback for generating suggestions, problem identification and solution, and structuring a system for tracking progress.

The importance of this relationship is the basis of current DoD initiatives described by John Mittino. Since quality has become such a significant issue in the acquisition process, DoD, as the customer, is reemphasizing policies and programs aimed at promoting improved quality practices by contractors.

"The Department [DoD] encourages commitment from top management and is promoting increased awareness and attention to quality problems during design and manufacturing. DoD is also re-examining its qualification and certification programs to determine whether quality is sufficiently stressed. Perhaps most importantly, we are trying to find new ways to include quality history in our source selection process." (Mittino)

Recommendation 9.2 Incorporate Quality Goals into All Organizational Activities

Quality goals must be understood in terms of the work that an organization performs, the process by which the work is performed and the management system under which the organization is run. As Richard Boyle of Honeywell has stated:

"When we talk about quality, we're not just talking about products. We're talking about three elements that must be present . . . quality of work, quality of work life and quality of management."

Specific goals must be established for all three elements. Quality of work is what most people mean when they speak of quality. Does the product or service meet the requirements? Is it satisfactory to the customer? This analysis involves all individuals and functions of the organization.

Quality of work life is the degree to which the work environment allows and motivates employees to contribute to the success of the organization. Does the environment offer challenge, responsibility and appropriate rewards? Boyle observes that:

"Quality of management is the key to sustained quality improvement. It involves fostering leadership that has the technical and intellectual skills to set the course for the organization."

The successful translation of quality goals into an organization's activities begins when employees can answer the question, "What is my job?" The job should be defined in terms of both the goods or services produced and the needs of the "customers" who receive them. When employees can answer

this question, the organization can then focus on quality goals to increase its effectiveness. Without quality goals and a plan for achieving them in all organizational activities, we cannot develop a process for continual improvement.

"The more effective approach has been to establish a quality improvement plan . . . The plan usually involves a system for rapid and accurate feedback . . . [so that] suggestions for improvement can be exchanged and progress can be tracked." (Richard Kraft, Matsushita)

Recommendation 9.3 Assess Organizational Activities and Processes As Well As Bottom Line Results

People and processes provide the conditions for quality improvement, which is the driver for productivity. As viewed by Carl Hirsch of Dana Corporation:

"The pursuit of quality is never finished, because the capacity of our people to produce quality is virtually unlimited. That's why we at Dana will not stop evolving and striving . . . It may be good—but excellence is never really enough."

Management must continually strive to improve the quality of its products, as well as the capabilities of its processes. Responsibility rests with all levels of management to review these processes and determine, through analysis, what they contribute to the bottom line. These reviews must be conducted at key points and be based on facts. Moreover, these reviews should focus on defect prevention.

"Screening by rejection only increases cost. Therefore, efforts must be made to manufacture right the first time.

This is the real quality control. You must be able to obtain the desired level of quality with the least waste." (Wada)

Richard Kraft recommends following the Japanese example of accepting the quality teachings of Dr. W. Edwards Deming, Dr. J.M. Juran and others. The Japanese have accepted the premise that superior quality leads to competitive success, costs little and creates a worldwide demand for goods because of their reputation. □

• • •

NASA's Office of Productivity Programs will host both a conference and a national symposium on quality and productivity in 1986. The Third Annual NASA Contractors Conference will be held at Ames Research Center, Sunnyvale, California, in June 1986. The national symposium, "Strategies for Revitalizing Maturing Organizations," will be held December 2—3, 1986, in Washington, D.C. For more information on these programs, contact David Braunstein, director, NASA Productivity Programs, NASA Headquarters, Code ADA, Washington, D.C. 20546.

- **Free Publicity**
- **Improved Public Relations**
- **Increased Sales**

—All three are possible if we can describe how your company has used NASA technology to develop and improve its products.

For more information, call:
Linda Watts, (301) 621-0241
NASA Spinoffs

Letters

The "Letters" column is designed to encourage a wide exchange of ideas among NASA Tech Briefs readers. To contribute a request for information or to respond to such a request, use the feedback cards in this issue, or write or call: Manager/Technology Transfer Division, P.O. Box 8757, Baltimore/Washington International Airport, MD 21240; (301) 859-5300. While we can print only a small number of letters, we will endeavor to select those that are of varied and wide interest.

TO MAKE A LONG STORY SHORT

As usual I was very pleased to receive the most recent March/April 1986 issue of NASA Tech Briefs. Although at first glance many of the topics may appear to be very narrow in scope, upon more careful scrutiny and with a little imagination, new applications may become apparent.

I would like to set the record straight in regard to the development of using cross-linked EVA material in the cooling garments used on the space shuttle suits [NTB March/April, p. 139]. It was Johnson Space Center who initially contacted Thermoplastic Processes Inc. in Stirling, New Jersey, pertaining to a problem they were experiencing with plasticizers leaching out into the cooling solutions. At their request, we submitted the first samples of product code 1861 Micro-Line tubing for evaluation. Although this initial sample was less flexible than desired, it proved superior to what they were previously using. We asked NASA how they planned on bonding this rather inert tubing to the then existing flexible PVC fittings. We were told that they would use epoxy. We said, "Good luck."

A few days later NASA called back and said, "We give up. How are you supposed to bond it?" Thermoplastic Processes Inc. suggested that heat fusing be looked into. We then supplied NASA with samples of telescopic sizes of our cross-linked Bev-A-Line VHT tubing for the initial heat fusion tests, and made an offer that if NASA were to supply samples of the EVA fittings to us we would cross-link them through irradiation so that the dimensional stability of the various components would allow them to be heat fused together with minimum distortion! Eventually we supplied softer versions of cross-linked EVA for even more flexibility.

There is no doubt that the very talented and dedicated people at ILC Dover sophisticated this technique to a new standard of excellence. However, I believe it is only fair for my employer, Thermoplastic Processes Inc., to receive their due credit.

Joseph Rene DuPont
Gillette, NJ

MORE Q's & A's

What do we do if we are interested in tech briefs marked "No further documentation is available"?

D.W. Hejde
Washington, DC

When no Technical Support Package (TSP) is available for a particular tech brief, or if you have further questions about applying the technology described in a TSP, you should contact the Technology Utilization Officer at the NASA Field Center that sponsored the research. He can put you in touch with the individuals who conducted the R&D that led to the innovation. The names,

addresses, and phone number of NASA's Technology Utilization Officers are listed on page 29 of this issue.

Do you publish an annual list of all NASA Tech Brief entries?

Indices for Tech Briefs published prior to 1980 are available from the National Scientific and Technical Information Facility, Technology Utilization Office, P.O. Box 8757, Baltimore/Washington Int'l. Airport, MD 21240. We regret that no indices are currently available for Tech Briefs published after 1980. Publication of these indices is expected in the near future and will be announced in NASA Tech Briefs.

How do I go about getting information on the price and availability of the NASA Patent Abstract Bibliography (PAB)?

The NASA Patent Abstract Bibliography, containing abstracts of all NASA inventions, can be purchased from the National Technical Information Service (NTIS), 5285 Port Royal Road, Springfield, VA 22161. The PAB is updated semi-annually. NTIS furnishes the PAB to subscribers who place a standing order by opening a deposit account in the amount of \$25. The price of each PAB is then charged against this amount.

For more information, write NTIS at the above address or phone (703) 487-4630.

POETRY IN MOTION

After I had already finished making the improvements for the GM auto washer pump, the schematic for fluidic devices published in NASA Tech Briefs was brought to my attention. From the knowledge gained, I was able to develop a simple, non-mechanical device costing 15 cents to 25 cents, as against the GM washer pump's \$18.00 to \$20.00 manufacturing cost.

More importantly, the bending of a fluid stream in a horizontal plane is clearly observable in this device. This phenomenon may be likened to "light from a distant star bent by a curve in space-time caused by the mass of the sun" (Einstein).

John Izumi
Izumi Co.
Glen Ellyn, IL

QUALITY & PRODUCTIVITY

Your articles on "Improving Quality and Productivity in Government and Industry" were magnificent! Best stuff I have read in many years. As a government employee with 17 years invested in the system, I can tell you that everything said about stifling creativity was right on the money. Every day the government kills 1000 good ideas with the same weapon Sampson used to slay the Philistines!!

John R. Jay
Pacific Missile Test Center
Point Mugu, CA

Please let me know how to get a copy of the recommendations of the 1984 Symposium on Quality and Productivity, referred to on page 182 of the Winter 1985 issue of NASA Tech Briefs. Looks like a very interesting item.

G.M. Clark
CIBA-GEIGY Corp.
McIntosh, AL

With this issue, NASA Tech Briefs concludes its presentation of the themes and recommendations of the 1984 Symposium on Quality and Productivity by reprinting themes 7-9, beginning on page 157. Themes 1-3 were reprinted in the Fall 1985 issue of

NTB, and themes 4-6 can be found in the Winter 1985 issue. NASA Tech Briefs chose to reprint these findings not only because we thought our readers would find them informative, but also because only a limited number of reports were available from NASA's Office of Productivity Programs, which sponsored the 1984 symposium.

NASA's Office of Productivity Programs will host another national symposium on quality and productivity in 1986. For more information on this program, contact David Braunstein, director, NASA Productivity Programs, NASA Headquarters, Code ADA, Washington, DC 20546.

GETTING THE BIG PICTURE

NASA Tech Briefs articles present not merely design techniques but an important way of thinking about systems which ought to be understood by project engineering teams. The presented techniques light the highest levels of systems conceptualization down to the lowest level of product design. The articles, though very brief, often help to change the conceptual thinking, while at the same time providing a directory to important engineering information.

Julian J. Dec
Comstock Engineering, Inc.
Butler, PA

In our organization, it is necessary for proposals for new contracts to keep current with all new aerospace developments that can impact how we design and produce new products. NASA Tech Briefs has been very useful to us in doing this.

Ralph I. Olsen
Boeing Aerospace
Seattle, WA

I am a mechanical engineer who's been reading Tech Briefs for many years. I'm keenly interested in the content of this magazine overall, because of the added knowledge and insight it gives me. I have an insatiable interest in unique solutions to design engineering problems. Tech Briefs, more than any other publication, has piqued that interest consistently.

Keith Whaley
Hughes Aircraft
Los Angeles, CA

I like the ads! Not only do they offset the cost of producing NASA Tech Briefs, but they let high-tech companies know about other high-tech companies.

Keep up the good work. NASA is the only branch of the federal government I would like to pay more taxes to support!

Douglas C. Smith
AT&T Information Systems
Middletown, NJ

SONS AND MOTHERS

Our company is primarily involved with computer simulation and technical analysis. I hope that we will be able to learn much more from Tech Briefs. My mother, who receives Tech Briefs, has always loved your publication and has been able to use what she has learned from your publication.

Richard V. Rudofski
Jaycor
Fairborn, OH

CORRECTION

The following equation for correcting nonlinearity in a photodetector appeared incorrectly on page 48 of the March/April issue of NASA Tech Briefs. In its proper form, the equation is:

$$R_3 = \frac{R_1 R_2}{R_s R_b} \left(\frac{R_s + R_b}{R_1 + R_2} \right)$$

Advertiser's Index

Aerospace Research Applications

Center	(RAC* 436)	150
Allied Bendix Aerospace	(RAC 421)	99
Alslys, Inc.	(RAC 341)	75
A.O. Smith Data Systems, Inc.	(RAC 426)	51
Aptec Computer Systems	(RAC 314)	84-85
Aurora Bearings	(RAC 413)	6
BitWise Designs, Inc.	(RAC 301)	24
Boeing Technology Services	(RAC 367)	93
Celerity Computing	(RAC 352)	15
Contel SpaceCom	(RAC 398)	127
Control Laser	(RAC 315)	53
CTS Corporation	(RAC 350,351,375-377)	31
Data-Control Systems	(RAC 371)	89
Data General Corporation	(RAC 353)	76-77
Datalab Products	(RAC 304)	52
Data Precision	(RAC 432, 433)	45
Datatype Incorporated	(RAC 340)	19
DDC International	(RAC 406)	27
EcoTech, Inc. Computer Systems	(RAC 440)	79
E G & G Electro-Optic	(RAC 431)	60
Engineering & Research Assoc., Inc.	(RAC 382)	105
Fairchild Control Systems Co.	(RAC 357)	21
Fairchild Weston Systems, Inc.	(RAC 441)	159
Fiberite	(RAC 307)	68-69
Ford Aerospace & Communications Corp.	(RAC 342)	91
General Motors Corporation		7-9
Greene, Tweed & Co.	(RAC 328)	146
GRQ, Inc.	(RAC 445)	163
Guideline Instruments, Inc.	(RAC 324)	73
Harris Aerospace	(RAC 410)	16-17
Honeywell Inc. Space and Strategic Avionics Division	(RAC 364)	166, Cov.III
IBM/Information Systems Group	(RAC 325)	4-5
IFR, Inc.	(RAC 317)	55
IMSL	(RAC 300)	116
Inland Motor, Specialty Products Group	(RAC 423)	113
Ion Laser Technology	(RAC 362)	63
ITT Electro-Optical Products	(RAC 403)	32
Keve Corporation	(RAC 442)	71
Kinetic Systems	(RAC 316)	88
Klinger Scientific Corp.	(RAC 368)	61
Lee Laser, Inc.	(RAC 370)	46
Laser Precision	(RAC 302)	50
Martin Marietta		Cov.II-1
McDonnell Douglas Corp.	(RAC 372)	Cov.IV
McDonnell Douglas Corp.	(RAC 373)	47
McDonnell Douglas Corp.	(RAC 374)	23
NEC America, Inc.	(RAC 369)	43
NTS Testing	(RAC 358)	160
Pace Incorporated	(RAC 318)	25
Pennwalt Corporation	(RAC 425)	35
Pressure Systems, Inc.	(RAC 378)	10
Spacehab, Inc.	(RAC 347)	95
STAC	(RAC 345)	158
Systonetics	(RAC 391)	72
Tex-Tech Industries, Inc.	(RAC 392)	147
Texas Instruments DSG		90
3 M Comtal	(RAC 319)	87
3 M Federal Systems	(RAC 422)	11
Tycor Electric Products Ltd.	(RAC 308)	150
Tycor Electric Products Ltd.	(RAC 309)	151
Valcor Engineering Corp.	(RAC 326)	107
Vitro Corporation	(RAC 394)	2
Yellow Springs Instrument Co.	(RAC 448)	143
Zenith Data Systems	(RAC 349)	81

*RAC stands for Reader Action Card. For further information on these advertisers, please circle the RAC number on the Reader Action Card elsewhere in this issue. This index has been compiled as a service to our readers and advertisers. Every precaution is taken to ensure its accuracy, but the publisher assumes no liability for errors or omissions.



Who Sells and Licenses Technology?
Who Buys It?
Who Are The Brokers?

TECHNOLOGY TRANSFER DIRECTORY 1986

A guide to Organizations, Agents, Buyers, Sellers, and Information Sources for the business of Seeking, Licensing, Acquiring, and Trading Technology. Covers:

Universities	Industrial Firms
Government Agencies	Patent Organizations
Research Institutes	Inventors Organizations
Business Development Centers	Commercial Broker Firms

WHO CAN USE THIS DIRECTORY

Licensing Agents	Research Administrators	Directors of Licensing
University Administrators	Technology Consultants	Holders of Marketable Patents
Inventors	Chambers of Commerce	Exporters & Importers of Technology
Patent Lawyers & Officers	Market Research Analysts	Business Brokers
New Opportunity Seekers	Technology Developers	Area Development Organizations
Corporate Strategists	High Technology Venturers	Commercial Development Agents

Mail this order form today to:

GRQ, Inc., 19 East Central Avenue, Paoli, Pennsylvania 19301

☐ Send _____ copies of Technology Transfer Directory 1986 at \$110 per book.
(Pa. resident add 6% sales tax) (\$140 outside of North America)

☐ Payment enclosed \$ _____ ☐ Visa ☐ Master Card

Credit Card # _____ Exp. Date _____

Signature _____

Name _____

Title _____

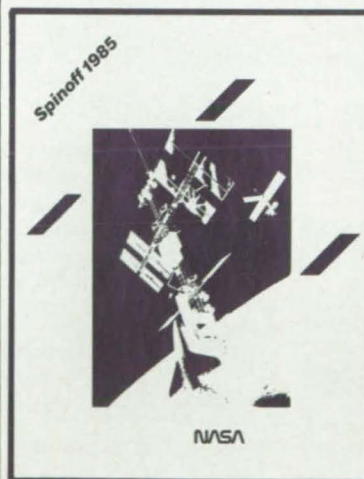
Company _____

Address _____

City _____ State _____ Zip _____ Country _____

Circle Reader Action No. 445

FREE PUBLICITY



NASA Spinoffs is an annual publication designed to tell consumers how NASA technology is being applied by industry to benefit all Americans. If you have applied NASA technology in any of your products or processes, you can receive valuable free publicity for your company in NASA Spinoffs.

To find out if you qualify, call Linda Watts at (301) 621-0241, or send in the Feedback Card bound into this issue.

NASA Spinoffs
Technology Transfer Division
P.O. Box 8757
BWI Airport, MD 21240

ABOUT THE NASA TECHNOLOGY UTILIZATION PROGRAM

Thumb Index



NASA TU Services



New Product Ideas



Electronic Components and Circuits



Electronic Systems



Physical Sciences



Materials



Computer Programs



Mechanics



Machinery



Fabrication Technology



Mathematics and Information Sciences



Life Sciences



Subject Index

This document was prepared under the sponsorship of the National Aeronautics and Space Administration. NASA Tech Briefs is published bi-monthly and is free to engineers in U.S. industry and to other domestic technology transfer agents. It is both a current-awareness medium and a problem-solving tool. Potential products... industrial processes... basic and applied research... shop and lab techniques... computer software... new sources of technical data... concepts... can be found here. The short section on New Product Ideas highlights a few of the potential new products contained in this issue. The remainder of the volume is organized by technical category to help you quickly review new developments in your areas of interest. Finally, a subject index makes each issue a convenient reference file.

Further information on innovations—Although some new technology announcements are complete in themselves, most are backed up by Technical Support Packages (TSP's). TSP's are available without charge and may be ordered by simply completing a TSP Request Card, found at the back of this volume. Further information on some innovations is available for a nominal fee from other sources, as indicated. In addition, Technology Utilization Officers at NASA Field Centers will often be able to lend necessary guidance and assistance.

Patent Licenses—Patents have been issued to NASA on some of the inventions described, and patent applications have been submitted on others. Each announcement indicates patent status and availability of patent licenses if applicable.

Other Technology Utilization Services—To assist engineers, industrial researchers, business executives, Government officials, and other potential users in applying space technology to their problems, NASA sponsors Industrial Applications Centers. Their services are described on pages 28-29. In addition, an extensive library of computer programs is available through COSMIC, the Technology Utilization Program's outlet for NASA-developed software. See special section on computer programs on page 74.

Applications Program—NASA conducts applications engineering projects to help solve public-sector problems in such areas as safety, health, transportation, and environmental protection. Two applications teams, staffed by professionals from a variety of disciplines, assist in this effort by working with Federal agencies and health organizations to identify critical problems amenable to solution by the application of existing NASA technology.

Reader Feedback—We hope you find the information in *NASA Tech Briefs* useful. A reader-feedback card has been included because we want your comments and suggestions on how we can further help you apply NASA innovations and technology to your needs. Please use it; or if you need more space, write to the Manager, Technology Transfer Division, P.O. Box 8757, Baltimore/Washington International Airport, Maryland 21240.

Advertising Reader Service—Reader Action Card (RAC): For further information on the advertisers, please circle the RAC number on the separate Reader Action Card in this issue.

Change of Address—If you wish to have *NASA Tech Briefs* forwarded to your new address, use the Subscription Card enclosed at the back of this volume of *NASA Tech Briefs*. Be sure to check the appropriate box indicating change of address, and also fill in your identification number (T number) in the space indicated.

This document was prepared under the sponsorship of the National Aeronautics and Space Administration. Neither Associated Business Publications, Inc., nor anyone acting on behalf of Associated Business Publications, Inc., nor the United States Government nor any person acting on behalf of the United States Government assumes any liability resulting from the use of the information contained in this document, or warrants that such use will be free from privately owned rights. The U.S. Government does not endorse any commercial product, process, or activity identified in this publication.

Mission **A**ccomplished

Through the technology transfer process, many of the systems, methods and products pioneered by NASA are re-applied in the private sector, obviating duplicate research and making a broad range of new products and services available to the public.



This nuclear magnetic resonance (NMR) image of the human brain was enhanced using NASA remote sensing technology. The image describes a tumor on the left lobe (the yellow mass on the right side of the image). The opposite lobe is normal except for some swelling (also in yellow), which appears around the cerebral spinal fluid cavity (shown in red).

For many of us, the subject of remote sensing is remote indeed. We tend to think of complex satellite and radar systems, and in doing so we forget that mechanisms as common as the camera are designed for the same purpose: to gather information about an object without coming into physical contact with it.

In the medical world, the x-ray machine is probably the most widely-used remote sensing instrument. It gathers information about the body based on its sensitivity to bone density. X-rays, however, are limited by their inability to penetrate bone, and thus are inadequate when images of soft tissues are required.

To obtain images of soft tissues, especially the brain, a NASA Tech Briefs, May/June 1986

relatively new technique called nuclear magnetic resonance (NMR) imaging has been developed. NMR data is gathered by measuring the energy the body's hydrogen protons release after the temporary imposition of an electromagnetic field. Then, with the help of a computer, this data is converted into images that, like x-rays, are useful in medical diagnostics.

While the technology for generating NMR data is relatively advanced, NMR data processing and analysis systems are not yet fully developed. Consequently, NMR images tend to lack definition, which makes them difficult to interpret. But recently the NMR data processing system has been greatly improved. Reformating NMR data to make it compatible with NASA remote sensing software has dramatically enhanced the clarity and consistency of NMR images, making them much more useful in medical diagnostics.

To process and analyze the digital data provided by its remote sensors, scientists at NASA's National Space Technology Laboratories, Bay St. Louis, Mississippi, developed the Earth Resources Laboratory Applications Software (ELAS). This conglomeration of 300 separate executable programs analyzes satellite and other remotely gathered data and converts it into colorful and highly detailed images.

In much the same way that NASA scientists use computer-enhanced images to assess the status of earth resources, medical diagnosticians use NMR images to detect anomalies, such as blood clots and tumors, in soft tissues. Enhancing NMR imaging technology is the goal of a three-year collaborative effort between doctors at the Mallinckrodt Institute of Radiology of the Washington University Medical Center, St. Louis, Missouri, and NASA scientists. Kennedy Space Center is providing funding and overall coordination for the project, while Washington University is supplying medical expertise and data. NSTL scientists are providing analytical capabilities based on the ELAS software and the expertise they've acquired through years of image processing and analysis.

One of the preliminary tasks of the NSTL scientists was to eliminate the systematic errors and high-frequency noise contained in the NMR data. This was partially accomplished by determining the necessary correction factors with the ELAS software. Then, using the computer, they enhanced the typically black and white NMR images by assigning color values to the digital data. Current efforts focus on further enhancing the color images to the point where they provide information on the biological behavior of a soft tissue anomaly, in addition to determining its size and location. This enhancement will allow diagnosticians to non-surgically differentiate blood clots from tumors, and further, determine whether a tumor is benign or malignant.

By using NASA software and analytical expertise to maximize the interpretability of NMR images, the rate of soft tissue disease detection will be greatly enhanced. From there it follows that treatment can be started earlier, hopefully in time to alter the course of life-threatening disease. □





Zero defects at zero gravity.

When you're working on America's first space station, the requirement is zero defects at zero gravity.

Which is why NASA depends on Honeywell Reliability to make advanced space concepts a reality.

Honeywell has played a major role in every one of NASA's manned space missions, from the X15 through Gemini and Apollo, to SkyLab and the Space Shuttle. And now we're working with other leaders in the aerospace industry to engineer critical control systems for life support, power distribution as well as guidance and navigation for NASA's first space station, scheduled for deployment in the mid-1990s.

Honeywell combines advanced technology with reliable performance to ensure America's space program will succeed well into the 21st century—and beyond.

Honeywell Reliability

Together, we can find the answers.

Honeywell

Circle Reader Action No. 364

©1986 Honeywell Inc.

BREAKTHROUGH: A VIDEODISC YOU CAN CHANGE WHENEVER YOU CHANGE YOUR MIND.

Videodiscs have long held many advantages over videotape. But the high cost and long turnaround time for changing the information on these rigid plastic discs have made them impractical for many uses.

Now, McDonnell Douglas engineers have perfected the process of recording videodiscs by projecting a laser light beam onto flexible film. New visuals and sound can be added or deleted, using a speedy and inexpensive photographic process. It's a practical idea that opens the door for dozens of new videodisc applications in training, marketing and product maintenance.

We're creating breakthroughs that make a difference in the way people work and the way people live.

We're McDonnell Douglas.

*For more information,
write to: Laserfilm,
McDonnell Douglas,
Box 14526
St. Louis, MO 63178*



MCDONNELL DOUGLAS

TRAINING SYSTEMS

SPACE & MISSILES

AIRCRAFT & HELICOPTERS

HEALTH CARE

INFORMATION SYSTEMS

FINANCING

ENERGY



© 1986 McDonnell Douglas Corporation

Circle Reader Action No. 372